TRAKYA UNIVERSITY

# JOURNAL OF NATURAL SCIENCES

22 Volume 1 Number April 2021

# TRAKYA UNIVERSITY JOURNAL OF NATURAL SCIENCES

TUJNS

**Trakya Univ J Nat Sci**
ISSN 2147-0294
e-ISSN 2528-9691

# Trakya University
# Journal of Natural Sciences

**Volume: 22** **Number: 1** **April** **2021**

# Trakya Univ J Nat Sci

http://dergipark.org.tr/trkjnat
e-mail: tujns@trakya.edu.tr

ISSN 2147-0294
e-ISSN 2528-9691

ISSN 2147-0294
e-ISSN 2528-9691

*Trakya University Journal of Natural Sciences*
*http://dergipark.org.tr/trkjnat*
*Volume 22, Number 1, April 2021*



***Correspondence Address***
Trakya Üniversitesi Fen Bilimleri Enstitüsü Binası, Balkan Yerleşkesi – 22030 Edirne / TÜRKİYE
e-mail: tujns@trakya.edu.tr
Tel: +90 284 2358230
Fax: +90 284 2358237

*This Journal is a peer reviewed journal and is indexed by CAB Abstract, CiteFactor, DOAJ (Directory of Open Access Journal), DRJI (Directory of Research Journal Indexing), ESCI (Emerging Sources Citation Index), Google Scholar, ResearchBib, Science Library Index, SIS (Scientific Indexing Services), TUBITAK-ULAKBIM Life Sciences Database (Turkish Journal Index) and Zoological Record.*

***Publisher***
Trakya Üniversitesi Matbaa Tesisleri / Trakya University Publishing Centre

# TRAKYA UNIVERSITY JOURNAL OF NATURAL SCIENCES

**Volume 22** **Number 1** **April** **2021**

## REVIEWER LIST

ISSN 2147-0294
e-ISSN 2528-9691

*Trakya University Journal of Natural Sciences*
*http://dergipark.org.tr/trkjnat*
*Volume 22, Number 1, April 2021*

## CONTENTS

### Research Article

*http://dergipark.org.tr/trkjnat*
*Trakya University Journal of Natural Sciences, 22(1): 1-8, 2021*
*ISSN 2147-0294, e-ISSN 2528-9691*
*DOI: 10.23902/trkjnat.770526*

**Research Article**

# DIET COMPOSITION OF THE WINTERING *Asio otus* L. (STRIGIFORMES: STRIGIDAE) IN TWO DIFFERENT HABITAT TYPES IN TURKEY

Ahmet Yesari SELÇUK[1], Ömral Ünsal ÖZKOÇ[2*], Melisa BAL[3], Osman Özmen YELTEKİN[4], Umut GÜNGÖR[3]

[1] Neighbourhood of Yüzüncü Yıl, Site of Tekart, 01170, Çukurova, Adana, TURKEY
[2] Department of Biology, Graduate School of Sciences, Ondokuz Mayıs University, 55200, Samsun, TURKEY
[3] Department of Forest Engineering, Institute of Graduate Studies, İstanbul University-Cerrahpaşa, Istanbul, TURKEY
[4] Department of Biology, Institute of Science, Trakya University, Edirne, TURKEY

**Cite this article as:**

Selçuk A.Y., Özkoç Ö.Ü., Bal M., Yeltekin O.Ö. & Güngör U. 2021. Diet Composition of the Wintering *Asio otus* L. (Strigiformes: Strigidae) *i*n Two Different Habitat Types in Turkey. *Trakya Univ J Nat Sci*, 22(1): 1-8, DOI: 10.23902/trkjnat.770526

Received: 16 July 2020, Accepted: 04 October 2020, Online First: 01 November 2020, Published: 15 April 2021

***Edited by:***
*Coşkun Tez*

****Corresponding Author:***
*Ömral Ünsal Özkoç*
*omral.ozkoc@yahoo.com.tr*

***ORCID ID:***
*orcid.org/0000-0002-5918-8664*

***Key words:***
*Long-eared Owl*
*Feeding ecology*
*Winter diet*
*Pellet analysis*
*Small mammals*

**Abstract:** In this study, we analysed a total of 691 pellets of the Long-eared Owl (*Asio otus* L.) collected from Edirne (Suburban), İstanbul (Suburban) and Kars (High altitude steppe) provinces in January-February 2019. Dietary contents of the Long-eared Owl were considering the different habitat (steppe and suburban) types. Small mammals constituted the majority of the diet content in all areas, but a small amount of bird remains were also found in pellets. 1474 prey items belonging to 7 different mammal taxa (*Apodemus* sp., *Cricetulus* sp., *Crocidura* sp., *Micromys* sp., *Microtus* sp., *Mus* sp., *Rattus* sp.) were identified. High amount of *Mus* sp. was found in pellets collected from Edirne (50.34%) and İstanbul (41.42%). On the other hand, *Microtus* sp. was the main prey species in Kars. Overall, our study supported that the Long-eared Owl acts as an opportunistic predator and change its dietary contents according to different environmental conditions. Incompatible results were obtained between the trapping study and pellet examination. The reasons could be that some mammal species can be caught by chance, trapping area cannot represent the entire hunting area and some mammal species could avoid trapping.

**Özet:** Bu çalışmada, Ocak-Şubat 2019'da Edirne (Suburban), İstanbul (Suburban) ve Kars (Dağ bozkırı) illerinden toplanan toplam 691 adet kulaklı orman baykuşu peleti analiz edilmiştir. Diyet içeriği farklı habitat türlerine (bozkır ve suburban) göre karşılaştırılmıştır. Küçük memeliler tüm alanlarda diyet içeriğinin çoğunu oluşturmaktadır, ayrıca peletlerde az miktarda kuş kalıntısı tespit edilmiştir. 7 farklı memeli taksonuna (*Apodemus* sp., *Cricetulus* sp., *Crocidura* sp., *Micromys* sp., *Microtus* sp., *Mus* sp., *Rattus* sp.) ait 1474 av belirlenmiştir. Edirne (%50,34) ve İstanbul'dan (%41,42) toplanan peletlerde yüksek miktarda *Mus* sp. tespit edilmiştir. Kars'tan toplanan peletlerde ise *Microtus* sp. ana av türüdür. Genel olarak, çalışmamız kulaklı orman baykuşunun fırsatçı bir avcı olarak beslendiğini ve diyet içeriğini farklı çevresel koşullara göre değiştirdiğini desteklemiştir. Kapanlama çalışması ile pelet analizi arasında uyumsuz sonuçlar elde edilmiştir. Bunun nedenleri, bazı memeli türlerinin tesadüfen yakalanabilmeleri, kapanlama alanının, baykuşun tüm avlanma alanını temsil edememesi ve bazı memeli türlerinin tuzaktan kaçınmaları olabilir.

## Introduction

Pellet analysis is a common, easy and inexpensive way to study owl's diet and behaviour. Owls usually ingest their prey as a whole and then digest them. After the digestion, they eject the indigestible parts of the prey as a compressed pellet. Pellets are elliptical shaped and contain some remains such as bones, furs, feathers, chitinous body parts, claws, mollusc shells and fish scales (Lynch 2007, König & Weick 2008, Yalden 2009). Even the smallest bone parts are preserved well in owl pellets, unlike pellets of birds of prey (König & Weick 2008). Owl pellets may provide a useful method for sampling small mammal communities by being more cost-effective (Heisler *et al*. 2016) because owls are specialized to prey rare and hard-to-detect micro mammal species making traditional standard traps relatively impractical (Teta *et al*. 2010).

The Long-eared Owl (*Asio otus* L.) is a widespread member of Strigidae throughout the Holarctic (Cramp & Simmons 1985). Its range extends to Continental Europe and the British Isles, Northwest Africa (Morocco and Tunisia), the Middle East including Asia Minor, Asia, and North America, south to New Mexico (Weick 2007, König & Weick 2008). It is mostly a resident and a

wintering species, very common in most parts of Turkey except its relatively local distribution in Eastern Anatolia (Kirwan *et al.* 2008). The species can be found in Turkey in all types of habitats with trees (Kirwan *et al.* 2008) and also frequently found in areas close to human settlements (Dziemian *et al.* 2012).

The hunting techniques and feeding niche of *A. otus* in the Palearctic have been well documented. Its diet is usually composed predominantly of small mammals (Birrer 2009). If a certain vole species is abundant in the hunting area, the owl specializes on this particular species (Romanowski & Zmihorski 2008, Basova 2009, Volkov *et al.* 2009, Ekimov 2010, Golova 2011). However, if the vole density is low in the diet, the proportion of prey other than small mammals may increase (Alivizatos & Goutner 1999, Pirovano *et al*. 2000, Rubolini *et al.* 2003, Shao & Liu 2006, Kiat *et al.* 2008, Song *et al.* 2010, Tian *et al.* 2015, Göçer 2016). The diet content can also vary according to seasonal conditions (Kafkaletou-Diez *et al.* 2008, Tome 2009), habitat differences (desert, urban, suburban, woodland, etc.) (Tian *et al.* 2015) and prey density in the hunting area.

The diet content of *A. otus* in Anatolia has been the subject of various studies (Turan 2005, Seçkin & Çoşkun 2006, Bulut *et al*. 2012, Hizal 2013, Göçer 2016, Kaya & Çoşkun 2017, Selçuk *et al.* 2017, 2019, Yorulmaz & Arslan 2019). Nonetheless, no data about the dietary content of the species is available for the population distributed in Thrace region of Turkey. In this study, we present data on the wintering diet of *A. otus* in two different suburban areas in Thrace region (Edirne and Istanbul, northwest of Turkey) and an open dry habitat in Kars (Northeast of Turkey).

## Materials and Methods

*Study areas*

The pellets of *A. otus* were collected between 20th of January and 28th of February 2019 in three areas in Edirne, İstanbul and Kars provinces (Fig. 1). Short descriptions of the collecting areas are provided below and further details of these areas are presented in Table 1. The areas where previous studies were performed are presented in Fig. 1. Each pellet was labelled and bagged individually and only the well-preserved pellets were included in the analyses. All collecting areas were communal winter roosting sites and the roosting groups were determined to be consisted of 2 to 35 birds which perched on coniferous and deciduous trees.

The collecting area in the Thrace region of Turkey is located in Edirne Province (N41.619521, E26.652396). The area is a common garden of a small settlement surrounded by a cultivated area and a breeding site of *A. otus*. Pellets were collected under the Mediterranean cypress (*Cupressus sempervirens* L.), Arizona cypress (*Cupressus arizonica* Greene), Oriental arborvitae (*Platycladus orientalis* L.) and Black locust (*Robinia pseudoacacia* L.) trees on which both first-winter and adult owls were observed. The number of owls varied from 3 to 35 in this area.


**Fig. 1.** Map showing the available locations where diet studies of *A. otus* in Turkey were performed so far. The black stars denote the localities of the present study and the numbers denote previous studies ([1]Turan, 2005, [2]Seçkin & Çoşkun, 2006, [3]Bulut *et al.*, 2012, [4]Hizal, 2013, [5]Göçer, 2016, [6,7]Selçuk *et al*., 2017, 2019, [8]Kaya & Çoşkun, 2017, [9]Yorulmaz & Arslan, 2019).

**Table 1.** Some climatological data about the collection areas (MGM, 2019).

| Collection Areas | Altitude (m) | Temperature (Monthly Average) (ºC) | | Temperature (Annual Average) (ºC) | Precipitation (Monthly Average) (mm) | | Precipitation (Annual Average (mm) |
|---|---|---|---|---|---|---|---|
| | | January | February | | January | February | |
| **Edirne** | 90 | 2.7 | 4.6 | 13.8 | 66.5 | 53.2 | 608.1 |
| **İstanbul** | 35 | 6.0 | 6.1 | 14.4 | 105.5 | 77.8 | 823.0 |
| **Kars** | 1,750 | -10.3 | -8.6 | 4.9 | 21.3 | 22.1 | 502.7 |

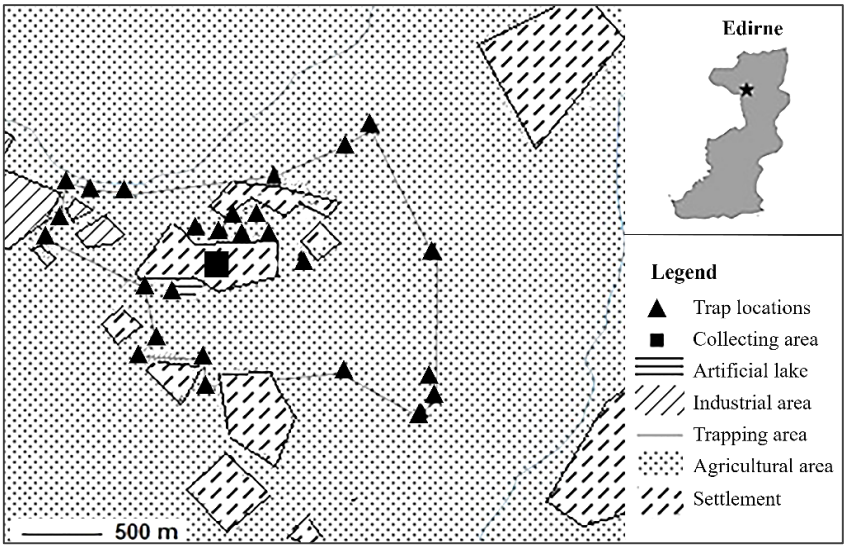


**Fig. 2.** The collecting area and the trapping localities in Edirne Province.

The collecting area in İstanbul (N41.03887, E28.54947**)** is located in the European side (Thrace region). Pellets were collected under Mediterranean cypress (*Cupressus sempervirens*) trees in a cemetery. The cemetery is surrounded by suburban settlements and cultivated areas and is about 1 km away from the southwestern coast of Büyükçekmece Lake. The number of owls varied from 2 to 8 in this area.

The collecting area in Kars Province (N40.576547, E43.042095**)** is located in Eastern Anatolia. Pellets were collected under Scots pine (*Pinus sylvestris* L.) trees in the campus of the Kafkas University. The collecting area is surrounded by high altitude steppe and is located about 1 km from the east side of Kars River. The number of owls varied from 6 to 7 in this area.

*Identification of prey and analysis of the pellets*

The identification of small mammals was performed according to Kryštufek & Vohralik (2001, 2005, 2009) and Barciova & Macholan (2009). Skull and lower jaw remains were used for identifications.

Since many species may show geographic, sexual and individual-related differences in body weight (biomass), uncertain biomass calculations may occur in pellet studies (Birrer 2009). Therefore, the data from Kryštufek & Vohralik (2001, 2005, 2009) was evaluated for biomass calculations since it reflected former samplings in Turkey. The identification of avian taxa was performed according to Svensson (1992) and Brown *et al.* (2003).

The minimum number of individuals, frequency, average prey and biomass ratios of small mammals and birds contained in each pellet were calculated.

*Trapping small mammals*

The trapping study was carried out between February 18$^{th}$ and 28$^{th}$ 2019 in order to identify small mammals in the collecting area in Edirne. Around this area, 200 Sherman-type live-capture traps were placed inside an area of approximately 2.82 km$^2$ (Fig. 2). The size of the trapping area was calculated as a minimum convex polygon in ArcMAP 10.7. The traps were placed in different types of habitat, such as shrub communities on the edge of agricultural areas, riparian areas, and dense shrub communities in urban areas and under a pine plantation site and checked every morning and evening during 10 days (2000 trapping night). All trapped specimens are preserved in the cytogenetic laboratory of Biology Department, Faculty of Science, Ondokuz Mayıs University.

The Chi-square analysis was applied to check if the observed availability of micro-mammals fits their expected frequency in the owl's diet.

## Results

*Pellet analysis*

A total of 691 pellets were collected, 521 from Edirne, 144 from İstanbul and 26 from Kars. 1170 preys belonging to 7 different taxa (6 small mammals and 1 bird) were determined in the pellets collected in Edirne province. The prey rate per pellet is 2.28. A significant portion of the diet content (F=97.86%; B=98.36%) consists of small mammals. Rodentia has the highest rate of diet content (97.18%). *Mus* sp. (F=50.34%; B=31.15%) were the main prey in the diet followed by *Microtus* sp. (F=27.26%; B=46.64%) (Table 2). 239 preys belonging to 7 different taxa (6 small mammals and 1 bird) were determined in the pellets collected in İstanbul province. The prey rate per pellet is 1.65. A significant portion of the diet content (F=92.89%; B=95.37%) consists of small mammals. *Mus* sp. (F=41.42%; B=21.71%) were the main prey in the collecting area followed by *Microtus* sp. (F=38.08%; B=55.17%) (Table 2). 65 preys belonging to 5 different taxa (4 small mammals and 1 bird) were determined in the pellets collected in Kars province. The prey rate per pellet is 2.50. A significant portion of the diet content (F=96.92%; B=98.34) consists of small mammals. *Microtus* sp. (F=64.62%; B=77.63%) were the main prey in the collecting area followed by *Mus* sp. (F=15.38%; B=6.69%) (Table 2).

**Table 2.** Diet composition of *Asio otus* as revealed by pellet analysis collected from Edirne, İstanbul and Kars provinces in Turkey in winter season. MNI: the minimum number of individuals, F%: frequency (F%), B%: biomass.

| Prey | Weight (g) | Edirne (Thrace Region) | | | İstanbul (Thrace Region) | | | Kars (Northeast of Turkey) | | |
|---|---|---|---|---|---|---|---|---|---|---|
| | | MNI | F% | B% | MNI | F% | B% | MNI | F% | B% |
| ***Apodemus* sp.** | 28.7 | 199 | 17.01 | 18.76 | 27 | 11.30 | 10.56 | 6 | 9.23 | 7.15 |
| ***Cricetulus* sp.** | 33.1 | 8 | 0.68 | 0.87 | - | - | - | 5 | 7.69 | 6.87 |
| ***Crocidura* sp.** | 8.4 | 8 | 0.68 | 0.22 | 1 | 0.42 | 0.11 | - | - | - |
| ***Micromys* sp.** | 9.9 | 22 | 1.88 | 0.72 | 1 | 0.42 | 0.13 | - | - | - |
| ***Microtus* sp.** | 44.5 | 319 | 27.26 | 46.64 | 91 | 38.08 | 55.17 | 42 | 64.62 | 77.63 |
| ***Mus* sp.** | 16.1 | 589 | 50.34 | 31.15 | 99 | 41.42 | 21.71 | 10 | 15.38 | 6.69 |
| ***Rattus* sp.** | 188 | - | - | - | 3 | 1.26 | 7.68 | - | - | - |
| **Total mammals** | | **1145** | **97.86** | **98.36** | **222** | **92.89** | **95.37** | **63** | **96.92** | **98.34** |
| **Birds** | 20.0 | 25 | 2.14 | 1.64 | 17 | 7.11 | 4.63 | 2 | 3.08 | 1.66 |
| **Total prey** | | **1170** | **100** | **100** | **239** | **100** | **100** | **65** | **100** | **100** |
| **Number of preys per pellet** | | 2.28+-1.06 Min-max: 1-6 | | | 1.65+-0.79 Min-max:1-4 | | | 2.5+-1.06 Min-max:1-6 | | |
| **Number of pellets** | | 521 | | | 144 | | | 26 | | |

A total of 96 small mammals belonging to 6 taxa were caught in the collecting area of Edirne Province (Table 3). The most common small mammals were *Apodemus* spp. (n=30 for *A. flavicollis* (Melchior) and n=32 for *A. sylvaticus* (L.)) (F%=64.58) followed by *Crocidura suaveolens* Pallas (n=12), *Mus macedonicus* Petrov & Ruzic (n=7) and *M. domesticus* Schwarz and Schwarz (n=14), respectively (Table 3). *Microtus levis* Miller was captured only once (F%=1.04). There is a significant difference between the frequency of small mammals in pellets and trapping results ($x^2$: 213.355; df: 5; $p < 0.0001$).

**Table 3.** Number and frequency of mammalian preys.

| Species | Number of Individuals (F) | Frequency (F%) |
|---|---|---|
| ***Apodemus* sp.** | 62 | 64.58 |
| ***Crocidura* sp.** | 12 | 12.5 |
| ***Microtus* sp.** | 1 | 1.04 |
| ***Mus* sp.** | 21 | 21.88 |
| **Total** | **96** | **100** |

## Discussion

The diet of *A. otus* has been revealed in detail particularly in Central Europe but the data in some other areas, such as Africa and Asia, are under-represented (Birrer 2009). Many studies were conducted to determine the diet of *A. otus* in Turkey except Thrace region. Birrer (2009) reviewed more than 475 studies and reported that main preys of *A. otus* are members of the order Rodentia. The present study corroborated the previous findings that rodents are dominant prey. On the other hand, it is a fact that the diet content of *A. otus* depends on the sampling season (Kafkaletou-Diez *et al.* 2008, Romanowski & Zmihorski 2008, Tome 2009, Song *et al.* 2010, Gryz & Krauze-Gryz 2015) and habitat type where the individuals are sampled (Capizzi & Luiselli 1998, Romanowski & Zmihorski 2008, Tian *et al.* 2015, Lesinski *et al*. 2016).

*Asio otus* is an opportunistic predator (Bertolino *et al.* 2001, Shao & Liu 2006, Tulis *et al.* 2015,). Therefore, if the density of rodent species in its diet is low or if rodents are completely absent, its tendency to prey on other species may increase (e.g. bird preys: Kiat *et al.* 2008, Sándor & Kiss 2008, Göçer 2016; bat preys: Tian *et al.* 2015). The main reason for this change in dietary content is the availability of different prey in different types of habitats and the adaptability of the owl regarding its choice of prey. Moreover, *A. otus* may change its prey preference according to the prey density in the hunting area (Song *et al.* 2010). Except for the results of study on the urban habitat (Göçer 2016), *Microtus* sp. are the dominant prey in Turkey. However, according to the results of this study, primary prey differs in Thrace region (Edirne and İstanbul) and Kars (steppe habitat) province. According to the optimal foraging theory, owls feed on the most beneficial prey. Therefore, it is expected to expand its feeding niche when the density of the main prey decreases in the hunting area. On the contrary, when the density of the main prey species increases and they become more available, the predators are more selective in capturing more profitable species (Schoener 1971, Pyke 1984).

Kontogeorgos (2019) suggested that the prey-size is another important factor in feeding habits and behaviour of predator species. *Asio otus* usually prefer preys smaller than 50 g but they were observed to catch preys larger than 50 g when the prey is weak or young (Vorisek *et al.* 1998, Manegold, 2000, Pirovano *et al.* 2000, Tome 2000, Birrer 2009). Kontogeorgos (2019) showed that rats weighing 250 g in the area selected for the study were consumed less. The reason could be that catching rats is not cost-

effective (Mori & Bertolini 2015). This study showed that the occurrence of rats in the diet ($F_{Edirne}$=0%, $F_{İstanbul}$=1.26%, $F_{Kars}$=0%) was significantly lower than other preys, as in previous studies (Escala *et al.* 2009, Cecere *et al.* 2013, Kontegeorgos 2019, Tulis *et al.* 2019).

Many diet studies reported that *Microtus* species were the primary food source of *A. otus* (Balčiauskienė *et al.* 2006, Sergio *et al.* 2008, Birrer 2009, Dziemian *et al.* 2012, Milchev & Ivanov 2016,). Studies conducted in different seasons and habitats in Anatolia (except Göçer 2016) reported that *Microtus* spp. were the main prey in the diet. *Microtus* sp. was the main prey in both winter diet determined in the present study (F=64.62%) and summer diet of the previous study performed in Selim district in Kars (F=81.63%) (Selçuk *et al.* 2019). However, when the population density of *Microtus* species in the hunting area is low or if they are completely absent, *Apodemus* or *Mus* spp. become the main prey in the diet of the species (Galeotti & Canova 1994, Bertolino *et al.* 2001, Escala *et al.* 2009). In Edirne and İstanbul (in this study), and in Porto Lagos (Western Thrace, Greece) (Alivizatos & Goutner 1999), *Mus* spp. was found to be the main prey. Palomo *et al.* (2007) reported that the reason for *Mus* spp. becoming the primary prey was the habitat degradation as a result of human activity. In rare cases, groups such as *Arvicola* spp. (Nilsson 1981), *Meriones* spp. (Shao & Liu 2006), *Cricetulus* spp. (Ma & Xiao 1995), *Rattus* spp. (Pirovano *et al.* 2000) and *Sigmodon* spp. (Noland *et al.* 2013, González- Rojas *et al.* 2017) may also be the primary or secondary prey. Additionally, when the prey availability is quite low in winter, owls can even feed on carrion (Mori *et al.* 2014).

*Asio otus* usually avoids hunting shrew species as a result of their undesirable taste. Therefore, in numerous studies, the ratio of shrew species in the dietary content is quite low (Birrer 2009). However, other studies reported that it was occasionally the secondary prey in the dietary content (F=22.4%, Dupal & Chernyshov 2013). The ratio of the shrew species in the diet studies conducted in Turkey is lower than 5% (Turan 2005, Seçkin & Çoşkun 2006, Bulut *et al.* 2012, Hizal 2013, Göçer 2016, Selçuk *et al.* 2017, 2019, Yorulmaz & Arslan 2019, in this study).

Birds in the dietary content have been reported to constitute less than 10% in most studies in Europe (Wijnandts 1984, Korpimäki 1992, Tome 1994, Pirovano *et al.* 2000, Navarro *et al.* 2003, Kovinka & Sharikov 2020). However, the proportion of birds in dietary content could be increasing in urban and suburban areas (Wijnandts 1984, Göçer 2016). In addition, urban cemeteries serve as shelters for birds and have a rich bird diversity (Lussenhop 1977, Čanády & Mošanský 2017). We observed that the frequency of birds found in pellets was higher in the collecting area in İstanbul, which is a cemetery in contrast to Kars (steppe area) and Edirne (suburban area) (Table 2).

In this study, and in many others, the composition of small mammalian in the diet from the pellet and from the trapping is different (Perrin, 1982, Yom-Tov & Wool 1997, Petrovici *et al.* 2013). In Edirne Province, although the predominant prey was found to be *Mus* spp. as a result of pellet analysis, *Apodemus* spp. had the highest rate (64.58%) in the trapping study. This may be due to the fact that some mammal species can be caught by chance (e.g. *Micromys* sp., *Cricetulus* sp.), the surface of the trapping area cannot represent the entire hunting area of *A. otus* (Petrovici *et al.* 2013), and the efficiency of capture methods (Vieira *et al.* 2014). Although owl pellets are an important alternative option for more detailed small mammal studies, it is still not recommended to rely on pellets to completely replace traditional trapping methods (Heisler *et al.* 2016).

The diet composition of *A. otus* in this study supports that this species has an opportunistic foraging behaviour. Our results also support the hypothesis that feeding strategy can vary depending on the type of habitat, climatic conditions and distribution, diversity and abundance of potential prey. We emphasize that Turkey has a great potential to investigate the diet of *A. otus*, because of vegetation, altitude, climatic conditions, and prey diversity vary greatly throughout the country.

**Acknowledgement:** The authors are grateful to Barış Yıldız, PhD for his support in fieldwork. We also thank Assist. Prof. Dr. Necmettin Güler (Edirne) for identification of the tree species.

**Author Contributions:** Concept: A.Y.S., Ö.Ü.Ö., Design: A.Y.S., Ö.Ü.Ö., M.S., Execution: A.Y.S., Ö.Ü.Ö., Material supplying: A.Y.S., O.Ö.Y., U.G., Data acquisition: A.Y.S., Ö.Ü.Ö., M.S., Data analysis/interpretation: A.Y.S., Ö.Ü.Ö., M.S., Manuscript writing: A.Y.S., Ö.Ü.Ö., M.S., Critical revision: A.Y.S., Ö.Ü.Ö., Small mammals field study and species identification: A.Y.S.

**Ethics Committee Approval:** Since the article does not contain any studies with human or animal subject, its approval to the ethics committee was not required.

**Conflict of Interest:** The authors have no conflicts of interest to declare.

**Funding:** The author declared that this study has received no financial support.

## References

1. Alivizatos, H. & Goutner V. 1999. Winter diet of the Barn Owl (*Tyto alba*) and Long-eared Owl (*Asio otus*) in northeastern Greece: a comparison. *Journal of Raptor Research*, 33: 160-163.
2. Balčiauskienė, L., Jovaišas, A., Naruševičius, V., Petraška, A. & Skuja, S. 2006. Diet of Tawny Owl (*Strix aluco*) and Long-eared Owl (*Asio otus*) in Lithuania as found from pellets. *Acta Zoologica Lituanica*, 16(1): 37-45.
3. Barciova, L. & Macholan, M. 2009. Morphometric key for the discrimination of two wood mice species, *Apodemus sylvaticus* and *A. flavicollis*. *Acta Zoologica Academiae Scientiarum Hungaricae*, 55(1): 31-38.
4. Basova, V.B. 2009. Comparative ecology of Long-eared and Short-eared Owls, *Asio otus* and *A. flammeus*. Extended abstract of dissertation for scientific degree of candidate of biological sciences, Moscow.

5. Bertolino, S., Ghiberti, E. & Perrone, A. 2001. Feeding ecology of the Long-eared Owl (*Asio otus*) in northern Italy: is it a dietary specialist? *Canadian Journal of Zoology*, 79: 2192-2198.

6. Birrer, S. 2009. Synthesis of 312 studies on the diet of the Long-eared Owl *Asio otus*. *Ardea*, 97: 615-24.

7. Brown, R., Ferguson, J., Lawrence, M. & Lees, D. 2003. *Tracks and Signs of the Birds of Britain and Europe*. 2nd edition. London: Christopher Helm. 336 pp.

8. Bulut, Ş., Akbaba, B. & Ayaş, Z. 2012. Analysis of mammal remains from owl pellets (*Asio otus*) in a suburban area in Beytepe, Ankara. *Hacettepe Journal of Biology and Chemistry*, 40: 233-237.

9. Čanády, A. & Mošanský, L. 2017. Public cemetery as a biodiversity hotspot for birds and mammals in the urban environment of Kosice city (Slovakia). *Zoology and Ecology*, 27(3-4): 185-195.

10. Capizzi, D. & Luiselli, L. 1998. A comparative study of the variability of owl diets in three localities of central Italy. *Revue d'écologie-La Terre Et La Vie*, 53: 367-385.

11. Cecere, J.G., Bombino, S. & Santangeli, A. 2013. Winter diet of Long-eared Owl *Asio otus* in a Mediterranean fragmented farmland. *The Wilson Journal of Ornithology*, 125(3): 655-658.

12. Cramp, S. & Simmons, K. 1985. The birds of the western Palearctic Handbook of the Birds of Europe the Middle East and North Africa, 4. Oxford: Oxford University Press. 960 pp.

13. Dupal, T.A. & Chernyshov, M.V. 2013. Small mammals in the diets of the Long-eared Owl (*Asio otus*) and Short-eared Owl (*Asio flammeus*) in the South of Western Siberia. *Russian Journal of Ecology*, 44(5): 397-401.

14. Dziemian, S., Piłacińska, B. & Pitucha, G. 2012. Winter diet composition of urban Long-eared Owls (*Asio otus*) in Rzeszów (SE Poland). *Biological Letters*, 49(2): 107-114.

15. Ekimov, E.V. 2010. Zonal features of trophic connections of the Long-eared Owl in steppes and semideserts of Tuva, Vestn. *Krasnoyarsk State Agricultural University*, 8: 59-63.

16. Escala, C., Alonso, D., Mazuelas, D., Mendiburu, A., Vilches, A., Arizaga, J. & Scheme, A.R. 2009. Winter diet of Long-eared Owls *Asio otus* in the Ebro valley (NE Iberia). *Revista Catalana d'Ornitologia,* 25: 49-53.

17. Galeotti, P. & Canova, L. 1994. Winter diet of Long-eared Owls (*Asio otus*) in the Po plain (northern Italy). *Journal of Raptor Research*, 28(4): 265-268.

18. Golova, S.V. 2011. Feeding of the Long-eared Owl in agrarian areas of the Nizhni Novgorod Volga region, Russia. *Pernatye khishchniki i ikh okhrana (Birds of Prey and Their Protection)*, 21: 176-180.

19. González-Rojas, J.I., Padilla-Rangel, H., Ruvalcaba-Ortega, I., Cruz-Nieto, M.A., Canales-Del-Castillo, R. & Guzmán-Velasco, A. 2017. Winter diet of the Long-eared Owl *Asio otus* (Strigiformes: Strigidae) in the grasslands of Janos, Chihuahua, Mexico. *Revista chilena de historia natural*, 90(1): https://doi.org/10.1186/s40693-017-0064-3

20. Göçer, E. 2016. Diet of a nesting pair of Long-eared Owls, *Asio otus*, in an urban environment in southwestern Turkey (Aves: Strigidae). *Zoology in the Middle East*, 62: 25-28.

21. Gryz, J. & Krauze-Gryz, D. 2015. Seasonal variability in the diet of the Long-eared Owl *Asio otus* in a mosaic of field and forest habitats in central Poland. *Acta Zoologica Cracoviensia*, 58(2): 173-180.

22. Heisler, L.M., Somers, C.M. & Poulin, R.G. 2016. Owl pellets: a more effective alternative to conventional trapping for broad-scale studies of small mammal communities. *Methods in Ecology and Evolution*, 7(1): 96-103.

23. Hizal, E. 2013. Diet of the Long-eared Owl *Asio otus*, in Central Anatolia (Aves: Strigidae). *Zoology in the Middle East*, 59: 118-122.

24. Kafkaletou-Diez, A., Tsachalidis, E.P. & Poirazidis, K. 2008. Seasonal variation in the diet of the Long-eared Owl (*Asio otus*) in a northeastern agricultural area of Greece. *Journal of Biological Research-Thessaloniki*, 10: 181-189.

25. Kaya, A. & Çoşkun, Y. 2017. Erzurum'dan toplanan kulaklı orman baykuşu (*Asio otus*) peletlerinde memeli hayvan türleri. *Bitlis Eren University Journal of Science*, 6: 47-50.

26. Kiat, Y., Perlman, G., Balaban, A., Leshem, Y., Izhaki, I. & Charter, M. 2008. Feeding specialization of urban Long-eared Owls, *Asio otus* (Linnaeus, 1758), in Jerusalem, Israel. *Zoology in the Middle East*, 43: 49-54.

27. Kirwan, G.M., Boyla, K.A., Castell, P., Demirci, B., Özen, M., Welch, H. & Marlow, T. 2008. *The distribution, taxonomy and breeding of Turkish birds*. London: Christopher Helm. 512 pp.

28. Kontogeorgos, I. 2019. Feeding ecology and prey selection by wintering Long-eared Owls *Asio otus* in Mediterranean Agrosystems. *Ornithological Science*, 18: 95-110.

29. Korpimäki, E. 1992. Diet composition, prey choice, and breeding success of Long-eared Owls: effects of multiannual fluctuations in food abundance. *Canadian Journal of Zoology*, 70: 2373-2381.

30. Kovinka, T.S. & Sharikov, A.V. 2020. Selection of prey by size and sex in the Long-eared Owl *Asio otus*. *Bird Study*, 1-7.

31. König, C. & Weick, F. 2008. *Owls of the world.* London: Christopher Helm. 528 pp.

32. Kryštufek, B. & Vohralik, V. 2001. *Mammals of Turkey and Cyprus. Order Insectivora (Introduction, Checklist, Insectivora).* Koper, Knjiznica Annales Majora. 138 pp.

33. Kryštufek, B. & Vohralik, V. 2005. *Mammals of Turkey and Cyprus. Order Rodentia I (Introduction, Checklist, Rodentia).* Koper, Knjiznica Annales Majora. 292 pp.

34. Kryštufek, B. & Vohralik, V. 2009. *Mammals of Turkey and Cyprus. Order Rodentia II (Introduction, Checklist, Rodentia).* Koper, Knjiznica Annales Majora. 372 pp.

35. Lesinski, G., Romanowski, J. & Budek, S. 2016. Winter diet of the Long-eared Owl *Asio otus* in various habitats of central and north-eastern Poland. *Annals of Warsaw University of Life Sciences-SGGW*, 55(1): 81-88.

36. Lussenhop, J. 1977. Urban cemeteries as bird refuges. *The Condor*, 79(4): 456-461.

37. Lynch, W. 2007. *Owls of the United States and Canada. A Complete Guide to Their Biology and Behavior*. Baltimore: The Johns Hopkins University Press. 242 pp.

38. Ma, S.X. & Xiao, W. 1995. Ecology of the Long-eared Owl (*Asio otus*) in winter. *Sichuan Journal of Zoology*, 15: 78-79.

39. Manegold, A. 2000. Pathologisch veränderte Schädel der Feldmaus (*Microtus arvalis*) aus Eulengewöllen und die Abnahme ihres Anteils im Verlauf des Winters. *Populationsökologie Greifvogel- und Eulenarten*, 4:531-537.

40. MGM, 2019. https://www.mgm.gov.tr/veridegerlendirme/il-ve-ilceler-istatistik.aspx?k=H, (Date accessed: 10.04.2020).

41. Milchev, B. & Ivanov, T. 2016. Winter diet of Long-eared Owls *Asio otus* (L.) in a suburban landscape of north-eastern Bulgaria. *Acta Zoologica Bulgarica*, 68: 355-361.

42. Mori, E., Menchetti, M. & Dartora, F. 2014. Evidence of carrion consumption behaviour in the Long-eared Owl *Asio otus* (Linnaeus, 1758) (Aves: Strigiformes: Strigidae). *Italian Journal of Zoology*, 81 (3): 471-475.

43. Mori, E. & Bertolini, S. 2015. Feeding ecology of Long-eared Owls in winter: an urban perspective. *Bird Study*, 62: 257-261.

44. Navarro, J., Sanchez-Zapata, J.A., Carrete, M. & Botella, F. 2003. Diet of three sympatric owls in steppe habitats of eastern Kazakhstan. *Journal of Raptor Research*, 37(3): 256-258.

45. Nilsson, I.N. 1981. Seasonal changes in food of the Long-eared Owl in southern Sweden. *Ornis Scandinavica*, 12: 216-223.

46. Noland, R.L., Maxwell, T.C. & Dowler, R.C. 2013. Food habits of Long-eared Owls (*Asio otus*) at a winter communal roost in Texas. The Southwestern Naturalist, 58(2): 245-248.

47. Palomo, L.J., Gisbert, J. & Blanco, J. C. 2007. *Atlas y Libro Rojo de los Mamíferos Terrestres de España. Dirección General para la Biodiversidad*, Madrid: Secem-Secemu. 588 pp.

48. Perrin, M.R. 1982. Prey specificity of Barn Owl in the Great Fish River valley of the eastern cape province. *South African Journal of Wildlife Research*. 12: 14-25.

49. Petrovici, M., Molnar, P. & Sandor, A.D. 2013. Trophic niche overlap of two sympatric owl species (*Asio otus* Linnaeus, 1758 and *Tyto alba* Scopoli, 1769) in the north-western part of Romania. *North-Western Journal of Zoology*, 9(2), 250-256.

50. Pirovano, A., Rubolini, D., Brambilla, S. & Ferrari N. 2000. Winter diet of urban roosting Long-eared Owls *Asio otus* in northern Italy: the importance of the Brown Rat *Rattus norvegicus*. *Bird Study*, 47: 242-244.

51. Pyke, G.H. 1984. Optimal foraging theory: a critical review. *Annual Review of Ecology and Systematics*, 15(1): 523-575.

52. Romanowski, J. & Zmihorski, M. 2008. Effect of season, weather and habitat on diet variation of a feeding specialist: a case study of the Long-eared Owl, *Asio otus* in Central Poland. *Folia Zoologica*, 57: 411-419.

53. Rubolini, D., Pirovano, A. & Borghi, S. 2003. Influence of seasonality, temperature and rainfall on the winter diet of the Long-eared Owl, *Asio otus*. *Folia Zoologica*, 52: 67-76.

54. Sándor, A.D. & Kiss, B.J. 2008. Birds in the diet of wintering Long-eared Owls (*Asio otus*) in the Danube Delta, Romania. *Journal of Raptor Research*, 42: 292-295.

55. Schoener, T.W. 1971. Theory of feeding strategies. *Annual Review Ecology, Evolution and Systematics*, 2: 369-404.

56. Seçkin, S. & Coşkun, Y. 2006. Small mammals in the diet of the Long-Eared Owl, *Asio otus*, from Diyarbakır, Turkey. *Turkish Journal of Zoology*, 30: 271-278.

57. Selçuk, A.Y., Bankoğlu, K. & Kefelioğlu, H. 2017. Comparison of winter diet of Long-eared Owls *Asio otus* (L., 1758) and Short-eared Owls *Asio flammeus* (Pontoppidan, 1763) (Aves: Strigidae) in northern Turkey. *Acta Zoologica Bulgarica*, 69: 345-348.

58. Selçuk, A.Y., Özkoç, Ö.Ü., Bilir, M.A. & Kefelioğlu, H. 2019. Diet composition of the Long-eared Owl (*Asio otus*) in the eastern Anatolia (Turkey). *Türkiye Ormancılık Dergisi*, 20(2): 72-75.

59. Sergio, F., Marchesi, L. & Pedrini, P. 2008. Density, diet and productivity of Long-eared Owls *Asio otus* in the Italian Alps: the importance of Microtus voles. *Bird study*, 55(3): 321-328.

60. Shao, M. & Liu, N. 2006. The diet of the Long-eared Owls in the desert of Northwest China. *Journal of Arid Environments*, 65: 673-676.

61. Song, S., Zhao, W., Zhao, J., Shao, M. & Liu, N. 2010. Seasonal variation in the diet of Long-eared Owl, *Asio otus*, in the desert of Northwest China. *Animal Biology*, 60: 115-122.

62. Svensson, L. 1992. *Identification Guide to European Passerines.* Stockholm: Märstatryck, 368 pp.

63. Teta, P., González-Fischer, C.M., Codesido, M. & Bilenca, D.N. 2010. A contribution from Barn Owl pellets analysis to known micromammalian distributions in Buenos Aires province, Argentina. *Mammalia*, 74(1): 97-103.

64. Tian, L., Zhou, X., Shi, Y., Guo, Y. & Bao, W. 2015. Bats as the main prey of wintering Long-eared Owl (*Asio otus*) in Beijing: Integrating biodiversity protection and urban management. *Integrative Zoology*, 10: 216-226.

65. Tome, D. 1994. Diet composition of the Long-eared Owl (*Asio otus*) in central Slovenia: seasonal variation in prey use. *Journal of Raptor Research*, 28: 253-258.

66. Tome, D. 2000. Estimating individual weight of prey items for calculation of the biomass in the diet of Long-eared Owl (*Asio otus*): is it worth of extra effort? *Folia Zoologica*, 49: 205-210.

67. Tome, D. 2009. Changes in the diet of Long-eared Owl *Asio otus*: seasonal patterns of dependence on vole abundance. *Ardeola*, 56(1): 49-56.

68. Tulis, F., Balaz, M., Obuch, J. & Sotnar, K. 2015. Responses of the Long-eared Owl *Asio otus* diet and the numbers of wintering individuals to changing abundance of the Common Vole *Microtus arvalis*. *Biologia*, 70(5): 667-673.

69. Tulis, F., Ševčík, M. & Obuch, J. 2019. Long-eared Owls roosted in the forest, still hunted in open land. *Raptor Journal*, 13(1), 105-119.

70. Turan, L. 2005. Winter diet of a Long-eared Owl population in Ankara, Beytepe. *Hacettepe Journal of Biology and Chemistry*, 34: 69-76.

71. Vieira, A.L.M., Pires, A. S., Nunes-Freitas, A.F., Oliveira, N.M., Resende, A.S. & Campello, E.F.C. 2014. Efficiency of small mammal trapping in an Atlantic forest fragmented landscape: the effects of trap type and position, seasonality and habitat. *Brazilian Journal of Biology*, 74(3): 538-544.

72. Volkov, S.V., Sviridova, T.V., Sharikov, A.V., Grinchenko, O.S. & Kol'tsov, D.B. 2009. Patterns of biotopic and spatial distribution of the Short-eared Owl in agrolandscape: effect of qualitative characteristics of habitats. *Sovy Sever noi Evrazii: ekologiya, prostranstvennoe i biotopicheskoe raspredelenie (Owls in Northern Eurasia: Ecology and Spatial and Biotopic Distribution)*, Moscow, 188-203.

73. Vorisek, P., Votypka, J., Zwara, K. & Svobodova, M. 1998. Heteroxenous coccidia increase the predation risk of parasitized rodents. *Parasitology*, 117: 521-524.

74. Weick, F. 2007. *Owls (Strigiformes): Annotated and illustrated checklist.* Germany: Springer Science & Business Media, 384 pp.

75. Wijnandts, H. 1984. Ecological energetics of the Long-eared Owl (*Asio otus*). *Ardea*, 72: 1-92.

76. Yalden, D.W. 2009. *The Analysis of Owl Pellets*. 4th Edition. Southampton, Mammal Society, 28 pp.

77. Yom-Tov, Y. & Wool, D. 1997. Do the contents of Barn Owl (*Tyto alba*) pellets accurately represent the proportion of prey species in the field? *Condor*, 99: 972-976.

78. Yorulmaz, T. & Arslan, N. 2019. Investigation on diet of Long-eared Owl (*Asio otus*) inhabiting Fatih Natural Park (Turkey). *Bitlis Eren Üniversitesi Fen Bilimleri Dergisi,* 8(3): 859-865.

*http://dergipark.org.tr/trkjnat*
*Trakya University Journal of Natural Sciences, 22(1): 9-15, 2021*
*ISSN 2147-0294, e-ISSN 2528-9691*
*DOI: 10.23902/trkjnat.773302*

**Research Article**

# DISTINCTIVE *SIRE1* RETROTRANSPOSON PATTERNS ON BARLEY CHROMOSOMES?

Elif KARLIK[1*], Nermin GÖZÜKIRMIZI[2]

[1] İstinye University, Department of Molecular Biology and Genetics, İstanbul, TURKEY
[2] İstanbul University, Faculty of Sciences, Department of Molecular Biology and Genetics, İstanbul, TURKEY

**Cite this article as:**

Karlık E., Gözükırmızı N. 2021. Distinctive *SIRE1* Retrotransposon Patterns on Barley Chromosomes? *Trakya Univ J Nat Sci*, 22(1): 9-15, DOI: 10.23902/trkjnat.773302

Received: 24 July 2020, Accepted: 09 October 2020, Online First: 07 November 2020, Published: 15 April 2021

***Edited by:***
*Yıldız Aydın*

****Corresponding Author:***
*Elif Karlık*
*elif.karlik@istinye.edu.tr*

***ORCID ID:***
*orcid.org/0000-0003-0669-2725*

***Key words:***
*Fluorescence in situ hybridization*
*Retrotransposon*
*SIRE1*
*Barley*
*ENV*
*GAG*

**Abstract:** *SIRE1* is an active and relatively high copy-number retroelement belongs to the *Tyl/Copia* long terminal repeat (LTR) retrotransposon superfamily. Distinctive *SIRE1* elements (*ENV* and *GAG*) distributions in barley genome were observed by using fluorescent *in situ* hybridization (FISH). We performed PCR to obtain tetramethylrhodamine-dUTP (TRITC)-labelled probes. Localizations of *SIRE1 ENV* and *GAG* domains were demonstrated under confocal microscope on *Hordeum vulgare* L. cv. Hasat root preparations. Our results revealed the distributions of *SIRE1* elements *ENV* and *GAG* in barley genome. These results may provide to uncover the organization of SIRE retrotransposon pattern in barley genome.

**Özet:** *SIRE1*, *Tyl/Copia* Uzun Uç Tekrarlı (Long Terminal Repeats- LTR) retrotranspozon üst ailesine ait olan aktif, nispeten yüksek kopyalı bir retroementtir. Arpa genomundaki ayırt edici *SIRE1* elementlerinin (*ENV* ve *GAG*) dağılımları floresan *in situ* hibridizasyonu (FISH) kullanılarak gözlemlendi. Tetramethylrhodamine-dUTP (TRITC)-işaretli probların elde edilmesinde PCR gerçekleştirildi. *SIRE1 ENV* ve *GAG* domainlerinin yerleşimleri, *Hordeum vulgare* L. cv. Hasat kök preparatlarında konfokal mikroskobu altında gösterildi. Sonuçlarımız, arpa genomundaki *SIRE1* elementlerinin *ENV* ve *GAG* dağılımlarını göstermektedir. Bu sonuçlar, SIRE1 elementlerinin arpa genomunun organizasyonunun ortaya çıkarılmasına katkı sağlayacaktır.

## Introduction

Transposable elements (TEs) are mobile genetic elements and are distributed throughout the plant genome, over the 14% of *Arabidopsis thaliana* (L.) Heynh. genome, over the 80% maize genome and 80.8% of barley genome consist of TEs (AGI 2000, Schnable *et al.* 2009, Mascher *et al.* 2017). TEs constitute DNA fragments which can move through the genome using a DNA intermediate (DNA transposons) or an RNA intermediate (retrotransposons). Retrotransposons encode their own proteins for replication and integration back into the genome can be subdivided into two main subclasses as LTR retrotransposons and non-LTR retrotransposons. Although both LTR and non-LTR retrotransposons are located on plant genomes, LTR retrotransposons are more abundant than non-LTR retrotransposons (Voytas & Boeke 2002, Sandmeyer *et al.* 2002, Schulman & Wicker 2013) and are divided into two main superfamilies known as *Tyl/copia* and *Ty3/gypsy* groups (Wicker *et al.* 2007).

*Tyl/copia* (*Pseudoviridae*) elements are prevalent in plants and grouped into three genera: Pseudovirus (*Ty1*), Hemivirus (*Copia*) and the Sirevirus which are closely related to the retroviruses, but have a different *polyprotein* (*pol*) gene order (Kumar & Bennetzen 1999, Llorens *et al.* 2009). Sireviruses are plant specific unique retrotransposons among *Tyl/copia* elements (Gao *et al.* 2003, Bousios *et al.* 2010). Sequence studies revealed that highly conserved sequence motifs of Sireviruses have been found within the extremely divergent non-coding part of the genome (Bousios *et al.* 2010). Recently, Sireviruses are named after the *SIRE1* element from soybean, and they were originally named as Agroviruses according to their host specificity that they were only colonized in plants (Peterson-Burch & Voytas 2002). Two notable features of Sireviruses can be considered as that they consist of an *env*-like gene after *pol* and encode a significantly larger *Gag* protein which differentiate them from other *Ty1/copia* genera (Peterson-Burch & Voytas 2002, Havecker *et al.* 2005). However, no known functions for either of these additional coding regions have been identified (Bousios *et al.* 2010).

Interestingly, some evidence indicated that individual retrotransposon families demonstrate typical patterns of chromosomal localizations (Presting *et al.* 1998, Friesen *et al.* 2001). However, with the completion of the DNA

sequencing project of *Arabidopsis thaliana* genome and various plant species, including barley, with large genome allowed the analysis of the retroelement distribution, and these studies revealed that TEs demonstrated non-random distribution through chromosomes (AGI 2000, Mascher *et al.* 2017). In barley genome project, Mascher *et al.* (2017) revealed that 3.7 Gb (80.8%) of barley genome consists of transposable elements and that only 10% of them are intact and potentially active. They distinguished the seven barley chromosomes into three fractions as fractions 1, 2 and 3. In the proximal fraction 3 -where older transposable elements are diverged, unique and predominated- contains mostly repetitive 20-mers. Moreover, fraction 3 is favoured by *Gypsy* retrotransposons, while fractions 1 and 2 are populated by *Copia* elements. These differences in the relative abundance of retrotransposon families are considered as distinct distributions of functional domains. Additionally, *Mariner* transposons preferentially occupy within 1 kb up- or downstream of the coding regions of genes. However, *Harbinger* and long interspersed elements are observed to be located further away from genes. Selective pressures are considered to underlie the distribution of different types of transposable elements around genes. As expected, the smallest transposable elements such as Mariner may be more tolerated in regions close to the genes. However, intriguingly, the Harbinger superfamily elements possess a clear preference for promoter regions, while long interspersed elements preferentially possess for downstream regions of genes. Moreover, the large transposable elements such as LTR retrotransposons and CACTA elements are located at greater distances from genes (Mascher *et al.* 2017).

Fluorescence *in situ* hybridization (FISH) using target-specific DNA probes have become a routine technique in modern molecular biology, cell research and medical diagnosis (Hausmann & Cremer 2003). However, application of FISH has been shown to be more difficult, because of the cell wall, the cytoplasm, which prevents chromosome spreading, low metaphase indices and often similar chromosome morphology (Salvo-Garrido *et al.* 2001). The distribution of retrotransposon families has been analysed in a variety of plant genomes including, *Allium cepa*, *Aegilops speltoides*, *Brachypodium distachyon* and *Glycine max* using FISH (Lin *et al.* 2005, Kiseleva *et al.* 2014, Shams and Olga Raskina 2018, Li *et al.* 2018). Li *et al.* (2018) performed FISH analysis on pachytene chromosomes of soybean BAC and three subclones. FISH analysis revealed that a recently inserted *SIRE1*, a solo *SIRE1* LTR and fragments of *Calypso*-like retroelements were located within this BAC. In barley, Acevedo-Garcia *et al.* (2013) used FISH analysis and YAC library to isolate *Ror1* gene, which encodes *Required for mlo-specified resistance* genes and important for basal defence, due to fine mapping and gene synteny strategies. Additionally, BAC clones have also been used to demonstrate *BARE1* patterns on barley chromosomes by FISH (Vicient *et al.* 1999).

The aim of this study was to present the localization of *SIRE1* patterns in *Hordeum vulgare* L. chromosomes using labelled-PCR products via FISH. *SIRE1* patterns were observed under confocal microscope on barley root preparations. Our results indicated the *SIRE1* localizations in barley genome.

## Materials and Methods

### *Plant materials*

*Hordeum vulgare* L.cv. Hasat was provided from the Directorate of Trakya Agricultural Research Institute. The plants were grown in a growth chamber under 16 h light/8 h dark and 25°C ± 2°C conditions. Relative humidity was kept at 60-75%. After 72 hours, plants were harvested, directly treated with liquid nitrogen and then stored at –80°C until DNA extraction.

### *gDNA Extraction*

gDNA were extracted from 200 mg of the samples by using a modified version of the cetyltrimethylammonium bromide (CTAB) precipitation method described in Mafra *et al.* (2008). Specifically, 200 mg homogenized sample was incubated with 1 ml Edward's buffer (0.5% (w/v) SDS, 250 mM NaCl, 25 mM EDTA, 200 mM Tris pH 8.0) at 95ºC for 5 min (Cold Spring Harbor Laboratory, 2005). The mixture was centrifugated at 16,000 g for 15 min. afterwards, the supernatant was extracted twice with chloroform. The aqueous phase was incubated with 2 volumes of CTAB precipitation solution, then the CTAB protocol was followed as previously described (Mafra *et al.* 2008). DNA yield and purity were measured by UV spectrophotometry at 230, 260 & 280 nm using a NanoDrop 2000c instrument (Thermo Scientific, Wilmington, DE, USA). DNA integrity was evaluated by agarose gel electrophoresis with which samples were separated on 1% agarose gels in 1X TAE buffer.

### *Chromosome preparation for FISH analysis*

Seeds were placed randomly in Petri dishes containing filter paper soaked in only water to germinate in an incubator at 18-25°C in the dark for 3 days. Root tips were harvested, directly fixed in Carnoy fixative (3:1 ethanol:acetic acid solution) without any chemical pre-treatment and stored at 4ºC. Chromosome preparations and FISH analysis were performed according to Jenkins & Hasterok (2001, 2007) with modifications. The slides were checked under the light microscope (Olympus U-TVO.5XC-3) and kept in a freezer at -20ºC.

### *Development of probes and labelling*

The FISH probes used in this study were generated from two sets of data which are the *ENV* (*envelope-like*) and *GAG* (encoding a structural protein) genes of *SIRE1*. To investigate the distribution of *SIRE1*, we amplified *ENV* and *GAG* domains of *SIRE1* using designed specific primer sets (Table 1). The probes for *ENV* and *GAG* domains were designated by using IDT's PrimerQuest© Tool (2012). GC% and Tm values of the probes were around 62 and between 47°and 55°C, respectively. The

sequences of *SIRE1 ENV and GAG* were obtained from barley (KP420209 for *GAG* and KP420210 for *ENV*).

Probe synthesis was carried out individually by using *SIRE1 ENV* and *GAG* primers. The reactions were performed in a total volume of 50 µl including 18.25 µl nuclease-free $dH_2O$, 25 µl of HotStart PCR Master Mix (Bio-Rad), 1.5 µl of each primer (10 µM/µl), 1.75 µl of tetramethylrhodamine-dUTP (TRITC) (1 mM), and 2 µl template DNA (40 ng/µl). PCR conditions were as follows: 94°C for 5 min followed by 40 cycles of 94°C for 25 s, annealing 50°C for 25 s and 72°C for 30 s. The reaction was completed by a final extension step at 72°C for 5 min.

**Table 1.** Primers used in this study.

| No | Primer Name | Sequence (5'→3') |
|---|---|---|
| 1 | *SIRE1 ENV F* | CGACAACACCAGAGGAGAATG |
| 2 | *SIRE1 ENV R* | CGCCTTGGTGGCCAATTA |
| 3 | *SIRE1 GAG F* | AACCGAGATGGAGGTAGTACA |
| 4 | *SIRE1 GAG R* | GAAACGGCACACGCTAGA |

*Fluorescence in situ hybridization (FISH) analysis*

The FISH analysis protocol was adopted from Jenkins and Hasterok (2001, 2007) protocol with modifications. Chromosome spreads were scanned under light microscope with ×40 objective to determine the number and quality of well-spread metaphase plates, and then they were treated with 100 µg/ml of RNase at 37°C for 1 h. The hybridization mixture contains 20 µl of deionised formamide (50%), 8 µl of dextran sulphate (10%), 4 µl of 20X SSC (2X SSC), 2 µl of 10% SDS (0.5%), 10 µl of probe (75-200ng/slide), 1 µl of blocking DNA (sonicated salmon sperm DNA) (25-100X probe) and added sterile $dH_2O$ to bring final volume 40 µl. Final concentrations were indicated in parenthesis. The mixture was denatured at 85°C for 10 min and kept on ice for 10 min. A 38 µl aliquot of the hybridization mixture was applied onto each slide, covered with a coverslip and sealed with paper bond. Both chromosomal DNA and probe DNA on the slides were denatured together in a thermal cycler at 70°C for 6 min and hybridized with each other at 37°C overnight in a humid dark box. Afterwards, hybridized the chromosome spreads were washed three times in 2X SSC: once 2X SSC to float coverslips off, once in 15% formamide/0.1X SSC and again once in 15% formamide/0.1X SSC, each for 10 min at 42°C. Then, the slides were washed in 2X SSC for 3 min at 42°C. This step was repeated twice with fresh 2X SSC at 42°C. Ultimately, the slides were washed three times in 2X SSC for 3 min at RT. Then, the slides were dehydrated in alcohol series (70, 90 and 100%), each for 1 min at RT and waited in the dark for 15-20 min. Vectashield-DAPI mounting-staining medium (7-10 µL) was dropped onto the chromosome spreads, which were then stored at 4°C until used.

*Image acquisition*

To image the slides, 551-575 nm wavelengths for probes labelled with TRITC and 420-480 nm wavelengths for DAPI were used for fluorescence detection in the Leica DM5500 confocal microscope. The different fluorescent images were acquired separately. Afterwards, they were merged into single composite images. The signal images were analysed by Adobe Photoshop CC 2014.

## Results

To characterize the abundance and localization patterns of soybean *SIRE1 ENV* and *GAG* domains in barley, we used root tip cells and *SIRE1 ENV* and *GAG* probes were labelled with TRITC. Specifically, we observed TRITC labelled *SIRE1 ENV* exhibited characteristic patterns at prophase in nucleus (Fig. 1). TRITC labelled *SIRE1 GAG* probes also demonstrated distinctive patterns in prophase phase in barley chromosomes (Fig. 2).

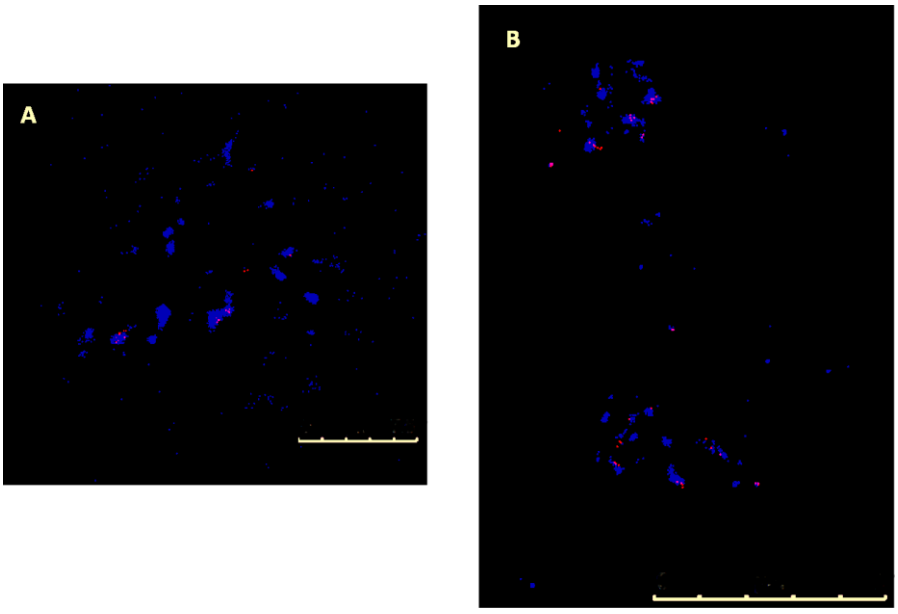


**Fig. 1.** Display of SIRE1 ENV distributions in barley root preparations *via* FISH. According to FISH results, characteristic feature of *SIRE1 ENVs* are localized in centred regions. Scale bar=7.5 and 25 µm for A and B, respectively.

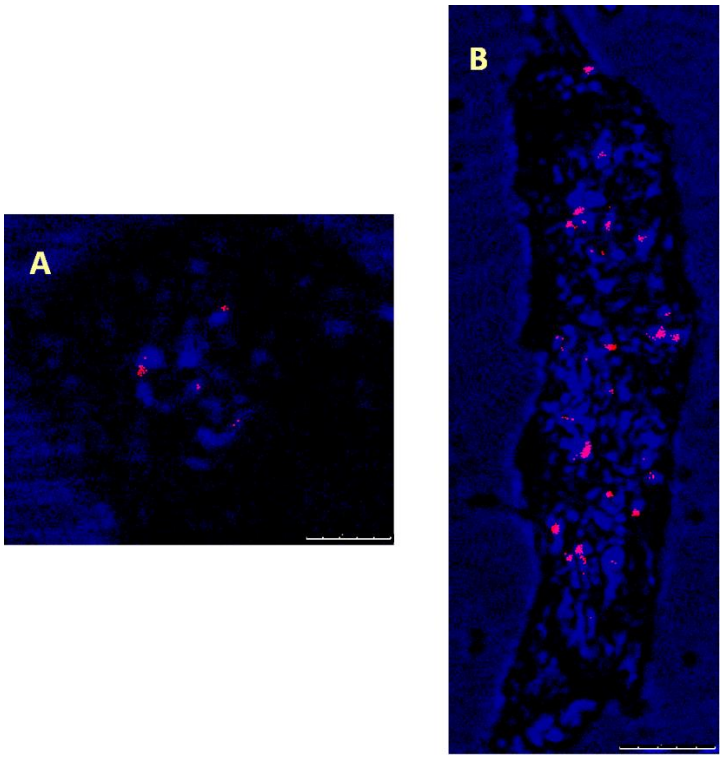


**Fig. 2.** Demonstrations of *SIRE1 GAG* localizations in barley root preparations *via* FISH. According to FISH results, *SIRE GAGs* are distinctively localized close to centred regions, similarly *SIRE1 ENV*. Scale bar=5 and 10 µm for A and B, respectively.

## Discussion

In plants, retroelements cover a large zone of genomes and are considered to have participated in the genome organization and evolution (McCarthy *et al.* 2002). Several studies have focused to detecting the chromosomal position of *Ty1-copia* retroelements, including *SIRE1* and anticipating their copy number (Pearce *et al.* 1996, Lin *et al.* 2005, Alipour *et al.* 2013, Kolano *et al.* 2013, Lee *et al.* 2013). In the current study, localizations of *SIRE1 ENV* and *GAG* domains were indicated on barley chromosomes (see Fig. 1 and 2). The results were obtained from *Hordeum vulgare* L. cv. Hasat root tips preparations using FISH analysis. Due to the large genome size of barley, researchers mostly prefer to use single-copy probes derived from BAC or YAC contigs (Vicient *et al.* 1999, Acevedo-Garcia *et al.* 2013, Bustamante *et al.* 2017). In our study, we used direct PCR products derived from barley DNA to produce single-stranded probes were small, appx. 233 bp for *ENV* and 120 bp for *GAG*. These small PCR probes were highly specific and stable for hybridization thus, it leads to very good amplification of the signals. By using short size of probes, we were able to visualize the first time *SIRE1 ENV* and *GAG* distribution patterns on barley chromosomes, indicating they intend to demonstrate different patterns. Additionally, it is possible to observe localization of lncRNAs on chromosomes and in the cells using direct labelled-PCR products *via* FISH techniques (Karlik *et al.* 2018).

In plant genomes, most of the TEs are amplified to thousands of copies and present as low- or moderate-number copies (Baucom *et al.* 2009). Besides increasing genome sizes, TEs can impact on genome structure and gene expression at a global scale. Moreover, deletions of the interleaving genome sequences or creations of new chromosomal rearrangements can be generated by recombination between two TEs (Weil & Wessle 1993, Hughes *et al.* 2003, Vicient & Casacuberta 2017). However, TE karyotype differences may be significant tool contributing to reproductive isolations of TEs and crop domestication, to discriminate species diversification in plants (Vicient & Casacuberta 2017). Also, the abundance and size of LTR retrotransposons in plant genomes exert interesting questions on how they affect genes and how they are regulated so that their insertions do not negatively influence the host genome (Galindo-González *et al.* 2017). Mascher *et al.* (2017) identified 3.7 Gb (80.8%) of the assembled barley genome sequence as derived from TEs, most of them were present as truncated and degenerated copies. Interestingly, only 10% of mobile elements are intact and potentially active. According to the sequencing results of Mascher *et al.* (2017), TEs presented notable variation in their insertion site preferences. The distribution of *SIRE1 ENV* and *GAG* barley were consistent with each other that they were mostly characterized close to the centromere regions (see Fig. 1 and 2). Presting *et al.* (1998) demonstrated the centromere of barley is enriched with *cereba* is a member of the *Ty3/Gypsy* class, that ~200 copies of *cereba* have been determined in each barley centromere (Hudakova *et al.* 2001, Houben & Schubert 2003). Two conserved centromere-specific repeats [Cereal Centromeric Sequence1 (CCS1) and Sau3A9] were reported, later is

revealed that they are related to *Ty3/Gypsy*-like retrotransposons. In barley, parts of the LTRs of *cereba* element and parts of integrase region of its polygene correspond to CCS1 and Sau3A9, respectively (Hudakova *et al*. 2001). Our results also indicated that presence of *SIRE1* is favoured mostly in regions close to centre locations that as we know *SIRE1* is active and belongs to the *Tyl/Copia* retrotransposon superfamily (Lin *et al*. 2005). However, *SIRE1* may be related to the centromeric repeats BCS1/CCS1 (barley cereal centromeric sequence), thus these elements may also contribute to *SIRE1* elements movements. Lin et al. (2005) reported the presence of a 102-bp tandem repeat (STR102) which was a *SIRE1* element and a *SIRE1* solo LTR in soybean. However, the flanking sequences of 3 of 10 *SIRE1* insertions were found to be repetitive, belonging to either *Ty3*/*gypsy* or other repetitive families (Laten *et al.* 1998). Moreover, these fragments have been demonstrated for maize and rice (Ananiev *et al*. 1998, Cheng *et al.* 2002) suggesting that they are common motifs of higher plants of centromeric/pericentromeric regions (Martinez-Zapater *et al.* 1986, Ananiev *et al.* 1998, Cheng *et al.* 2002, Lin et al. 2005), which is also consistent with our results. In soybean, Lin et al. (2005) also considered that *SIRE1* may preferentially get in heterochromatic and/or pericentromeric regions which may alternatively be selected against the gene-rich euchromatic regions. In barley, we also observed that *SIRE1* elements were mostly concentrated in centred regions. FISH analysis of barley *SIRE1* elements provided us to allow cursory insight into the barley genome organization.

In conclusion, we were able to observe the distinctive distributions of the *SIRE1 ENV* and *GAG* elements via FISH analysis by using labelled-PCR products as probes in barley root preparations. How these elements function to organize genome is still a mystery, however the applications of FISH analysis of TEs may have an important potential to uncover the organization of higher plant genomes.

**Acknowledgement**

The authors thank Dr. Stuart James Lucas for his kind revision.

**Author Contributions:** Execution: E.K., Material supplying: E.K., Manuscript writing: E.K., Critical revision: N.G.

**Ethics Committee Approval:** Since the article does not contain any studies with human or animal subject, its approval to the ethics committee was not required.

**Conflict of Interest:** The authors have no conflicts of interest to declare.

**Funding:** The author declared that this study has received no financial support.

## References

1. Acevedo-Garcia, J., Collins, N.C., Ahmadinejad, N., Ma, L., Houben, A., Bednarek, P., Benjdia, M., Freialdenhoven, A., Altmüller, J., Nürnberg, P., Reinhardt, R., Schulze-Lefert, P. & Panstruga, R. 2013. Fine mapping and chromosome walking towards the *Ror1* locus in barley (*Hordeum vulgare* L.). *Theoretical and Applied Genetics*, 126(12): 2969-2982. https://doi.org/10.1007/s00122-013-2186-6
2. Alipour, A., Tsuchimoto, S., Sakai, H., Ohmido, N. & Fukui, K. 2013. Structural characterization of *copia*-type retrotransposons leads to insights into the marker development in a biofuel crop, L *Jatropha curcas*. *Biotechnology for Biofuel*, 6(1): 129. https://doi.org/10.1186/1754-6834-6-129
3. Ananiev, E.V., Phillips, R.L. & Rines, H.W. 1998. Chromosome-specific molecular organization of maize (*Zea mays* L.) centromeric regions. *Proceedings of the National Academy of Sciences of the USA*, 95 (22): 13073-13078. https://doi.org/10.1073/pnas.95.22.13073
4. Baucom, R.S., Estill, J.C., Chaparro, C., Upshaw, N., Jogi, A., Deragon, J.M., Westerman, R.P., Sanmiguel, P.J. & Bennetzen, J.L. 2009. Exceptional diversity, non-random distribution, and rapid evolution of retroelements in the B73 maize genome. *PLoS Genetics*, 5(11): e1000732. https://doi.org/10.1371/journal.pgen.1000732
5. Bousios, A., Darzentas, N., Tsaftaris, A. & Pearce, S.R. 2010. Highly conserved motifs in noncoding regions of Sirevirus retrotransposons: the key for their pattern of distribution within and across plants?. *BMC Genomics*, 11: 89. https://doi.org/10.1186/1471-2164-11-89
6. Bustamante, F.O., Aliyeva-Schnorr, L., Fuchs, J., Beier, S. & Houben, A. 2017. Correlating the genetic and physical map of barley chromosome 3H revealed limitations of the FISH-based mapping of nearby single-copy probes caused by the dynamic structure of metaphase chromosomes. *Cytogenetic and Genome Research*, 152(2): 90-96. https://doi.org/10.1159/000478631
7. Cheng, Z., Dong, F., Langdon, T., Ouyang, S., Buell, C.R., Gu, M., Blattner, F.R. & Jiang, J. 2002. Functional rice centromeres are marked by a satellite repeat and a centromere-specific retrotransposon. *Plant Cell*, 14(8): 1691-1704. https://doi.org/10.1105/tpc.003079
8. Friesen N., Brandes, A. & Heslop-Harrison, J. 2001. Diversity, origin and distribution of retrotransposons in conifers. *Molecular Biology and Evolution*, 18(7): 1176-1188. https://doi.org/10.1093/oxfordjournals.molbev.a003905.
9. Galindo-González, L., Mhiri, C., Deyholos, M.K. & Grandbastien, M.A. 2017. LTR-retrotransposons in plants: engines of evolution. *Gene*, 626: 14-25. https://doi.org/10.1016/j.gene.2017.04.051
10. Gao, X., Havecker, E.R., Baranov, P.V., Atkins, J.F. & Voytas, D.F. 2003. Translational recoding signals between gag and pol in diverse LTR retrotransposons. *RNA*, 9(12): 1422-1430. https://doi.org/10.1261/rna.5105503

11. Hausmann, M. & Cremer, C. 2003. Standardization of FISH-procedures: Summary of the first discussion workshop. *Analytical Cellular Pathology*, 25(4): 201-205. https://doi.org/10.1155/2003/427509

12. Havecker, E.R., Gao, X. & Voytas, D.F. 2005. The sireviruses, a plant-specific lineage of the *Ty1/copia* retrotransposons, interact with a family of proteins related to dynein light chain. *Plant Physiology*, 139(2): 857-868. https://doi.org/10.1104/pp.105.065680

13. Houben, A. & Schubert, I. 2003. DNA and proteins of plant centromeres. *Current Opinion in Plant Biology*, 6(6): 554-560. https://doi.org/10.1016/j.pbi.2003.09.007

14. Hudakova, S., Michalek, W., Presting, G.G., Ten Hoopen, R., Dos Santos, K., Jasencakova, Z. & Schubert, I. 2001. Sequence organization of barley centromeres. *Nucleic Acids Research*, 29(24): 5029-5035. https://doi.org/10.1093/nar/29.24.5029

15. Hughes, A.L., Friedman, R., Ekollu, V. & Rose, J.R. 2003. Non-random association of transposable elements with duplicated genomic blocks in *Arabidopsis thaliana*. *Molecular Phylogenetics and Evolution*, 29(3): 410-416. https://doi.org/10.1016/S1055-7903(03)00262-8

16. Jenkins, G. & Hasterok, R. 2001. Painting whole chromosome sets in hybrids using GISH, in *Advanced Molecular Cytogenetics -a practical course manual*. Wydawnictwo Uniwersytetu Śląskiego. 35-48.

17. Jenkins, G. & Hasterok, R. 2007. BAC 'landing' on chromosomes of *Brachypodium distachyon* for comparative genome alignment. *Nature Protocols*, 2: 88-98. https://doi.org/10.1038/nprot.2006.490

18. Karlik, E., Marakli, S. & Gozukirmizi, N. 2018. Two lncRNAs expression profiles in salt stressed barley (*Hordeum vulgare* L.) roots. *Cytologia*, 83(1): 37-43. https://doi.org/10.1508/cytologia.83.37

19. Kiseleva, A.V., Kirov, I.V. & Khrustaleva, L.I. 2014. Chromosomal organization of centromeric *Ty3/gypsy* retrotransposons in *Allium cepa* L. and *Allium fistulosum* L. *Russian Journal of Genetics*, 50(6): 670-676. https://doi.org/10.1134/S102279541404005X

20. Kolano, B., Bednara, E. & Weiss-Schneeweiss, H. 2013. Isolation and characterization of reverse transcriptase fragments of LTR retrotransposons from the genome of *Chenopodium quinoa* (Amaranthaceae). *Plant Cell Reports*, 32(10): 1575-1588. https://doi.org/10.1007/s00299-013-1468-4

21. Kumar, A. & Bennetzen, J.L. 1999. Plant retrotransposons. *Annual Review of Genetics*, 33: 479-532. https://doi.org/10.1146/annurev.genet.33.1.479

22. Laten, H.M., Majumdar, A. & Gaucher, E.A. 1998. *SIRE-1*, a *copia/Ty1*-like retroelement from soybean, encodes a retroviral envelope-like protein. *Proceedings of the National Academy of Sciences of the USA*, 95(12): 6897-6902. https://doi.org/10.1073/pnas.95.12.6897

23. Lee, S.I., Park, K.C., Son, J.H., Hwang, Y.J., Lim, K.B., Song, Y.S., Kim, J.H. & Kim, N.S. 2013. Isolation and characterization of novel *Ty1-copia*-like retrotransposons from lily. *Genome*, 56(9): 495-503. https://doi.org/10.1139/gen-2013-0088

24. Li, Y., Zuo, S., Zhang, Z., Li, Z., Han, J., Chu, Z., Hasterok, R. & Wang, K. 2018. Centromeric DNA characterization in the model grass *Brachypodium distachyon* provides insights on the evolution of the genus. *The Plant Journal*, 93(6): 1088-1101. https://doi.org/10.1111/tpj.13832

25. Lin, J.Y., Jacobus, B.H., Sanmiguel, P., Walling, J.G., Yuan, Y., Shoemaker, R.C., Young, N.D. & Jackson, S.A. 2005. Pericentromeric regions of soybean (*Glycine max* L. *Merr*.) chromosomes consist of retroelements and tandemly repeated DNA and are structurally and evolutionarily labile. *Genetics*, 170(3): 1221-1230. https://doi.org/10.1534/genetics.105.041616

26. Llorens, C., Munoz-Pomer, A., Bernard, L., Botella, H. & Moya, A. 2009. Network dynamics of eukaryotic LTR retroelements beyond phylogenetic trees. *Biology Direct*, 4(41). https://doi.org/10.1186/1745-6150-4-41

27. Mafra, I., Silva, S.A., Moreira, E.J.M.O., Ferreira Da Silva, C.S., Beatriz, M. & Oliveira, P.P. 2008. Comparative study of DNA extraction methods for soybean derived food products. *Food Control*, 19(12): 1183-1190. https://doi.org/10.1016/j.foodcont.2008.01.004

28. Martinez-Zapater, J.M., Estelle, M.A. & Somerville, C.R. 1986. A highly repeated DNA sequence in *Arabidopsis thaliana*. *Molecular and General Genetics*, 204(3): 417-423. https://doi.org/10.1007/BF00331018

29. Mascher, M., Gundlach, H., Himmelbach, A., Beier, S., Twardziok, S. O., Wicker, T., Radchuk, V., Dockter, C., Hedley, P. E., Russell, J., Bayer, M., Ramsay, L., Liu, H., Haberer, G., Zhang, X. Q., Zhang, Q., Barrero, R. A., Li, L., Taudien, S., Groth, M., Felder, M., Hastie, A., Šimková, H., Staňková, H., Vrána, J., Chan, S., Muñoz-Amatriaín, M., Ounit, R., Wanamaker, S., Bolser, D., Colmsee, C., Schmutzer, T., Aliyeva-Schnorr, L., Grasso, S., Tanskanen, J., Chailyan, A., Sampath, D., Heavens, D., Clissold, L., Cao, S., Chapman, B., Dai, F., Han, Y., Li, H., Li, X., Lin, C., McCooke, J. K., Tan, C., Wang, P., Wang, S., Yin, S., Zhou, G., Poland, J. A., Bellgard, M. I., Borisjuk, L., Houben, A., Doležel, J., Ayling, S., Lonardi, S., Kersey, P., Langridge, P., Muehlbauer, G. J., Clark, M. D., Caccamo, M., Schulman, A. H., Mayer, K. F. X., Platzer, M., Close, T. J., Scholz, U., Hansson, M., Zhang, G., Braumann, I., Spannagl, M., Li, C., Waugh, R. and Stein, N. 2017. A chromosome conformation capture ordered sequence of the barley genome. *Nature*, 26: 427-433. https://doi.org/10.1038/nature22043

30. Mccarthy, E.M., Liu, J., Lizhi, G. & Mcdonald, J.F. 2002. Long terminal repeat retrotransposons of *Oryza sativa*. *Genome Biology*, 3(10): 1-11. https://doi.org/10.1186/gb-2002-3-10-research0053

31. Pearce, S.R., Pich, U., Harrison, G., Flavell, A.J., Heslop-Harrison, J.S., Schubert, I. & Kumar, A. 1996. The *Ty1-copia* group retrotransposons of *Allium cepa* are distributed throughout the chromosomes but are enriched in the terminal heterochromatin. *Chromosome Research*, 4(5): 357–364. https://doi.org/10.1007/BF02257271

32. Peterson-Burch, B.D. & Voytas, D.F. 2002. Genes of the Pseudoviridae (*Ty1/copia* retrotransposons). *Molecular Biology and Evolution*, 19(11): 1832-1845. https://doi.org/10.1093/oxfordjournals.molbev.a004008

33. Presting, G.G., Malysheva, L., Fuchs, J. & Schubert, I. 1998. A *Ty3/gypsy* retrotransposon-like sequence localizes to the centromeric regions of cereal chromosomes. *The Plant Journal*, 16(6): 721–728. https://doi.org/10.1046/j.1365-313x.1998.00341.x

34. Salvo-Garrido, H.G., Travella, S., Schwarzacher, T., Harwood, W.A. & Snape, J.W. 2001. An efficient method for the physical mapping of transgenes in barley using *in situ* hybridization. *Genome*, 44(1): 104-110. https://doi.org/10.1139/gen-44-1-104

35. Sandmeyer, S.B., Aye, M. & Menees, T. 2002. Ty3, a position-specific, gypsy-like element in *Saccharomyces cerevisiae*. *In: Mobile DNA II*, Craig, N.L., Craigie, R., Gellert, M., Lambowitz, A.M. (eds.). Washington DC: ASM Press. 663-683.

36. Schnable, P.S., Ware, D., Fulton, R. S., Stein, J. C., Wei, F., Pasternak, S., Liang, C., Zhang, J., Fulton, L., Graves, T.A., Minx, P., Reily, A.D., Courtney, L., Kruchowski, S. S., Tomlinson, C., Strong, C., Delehaunty, K., Fronick, C., Courtney, B., Rock, S. M., Belter, E., Du, F., Kim, K., Abbott, R. M., Cotton, M., Levy, A., Marchetto, P., Ochoa, K., Jackson, S. M., Gillam, B., Chen, W., Yan, L., Higginbotham, J., Cardenas, M., Waligorski, J., Applebaum, E., Phelps, L., Falcone, J., Kanchi, K., Thane, T., Scimone, A., Thane, N., Henke, J., Wang, T., Ruppert, J., Shah, N., Rotter, K., Hodges, J., Ingenthron, E., Cordes, M., Kohlberg, S., Sgro, J., Delgado, B., Mead, K., Chinwalla, A., Leonard, S., Crouse, K., Collura, K., Kudrna, D., Currie, J., He, R., Angelova, A., Rajasekar, S., Mueller, T., Lomeli, R., Scara, G., Ko, A., Delaney, K., Wissotski, M., Lopez, G., Campos, D., Braidotti, M., Ashley, E., Golser, W., Kim, H., Lee, S., Lin, J., Dujmic, Z., Kim, W., Talag, J., Zuccolo, A., Fan, C., Sebastian, A., Kramer, M., Spiegel, L., Nascimento, L., Zutavern, T., Miller, B., Ambroise, C., Muller, S., Spooner, W., Narechania, A., Ren, L., Wei, S., Kumari, S., Faga, B., Levy, M. J., McMahan, L., Van Buren, P. & Vaughn, M.W. (2009). The B73 maize genome: Complexity, diversity, and dynamics. *Science*, 326(5956), 1112-1115. https://doi.org/10.1126/science.1178534

37. Schulman, A.H. & Wicker, T. 2013. A field guide to transposable elements, *In: Plant Transposons and Genome Dynamics in Evolution*, Fedoroff, N.V. (ed.). Oxford: Wiley Blackwell. 15-40.

38. Shams, I. & Raskina, O. 2018. Intraspecific and intraorganismal copy number dynamics of retrotransposons and tandem repeat in *Aegilops speltoides* Tausch (Poaceae, Triticeae). *Protoplasma*, 255(4): 1023-1038. https://doi.org/10.1007/s00709-018-1212-6

39. The *Arabidopsis* Genome Initiative. 2000. Analysis of the genome sequence of the flowering plant *Arabidopsis thaliana*. *Nature*, 408: 796-815. https://doi.org/10.1038/35048692

40. Vicient, C.M., Kalendar, R., Anamthawat-Jansson, K. & Schulman, A.H. 1999. Structure, functionality, and evolution of the *BARE-1* retrotransposon of barley. *Genetica*, 107(1-3): 53-63. https://doi.org/10.1023/A:1003929913398

41. Vicient, C.M. & Casacuberta, J.M. 2017. Impact of transposable elements on polyploid plant genomes. *Annals of Botany*, 120(2): 195-207. https://doi.org/10.1093/aob/mcx078

42. Voytas, D.F. & Boeke, J.D. 2002. Ty1 and Ty5 of *Saccharomyces cereviceae*, *In: Mobile DNA II*, Craig, N.L., Craigie, R., Gellert, M. & Lambowitz, A.M. (eds.). Washington DC: ASM Press. 631-662.

43. Wicker, T., Sabot, F., Hua-Van, A., Bennetzen, J., Capy, P., Chalhoub, B., Flavell, A.J., Leroy, P., Morgante, M., Panaud, O., Paux, E., Sanmiguel, P. & Schulman, A.H. 2007. A unified classification system for eukaryotic transposable elements. *Nature Reviews Genetics*, 8(12): 973-982. https://doi.org/10.1038/nrg2165

44. Weil, C.F. & Wessler, S.R. 1993. Molecular evidence that chromosome breakage by *Ds* elements is caused by aberrant transposition. *Plant Cell*, 5(5): 515-522. https://doi.org/10.1105/tpc.5.5.515

*http://dergipark.org.tr/trkjnat*
*Trakya University Journal of Natural Sciences, 22(1): 17-22, 2021*
*ISSN 2147-0294, e-ISSN 2528-9691*
*DOI: 10.23902/trkjnat.772976*

**Research Article**

# THE EFFECT OF EXTRACTION METHODS ON ANTIOXIDANT AND ENZYME INHIBITORY ACTIVITIES AND PHYTOCHEMICAL COMPONENTS OF *Galium aparine* L.

Merve BAT ÖZMATARA

Gebze Technical University, Faculty of Science, Kocaeli, TURKEY

**Cite this article as:**

Bat Özmatara M. 2021. The Effect of Extraction Methods on Antioxidant and Enzyme Inhibitory Activities and Phytochemical Components of *Galium aparine* L. *Trakya Univ J Nat Sci*, 22(1): 17-22, DOI: 10.23902/trkjnat.772976

Received: 24 July 2020, Accepted: 23 October 2020, Online First: 16 November 2020, Published: 15 April 2021

***Edited by:***
*Cem Vural*

***Corresponding Author:***
*Merve Bat Özmatara*
*mervebatt@gmail.com*

***ORCID ID:***
*orcid.org/0000-0002-6912-8825*

***Key words:***
*Galium aparine*
*Antioxidant activity*
*α-amylase inhibition*
*Phenolic compounds*

**Abstract:** *Galium aparine* L. is an annual herbaceous plant of Rubiaceae family. It has therapeutic effects as contains various bioactive components. The aim of this study was to investigate the effects of extraction methods on the amount of phytochemical components of *G. aparine*. The change in the amount of bioactive components directly affects antioxidant and antidiabetic activity. In this study, three different extraction methods, soxhlet, maceration and ultrasonic, using methanol as solvent, were used and the extractions were performed using of *G. aparine*. The phytochemical components of the extracts was analyzed both qualitatively and quantitatively. The soxhlet extraction showed that it contained the highest amount of flavonoids, tannins and phenolic compounds, compared to the other two extraction methods. Obtained soxhlet extraction contained 131.827 g quercetin acid equivalent (QE) flavonoids, 825.4 g as gallic acid equivalent (GAE) phenolic compunds, 366.998 mg as tallic acid (TAE) of tannins. Due to the high amount of phenolic compounds, flavonoids and tannins it contains, soxhlet extract has been shown to have α-amylase inhibition effect (46%) and much more radical scavenging activity than other extracts.

**Özet:** *Galium aparine* L. (yoğurt otu), Rubiaceae familyasına ait yıllık otsu bir bitkidir. Çeşitli biyoaktif bileşenler içerdiğinden terapötik etkilere sahiptir. Bu çalışmanın amacı ekstraksiyon yöntemlerinin bitkinin biyoaktif bileşen miktarına etkisini incelemektir. Biyoaktif bileşenlerin miktarındaki değişiklik doğrudan antioksidan ve antidiyabetik aktiviteyi etkiler. Bu çalışmada yoğurt otu kullanılarak çözücünün metanol olduğu soxhlet, maserasyon ve ultrasonik olmak üzere 3 farklı ekstraksiyon yöntemi kullanılmıştır. Ekstraktların fitokimyasal bileşeni hem kalitatif hem de kantitatif olarak analiz edilmiştir. Ekstraktlarda en fazla flavonoid, tanen ve fenolik bileşik içeren ekstraktın, soxhlet ekstraksiyonu sonucu elde edilen ekstrakt olduğu bulundu. Soxhlet ekstraktı, 131.827 kuersetin asit eşdeğeri (QE)/g, flavonoidler, 825.4 gallik asit eşdeğeri (GAE)/g, fenolik bileşikler 366.998 mg tallik asit eşdeğeri (TAE)/g tanenler içerir. İçerdiği fenolik bileşik, flavonoidler ve tanenlerle, soxhlet ekstraktının α- amilaz inhibisyon etkisine (%46) ve diğer ekstraktlardan çok daha fazla radikal temizleme etkinliğine sahip olduğu gösterilmiştir.

## Introduction

Free radicals are constantly produced by biochemical processes such as respiration, which represent an important part of aerobic life and our metabolism. Human body has routine antioxidant mechanisms to passifiy many free radicals, including produced superoxide ion, hydrogen peroxide and hydroxyl radicals, and protect the body against their harmful effects. However, under severe oxidative stress conditions where antioxidant defense is insufficient, biochemical changes caused by reactive oxygen species (ROS) are known to cause various diseases such as cancer, atherosclerosis, arthritis, inflammation and neurodegeneration (Shirwaikar *et al.* 2006). Many researches have been performed to investigate how to reduce or prevent oxidative diseases. It is focused on reducing the levels of oxidative stress in the body by increasing the amount of natural antioxidants with high consumption of vegetables and fruits. Natural antioxidants, especially polyphenolic compounds are safe and have antiradical activities. For this reason, extensive studies have been conducted recently to identify plants with antioxidant properties (Pohl & Lin, 2018, Kamble & Gacche, 2019).

There are approximately 350.000 plant species in the world and 80.000 of them are edible. However, it is estimated that about 150 species are bred for human consumption or as a feed source for animals (Füleky, 2009). It is known that foods rich in polyphenols increase the body's antioxidant capacity. More than 8,000 such

compounds identified from different plant species are considered to be rich sources of secondary metabolites (Pandey & Rizvi, 2009). However, the risk of getting many diseases such as cancer and diabetes decreases when a diet rich in plant polyphenols is consumed (Pandey & Rizvi, 2009, Young & Woodside, 2001).The fact that polyphenols have single oxygen pacifiers, metal chelators, hydrogen donors and ferric hemoglobin act as reducers according to their redox properties. Due to its redox properties, polyphenols act as single reducers of oxygen, metal chelators, hydrogen donors and ferric hemoglobin and show an antiradical activity in the body (Rice-Evans *et al.* 1995, Rice-Evans *et al.* 1997, Prior *et al.* 2005, López *et al.* 2007, Cíz *et al.* 2008,Gebick & Banasiak 2009). Natural products of plant origin such as flavonoids, terpenoids, steroids also have different pharmacological properties, including antioxidant and antitumor activity (Aslantürk *et al.* 2017).

It is known that the α-amylase enzyme is effective in controlling blood sugar level in treatment of diabetes. There are many studies investigating the potential of plant extracst to be used instead of enzyme inhibitors taken as medicines in treatment of diabetes (Soud *et al.* 2004, Tlilia & Sarikurkcu, 2020).

*Galium aparine L*. is a herbaceous perennial plant belonging to the Rubiaceae family, widely grown in Europe and Asia ( Senio *et al.* 2018). It is a natural antioxidant containing anthraquinones, iridoids, alkanes, flavonoids, tannins, polyphenolic acids and it is used in treatment of various diseases such as diabetes, cancer and hypertension (Saeed & Javed 2007).

Recently, researchers have been trying to isolate antioxidants and phytochemical constituents from plants as they act an alternative therapeutic (Airaodion *et al.* 2019). However, the effect of extraction method on apha amylase inhibition, antioxidant activity and phenolic compound amount in *G. aparine* has not been reported. The main aim of this study was to evaluate the effect of extraction method on enzyme inhibition, antioxidant activity and phytochemical compound amount in *G. aparine.*

## Materials and Methods

*Instrumentation*

Extraction of *G. aparine* was done with an ultrasonic bath (Çalışkan, Ankara, Turkey) with a constant frequency of 40 kHz and a power setting of 60 W. The antioxidant activity, enzyme inhibitory activity and phytochemical components of *G. aparine* extracts were measured using a UV-Vis spectrophotometer (SpectraMax Plus 384 Microplate Reader, California, USA). A vortex mixer, (IKA MS3,SIEHE-IKA from Germany) was used to for mix samples.

*Materials and Chemicals*

*Galium aparine* was bought from a herbalist in İstanbul, Turkey. 1,1-diphenyl-2-picryl-hydrazyl (DPPH), [2,2'- azinobis- (3-ethylbenzothiazoline-6-sulfonic acid)] (ABTS), potassium persulfate ($K_2S_2O_8$), iron (III) chloride ($FeCl_3$), sodium carbonate ($Na_2CO_3$), citric acid monohdyrate were purchased from Sigma (USA). N,N-dimethyl-p-phenylenediamine dihydrochloride (DMPD), ethanol, methanol, sulphuric acid, chloroform, acetic acid and sodium acetate were purchased from Merck. All solvents were of analytical grade.

*Extraction*

Soxhlet exctraction, ultrasound assisted extraction and maceration were used as extraction methods. For each method, 5 grams of plant samples were weighed and used. The soxhlet extraction was performed with 150 ml of methanol, the ultrasound assisted extraction was performed in 150 ml of methanol for 30 minutes and for maceration method, 5 grams sample was kept in methanol for 1 day. The filtration for soxhlet extraction was carried out and the sample was preserved at 4°C.

*Determination of antioxidant activity*

DPPH free radical scavenging activity

Assay for DPPH free radical scavenging activity is often used to evaluate the antioxidant capacity of compounds. The Brand-Williams method was used to test whether sample will bleach the stable DPPH radical. Thus, the DPPH radical scavenging activity was measured (Brand-Williams *et al.* 1995). 0.75 mL of plant extract was added over 1.50 mL of DPPH solution prepared in ethanol (0.05 mM). The mixture was kept at room temperature for 30 minutes. Then, the absorbance at 517 nm was measured in the UV-Vis spectrophotometer. The scavenging activity of DPPH radical was calculated using the following equation (Cioancă et al. 2015):

$$DPPHscavenging\ (\%) = \left[\frac{\text{Acontrol} - \text{Asample}}{\text{Acontrol}}\right] x100\ (Eq.1)$$

where $A_{control}$ shows the absorbance of the control (DPPH solution without sample) and $A_{sample}$ shows the absorbance of the test sample.

*ABTS radical scavenging activity*

This method, developed by Arnao *et al. (*2001) is based on the reduction of radical and color loss by adding antioxidants on the $ABTS^{\bullet+}$ radical cation formed by $K_2S_2O_8$ oxidation of ABTS [2,2'-azinobis-(3-ethylbenzothiazoline-6-sulfonic acid)]. Blue/green colored $ABTS^{\bullet+}$ radical gives strong absorption in 600-750 nm (Arnao *et al.* 2001).

7.4 mM ABTS solution and 2.6 mM potassium persulfate solution were mixed equally and kept in the dark for 12 hours at room temperature. 1 mL of the ABTS radical solution was diluted with an absorbance of 1.1 ± 0.02 at 734 nm in the spectrophotometer by adding about 60 mL of methanol. 150 µL of sample solutions and 2850 µL of $ABTS^{\bullet+}$ radical solution were left in dark for 2 hours for incubation. The control solution was prepared using distilled water instead of the sample. The absorbance at 734 nm was measured in the spectrophotometer. In the calculations, ABTS% radical scavenging effect was found with the following equation (Cioancă et al. 2015).

$$ABTS \bullet + scavenging(\%) = \left[\frac{\text{Acontrol} - \text{Asample}}{\text{Acontrol}}\right] x100 (Eq. 2)$$

where $A_{control}$ shows the absorbance of the control (ABTS solution without sample) and $A_{sample}$ shows the absorbance of the test sample.

*DMPD radical scavenging activity*

The method developed by Fogliano *et al.* (1999) was applied for this antioxidant capacity test. DMPD turns into cation radical form ($DMPD^{\bullet+}$) in acidic pH or in the presence of oxidant. After 100 mM DMPD solution was prepared, radical was formed by adding 100 mL of 0.1 M acetate buffer (pH 5.3) and 0.2 mL of 0.05 M $FeCl_3$ onto 1 mL of this solution. Next, the sample solution and the control solution prepared by replacing the sample with distilled water were added. After 10 minutes, the absorbance at 505 nm was measured on spectrophotometer. $DMPD^{\bullet+}$ radical scavenging activity was calculated according to the equation below (Cioancă et al. 2015).

$$DMPD \bullet + scavenging\ (\%) = \left[\frac{\text{Acontrol} - \text{Asample}}{\text{Acontrol}}\right] x100\ (Eq. 3)$$

where $A_{control}$ shows the absorbance of the control (ABTS solution without sample) and $A_{sample}$ shows the absorbance of the test sample.

*Quantitative phytochemical analysis*

Determination of total flavonoid content

Total flavonoid content was determined using the colorimetric method (Zhishen *et al.* 1999). 0.25 mL of standard quercetin (20-200 mg/mL) or extract solution (1 mg/mL) was taken and mixed with 1.25 mL distilled water. 75 µL of 5% (m/v) sodium nitrite and 150 µL of 10% (m/v) aluminum chloride solution were added. It was waited for 5 minutes before adding 0.5 mL of 1M sodium hydroxide solution. The mixture was completed to 2.5 mL with distilled water and the absorbance at 510 nm was measured in the spectrophotometer. The results were expressed as quercetin mg equivalent for 1 gram extract.

*Determination of total phenolic compounds*

The method developed by Slinkard-Singleton (1977) was used for total phenolic compound evaluation. After adding 45 mL distilled water, 1 mL Folin-Ciocalteau reagent to 1 mL sample solutions at a concentration of 1000 µg/mL, the mixture was thoroughly mixed with a shaking machine. After standing for 3 minutes in this mixture, 3 mL of 2% (w/v) $Na_2CO_3$ was added and incubated for 2 hours on the shaking machine. After incubation, the absorbances of the mixtures at 760 nm were measured. Distilled water was used instead of extract as blind and gallic acid was used as standard. Total phenolic substance content is expressed as the equivalent of the standard used per µg in 1 gram sample.

*Determination of total tannis content*

The total tannin content was determined by the method of Schanderl (1970). 1 mL of the plant extract mixed with 0.5 mL Folin's phenol reagent and 5 mL of 35% $Na_2CO_3$ was added. The mixture was allowed to stand for 5 min at room temperature. The blue color produced was read at 640 nm using UV/visible spectrophotometer. The tannin content was calculated by calibration curve of tannic acid and the results were expressed as tannic acid equivalent (mg/g).

*Qualitative phytochemical analysis*

Different methods have been used to qualitatively identify the phytochemical components of methanol extracts obtained by different extraction techniques (Harborne 1973, Trease & Evans 1989, Sofowora 1993, Odebiyi & Sofowora 1978, Roopashree 2008).

*Test for tannins*

0.5 ml extract and 20 ml of distilled water were boiled in a tube. 0.1% ferric chloride ($FeCl_3$) was added after filtering. Appearance of brownish green coloration showed the presence of tannins.

*Test for terpenoids*

0.5 ml extract and 2 ml of chloroform were mixed and sulphuric acid was added. Formation of red brown coloration showed the presence of terpenoids.

*Test for phenols*

1 ml extract and 2 ml of distilled water were mixed and few drops of 10% $FeCl_3$ was added. Blue colour showed the presence of phenols.

*Test for quinones*

1 ml extract and 1 ml of concentrated sulphuric acid were mixed. Formation of red colour showed the quinones.

*Test for steroids*

0.5 ml extract, 2 ml chloroform and 1 ml of sulphuric acid were mixed. Formation of reddish brown showed the presence of steroids.

*Enzyme inhibitory activity*

The extracts were analyzed for their α-amylase inhibitory activities using the method reported by Zengin *et al*. (2015). 25 µL of sample extract was mixed with 50 µL of alpha amylase in phosphate buffer (pH 6.9 containing 6 mM sodium chloride). After 10 min at 37°C, 50 µL of starch solution (0.05%) was added to start the reaction. After 10 min of incubation at 37°C, the reaction was stopped using 25 µL of HCl (1 M) and 100 µL of iodine- potassium iodide solution was added. Acarbose, a known α-amylase inhibitor was used as a standard drug. The absorbance was measured at 630 nm. The α-amylase inhibitory activity was calculated by using following equation (Cioancă et al. 2015):

$$Percantage\ of\ inhibition(\%) = \left[\frac{\text{Acontrol} - \text{Asample}}{\text{Acontrol}}\right] x100 (Eq. 4)$$

where $A_{control}$ shows the absorbance of the control (ABTS solution without sample) and $A_{sample}$ shows the absorbance of the test sample.

## Results

*Antioxidant activity of Galium aparine*

Results of the in vitro antioxidant activities using three different assays (DPPH radical scavenging, ABTS radical scavenging, DMPD radical scavenging) were expressed as percent inhibiton. Among the extracts obtained as a result of soxhlet, ultrasonic and maceration extraction methods, the soxhlet extract showed the highest radical scavenging activity and the extract obtained by maceration showed the lowest antioxidant activity. Results of DPPH, ABTS and DMPD scavenging activities are shown in Fig. 1.

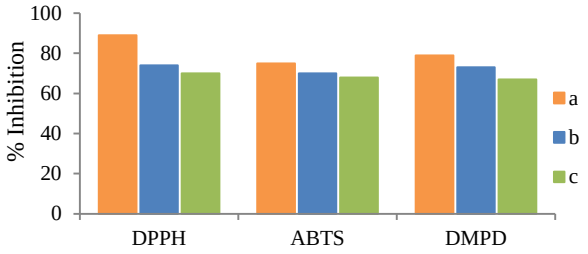


**Fig. 1.** DPPH, ABTS, DMPD radical scavenging activities of soxhlet (a), ultrasonic (b) and maceration (c) extracts.

In the DPPH test, the ability of *G. aparine* to act as a donor for hydrogen atoms or electrons to reduce DPPH to DPPH-H was spectrophotometrically measured, and the radical scavenging activity of the soxhlet extract was found to be greater than that of other extracts.

Neelam & Khan (2012) reported that methanol is the best solvent for cationic radical activity like DPPH. The methanol extract showed greater activity than the butylated hydroxy anisole used as standard. Studies in the literature support that when methanol is used, the radical scavenging activity increases.

In the ABTS test, the reaction between ABTS and potassium persulfate forms the ABTS radical cation ($ABTS^{+}$) and a blue green color is observed. When the antioxidant is present, the radical reverts to a colorless state. In a study conducted by Bokhari *et al.* (2013), it was shown that *G. aparine* has ABTS radical scavenging activity.

DMPD radical cation ($DMPD^{+}$) is generated through a reaction between DMPD and potassium persulfate and is subsequently reduced in the presence of hydrogen-donating antioxidants. Among the extracts, soxhlet was found to have the highest DMPD scavenging activity with 80%.

*Qualitative phytochemical screening*

The phytochemical analysis of the extracts obtained using different extraction techniques is shown in Table 1. Phytochemical analysis showed the presence of tannins, phenolic compounds, steroids, terpenoids and quinones in the plant extract. It is clear from the results that the tannins reached to high rates by soxhlet extraction, were at low rates by maceration and moderate concentration by ultrasonic method (Table 1). Soxhlet extract contains more terpenoid and phenolic compounds compared to other extracts. It was observed that quinones could not be obtained by maceration extraction. Steroids were represented with higher amounts in soxhlet extraction method compared with the other two methods. General results showed that soxhlet is the best extraction method in this experiment of phytochemicals.

**Table 1.** Qualitative phytochemical screening.

| Chemical Constituents | Soxhlet Extract | Ultrasonic Extract | Maceration Extract |
|---|---|---|---|
| Tannins | +++ | ++ | + |
| Terpenoids | +++ | + | ++ |
| Phenols | +++ | + | + |
| Quinones | ++ | + | - |
| Steroids | ++ | + | + |

+ = low concentration, ++ = moderate concentration, +++ = high concentration, - = absent.

*Quantitative phytochemical screening*

Table 2 summarizes the result of various quantitative phytochemical analysis of different extracts. The level of flavonoid content was found higher in soxhlet extract [131.827 mg quercetin acid equivalent (QE)/g) and lower in maceration extract (32.47 QE/g)]. When total phenolic compound amounts were measured, soxhlet extract was found to have the highest amount of phenolic compound with 825.4 µg gallic acid equivalent (GAE)/g. Maceration extract and ultrasonic extract have 186.7 µg GAE/g, 145.8 µg GAE/g phenolic compound, respectively. The level of tannin was found higher in soxhlet extract [366.998 mg tallic acid equivalent (TAE)/g) and lower in maceration extract (293.27 TAE/g)].

**Table 2.** Quantitative phytochemical screening.

| | Total Flavonoid Content (mg QE/g) | Total Phenolic Compound (µg GAE/ g) | Total Tannin Content (mg TAE/g) |
|---|---|---|---|
| **Soxhlet Extract** | 131.827± 0.008 | 825.4 ± 0.015 | 366.998 ± 0.004 |
| **Ultrasonic Extract** | 30.8 ± 0.009 | 145.8 ± 0.012 | 318.7 ± 0.0010 |
| **Maceration Extract** | 32.47 ± 0.010 | 186.7 ± 0.011 | 293.27 ± 0.013 |

Each value is the average of three analyses ± standard deviation.

In the study of Lakic *et al*. (2010), obtained total phenolic compound amounts of extracts by maceration method using methanol (2.44-4.65 mg and 4.57-5.16 mg)GAE / g dry extract) and flavonoid amount (6.38-13.40 µg and15.56-17.96 µg QE / g dry extract). When compared with other similar studies, soxhlet extraction and the use of 100% methanol appeared to be the most effective extraction methods for the total amount of phenolic compounds and flavonoids.

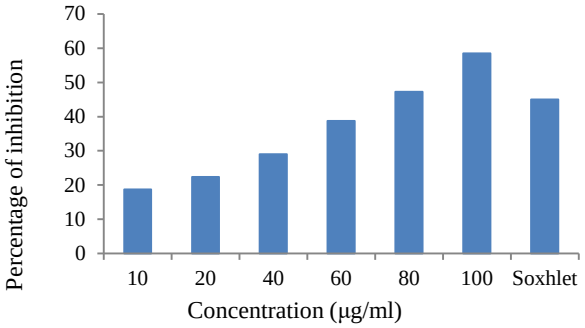


**Fig. 2.** α-amylase inhibitory activity of acarbose and soxhlet extract.

*Inhibitory activity of α-amylase*

Acarbose (at a concentrations 100 µg/mL) showed 58.45% inhibitory effects on the α-amylase activity. The inhibition effect of acarbose used as standards in different concentrations is given in Fig. 2. Soxhlet extract showed an effect close to the inhibition of 80 µg/ml of acarbose with 45% inhibition. Soxhlet extract was the only extract showing α- amylase inhibition. The anti-diabetic potency was defined by the inhibition of α-amylase activity. Therefore, it is only soxhlet extract that has anti-diabetic properties among the extracts.

## Conclusion

It has been shown that phytochemical compounds of *Galium aparine* has antioxidant and antidiabetic properties. Several in vitro studies have reported the antioxidant potential of *G. aparine* (Lindsey *et al.* 2002, Bokhari *et al*. 2013). Extracts from the seeds of the *G. aparine* also have therapeutic effects due to their phytochemical activity (Farcas *et al*. 2018). Since the extraction method used changes the phytochemical component of the extract, it also changes the antioxidant or antidiabetic activity. According to the results obtained, the most effective method for antioxidant and antidiabetic effect is the soxhlet extraction.

**Ethics Committee Approval:** Since the article does not contain any studies with human or animal subject, its approval to the ethics committee was not required.

**Conflict of Interest:** The authors have no conflicts of interest to declare.

**Funding:** The author declared that this study has received no financial support.

## References

1. Airaodion, A., Ogbuagu, E., Ekenjoku, J., Ogbuagu, U. & Airaodion, E. 2019. Therapeutic effect of methanolic extract of *Telfaira occidentalis* leaves against acute ethanol-induced oxidative stres in wistar rats. *International Journal of Bio-Science and Bio-Technology*,11(7): 179-189.
2. Arnao, M., Cano, A., Alcolea, J. & Acosta, M. 2001. Estimation of Free Radical-quenching activity of leaf pigment extracts. *Phytochemical Analysis*, 12(2): 138-143.
3. Aslantürk, Ö.S., Çelik, T.A., Karabey, B. & Karabey, F. 2017. Active Phytochemical Detecting, Antioxidant, Cytotoxic, Apoptotic Activities of Ethyl Acetate and Methanol Extracts of *Galium aparine* L. *British Journal of Pharmaceutical Research*, 15: 1-16.
4. Brand-Williams, W., Cuvelier, ME. & Berset, C. 1995. Use of a free radical method to evaluate antioxidant activity. *Lebensmittel-Wissenschaft & Technologie*, 28: 25-30.
5. Bokhari, J., Khan, M.R., Shabbir, M., Rashid, U., Jan, S & Zai, J.A. 2013. Evaluation of diverse antioxidant activities of *Galium aparine*. *Spectrochim Acta A:Molecular Biomolecular Spectrosopy*, 102: 24-29.
6. Cioancă, O., Mircea, C., Hritcu, L., Trifan, A., Mihasan, M., Aprotosoaie, A.C., Robu S., Gille, E. & Hancianu, M. 2015. In vitro-in vivo correlation of the antioxidant capacity of Salviae aetheroleum essential oil. *Farmacia*, 63(1): 34-39.
7. Cíz, M., Pavelková, M., Gallová, L., Králová, J., Kubala, L. & Lojek, A. 2008. The influence of wine polyphenols on reactive oxygen and nitrogen species production by murine macrophages RAW 264.7. *Physiological Research*, 57: 393-402.
8. Farcas, A.D., Mot, A.C., Zagrean-Tuza, C., Toma, V., Cimpoiu, C., Hosu, A., Parvu, M., Roman, I & Silaghi-Dumitrescu, R. 2018. Chemo-mapping and biochemical modulatory and antioxidant/prooxidant effect of *Galium verum* extract during acute restraint and dark stress in female rats. *PLoS One*, 13: 7.
9. Fogliano, V., Verde, V., Randazzo, G. & Ritieni, A. 1999. Method for measuring antioxidant capacity of wines. *Journal of Agricultural and Food Chemistry*, 47: 1035-1040.
10. Füleky, G. 2009. *Cultivated Plants, Primarily As Food Sources*. Eolss Publishers Co Ltd, 372 pp.
11. Gebick, L. & Banasiak, E. 2009. Role of medicinal in oxidative stres. *Acta Biochimica Polonica*, 56: 509-513.
12. Harborne, J.B. 1973. *Phytochemical methods*, London. Chapman and Hall, Ltd., 188 pp.
13. Kamble, S. & Gacche, R. 2019. Evaluation of anti-breast cancer, anti-angiogenic and antioxidant properties of selected medicinal plants. *European Journal of Integrative Medicine*, 25: 13-19.
14. Lakić, N., Dukić, N., Isak, J. & Božin, B. 2010. Antioxidant properties of *Galium verum* L. (Rubiaceae) extracts. *Central European Journal of Biology*, 5(3): 331-337.
15. Lindsey, K.L., Motsei, M.L & Jäger, A.K. 2002. Screening of South African food plants for antioxidant activity. *Journal of Food Sciences*, 67: 2129-2131.
16. López, D., Pavelkova, M., Gallová, L., Simonetti, P., Gardana, C., Lojek, C., Loaiza, R. & Mitjavila, M. 2007. Dealcoholized red and white wines decrease oxidative stres associated with inflammation in rats. *British Journal of Nutrition*, 98: 611-619.
17. Neelam, S. & Khan, Z. 2012. Antioxidant activity of *Galium aparine L.*from Punjab, Pakistan. *Pakistan Journal of Botany*, 44: 251-253.

18. Odebiyi, O.O. & Sofowora, F.A. 1978. Plytochemical Screening of Medical Plants IL. *Iloyidia*, 4(3): 234-246.

19. Pandey, K.B. & Rizvi, S.I. 2009. Plant polyphenols as dietary antioxidants in human health and disease. *Oxidative Medicine and Cellular Longevity*, 2: 270-278.

20. Pohl, F. & Lin, P. 2018. The potential use of plant natural products and plant extracts with antioxidant properties for the prevention/ treatment of neurodegenerative diseases: in vitro, in vivo and clinical trials. *Molecules*, 23(12): 3283.

21. Prior, R.L., Wu, X. & Schaich, K. 2005. Standardized methods for the determination of antioxidant capacity and phenolics in food and dietary supplements. *Journal of Agriculture and Food Chemistry*, 53: 4290-4302.

22. Rice-Evans, C.A., Miller, N.J., Bolwell, P.G., Bramley, P.M. & Pridham, J.B. 1995. The relative antioxidant activities of plant derived polyphenolic flavonoids. *Free Radical Research*, 22: 375-383.

23. Rice-Evans, C.A., Miller, N.J. & Paganga, G. 1997. Antioxidant properties of phenolic compounds. *Trends in Plant Science*, 2: 152-159.

24. Roopashree, T.S., Dang, R., Rani, R.H.S. & Narendra. C. 2008. Antibacterial activity of antipsoriatic herbs: *Cassia tora*, *Momordica charantia* and *Calendula officinalis*. *International Journal of Applied Research in Natural Products*, 1: 20-28.

25. Saeed, S.A. & Javed, S. 2007. Exploring the economic value of underutilized plant species in Ayubia national park. *Pakistan Journal of Botany*, 39: 1435-1442.

26. Schanderl, S.H. 1970. *Methods in food analysis*. New York: Academic Press, 709 pp.

27. Senio, S., Pereira, C., Vaz, J., Sokovic, M., Barros, L. & Ferreira, I. 2018. Dehydration process influences the phenolic profile, antioxidant and antimicrobial properties of *Galium aparine L. Industrial Crops and Products*, 120, 97-103.

28. Shirwaikar, A., Rajendran, K. & Punitha, I.S.R. 2006. *In vitro* antioxidant studies on the benzyl tetra isoquinoline alkaloid berberine. *Biological and Pharmaceutical Bulletin*, 29: 1906-1910.

29. Slinkard, K. & Singleton, V.L. 1977. Total Phenol Analysis: Automation and Comparison with Manual Methods. *American Journal of Enology and Viticulture*, 28: 49-55.

30. Sofowora, A. 1993. *In Phytochemical screening of medicinal plants and traditional medicine in Africa*, Spectrum Books Ltd Nigeria, 289 pp.

31. Soud, R., Hamdan, I. & Afifi, F. 2004. Alpha amylase inhibitory activitv of some plant extracts with hyporrlvcemic activitv. *Scientia Pharmaceutica*, 72: 25-33.

32. Tlilia, N. & Sarikurkcu, C. 2020. Bioactive compounds profile, enzyme inhibitory and antioxidant activities of water extracts from five selected medicinal plants. *Industrial Crops & Products*, 151 pp.

33. Trease, G.E. & Evans, W.C. 1989. *Phenols and Phenolic glycosides.* In: Textbook of Pharmacognosy. Balliese, Tindall and Co Publishers, London, 616 pp.

34. Young, I.S. & Woodside, J.V. 2001. Antioxidants in health and disease. *Journal of Clinical Pathology*, 54: 176-186.

35. Zengin, G., Sarikurkcu, C., Gunes, E., Uysal, A., Ceylan, R., Uysal, S., Gungor, H. & Aktumsek, A. 2015. Two Ganoderma species: profiling of phenolic compounds by HPLC-DAD, antioxidant, antimicrobial and inhibitory activities on key enzymes linked to diabetes mellitus, Alzheimer's disease and skin disorders. *Food & Function*, 6(8): 2794-2802.

36. Zhishen, J., Mengcheng, T. & Jianming, W. 1999. The Determination of Flavonoid Contents in Mulberry and Their Scavenging Effects on Superoxide Radicals. *Food Chemistry*, 64: 555-559.

*http://dergipark.org.tr/trkjnat*
*Trakya University Journal of Natural Sciences, 22(1): 23-33, 2021*
*ISSN 2147-0294, e-ISSN 2528-9691*
*DOI: 10.23902/trkjnat.774926*

**Research Article**

# SARS CoV-2 SPIKE GLYCOPROTEIN MUTATIONS AND CHANGES IN PROTEIN STRUCTURE

Ekrem AKBULUT

Department of Bioengineering, Faculty of Engineering and Natural Sciences, Malatya Turgut Özal University, Malatya, TURKEY

**Cite this article as:**

Akbulut E. 2021. SARS CoV-2 Spike Glycoprotein Mutations and Changes in Protein Structure. *Trakya Univ J Nat Sci*, 22(1): 23-33, DOI: 10.23902/trkjnat.774926

Received: 28 July 2020, Accepted: 23 November 2020, Online First: 04 December 2020, Published: 15 April 2021

***Edited by:***
*Enes Taylan*

***Corresponding Author:***
*Ekrem Akbulut*
*ekrem.akbulut@ozal.edu.tr*

***ORCID ID:***
*orcid.org/0000-0002-7526-9835*

***Key words:***
*SARS CoV-2*
*COVID19*
*Spike protein*
*Mutational changes*
*Protein structure*

**Abstract:** Severe Acute Respiratory Syndrome Corona Virus-2 (SARS CoV-2) is a single-stranded positive polarity RNA virus with a high virulence effect. Spike (S) glycoprotein is the outermost component of the SARS CoV-2 virion and is important in the entry of the virus into the cell via the angiotensin converting enzyme 2 (ACE2) receptor. ACE2 plays an important role in the regulation of human blood pressure by converting the vasoconstrictor angiotensin 2 to the vasodilator angiotensin 1-7. In this study, the changes that mutations in Asian isolates may cause in S glycoprotein structure were analyzed and modeled to contribute to drug and vaccine targeting studies. Genome, proteome and mutation analyses were done using bioinformatics tools (MAFFT, MegaX, PSIPRED, MolProbity, PyMoL). Protein modelling was performed using ProMod3. We detected 26 mutations in the S glycoprotein. The changes that these mutations reveal in the general topological and conformational structure of the S glycoprotein may affect the virulence features of SARS CoV-2. It was determined that mutations converted the receptor binding domain (RBD) from down-formation to like-up formation. It is thought that conformational change occurring after mutation in RBD may cause an increase in receptor affinity. These findings could be beneficial for disease prevention of and drug/vaccine development for SARS CoV-2.

**Özet:** Şiddetli akut solunum yolu sendromu koronavirüsü-2 (SARS CoV-2) yüksek virülans etkiye sahip tek zincirli pozitif polariteli RNA virüsüdür. Spike (S) glikoprotein SARS CoV-2 virionunun en dıştaki bileşenidir ve anjiyotensin dönüştürücü enzim 2 (ACE2) reseptörü aracılığı ile virüsün hücreye girişinde önemlidir. ACE2, vazokonstriktör anjiyotensin 2'yi vazodilatör anjiyotensin 1-7'ye dönüştürerek insanda kan basıncının düzenlenmesinde önemli roller üstlenir. Bu çalışmada, Asya izolatlarındaki mutasyonların S glikoprotein yapısında neden olabileceği değişiklikler analiz edilmiş ve ilaç ve aşı hedefleme çalışmalarına katkıda bulunmak üzere modellenmiştir. Genom, proteom ve mutasyon analizleri biyoinformatik araçları (MAFFT, MegaX, PSIPRED, MolProbity, PyMoL) kullanılarak yapıldı. Protein modellemesi ProMod3 kullanılarak yapıldı. S glikoproteinde 26 mutasyon tespit edilmiştir. Bu mutasyonların S glikoproteininin genel topolojik ve konformasyonel yapısında ortaya çıkardığı değişiklikler, SARS CoV-2'nin virülans özelliklerini etkileyebilir. Mutasyonların reseptör bağlanma bölgesini (RBB) kapalı formasyondan açık formasyon benzeri bir yapıya dönüştürdüğü belirlenmiştir. RBB'de mutasyondan sonra meydana gelen konformasyonel değişimin reseptör afinitesinde bir artışa neden olabileceği düşünülmektedir. Bu bulgular hastalığın önlenmesi ve SARS CoV-2 ilaç ve aşı geliştirme çalışmaları için faydalı olabilir.

## Introduction

SARS CoV-2 is a single-stranded RNA virus with positive polarity (Baltimore 1971, Perlman 2020). COVID-19 infection caused by SARS-CoV-2 has affected 6.8 million people in approximately 179 countries, resulting in 398 thousand deaths from December 2019 to June 06, 2020. Asia is one of the major centres affected by the disease, with 1.3 million cases and 33.791 deaths (Worldometer 2020). The etiology of the disease, which first appeared in Hubei province of China, has not been fully clarified (Bogoch *et al*. 2020). Although the origin of the virus is not known for certain, evidence suggests that it may have a bat origin (Zhou *et al*. 2020, Zhu *et al.* 2020). The disease is manifested by nonspecific symptoms such as cough, fever and fatigue. Subsequently, shortness of breath and acute respiratory distress lead to mechanical ventilation and multiple organ failure in patients (Chen *et al.* 2020, Huang *et al.* 2020).

The SARS CoV-2 genome is a single-stranded RNA containing 12 protein-encoding regions with a length of 29,903 nucleotides (Wu *et al.* 2020). Similar to other beta-coronavirus, SARS-CoV-2 has a long ORF1ab polyprotein at the 5′ end, followed by four major structural proteins, including the spike surface glycoprotein, small envelope protein, matrix protein and nucleocapsid protein (Phan 2020). RNA virus genomes have high mutation potential (Drake 1993). In RNA viruses, mutations are thought to be the basis for adaptation and escape from the host cell's immune response (Kuljića & Budisin 1992). Mutations in some cases result in the weakening or complete eradication of the pathogenic effects of the viruses, and in other cases it may result in an increase in the severity of the infection with an opposite effect (Conenello *et al.* 2007, Zhang *et al.* 1998). To enter host cells, coronaviruses first bind to a cell surface receptor for viral attachment, subsequently enter endosomes, and eventually fuse viral and lysosomal membranes (Shang *et al.* 2020a). The trimeric S glycoprotein plays an important role in the entry of the virus into the cell by binding to ACE2 receptor of the host cell (Gallagher & Buchmeier 2001, Li *et al.* 2005). ACE2 cleaves angiotensin II to angiotensin (1-7), which exerts vasodilating, anti-inflammatory, and anti-fibrotic effects through binding to the Mas receptor (Bourgonje *et al.* 2020). The stability of the S glycoprotein and ACE2 linkage is closely related to the severity of the viral infection. S glycoprotein is a critical determinant of viral host range and tissue tropism and a major inducer of host immune responses. S glycoprotein contains a large ectodomain, a single-pass transmembrane anchor, and a short intracellular tail (Li 2016). S glycoprotein binds to ACE2 on the host cell surface through its S1 subunit and then fuses viral and host membranes through its S2 subunit. In addition to S glycoprotein activity, transmembrane protease serine 2 (TMPRSS2), lysosomal proteases and Neuropilin 1 (NRP1) activities are also important in the entry of the virus into the cell (Daly *et al.* 2020, Hoffman *et al.* 2020, Ou *et al.* 2020).

Clarification of the virus-host interactions will provide significant opportunities not only for the elucidation of the pathogenesis of the disease but also for the development of antiviral drugs (Mahajan *et al.* 2018).

Mutations in spike glycoprotein can cause conformational and structural changes that affect the affinity of binding to the receptor. The receptor binding domain in which the virus interacts with the ACE2 receptor can be folded independently from the rest of the spike protein, and this makes the structural changes that occur in this region even more important in terms of antiviral drug design studies (Li *et al.* 2005).

In this study, the S glycoprotein structure of 128 SARS CoV-2 Asian isolates was analyzed for possible mutational changes in the secondary, tertiary and quaternary structure to contribute to target identification studies involved in drug and vaccine design.

## Materials and Methods

### *Sequence Data*

Nucleotide and protein sequence information of 128 isolates from Asia continent were obtained from NCBI Virus database (NCBI 2019). Reference spike glycoprotein accesion code is YP_009724390.

### *Bioinformatic Tools*

Protein sequence information of 128 isolates were aligned with the MAFFT (v7.463) multiple sequence alignment program FFT-NS-i algorithm (Carroll *et al.* 2007, Katoh 2002, Katoh *et al.* 2018). The scoring matrix BLOSUM 80 was chosen for the amino acid sequences (Mount 2008). Gap opening penalty was used as 2.0. The mutated residues were analyzed with MegaX bioinformatic workbench (Kumar *et al.* 2018). MolProbity tool was used for structural validation and model quality (covalent geometry, torsion angle, optimized hydrogen placement and whole atom contact analysis) of wild type and variant spike proteins (Chen *et al.* 2010). Physiochemical properties of wild type and variant spike proteins were estimated by ProtParam tool from ExPASy portal (Wilkins *et al.* 1999). Secondary structure components (random coils, beta strands alpha helices) of spike protein were identified by using PSIPRED web server (Buchan *et al.* 2013). Three-dimensional model of wild type and variant spike proteins was generated by the method of homology modeling using Swiss-Model (Waterhouse *et al.* 2018). 3D structure alignments were performed by PyMOL (Ver2.3.4 Schrödinger).

### *Template Search*

Template search with BLAST (Basic Local Alignment Search Tool) and HHBlits (Hidden Markov Model-HMM-based lightning-fast iterative sequence search) was performed against the SWISS-MODEL template library. The target sequence was searched with BLAST against the primary amino acid sequence contained in the SMTL (Swiss Model Template Library) (Camacho *et al.* 2009). A total of 170 templates were found. An initial HHblits profile was built using the procedure outlined in Remmert *et al.* (2012), followed by 1 iteration of HHblits against NCBI non-reductant protein sequence database (NR20). The obtained profile was then searched against all profiles of the SMTL. A total of 685 templates were found. SMTL ID (6vxx) was selected as template.

### *Model Building*

Models were built based on the target-template alignment using ProMod3. Coordinates which were conserved between the target and the template were copied from the template to the model. Insertions and deletions were remodelled using a fragment library. Side chains were then rebuilt. Finally, the geometry of the resulting model was regularized by using a force field (Guex *et al.* 2009).

**Table 1.** SARS-CoV-2 S glycoprotein mutations.

| Site | Residue number | Wild Type | Variant | NCBI Acc | Origin |
|---|---|---|---|---|---|
| **Signal peptide** | 8 | L | V | QIT07011<br>QIT08268<br>QIT08280 | Hong Kong<br>Hong Kong<br>Hong Kong |
| **N-terminal domain** | 28 | Y | H | QJF77846 | India |
| | 28 | Y | N | QIA20044 | China |
| | 49 | H | Y | QJD47718 | Taiwan |
| | 50 | S | L | QIU80913 | China |
| | 74 | N | K | QIO04367 | China |
| | 144 | Y | Deletion | QHS34546 | India |
| | 221 | S | W | QHZ00379 | China |
| | 271 | Q | R | QJC19491 | India |
| | 292 | A | V | QJD23249 | Malaysia |
| | 293 | L | M | QJD23249 | Malaysia |
| | 294 | D | I | QJD23249 | Malaysia |
| | 295 | P | H | QJD23249 | Malaysia |
| | 296 | L | F | QJD23249 | Malaysia |
| | 297 | S | W | QJD23249 | Malaysia |
| **Receptor binding domain** | 367 | V | F | QJC20993 | HongKong |
| | 408 | R | I | QHS34546 | India |
| | 519 | H | Q | QJD23249 | Malaysia |
| **S1 subunit** | 570 | A | V | QIU81885 | Beijing |
| | 614 | D | G | QIT08292<br>QIT08304<br>QJF77858<br>QJF77882<br>QJD47812<br>QJD47824<br>QJD47836<br>QJD47848<br>QJD47860<br>QJD47872<br>QJD47884<br>QJD47896<br>QJD20849<br>QJD20861<br>QJC19491 | Hong Kong<br>Hong Kong<br>India<br>India<br>Taiwan<br>Taiwan<br>Taiwan<br>Taiwan<br>Taiwan<br>Taiwan<br>Taiwan<br>Taiwan<br>Sri Lanka<br>Sri Lanka<br>India |
| | 653 | A | V | QIU81873 | Beijing |
| **S2 subunit** | 765 | R | L | QJD47800 | Taiwan |
| | 772 | V | I | QIZ16509 | Turkey |
| **Fusion peptide** | 791 | T | I | QJD47728<br>QJD47740<br>QJD47752<br>QJD20632<br>QJD20656 | Taiwan<br>Taiwan<br>Taiwan<br>Taiwan<br>Taiwan |
| **S2 subunit** | 884 | S | F | QJD47718 | Taiwan |
| **HR1** | 930 | A | V | QIA98583 | India |

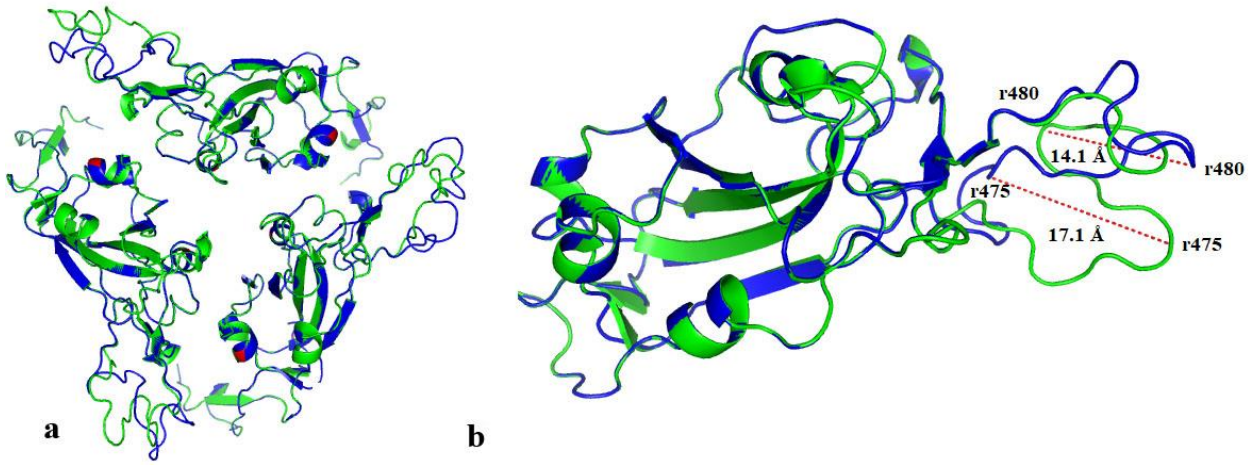


**Fig. 1.** Cartoon illustration of SARS CoV-2 S glycoprotein receptor binding domain. a) homo-trimer structure, aligned wild type (blue color)-variant (green colour), b) monomer structure, aligned wild type-variant, inter-residual displacement (r: residue).

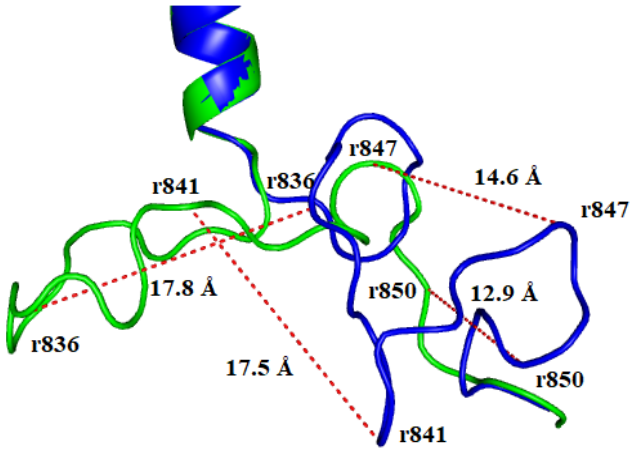


**Fig. 2.** SARS CoV-2 S glycoprotein fusion peptide domain-cartoon illustration of aligned wild type (blue color)-variant (green colour), inter-residual displacement.

*Model Quality Estimation*

The global and per-residue model quality was assessed using the QMEAN (Qualitative Model Energy Analysis) scoring function and MolProbity workbench (Benkert *et al.* 2011).

*Oligomeric State Conservation*

The quaternary structure annotation of the template was used to model the target sequence in its oligomeric form. The method is based on a supervised machine learning algorithm, Support Vector Machines (SVM), which combines interface conservation, structural clustering, and other template features to provide a quaternary structure quality estimate (QSQE) (Bertoni *et al.* 2017). The QSQE score is a number between 0 and 1, reflecting the expected accuracy of the interchain contacts for a model built based on a given alignment and template. Higher numbers indicate higher reliability. This complements the GMQE (Global Model Quality Estimation) score which estimates the accuracy of the tertiary structure of the resulting model.

## Results

In this study, a total of 26 mutations were detected in the S glycoprotein of SARS CoV-2 in Asian isolates (Table 1). Most of these mutations were found in the structurally and functionally important regions of the S glycoprotein, which function in virus-host interaction. Fourteen mutations were detected in the N-terminal domain and three in the C-terminal domain of the S glycoprotein. The mutations 367V>F, 408R>I and 519H>Q were detected in the receptor binding domain, where the S glycoprotein interacts with the ACE2 receptor of the host cell (Fig. 1).

The 791 T>I mutation was detected in the fusion peptide region, which plays an important role in viral fusion and disruption of the membrane integrity of the host cell (Fig. 2). The 8L>V mutation was detected in the signal peptide sequence involved in the translocation of the viral protein. The 930A>V mutation was observed in the heptad repeat (HR) 1 domain. HR1 promotes the fusion process of the host cell membrane with the viral envelope by bringing the fusion peptide closer to the C-terminal domain of the ectodomain which is the domain of the membrane protein that extends into the extracellular space (Lu *et al.* 2008). Ectodomains are usually the parts of proteins that initiate contact with surfaces and cause signal transduction.

The residues in which the mutation was determined were rearranged using the MegaX software to obtain the mutant spike protein sequence. Protein 3D structures were modelled with the Swiss-Model web service using wild type and variant amino acid sequences (Fig. 3).

Structural differences between the wild type and variant were analyzed using bioinformatics tools. Model quality was assessed by QMEAN and MolProbity. The MolProbity score was 1.38 for the variant and 1.42 for the wild type. The MolProbity score of the model used as a template (6vxx) was 2.8. The MolProbity score of the model was lower than that of the model used as a template, suggesting that the quality of the model was better than the average structure at this resolution (Davis *et al.* 2007). The GMQE score was 0.75, QMEAN score

was -2.07, Clash score was 1.57, Ramachandran favoured sites were 91.5% and Ramachandran outliers were 1.82% for the wild type protein. On the other hand, the Clash score was 1.45, GMQE score was 0.75, QMEAN score was −1.86, Ramachandran favoured sites were 91.8% and Ramachandran outliers were 1.64% for the variant protein. The Ramachandran plots (Fig. 4) suggest that the protein models produced have acceptable polypeptide backbone and phi (φ) and psi (Ψ) torsion angles for the alpha-helix and beta-strand regions (Lovell *et al*. 2003). The scores obtained are considered to be within the appropriate limits in terms of model quality (Benkert *et al.* 2011).

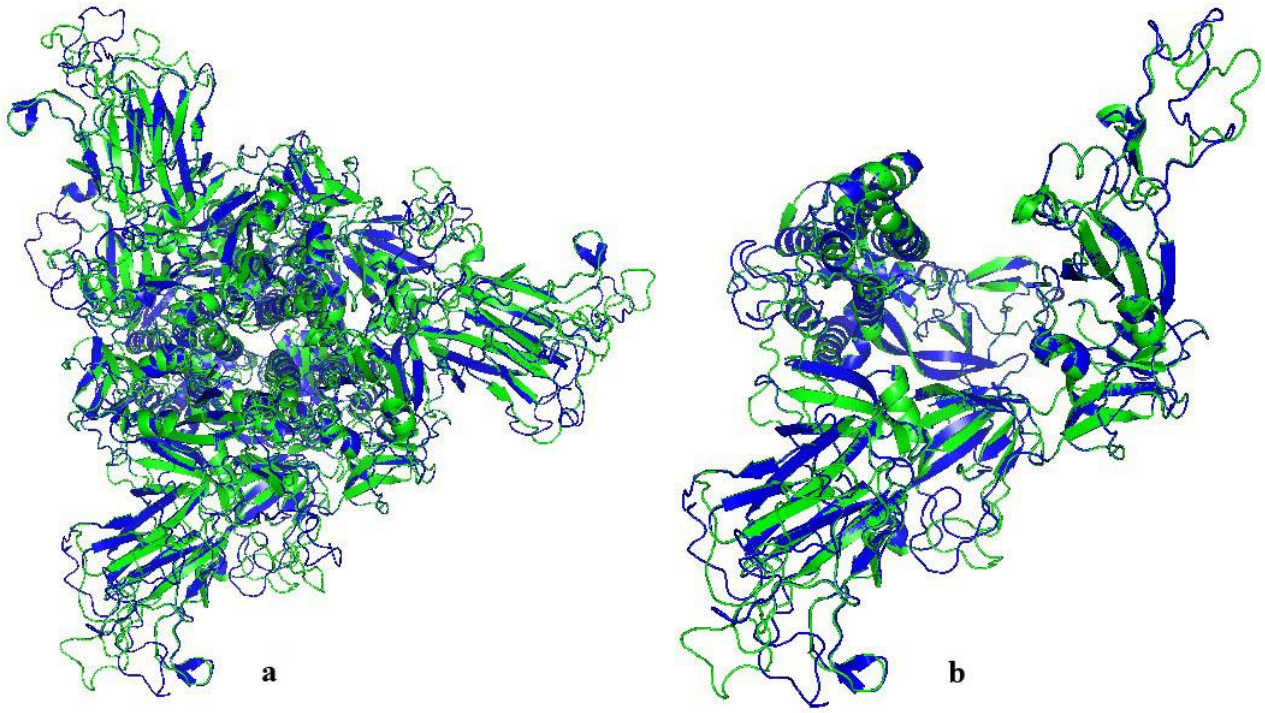


**Fig. 3.** Homology model of SARS CoV-2 S glycoprotein (cartoon illustration). a) homo-trimer structure of SARS CoV-2 S glycoprotein, aligned wild type (blue colour)-variant (green colour), b) monomer structure of SARS CoV-2 S glycoprotein, aligned wild type-variant.

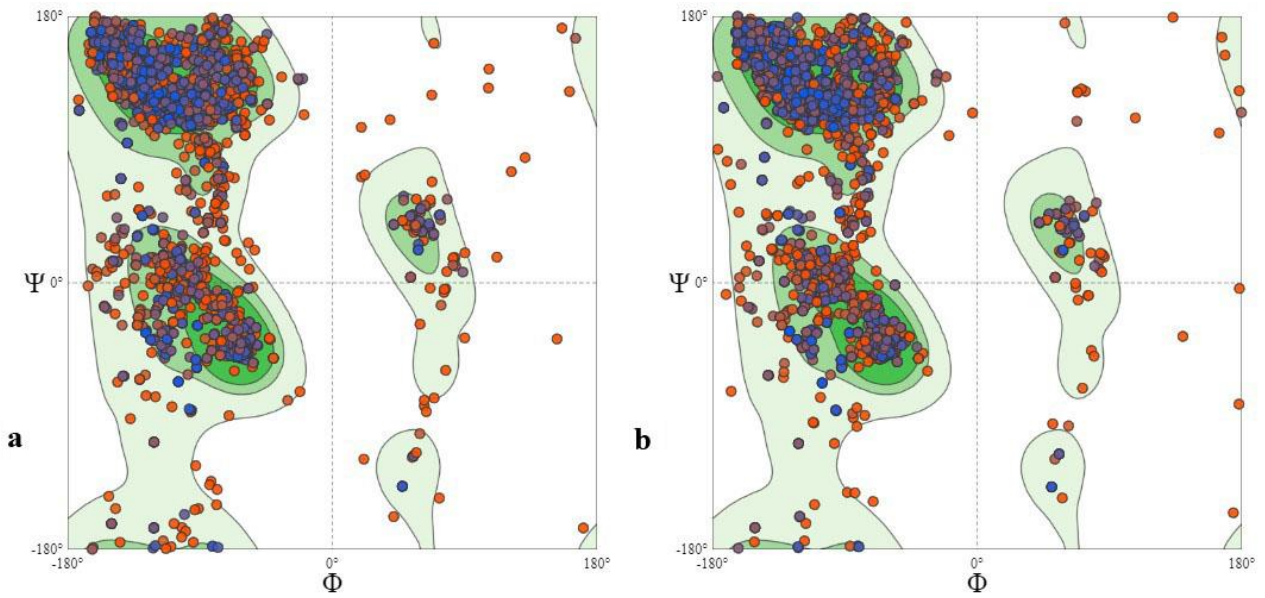


**Fig. 4.** Model quality data of SARS CoV-2 S glycoprotein. a) Ramachandran plot of wild model, b) Ramachandran plot of variant model.

Secondary structure predictions were performed using the PSIPRED workbench, which predicted that the wild type glycoprotein has 65 helices and 20 beta strands, while the variant glycoprotein has 65 helices and 22 beta strands (Fig. 5). It seems that mutations can cause changes in the conformational and topological structure of the spike glycoprotein (RMSD value: 0.047) (Fig. 6).

Structural analysis data revealed the presence of tryptophan-rich conserved region (1208-YIKWPWYIWL-1219), called the proximal transmembrane region, in S glycoprotein S2 subunit in both wild type and variant models. The last five residues of this region, which are conserved in other coronavirus species, are located in the transmembrane domain and are responsible for viral infectivity (Lu *et al*. 2008).

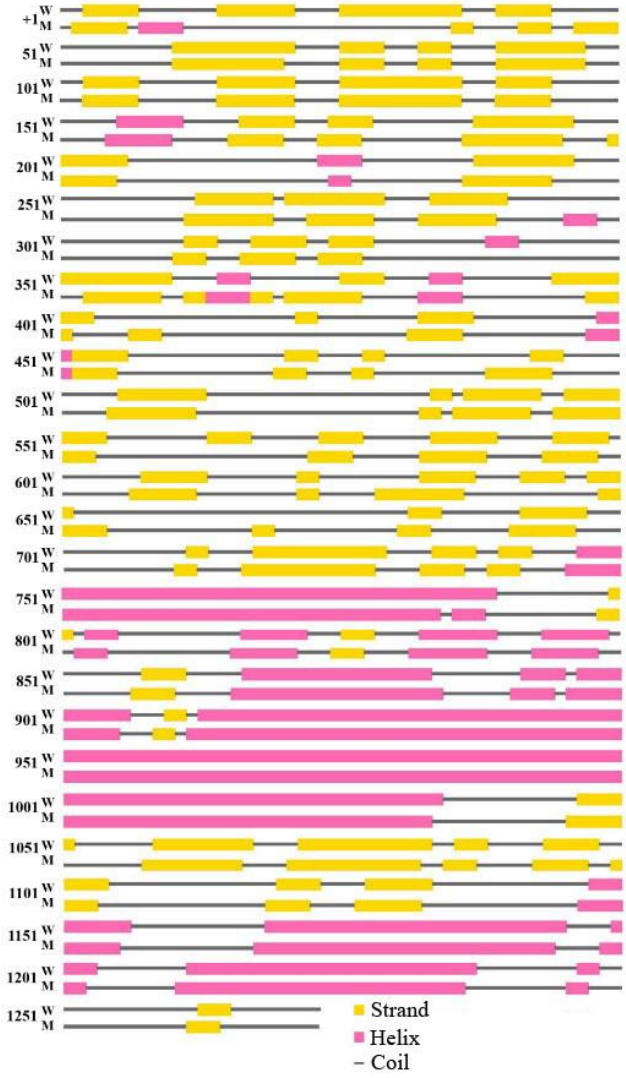


**Fig. 5.** Comparative illustration of secondary structure of SARS CoV-2 S glycoprotein (W-wild structure; M-variant structure)

## Discussion

In our study, changes in the secondary (Fig. 5) and quaternary (Fig. 6) structure of the spike glycoprotein caused by the 26 mutations seen in SARS CoV-2 Asian isolates were modeled. It was observed that mutation-derived changes in the wild type S glycoprotein secondary structure may cause changes that affect the topological and conformational structure of the S glycoprotein. The emergence of additional 2 beta strand formation in the variant structure at the S glycoprotein receptor binding site may result in an increase in the structural stability of the binding site.

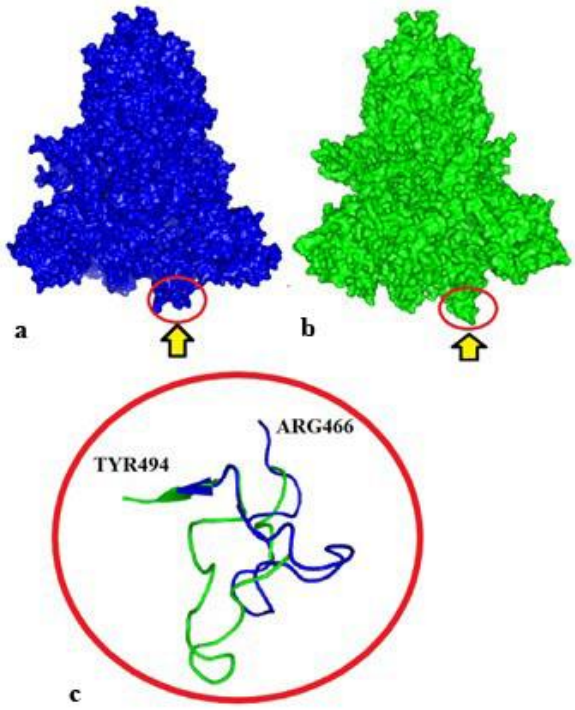


**Fig. 6.** Representation of changes in the general structure of the SARS CoV-2 S glycoprotein. a) wild model-down formation, b) variant model-like up formation, c) focused-aligned representation of RBD-cartoon illustration. Arrow indicates change in receptor binding site.

The entry of the coronaviruses into the cell occurs via two stages. In the first stage, the virus recognises the host cell ACE2 receptor for viral binding, and in the second stage, the viral and host membranes merge (Li 2016). Receptor recognition and binding is the first stage of viral infection. This affects the determination of the host cell type and tissue tropism (Li *et al*. 2006). The SARS CoV-2 S glycoprotein and its affinity to the human ACE2 (*hACE2*) receptor are thought to be associated with the severity of the disease and the spread of the virus (Li *et al.* 2005). The high spreading rate and virulence effect of SARS CoV during its first occurrence in 2002 were not seen at the same severity when it reappeared in 2004, and this has been associated with decreased receptor affinity of spike glycoprotein (Kan *et al*. 2005, Walls *et al*. 2020.) While 24 residues in SARS CoV S glycoprotein interact with 53 residues in *hACE2*, we identified that 37 residues in SARS CoV-2 S glycoprotein interact with 77 residues in *hACE2*. The strong relationship of SARS CoV-2 S glycoprotein with *hACE2* may bring important problems in terms of the prognosis of the disease, considering the metabolic function of *hACE2*. SARS CoV-2-mediated down-regulation of ACE2 causes hyperinflamation

through dysregulation of the renin-angiotensin-aldosterone system, attenuation of Mas receptor, increased activation of (des-Arg9)-bradykinin, and activation of the C5a and C5b-9 complement system (Mahmudpour *et al*. 2020). Hyperinflammation results in severe lung tissue damage and loss of lung function (Gustine & Jones 2020).

In addition, it is thought that apart from the S glycoprotein-ACE2 receptor relationship, host gender, comorbidity, presence of immunosuppressive states and ACE2 polymorphism may also have a role in the observation of different mortality rates in different populations (Li *et al.* 2020, Bosso *et al.* 2020). In the study conducted by Srivastava *et al.* (2020) in Indian population, it was stated that ACE2 rs228566 A>G polymorphism increased ACE2 expression by up to 50%, and this situation was associated with the relatively low mortality and morbidity rates in India. ACE2 has two forms in the body. The full-length form with a transmembrane domain contains 808 amino acids, while the soluble form contains 740 amino acids (Marquez *et al.* 2020). The circulating soluble ACE2 interaction with SARS CoV-2 can limit the interaction of the virus with membrane-bound ACE2 and prevent the virus from entering the cell. In this context, increased ACE2 expression may limit viral infection (Davidson *et al.* 2020, Kruse 2020, Khan *et al.* 2017). On the other hand, reduced S glycoprotein receptor affinity may activate the normalization of the peptide receptor relationship, thus the conversion process of angiotensin II to angiotensin (1-7). Angiotensin (1-7) may limit the inflammatory response by inducing the conversion of proinflammatory des-arg$^{9}$ bradykinin 1-8 to bradykinin 1-7 (Davidson *et al.* 2020, Santos *et al.* 2019). It is seen that the protein structure formed after mutations in S glycoprotein is not alone a determinant in host virus interaction and the development of viral infection and will affect this process in many biological pathways and factors.

Two conformational states are observed in the S glycoprotein receptor binding site. One of them is the down-formation in which the receptor binding site is hidden / masked, and the other is the up-formation, which is accessible to the receptor binding site and exhibits less stable structure (Gui *et al.* 2017, Walls *et al.* 2017, Wrapp *et al.* 2020). The findings of this study indicate that the changes in the *hACE2* binding region of the S glycoprotein transform the spike protein binding region from down-formation to like-up formation (Fig. 6). It is known that mutations that occur in the receptor binding domain will affect the S glycoprotein receptor affinity (Jia *et al.* 2020, Kim *et al.* 2019, Ou *et al.* 2020). The data we obtained in the study point to the structure transformed into a like-up formation. This transformation may result in an increase in S protein receptor affinity, viral infection severity, and transmission. These data support the view that the enhanced affinity of SARS CoV-2 to the receptor increases the severity and spread of the disease. He *et al*. (2020) emphasised that the affinity of SARS CoV-2 spike glycoprotein to the *hACE2* receptor is higher than that of the SARS CoV spike glycoprotein and that it may be associated with the severity of infection. Mutations in spike glycoprotein may result in the tropism of the virus to new host or receptors, increasing or decreasing the virulence effect (Shang *et al.* 2020b). It is believed that the mutations of 367V>F, 408R>I, and 519H>Q detected at the receptor binding domain may affect the binding dynamics. The topological and conformational changes that these mutations reveal in coils (Mason & Arndt 2004), which have important structural roles in binding action can affect the clamping of three receptor binding S1 structures that are embedded on the homo-trimeric S2 stem. 510D>G and 529I>T mutations in MERS CoV spike glycoprotein were reported to reduce the receptor affinity and may play a role in reducing the virulence effects of the disease (Kim *et al.* 2016). Changes in the receptor binding domain of SARS CoV-2 are also likely to lead to similar results as well as opposite results. Mutation can also cause enhanced affinity and virulence. The increase in SARS CoV-2 S glycoprotein receptor affinity increases the rate of human-to-human transmission of the virus (Shang *et al.* 2020c).

The mutation in the HR1 region (930A> V) involved in the fusion process caused minor changes in the conformational structure of HR1. The HR regions play important roles in membrane fusion and viral entry. Chan *et al.* (2006) reported that 927P, 941P, 955P, and 1165P mutations in the HR region of SARS CoV S glycoprotein resulted in inhibition of membrane fusion and impairment of viral entry. Cavallo and Oliva (2020) noticed that the 929S>I, 939S>F and 936D>Y mutations seen in the HR region of SARS CoV-2 S glycoprotein caused a loss in the stability of the construct after fusion. The 936D>Y mutation was found to cause the loss of the 936D-1185R salt bridge, a strong inter-monomer interaction, and weaken the post-fusion assembly (Cavallo & Oliva 2020).

The 791T> I mutation was detected in the fusion peptide region, which was involved in the entry of viruses into the cell, deterioration of host cell membrane stability, fusion pore formation and fusion of the viral envelope with cellular membranes (Ou *et al*. 2016, Peisajovich & Shai 2003). Many studies showed that changes caused by inhibition or mutation in fusion peptide prevent fusion (Duffus *et al.* 1995, Perin *et al.* 2016, Ding *et al*. 2017, Kadam and Wilson 2017). Perin et al. (2016) showed that in the study of drug-based inhibition of hepatitis C virus (HCV) fusion peptide prevented the fusion of HCV to the cell membrane. It is known that signal peptides play an important role in the translocation of viral and bacterial proteins into host cells (Garcia *et al.* 1988, Ignatova *et al.* 2002, Lumangtad & Bell 2020, Vermeire *et al.* 2014). A study by Li *et al*. (2020) showed that the signal peptide can contribute to the severity of infection through viral protein translocation. The 8L>V mutation detected in the signal peptide region may affect the translocation properties of the viral protein structure and therefore the virulence of SARS CoV-2 (Fig. 2).

Mutations in S glycoprotein, which is an important structural target for treatment and prophylaxis, will affect not only the change in virulence properties but also the validity and stability of the vaccine to be developed. The change in the antigenic structure after the mutations detected in influenza virus necessitates periodic adjustments in influenza vaccine (Yang *et al.* 2019, CDC 2019, Agor & Özaltın 2018). Yang *et al*. (2019) showed that influenza A (H1N1) virus 127D>E, 191L>I, 222D>G/N and 223Q>R mutations caused change in antigen and decreased receptor affinity. In vaccine validity studies conducted with hepatitis B virus (HBV), which is a DNA virus with a lower mutation risk than RNA viruses. It has been reported that there is a significant decrease in the sensitivity of the vaccine used in hepatitis B prophylaxis against variant forms (Torresi 2008, Hsu *et al.* 2004). In the study conducted by Kamili (2010), it was observed that HBV 173V>L, 180L>M, 204M>V and 145G>R mutations had a negative effect on the protective properties of the vaccine, and the vaccine did not provide prophylaxis against variant forms. It is known that SARS CoV-2 mutations will produce 2 different results for the COVID19 vaccine to be developed. Either a new vaccine will be required for each new mutation, as in seasonal influenza, or it will remain valid without causing a change in the immune response. Analysis and modeling of mutation data will contribute to the determination of the correct target structure, the interpretation of changes in the viral proteome, and preventive/ therapeutic approaches.

## Conclusion

As a result, it was determined that mutations converted the receptor binding site from down-formation to like-up formation. It is thought that conformational change occurring after mutation in RBD may result in an increase in receptor affinity. The changes that these mutations reveal in the general topological and conformational structure of the S glycoprotein may affect the virulence features in the functional structure. These findings could be beneficial for the disease prevention and drug/vaccine development of SARS CoV-2.

**Ethics Committee Approval:** Since the article does not contain any studies with human or animal subject, its approval to the ethics committee was not required.

**Conflict of Interest:** The authors have no conflicts of interest to declare.

**Funding:** The author declared that this study has received no financial support.

## References

1. Agor, J.K. & Özaltın, O.Y. 2018. Models for predicting the evolution of influenza to inform vaccine strain selection. *Human Vaccines Immunotherapeutics*, 14(3): 678-683.
2. Baltimore, D. 1971. Expression of animal virus genomes. *Bacteriological Reviews*, 35(3): 235-241.
3. Benkert, P., Biasini, M. & Schwede, T. 2011. Toward the estimation of the absolute quality of individual protein structure models. *Bioinformatics*, 27(3): 343-350.
4. Bertoni, M., Kiefer, F., Biasini, M., Bordoli, L. & Schwede, T. 2017. Modeling protein quaternary structure of homo- and hetero-oligomers beyond binary interactions by homology. *Scientific Reports*, 7(1): 1-15.
5. Bogoch, I.I., Watts, A., Thomas-Bachli, A., Huber, C., Kraemer, M.U.G. & Khan, K. 2020. Pneumonia of unknown aetiology in Wuhan, China: Potential for international spread via commercial air travel. *Journal of Travel Medicine*, 27(2): 1-3.
6. Bosso, M., Thanaraj, T.A., Abu-Farha, M., Alanbaei, M., Abubaker, J.& Al-Mulla, F. 2020. The two faces of ACE2: The role of ACE2 receptor and its polymorphisms in hypertension and COVID-19. *Molecular Therapy Methods&Clinical Development*, 18: 321-327.
7. Bourgonje, A.R., Abdulle, A.E., Timens, W., Hillebrands, J.L., Navis, G.J., Gordijn, S.J., Bolling, M.C., Dijkstra, G., Voors, A.A., Osterhaus, A.D., van der Voort, P.H., Mulder, D.J. & van Goor, H. 2020. Angiotensin-converting enzyme-2 (ACE2), SARS-CoV-2 and pathophysiology of coronavirus disease 2019 (COVID-19). *The Journal of Pathology*, 251(3): 228-248.
8. Buchan, D.W.A., Minneci, F., Nugent, T.C.O., Bryson, K. & Jones, D.T. 2013. Scalable web services for the PSIPRED Protein Analysis Workbench. Nucleic Acids Research, 41(Web Server issue): W349-W357.
9. Camacho, C., Coulouris, G., Avagyan, V., Ma, N., Papadopoulos, J., Bealer, K. & Madden, T.L. 2009. BLAST+: Architecture and applications. *BMC Bioinformatics*, 10(1): 421.
10. Carroll, H., Beckstead, W., O'Connor, T., Ebbert, M., Clement, M., Snell, Q. & Mcclellan, D. 2007. DNA reference alignment benchmarks based on tertiary structure of encoded proteins. *Bioinformatics*, 23(19): 2648-2649.
11. Cavallo, L. & Oliva, R. 2020. D936Y and other mutations in the fusion core of the SARS-Cov-2 spike protein heptad repeat 1 undermine the post-fusion assembly. *bioRxiv*, https://doi.org/10.1101/2020.06.08.140152
12. CDC-Centers for Disease Control and Prevention, National Center for Immunization and Respiratory Diseases (NCIRD). 2019. How the flu virus can change: "drift" and "shift" https://www.cdc.gov/flu/about/viruses/change.htm (Data accessed: 01.05.2020).
13. Chan, W.E., Chuang, C.K., Yeh, S.H., Chang, M.S. & Chen, S.S.L. 2006. Functional characterization of heptad repeat 1 and 2 mutants of the spike protein of severe acute respiratory syndrome Coronavirus. *Journal of Virology*, 80(7): 3225-3237.
14. Chen, N., Zhou, M., Dong, X., Qu, J., Gong, F., Han, Y., Qiu, Y., Wang, J., Liu, Y., Wei, Y., Xia, J., Yu, T., Zhang, X. & Zhang, L. 2020. Epidemiological and clinical characteristics of 99 cases of 2019 novel coronavirus pneumonia in Wuhan, China: a descriptive study. *The Lancet*, 395(10223): 507-513.

15. Chen, V.B., Arendall, W.B., Headd, J.J., Keedy, D.A., Immormino, R.M., Kapral, G.J., Murray, L.W., Richardson, J.S. & Richardson, D.C. 2010. MolProbity: All-atom structure validation for macromolecular crystallography. *Acta Crystallographica Section D: Biological Crystallography*, 66(1): 12-21.

16. Conenello, G.M., Zamarin, D., Perrone, L.A., Tumpey, T. & Palese, P. 2007. A single mutation in the PB1-F2 of H5N1 (HK/97) and 1918 influenza A viruses contributes to increased virulence. *PLoS Pathogens*, 3(10): 1414-1421.

17. Daly, J.L., Simonetti, B., Klein, K., Chen, K., Williamson, M.K., Antón-Plágaro, C., Shoemark, D.K., Gracia, L.S., Bauer, M., Hollandi, R., Greber, U.F., Horvath, P., Sessions, R.B., Helenius, A., Hiscox, J.A., Teesalu, T., Matthews, D.A., Davidson, A.D., Collins, B.M., Cullen, P.J. & Yamauchi, Y. 2020. Neuropilin-1 is a host factor for SARS-CoV-2 infection. *Science*, eabd3072: 1-8.

18. Davidson, A.M., Wysocki, J. & Batlle, D. 2020. Interaction of SARS-CoV-2 and other coronavirus with ACE (Angiotensin-Converting Enzyme)-2 as their main receptor- therapeutic implications. *Hypertension*, 76(5): 1339-1349.

19. Davis, I.W., Leaver-Fay, A., Chen, V.B., Block, J.N., Kapral, G.J., Wang, X., Murray, L.W., Arendall, W.B., Snoeyink, J., Richardson, J.S. & Richardson, D.C. 2007. MolProbity: All-atom contacts and structure validation for proteins and nucleic acids. *Nucleic Acids Research*, 35(2): 375-383.

20. Ding, X., Zhang, X., Chong, H., Zhu, Y., Wei, H., Wu, X., He, J., Wang, X. & He, Y. 2017. Enfuvirtide (T20)-based lipopeptide is a potent HIV-1 cell fusion Inhibitor: implications for viral entry and inhibition. *Journal of Virology*, 91(18): 1-20.

21. Drake, J.W. 1993. Rates of spontaneous mutation among RNA viruses. *Proceedings of the National Academy of Sciences of the United States of America*, 90(9): 4171-4175.

22. Duffus, W.A., Levy-Mintz, P., Klimjack, M.R. & Kielian, M. 1995. Mutations in the putative fusion peptide of Semliki Forest virus affect spike protein oligomerization and virus assembly. *Journal of Virology*, 69(4): 2471-2479.

23. Gallagher, T.M. & Buchmeier, M.J. 2001. Coronavirus spike proteins in viral entry and pathogenesis. *Virology*, 279(2): 371-374.

24. Garcia, P.D., Ou, J.H., Rutter, W.J. & Walter, P. 1988. Targeting of the hepatitis B virus precore protein to the endorplasmic reticulum membrane: After signal peptide cleavage translocation can be aborted and the product released into the cytoplasm. *Journal of Cell Biology*, 106(4): 1093-1104.

25. Guex, N., Peitsch, M.C. & Schwede, T. 2009. Automated comparative protein structure modeling with SWISS-MODEL and Swiss-PdbViewer: A historical perspective. *Electrophoresis*, 30(SUPPL. 1): S162-S173.

26. Gui, M., Song, W., Zhou, H., Xu, J., Chen, S., Xiang, Y. & Wang, X. 2017. Cryo-electron microscopy structures of the SARS-CoV spike glycoprotein reveal a prerequisite conformational state for receptor binding. *Cell Research*, *27*(1): 119-129.

27. Gustine, J.N. & Jones, D. 2020. Immunopathology of yyperinflammation in COVID-19. *The American Journal of Pathology*, https://doi.org/10.1016/j.ajpath.2020.08.009

28. He, J., Tao, H., Yan, Y., Huang, S.Y. & Xiao, Y. 2020. Molecular mechanism of evolution and human infection with SARS-CoV-2. *Viruses*, 12(4): 428.

29. Hoffmann, M., Kleine-Weber, H., Schroeder, S., Krüger, N., Herrler, T., Erichsen, S., Schiergens, T.S., Herrler, G., Wu, N.H., Nitsche, A., Müller, M.A., Drosten, C. & Pöhlmann, S. 2020. SARS-CoV-2 cell entry depends on ACE2 and TMPRSS2 and is blocked by a clinically proven protease inhibitor. *Cell*, 181: 271-280.

30. Hsu, H.Y., Chang, M.H., Ni, Y.H. & Chen, H.L. 2004. Survey of hepatitis B surface variant infection in children 15 years after a nationwide vaccination programme in Taiwan. *Gut*, 53(10): 1499-1503.

31. Huang, C., Wang, Y., Li, X., Ren, L., Zhao, J., Hu, Y., Zhang, L., Fan, G., Xu, J., Gu, X., Cheng, Z., Yu, T., Xia, J., Wei, Y., Wu, W., Xie, X., Yin, W., Li, H., Liu, M., Xiao, Y., Gao, H., Guo, L., Xie, J., Wang, G., Jiang, R., Gao, Z., Jin, Q., Wang, J. & Cao, B. 2020. Clinical features of patients infected with 2019 novel coronavirus in Wuhan, China. *The Lancet*, 395(10223): 497-506.

32. Ignatova, Z., Hörnle, C., Kasche, V. & Nurk, A. 2002. Unusual signal peptide directs penicillin amidase from Escherichia coli to the tat translocation machinery. *Biochemical and Biophysical Research* Communications, 291(1): 146-149.

33. Jia, Y., Shen, G., Zhang, Y., Huang, K.-S., Ho, H.-Y., Hor, W.-S., Yang, C.H., Li, C. & Wang, W.L. 2020. Analysis of the mutation dynamics of SARS-CoV-2 reveals the spread history and emergence of RBD mutant with lower ACE2 binding affinity. *BioRxiv*, 2020.04.09.034942. https://doi.org/10.1101/2020.04.09.034942

34. Kan, B., Wang, M., Jing, H., Xu, H., Jiang, X., Yan, M., Liang, W., Zheng, H., Wan, K., Liu, Q., Cui, B., Xu, Y., Zhang, E., Wang, H., Ye, J., Li, G., Li, M., Cui, Z., Qi, X., Chen, K., Du, L., Gao, K., Zhao, Y., Zou, X., Feng, Y., Gao, Y., Hai, R., Yu, D., Guan, Y. & Xu, J. 2005. Molecular Evolution Analysis and Geographic Investigation of Severe Acute Respiratory Syndrome Coronavirus-Like Virus in Palm Civets at an Animal Market and on Farms. *Journal of Virology*, 79(18): 11892-11900.

35. Kadam, R.U. & Wilson, I.A. 2017. Structural basis of influenza virus fusion inhibition by the antiviral drug Arbidol. *PNAS*, 114(2): 206-214.

36. Kamili, S. 2010. Infectivity and vaccination efficacy studies in animal models of HBV S and pol gene mutants. *Antiviral Therapy*, 15(3): 477-485.

37. Katoh, K. 2002. MAFFT: a novel method for rapid multiple sequence alignment based on fast Fourier transform. *Nucleic Acids Research*, 30(14): 3059-3066.

38. Katoh, Kazutaka, Rozewicki, J. & Yamada, K.D. 2018. MAFFT online service: Multiple sequence alignment, interactive sequence choice and visualization. *Briefings in Bioinformatics*, 20(4): 1160-1166.

39. Khan, A., Benthin, C., Zeno, B., Albertson, T.E., Boyd, J., Christie, J.D., Hall, R., Poirier, G., Ronco, J.J., Tidswell, M., Hardes, K., Powley, W.M., Wright, T.J., Siederer, S.K.,

Fairman, D.A., Lipson, D.A., Bayliffe, A.I. & Lazaar, A.L. 2017. A pilot clinical trial of recombi-nant human angiotensin-converting enzyme 2 in acute respiratory distress syndrome. *Critical Care*, 21(234): 1-9.

40. Kim, Y., Cheon, S., Min, C.K., Sohn, K.M., Kang, Y.J., Cha, Y.J., Kang, J. Il, Han, S.K., Ha, N.Y., Kim, G., Aigerim, A., Shin, H.M., Choi, M.S., Kim, S., Cho, H.S., Kim, Y.S. & Choa, N.H. 2016. Spread of mutant middle east respiratory syndrome coronavirus with reduced affinity to human CD26 during the south Korean outbreak. *MBio*, 7(2): e00019-16.

41. Kim, Y.S., Aigerim, A., Park, U., Kim, Y., Rhee, J.Y., Choi, J.P., Park, W.B., Park, S.W., Kim, Y., Lim, D.G., Inn, K.S., Hwang, E.S., Choi, M.S., Shin, H.S. & Cho, N.H. 2019. Sequential emergence and wide spread of neutralization escape middle east respiratory syndrome coronavirus mutants, South Korea, 2015. *Emerging Infectious Diseases*, 25(6): 1161-1168.

42. Kruse, R.L. 2020. Therapeutic strategies in an outbreak scenario to treat the novel coronavirus originating in Wuhan, China. *F1000Research*, 9(72): 1-15.

43. Kuljić-Kapulica, N. & Budisin, A. 1992. Coronaviruses. In *Srpski arhiv za celokupno lekarstvo*, 120(7-8): 215-218.

44. Kumar, S., Stecher, G., Li, M., Knyaz, C. & Tamura, K. 2018. MEGA X: Molecular evolutionary genetics analysis across computing platforms. *Molecular Biology and Evolution*, 35(6): 1547-1549.

45. Li, D., Wu, J., Chen, J., Zhang, D., Zhang, Y., Qiao, X., Yu, X., Zheng, Q. & Hou, J. 2020. Optimized expression of classical swine fever virus E2 protein via combined strategy in Pichia pastoris. *Protein Expression and Purification*, 167(105527): 1-7.

46. Li, Q., Cao, Z. & Rahman, P. 2020. Genetic variability of human angiotensin-converting enzyme 2 (hACE2) among various ethnic populations. *Molecular Genetics & Genomic Medicine*, 8(e1344): 1-6.

47. Li, F. 2016. Structure, function and evolution of coronavirus spike proteins. *Annual Review of Virology*, 3(1): 237-261.

48. Li, F., Li, W., Farzan, M. & Harrison, S.C. 2005. Structural biology: Structure of SARS coronavirus spike receptor-binding domain complexed with receptor. *Science*, 309(5742): 1864-1868.

49. Li, W., Wong, S.-K., Li, F., Kuhn, J.H., Huang, I.C., Choe, H. & Farzan, M. 2006. Animal Origins of the Severe Acute Respiratory Syndrome Coronavirus: Insight from ACE2-S-protein interactions. *Journal of Virology*, 80(9): 4211-4219.

50. Li, W., Zhang, C., Sui, J., Kuhn, J.H., Moore, M.J., Luo, S., Wong, S.K., Huang, I.C., Xu, K., Vasilieva, N., Murakami, A., He, Y., Marasco, W.A., Guan, Y., Choe, H. & Farzan, M. 2005. Receptor and viral determinants of SARS-coronavirus adaptation to human ACE2. *EMBO Journal*, 24(8): 1634-1643.

51. Lovell, S.C., Davis, I.W., Arendall, W.B., De Bakker, P.I.W., Word, J.M., Prisant, M.G., Richardson, J.S. & Richardson, D.C. 2003. Structure validation by Cα geometry: φ,ψ and Cβ deviation. *Proteins: Structure, Function and Genetics*, 50(3): 437-450.

52. Lu, Y., Neo, T.L., Liu, D.X. & Tam, J.P. 2008. Importance of SARS-CoV spike protein Trp-rich region in viral infectivity. *Biochemical and Biophysical Research Communications*, 371(3): 356-360.

53. Lumangtad, L.A. & Bell, T.W. 2020. The signal peptide as a new target for drug design. *Bioorganic and Medicinal Chemistry Letters*, 30(10): 127115.

54. Mahajan, M., Chatterjee, D., Bhuvaneswari, K., Pillay, S. & Bhattacharjya, S. 2018. NMR structure and localization of a large fragment of the SARS-CoV fusion protein: Implications in viral cell fusion. *Biochimica et Biophysica Acta - Biomembranes*, 1860(2): 407-415.

55. Mahmudpour, M., Roozbeh, J., Keshavarz, M., Farrokhi, S. & Nabipour, I. 2020. COVID-19 cytokine storm: The anger of inflammation. Cytokine, 133(155151): 1-10.

56. Marquez, A., Wysocki, J., Pandit, J. & Batlle, D. 2020. An update on ACE2 amplification and its therapeutic potential. *Acta Physiologica*, e13513: 1-14.

57. Mason, J.M. & Arndt, K.M. 2004. Coiled coil domains: Stability, specificity, and biological implications. *ChemBioChem*, 5(2): 170-176.

58. Mount, D.W. 2008. Using BLOSUM in sequence alignments. *Cold Spring Harbor Protocols*, 3(6): 1. https://doi.org/10.1101/pdb.top39

59. NCBI. 2019. *NCBI Virus*. Www.Ncbi.Nlm.Nih.Gov/Labs/Virus. https://www.ncbi.nlm.nih.gov/labs/virus/vssi/#/

60. Ou, J., Zhou, Z., Dai, R., Zhang, J., Lan, W., Zhao, S., Wu, J., Seto, D., Cui, L., Zhang, G. & Zhang, Q. 2020. Emergence of RBD mutations from circulating SARS-CoV-2 strains with enhanced structural stability and higher human ACE2 receptor affinity of the spike protein. *BioRxiv*, 2020.03.15.991844. https://doi.org/10.1101/2020.03.15.991844

61. Ou, X., Liu, Y., Lei, X., Li, P., Mi, D., Ren, L., Guo, L., Guo, R., Chen, T., Hu, J., Xiang, Z., Mu, Z., Chen, X., Chen, J., Hu, K., Jin, Q., Wang, J. & Qian, Z. 2020. Characterization of spike glycoprotein of SARS-CoV-2 on virus entry and its immune cross-reactivity with SARS-CoV. *Nature Communications*, 11(1620): 1-12.

62. Ou, X., Zheng, W., Shan, Y., Mu, Z., Dominguez, S.R., Holmes, K.V. & Qian, Z. 2016. Identification of the Fusion Peptide-Containing Region in Betacoronavirus Spike Glycoproteins. *Journal of Virology*, 90(12): 5586-5600.

63. Peisajovich, S.G. & Shai, Y. 2003. Viral fusion proteins: Multiple regions contribute to membrane fusion. *Biochimica et Biophysica Acta - Biomembranes*, 1614(1): 122-129.

64. Perin, P.M., Haid, S., Brown, R.J.P., Doerrbecker, J., Schulze, K., Zeilinger, C., Schaewen, M., Heller, B., Vercauteren, K., Luxenburger, E., Baktash, Y.M., Vondran, F.W.R., Speerstra, S., Awadh, A., Mukhtarov, F., Schang, L.M., Kirschning, A., Müller, R., Guzman, C.A., Kaderali, L., Randall, G., Meuleman, P., Ploss, A. & Pietschmann, T. 2016. Flunarizine prevents hepatitis C virus membrane fusion in a genotype-dependent manner by targeting the potential fusion peptide within E1. *Hepatology*, 63(1): 49-62.

65. Perlman, S. 2020. Another decade, another coronavirus. In *New England Journal of Medicine*, 382(8): 760-762.

66. Phan, T. 2020. Novel coronavirus: From discovery to clinical diagnostics. *Infection, Genetics and Evolution*, 79(104211): 1-2.

67. Remmert, M., Biegert, A., Hauser, A. & Söding, J. 2012. HHblits: Lightning-fast iterative protein sequence searching by HMM-HMM alignment. *Nature Methods*, 9(2): 173-175.

68. Santos, R.A.S., Oudit, G.Y., Verano-Braga, T., Canta, G., Steckelings, U.M. & Bader, M. 2019. The renin-angiotensin system: going beyond the classical paradigms. *American Journal of Physiology-Heart and Circulatory Physiology*, 316(5): 958-970.

69. Shang, J., Wan, Y., Luo, C., Ye, G., Geng, Q., Auerbach, A. & Li, F. 2020a. Cell entry mechanisms of SARS-CoV-2. *PNAS*, 117(21): 11727-11734.

70. Shang, J., Wan, Y., Liu, C., Yount, B., Gully, K., Yang, Y., Auerbach, A., Peng, G., Baric, R. & Li, F. 2020b. Structure of mouse coronavirus spike protein complexed with receptor reveals mechanism for viral entry. *PLoS Pathogens*, 16(3): e1008392.

71. Shang, J., Ye, G., Shi, K., Wan, Y., Luo, C., Aihara, H., Geng, Q., Auerbach, A. & Li, F. 2020c. Structural basis of receptor recognition by SARS-CoV-2. *Nature*, 581, 221-224.

72. Srivastava, A., Bandopadhyay, A., Das, D., Pandey, R.K., Singh, V., Khanam, N., Srivastava, N., Singh, P.P., Dubey, P.K., Pathak, A., Gupta, P., Rai, N., Sultana, G.N.N. & Chaubey, G. 2020. Genetic association of ACE2 rs2285666 polymorphism with Covid-19 spatial distribution in India. Frontiers in Genetics, 11(564741): 1-6.

73. Torresi, J. 2008. Hepatitis B antiviral resistance and vaccine escape: Two sides of the same coin. *Antiviral Therapy*, 13(3): 337-340.

74. Vermeire, K., Bell, T.W., Van Puyenbroeck, V., Giraut, A., Noppen, S., Liekens, S., Schols, D., Hartmann, E., Kalies, K.U. & Marsh, M. 2014. Signal Peptide-Binding Drug as a Selective Inhibitor of Co-Translational Protein Translocation. *PLoS Biology*, 12(12): e1002011.

75. Walls, A.C., Park, Y.J., Tortorici, M.A., Wall, A., McGuire, A.T. & Veesler, D. 2020. Structure, Function, and Antigenicity of the SARS-CoV-2 Spike Glycoprotein. *Cell*, 181(2): 281-292.

76. Walls, A.C., Tortorici, M.A., Snijder, J., Xiong, X., Bosch, B.J., Rey, F.A. & Veesler, D. 2017. Tectonic conformational changes of a coronavirus spike glycoprotein promote membrane fusion. *Proceedings of the National Academy of Sciences of the United States of America*, 114(42): 11157-11162.

77. Waterhouse, A., Bertoni, M., Bienert, S., Studer, G., Tauriello, G., Gumienny, R., Heer, F.T., De Beer, T.A.P., Rempfer, C., Bordoli, L., Lepore, R. & Schwede, T. 2018. SWISS-MODEL: Homology modelling of protein structures and complexes. *Nucleic Acids Research*, 46(W1): W296-W303.

78. Wilkins, M.R., Gasteiger, E., Bairoch, A., Sanchez, J.C., Williams, K.L., Appel, R.D. & Hochstrasser, D.F. 1999. Protein identification and analysis tools in the ExPASy server. *Methods in Molecular Biology*, 112: 531-552.

79. Worldometer. 2020. Coronavirus Cases. In *Worldometer* (pp. 1-22).

80. Wrapp, D., Wang, N., Corbett, K.S., Goldsmith, J.A., Hsieh, C.L., Abiona, O., Graham, B.S. & McLellan, J.S. 2020. Cryo-EM structure of the 2019-nCoV spike in the prefusion conformation. *Science*, 367(6483): 1260-1263.

81. Wu, F., Zhao, S., Yu, B., Chen, Y.-M., Wang, W., Hu, Y., Song, Z.-G., Tao, Z.-W., Tian, J.-H., Pei, Y.-Y., Yuan, M.-L., Zhang, Y.-L., Dai, F.-H., Liu, Y., Wang, Q.-M., Zheng, J.-J., Xu, L., Holmes, E.C. & Zhang, Y.Z. 2020. Complete genome characterisation of a novel coronavirus associated with severe human respiratory disease in Wuhan, China. *BioRxiv*, 2020.01.24.919183. https://doi.org/10.1101/2020.01.24.919183

82. Yang, L., Cheng, Y., Zhao, X., Wei, H., Tan, M., Li, X., Zhu, W., Huang, W., Chen, W., Liu, J., Li, Z., Shu, Y. & Wang, D. 2019. Mutations associated with egg adaptation of influenza A(H1N1)pdm09 virus in laboratory based surveillance in China, 2009-2016. *Biosafety and Health*, 1(1): 41-45.

83. Zhang, M., Zeng, C.Q.-Y., Dong, Y., Ball, J.M., Saif, L.J., Morris, A.P. & Estes, M.K. 1998. Mutations in Rotavirus Nonstructural Glycoprotein NSP4 Are Associated with Altered Virus Virulence. *Journal of Virology*, 72(5): 3666-3672.

84. Zhou, P., Yang, X.-L., Wang, X.G., Hu, B., Zhang, L., Zhang, W., Si, H.R., Zhu, Y., Li, B., Huang, C.L., Chen, H.D., Chen, J., Luo, Y., Guo, H., Jiang, R.-Di, Liu, M.Q., Chen, Y., Shen, X.R., Wang, X., Zheng, X.S., Zhao, K., Chen, Q.J., Deng, F., Liu, L.L., Yan, B., Zhan, F., Wang, Y., Xiao, G.F. & Shi, Z.L. 2020. A pneumonia outbreak associated with a new coronavirus of probable bat origin. *Nature*, 579(7798): 270-273.

85. Zhu, N., Zhang, D., Wang, W., Li, X., Yang, B., Song, J., Zhao, X., Huang, B., Shi, W., Lu, R., Niu, P., Zhan, F., Ma, X., Wang, D., Xu, W., Wu, G., Gao, G.F. & Tan, W. (2020). A novel coronavirus from patients with pneumonia in China, 2019. *New England Journal of Medicine*, 382(8): 727-733.

*http://dergipark.org.tr/trkjnat*
*Trakya University Journal of Natural Sciences, 22(1): 35-42, 2021*
*ISSN 2147-0294, e-ISSN 2528-9691*
*DOI: 10.23902/trkjnat.806802*

**Research Article**

# EFFECT OF MODERATE STATIC MAGNETIC FIELD ON HUMAN BONE MARROW MESENCHYMAL STEM CELLS: A PRELIMINARY STUDY FOR REGENERATIVE MEDICINE

Kaya MOLO, Emel ORDU*

Department of Molecular Biology and Genetics, Faculty of Arts and Science, Yıldız Technical University, İstanbul, TURKEY

**Cite this article as:**

Molo K. & Ordu E. 2021. Effect of Moderate Static Magnetic Field on Human Bone Marrow Mesenchymal Stem Cells: a Preliminary Study for Regenerative Medicine. *Trakya Univ J Nat Sci*, 22(1): 35-42, DOI: 10.23902/trkjnat.806802

Received: 07 October 2020, Accepted: 21 January 2021, Online First: 17 February 2021, Published: 15 April 2021

**Abstract:** Static Magnetic Field (SMF) is one of the biophysiological stimulants which modulates physiological processes in different cell lines. Mesenchymal stem cells (MSCs) are important biological tools for regenerative medicine. Although it is known that SMFs cause a change in cellular membrane polarization, oxidative product concentrations, gene expression patterns and cell propagation rates, depending on exposure time and intensity, their effects on MSCs have not been properly explained yet. In this study, MSCs derived from human bone marrow were treated with moderate 328 mT SMF by using cylindric Neodymium Iron Boron ($Nd_2Fe_{14}B$) magnets to investigate its influence on orientation, proliferation rates and morphologies. Results showed that the treated cells gained more homogenous orientation than the non-treated cells, however SMF influence did not significantly change proliferation rates.

The cells were grown under both chemically osteogenic induction and SMF to observe the osteogenic differentiation and biomineralization. Alkaline phosphatase (ALP) activity decreased significantly in the cells treated with SMF compared to the control groups. Alizarin Red S staining showed that mineralization also decreased in the cells. The results showed that an easily produced moderate SMF can be a useful physical stimulant to control the fate of MSC both *in vitro* and *in vivo*.

**Özet:** Statik Manyetik Alan (SMA), farklı hücre hatlarında fizyolojik süreçleri düzenleyen biyofizyolojik uyarıcılardan biridir. Mezenkimal kök hücreler (MKH'ler) rejeneratif tıp için önemli biyolojik araçlardır. SMA'ların yoğunluğuna ve süresine göre hücre membran polarizasyonunu, oksidatif ürün konsantrasyonlarını, gen ekspresyon modellerini ve hücre çoğalma oranlarını değiştirdiği bilinmesine rağmen, MKH'ler üzerindeki SMA etkileri henüz tam olarak açıklanmamıştır. Bu çalışmada, insan kemik iliği kaynaklı MKH'ler, silindirik Neodimyum Demir Bor ($Nd_2Fe_{14}B$) mıknatıslar kullanılarak orta derecede 328 mT SMA etkisinde bırakıldı ve hücrelerin oryantasyonu, çoğalma oranı ve osteojenik farklılaşma potansiyelleri incelendi. Sonuçlar, tedavi edilen hücrelerin, tedavi edilmeyen hücrelerden daha homojen bir yönelim kazandığını, ancak SMF etkisinin çoğalma oranlarını önemli ölçüde değiştirmediğini gösterdi.

MKH'ler, osteojenik farklılaşmayı ve biyomineralizasyonu gözlemlemek için hem kimyasal olarak osteojenik indüksiyon hem de SMA altında büyütüldüğünde, Alkalin Fosfataz (ALP) aktivitesi kontrol gruplarına kıyasla önemli ölçüde azaldı. Alizarin Red S boyaması, uyarılan hücrelerde mineralleşmenin de azaldığını gösterdi. Sunulan sonuçlar, kolayca üretilen orta düzeyde bir SMA'nın *in vitro* veya *in vivo* olarak MKH kaderini kontrol etmek için yararlı bir fiziksel uyarıcı olabileceğinin altını çizmektedir.

***Edited by:***
*Reşat Ünal*

***Corresponding Author:***
*Emel Ordu*
*bemel@yildiz.edu.tr*

***ORCID iDs of the authors:***
*K.M. orcid.org/0000-0001-6168-2058*
*E.O. orcid.org/0000-0003-3060-2806*

***Key words:***
*Bone marrow mesenchymal stem/stromal cells,*
*Static magnetic field,*
*Osteogenesis*

## Introduction

In medicine, morphological and functional repair techniques, as well as regeneration of damaged or aged cells, tissues, or organs, are rapidly growing. These approaches need available cell sources that provide appropriate new tissue components or paracrine effects. Due to this reason, stem cells have been gaining much attention for the last three decades (Rajabzadeh *et al.* 2019, Suman *et al.* 2019).

Stem cells are commonly characterized by their unspecialized nature and their high ability for self-renewal and differentiation into functional cell types of the organism. After the embryonic development stage, multipotent stem cells reside in numerous tissues of the body. Tissues conserve their continuity and regulate their micro-environment by the functions of these stem cells (Rajabzadeh *et al.* 2019, Suman *et al.* 2019).

A new type of multipotent stem cells derived from bone marrow was discovered by the pioneering studies of Friedenstein *et al.* in the 1960s. These cells adhere to plastic surfaces and have a fibroblastic appearance. Although Friedenstein called them osteoprogenitors, subsequent studies showed that they can differentiate into osteoblasts, chondrocytes and adipocytes, and regulate the hematopoietic microenvironment in the bone marrow. This special stem cell type is currently known as mesenchymal stem/stromal cells (MSCs) (Keating 2017, Trohatou & Roubelakis 2017).

Although MSCs were first isolated from bone marrow, they can also be isolated by less invasive techniques from adipose tissue, placenta, Wharton jelly, umbilical cord blood, and amniotic fluid. In addition to their high self-renewal and differentiation potential *in vitro* and *in vivo*, they have paracrine effects that promote immunomodulation in addition to anti-apoptotic and anti-oxidative effects (Brown *et al.* 2019). These properties of MSCs make them a good tool for regenerative medicine.

During embryonic development and through the entire life of an organism, cells are constantly exposed to a variety of mechanical stimulations, e.g., muscle force, gravity, blood flow and other physical forces or processes. The interactions between cells and mechanical or physical factors are critical to the health and function of various tissues and organs of the body and are believed that they have important roles in diseases, e.g., atherosclerosis, osteoarthritis and osteoporosis (Guilak *et al.* 2009).

A static magnetic field (SMF) is described as a constant, non-changing vector field of an electrical current or a permanent magnet. The SMF is also a force that interacts with biological systems (Lohmann & Lohmann 2019). Magnetic Resonance Imagining (MRI) presents one of the interaction examples between SMF and tissues, cells or biomolecules (Marycz *et al.* 2018). Magnetism and its effects on healing also have a place in both traditional and modern medicine (Markov 2007, 2015).

We aimed to seek interaction between bone marrow-derived mesenchymal stem/stromal cells (BM-MSC) and moderate SMF in this preliminary study.

## Materials and Methods

*Bone Marrow Mesenchymal Stem/Stromal Cells Cell Culture*

Cryopreserved human BM-MSCs were purchased from Stem Cell and Gene Therapy Research and Application Center, Kocaeli University-Turkey. NutriStem Cell XF Basal Medium (Cat.# 05-200-1A, Biological Industries-USA) supplemented with NutriStem XF Supplement XF (Cat.# 05-201-1U, Biological Industries-USA) for BM-MSC propagation or Stempro Basal Medium (Cat.# A10069-01, Thermo Fisher-USA) supplemented with Stempro Osteogenesis Supplement (Cat.#A10066-01, Thermo Fisher-USA) for osteogenesis induction of BM-MSCs were used in cell cultures. The cells were incubated at 37 °C with 5 % $CO_2$ and 100 % humidity (Biosan ES20 incubator-Latvia) in all experiments.

*Static Magnetic Field Source and Magnetic Flux Density (B)*

Two cylindrical Neodymium-Iron-Boron ($Nd_2Fe_{14}B$) magnets with 22 mm diameters (Mıknatıs Teknik-Turkey) were used as SMF sources. The magnets were on top of each other underneath the 12-well plate (TPP-USA) (Figs 1a, b). Each of the magnets has enough surface area to cover one of the assay wells of 12-well plate (Fig. 1c). The diameter of each well in the 12-well plate was 21 mm. The magnetic field flux density or magnetic induction (B) produced by two magnets on top of each other was measured as 328 mT by AC/DC Magnetic Meter PCE-MFM 3000. B is the number of lines of force passing through a unit area of material (Stefanita CG 2012; Wills & Finch 2015). All control groups were grown in Earth's magnetic field.

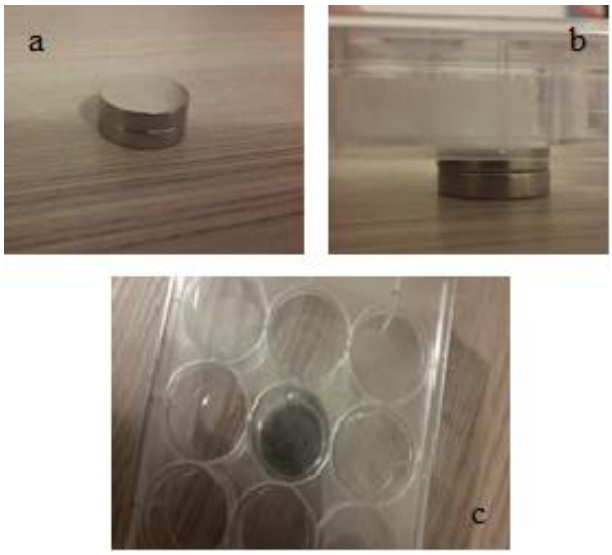


**Fig. 1.** Two cylindrical Neodymum-Iron-Boron ($Nd_2Fe_{14}B$) magnets provided the 328 mT SMF. **a)** All magnents were placed top on top, **b)** Assay wells of 12-well plates were put on surface of the magnets, **c)** Each of the magnets had enough surface area to cover interior surface of a well.

*Determination of Cell Orientation under 328 mT SMF Influence*

To observe and measure whether human BM-MSCs gain an orientation under 328 mT SMF, the cells in 12-well plates were grown in NutriStem Cell XF Basal Medium supplemented with NutriStem XF Supplement

XF with or without the SMF influence for 6 days. Two separate 12-well plates were used to minimize the magnetic exposure of the control group. On day 0, 10780 cells/well were plated into the three wells of each 12-well plates. One of the plates was used as the control and was not exposed to SMF. The second plate was placed on top of the $Nd_2Fe_{14}B$ magnets. On the 6$^{th}$ day, the cells were photographed under an inverted microscope with a camera attachment (Zeiss Axiovert A01-Germany). The camera was operated in 20x magnification.

All images were pre-processed with the open-source software ImageJ [http://imagej.nih.gov/ij/index.html] and a fully automated analysis of cell orientation was obtained utilizing the OrientationJ plugin.

*Determination of Cell Proliferation and Growth under 328 mT SMF Influence*

Two separate 12-well plates were used to minimize the magnetic exposure of the control group. On day 0, 10780 cells/well were plated into the three wells of each 12-well plates. One of the plates was used as the control without exposure to magnetic influence. The second plate was placed on top of the $Nd_2Fe_{14}B$ magnets. The cultures were fed with The NutriStem Cell XF Basal Medium supplemented with NutriStem XF Supplement XF. On the 6$^{th}$ day, the cell growth and propagation were measured after incubation for 3 hours with MTT (3-(4,5-dimethylthiazol-2-yl)- 2,5-diphenyltetrazolium bromide) salt (Cat# M2003, Sigma-USA). After the incubation, purple/blue formazan crystals were solubilized by the addition of 300 µL DMSO (dimethyl sulfoxide) (Cat# D2650, Sigma-USA). 100 µL solution was taken and measured at 570 nm and 650 nm in a spectrophotometric plate reader (BIOTEK-USA).

*Determination of Biomineral Accumulation and Osteogenic Differentiation under 328 mT SMF Influence*

To determine and measure biomineral accumulation and osteogenic differentiation, two control groups and two assay groups in separate 12 well plates were prepared. The cells were plated intro the three wells of each plates.. On day 0, 70000-80000 human BM-MSCs/ well were incubated in NutriStem Cell XF Basal Medium supplemented with NutriStem XF Supplement XF. On the 1$^{st}$ day, all medium was changed according to the experiment setting.

The 1$^{st}$ control group was the BM-MSCs which were incubated in NutriStem Cell XF Basal Medium supplemented with NutriStem XF Supplement XF. The 2$^{nd}$ control group was the BM-MSCs which were incubated in Stempro Basal Medium supplemented with Stempro Osteogenesis Supplement. The 1$^{st}$ assay group was the BM-MSCs that were incubated in NutriStem Cell XF Basal Medium supplemented with NutriStem XF Supplement XF under 328 mT SMF influence. The 2$^{nd}$ assay group was the BM-MSCs that were incubated in Stempro Basal Medium supplemented with Stempro Osteogenesis Supplement under 328 mT SMF influence. The experiment duration was 14 days in total.

Biomineralization was determined with Alizarin Red S (pH: 4.1-4.3) staining. On the 14$^{th}$ day, all medium was poured out. The cells were fixed by 500 µL 4 % buffered formalin solution for 30 minutes. After washing two times with $dH_2O$, 1 mL Alizarin Red S staining solution was added to every culture well and incubated for 20 minutes. After incubation, the control and assay wells were washed with $dH_2O$ four times. Stained control and assay wells were photographed.

Osteogenesis was determined with Alkaline Phosphatase (ALP) activity. On the 14$^{th}$ day, all medium was poured out. The cells were lysed by two freeze and thaw cycles in phosphate buffer containing 1 % (v/v) Triton x-100. 1 mg/mL ALP substrate (p-nitrophenol phosphate, p-npp) (20-106, Sigma-USA) solution was prepared in a solution containing 1 M diethanolamine, 0.5 M $MgCl_2$ (pH 9.8). 75 µL cell lysate and 25 µL ALP substrate solutions were mixed and incubated for 20 seconds. ALP activity was measured at 405 nm by a spectrophotometric plate reader.

*Statistical Analysis*

An unpaired student t-test was used to determine the statistical significance of the differences between control and assay groups with $P<0.05$ accepted as significant.

## Results

*328 mT SMF Effects on Human BM-MSCs Orientation*

The human BM-MSCs groups grown in wells without 328 mT SMF influence (Fig. 2a) and the human BM-MSCs groups grown in wells with 328 mT SMF influence (Fig. 2c) were photographed by 20x magnification after 6 hours of SMF exposure. OrientationJ, a plugin of ImageJ was used to infer the preferred orientation of structures in these images. OrientationJ computed histograms for the control groups (Fig. 2b) and the assay groups (Fig. 2d). The preferred orientation in Fig. 2d was seen as a homogenous histogram with a peak. However, the control group revealed a heterogenous histogram with multiple peaks (Fig 2b).

OrientationJ was also used to produce an orientation map. The images shown in Fig. 2a and Fig. 2c were colored according to their local directionality. The multi-directionality in Fig. 2a was seen as a multi-chromic plane. However, increased mono-directionality was seen as a mono-chromic plane (Fig. 2c).

*328 mT SMF Effects on Human BM-MSCs Proliferation and Growth*

Cell viability and growth in both the control and assay groups were determined by the MTT analysis after 8 hours of SMF exposure. Cell count in the control and assay groups reached to mean 199300 cells /well and 253744 cells/well, respectively (Table 1). The difference between the groups was not statistically significant (two-tailed $P = 0.2055$).

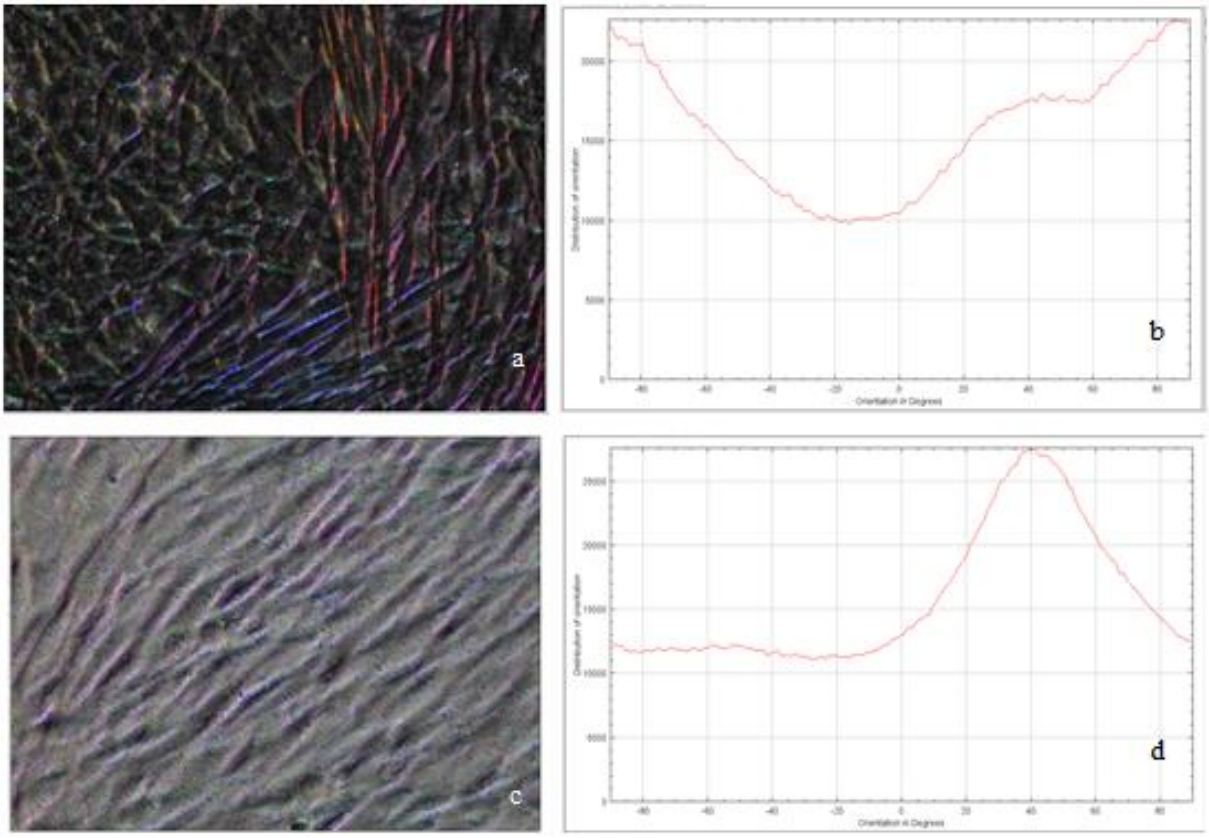


**Fig. 2.** 328 mT SMF effect on the human BM-MSC orientation. All microscopic photos were taken by 20x magnification. **a)** The cells grown as control group without artificial SMF influence. Multichromatic cells represent multi-directionality of the cells. **b)** shows the orientation, in degrees, of the cells in a. **c)** The cells were grown as assay group with artificial 328 mT SMF influence. Monochromatic cells irepresent mono-directionality of the cells. **d**) shows the orientation, in degrees, of the cells c.

**Table 1.** Compression of viable vell counts between the control and assay groups.

| Control Groups (Without 328 mT SMF Influence) | Viable Cell Count/well | Assay Groups (With 328 mT SMF Influence) | Viable Cell Count/well |
|---|---|---|---|
| 1st control well | 134,300 | 1st assay well | 256,633 |
| 2nd control well | 213,800 | 2nd assay well | 232,300 |
| 3rd control well | 249,800 | 3rd assay well | 272,300 |
| **Sample Number** | **3** | **Sample Number** | **3** |
| **Mean** | **199,300** | **Mean** | **253,744** |
| **Standard Deviation** | **59,099.49** | **Standard Deviation** | **20,155.85** |
| two tailed P = 0.2055 | | | |

*328 mT SMF Effects on Biomineral Accumulation and Osteogenic Differentiation of Human BM-MSCs*

To observe the effect of SMF on osteogenesis, two different cell culture mediums i) Stempro Basal Medium supplemented with Stempro Osteogenesis Supplement, an osteogenesis-stimulating medium, ii) NutriStem Cell XF Basal Medium for proliferation were compared. The osteogenesis process of BM-MSCs under the 328 mT SMF was evaluated by measuring ALP activity and biomineralization.

ALP activity of the cells were compared on the 14th day of incubation in NutriStem Cell XF Basal Medium supplemented with NutriStem XF Supplement XF with or without continuous 328 mT SMF treatment. The mean values of ALP activities of the cells treated and non-treated by continuous 328 mT SMF for 14 days were 11.844 IU/L and 13.575 IU/L, respectively (Table 2). Statistical evaluation of the ALP activities between the groups showed that the effect of SMF exposure was not significantly different (two-tailed P= 0.1015).

Osteogenesis was induced using the Stempro Osteogenesis Differentiation Kit and ALP activities of the cells were compared after 14 days of incubation in Stempro Basal Medium supplemented with Stempro Osteogenesis Supplement with or without continuous 328 mT SMF treatment. The mean ALP activities of the cells treated and non-treated by continuous 328 mT SMF for 14 days were 31.367 IU/L and 25.966 IU/L, respectively (Table 3). Results showed that the difference between ALP activities of the two groups was statistically significant (two-tailed P = 0.0336).

**Table 2.** IU/ALP activities of human BM-MSCs were grown in NutriStem Cell XF Basal Medium supplemented with NutriStem XF Supplement XF without or with 328 mT SMF treatment.

| 1st control (Without 328 mT SMF Influence) | 1st control IU/ALP Activity | 1st assay (With 328 mT SMF Influence) | 1st assay IU/ALP Activity |
|---|---|---|---|
| Control well | 10.549 | Assay well | 13.216 |
| Control well | 11.701 | Assay well | 13.589 |
| Control well | 13.280 | Assay well | 13.920 |
| **Sample Number** | **3** | **Sample Number** | **3** |
| **Mean** | **11.844** | **Mean** | **13.575** |
| **Standard Deviation** | **1.371** | **Standard Deviation** | **0.352** |
| two-tailed P = 0.1015 | | | |

**Table 3.** IU/ALP activities of human BM-MSCs were grown in Stempro Basal Medium supplemented with Stempro Osteogenesis Supplement without or with 328 mT SMF treatment.

| 2nd control (Without 328 mT SMF Influence) | 2nd control IU/ALP Activity | 2nd assay (With 328 mT SMF Influence) | 2nd assay IU/ALP Activity |
|---|---|---|---|
| Control well | 30.709 | Assay well | 26.517 |
| Control well | 32.768 | Assay well | 23.051 |
| Control well | 30.624 | Assay well | 28.331 |
| **Sample Number** | **3** | **Sample Number** | **3** |
| **Mean** | **31.367** | **Mean** | **25.966** |
| **Standard Deviation** | **1.214** | **Standard Deviation** | **2.682** |
| two-tailed P = 0.0336 | | | |

Biomineralization was compared by Alizarin Red S staining at the end of the 14th day of incubation in NutriStem Cell XF Basal Medium supplemented with NutriStem XF Supplement XF with or without continuous 328 mT SMF treatment. No difference was observed in staining patterns between the control and assay groups (Fig. 3a, b). When biomineralization was compared by Alizarin Red S staining in Stempro Basal Medium supplemented with Stempro Osteogenesis Supplement with or without continuous 328 mT SMF treatment, the results showed that the staining in the groups treated continuous 328 mT SMF for 14 days was less than the groups grown without 328 mT SMF influence (Figs 4a, b).

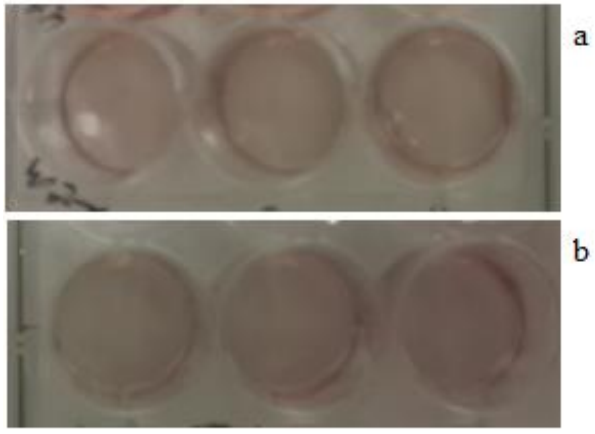


**Fig. 3.** After Alizarin Red S staining, comparison of the 1st control and 1st assay. **a)** 1st control, human BM-MSCs were grown in NutriStem Cell XF Basal Medium supplemented with NutriStem XF Supplement XF without 328 mT SMF Treatment, **b)** 1st assay, human BM-MSCs were grown in NutriStem Cell XF Basal Medium supplemented with NutriStem XF Supplement XF with 328 mT SMF treatment.

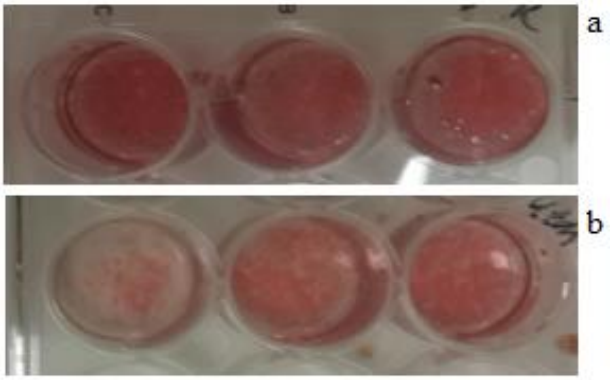


**Fig. 4.** After Alizarin Red S staining, comparison of the 2nd control and 2nd assay. **a)** 2nd control, human BM-MSCs were grown in Stempro Basal Medium supplemented with Stempro Osteogenesis Supplement without 328 mT SMF treatment, **b)** 2nd assay, human BM-MSCs were grown in Stempro Basal Medium supplemented with Stempro Osteogenesis Supplement with 328 mT SMF treatment.

## Discussion

A natural magnetic field (geomagnetic field) or an artificial magnetic field is a physical parameter of the environment just as temperature, humidity, or altitude. Magnetic fields impact biological or organic systems as well as inorganic systems or matters. These influences are determined by magnetic susceptibility of the objects, magnetic field intensity or magnetic field flux density, and gradient. However, the kind of a magnetic field source (an electrical flux or a permanent magnet) has no special effect on the results. Salmons and turtles determine their natal homing behavior by the geomagnetic changes or intensities (Lohmann & Lohmann 2019). Cells can give responses to any magnetic field with their various structures or biomolecules (membranes, mitochondria, nucleic acids, and proteins) (Zhang *et al.* 2017a). In this

preliminary study, $Nd_2Fe_{14}B$ magnets easily produced a SMF. In the SMF, the magnetic field intensity or magnetic field flux density does not change according to time. The geomagnetic field and magnetic field used in Magnetic Resonance Imagining (MRI) are the SMF. It is a more suitable magnetic field with less changeable parameters to observe its influence or effects on biological systems. The SMFs are classified according to their magnetic flux density (B) as weak (<1 mT), moderate (1 mT-1 T), strong (1 T-5 T), and ultrastrong (>5 T) (Zhang *et al.* 2017b). Although there is substantial evidence on the biological effects of moderate SMF, the results of the effects are controversial, and the mechanism of the effects are still not clear. In this study, moderate (328 mT) SMF effects on cells were evaluated.

Mesenchymal stem/stromal cells (MSCs) with differentiation ability to multiple into mesodermal cell types (osteoblast, chondrocyte, and adipocyte) and modulative secretome are the main tools for regenerative medicine and cell therapies (Fitzsimmons *et al.* 2018). Although the MSCs were isolated and propagated from various tissues or tissue areas including bone marrow, adipose tissue, dental pulp, placenta, Wharton Jelly, umbilical cord blood, and other perivascular areas with similar phenotypic characteristics and differentiation abilities, bone marrow-derived MSCs (BM-MSCs) are the most extensively studied one, especially for bone regeneration and osteogenesis.

The MSCs cultured *in vitro* can be chemically induced to differentiate to the bone and other mesodermal cell types. Common biochemical agents and growth factors for osteogenesis are dexamethasone, indomethacin, and Bone Morphogenic Proteins (BMPs). Tissue regeneration methods utilize these factors to produce tissue constructs *in vitro* that are ready for implantation *in vivo* and to reduce healing time. MSCs are also highly mechanosensitive *in vitro* and *in vivo*. A mechanical stimulation as tensile strain induces MSCs for osteogenesis and tendogenesis but inhibits adipogenesis. Other mechanical stimulations as hydrostatic pressure and compressive loading induce MSCs for chondrogenesis. Therefore, mechanical stimulations are also another effector for tissue regeneration methods to determine or modulate MSCs fate (Delaine-Smith & Reilly 2012). The SMF is one of the mechanical stimulants for cellular structures and electrochemical flux on cellular membranes. However, its effects on especially stem cell physiology are poorly discussed. If there are any SMF effects on stem cell fate, its degree, condition and mechanism should be determined by detailed studies (Marycz *et al.* 2018).

Murayama *et al.* (1965) were the first to report cell orientation under SMF influence. Deoxygenized sickled erythrocytes in a suspension gained a pendicular orientation under 0,35 T SMF influence. Kotani *et al.* (2002) observed MC3T3-E1 cells orientation toward magnetic field flux direction after constant 60 hours of 8 T SMF influence. Ogiue-Ikeda *et al.* (2004) showed that A7r5 cells (smooth muscle cell, spindle shape) were orientated after a 60 hour magnetic field (8T) exposure only when the cells were seeded with high cell density ($1x10^5$ cells/$cm^2$). On the other hand, when the cells were in confluent condition at the start point of the magnetic field exposure, the cells were not oriented. Sadri *et al.* (2018) showed that Wharton Jelly derived mesenchymal stem cells gain parallel orientation in 8 hours and 18 mT SMF influence. However, orientation in SMF influence depends on cell shape. For example, Human kidney HFK293 cells in 8 T SMF influence and Human glioblastoma cells 10 T SMF influence, which are both polygonal shaped cells preferred orientation was not observed. Also, cellular orientation in the SMF influence depends on magnetic flux density or magnetic intensity. This orientation tendency is produced by the SMF influence on non-global diamagnetic anisotropic particles or molecules. This creates a torque on these structures. This effect is especially seen in membrane proteins, microtubes and actin filaments (Zhang, *et al.* 2017b). In our study, we observed that human BM-MSCs in high density but still proliferating cultures gain orientation in moderate 328 mT SMF influence (Figs 2a-d). Although the floating cells as erythrocytes gain an orientation under a static magnetic field in few seconds, the time for adherent cells such as osteoblasts gaining an orientation is in 10 times longer. The starting cell density and assay duration give a chance for orientation under the static magnetic field exposure.

There are contradictory results about the SMF effect on cell proliferation and growth. Kim *et al.* (2015) observed an increased BM-MSC proliferation during 3 mT, 15 mT, and 50 mT SMF treatment for 1, 3, 5, 7, and 9 days exposures, respectively. Maredziak *et al.* (2017) also determined an increasing proliferation in adipose tissue-derived MSCs in 0,5 T SMF treatment for 7 days. However, Silva *et al.* (2018) observed decreased viability of mouse BM-MSC with or without magnetized nanoparticles in 0.3-0.45 T SMF treatment for 48 hours. Cunha *et al.* (2012) also observed decreased proliferation and growth rate of human osteoblast in 320 mT SMF treatment for 1, 3, and 7 days. Yamamato *et al.* (2003) observed an unchanged proliferation and growth rates of rat osteoblasts in 280 mT or 340 mT SMF treatment for 2, 4, 6, 8, and 10 days. We also observed an unchanged proliferation and growth rate of human BM-MSC in 328 mT SMF for 6 days (Table 1 and Fig. 3). Yamamato *et al.* (2003) explained the unchanged proliferation rates as an increased S phase but non-triggered G2/M transition.

A metalloenzyme Alkaline Phosphatase (ALP) is expressed in high concentrations in bone tissues and hydrolases phosphomonoesters. During biomineralization, ALP local concentration increases and triggers the process. ALP activity decreases and the bones become soft with insufficient biomineralization in a heredity hypo-phosphatase disorder (Golub & Boesze-Battaglia 2007). In this study, the ALP activity was compared between groups treated with or without

continuous 328 mT SMF for 14 days. It was observed that the ALP activity decreased in the groups treated with 328 mT SMF. Decreased biomineralization or staining with Alizarin Red S was also seen in the groups treated with continuous 328 mT SMF for 14 days. Wang *et al*. (2016) observed a decreased osteogenic differentiation in adipose tissue-derived MSCs treated with continuous 0.5 T for 7 days. Also, Yang *et al.* (2018) observed a decreased ALP activity and biomineralization in MC3T3-E1 cells treated continuous 200 mT SMF for 8 days. However, there are also contradictory results in this regard. Increased ALP activity and biomineralization in MC3T3-E1 cells treated with 16 T SMF were observed (Yang *et al.* 2018).

In conclusion, a static magnetic field is an easily obtainable and controllable physical stimulant for organisms and cells. Therefore, it can be an effective medical tool. MSCs have a main role in tissue regeneration and cell therapies by differentiation and paracrine effects. Their affectivity and distribution can be controlled by the SMF influence.

**Ethics Committee Approval:** Since the article does not contain any studies with human or animal subject, its approval to the ethics committee was not required.

**Author Contributions:** Design: E.O., Execution: K.M., Data analysis/interpretation: K.M., E.O., Manuscript writing: K.M., E.O.

**Conflict of Interest:** The authors have no conflicts of interest to declare.

**Funding:** This work was supported by the Research Fund of Yıldız Technical University, Project Number: FYL-2019-3520.

## References

1. Brown, C., McKee, C., Bakshil, S., Walker, K., Hakman, E., Halassy, S., Svinarich, D., Dodds, R., Govind, C.K. & Chaudhry, G.R. 2019. Mesenchymal stem cells: Cell therapy and regeneration. *Journal of Tissue Engineering and Regenerative Medicine*, 13(9): 1738-1755. https://doi.org/ 10.1002/term.2914
2. Cunha, C., Panseri, S., Marcacci, M., Tampieri, A. 2012. Evaluation of the effects of a moderate intensity static magnetic field application on human osteoblast-like cells. *American Journal of Biomedical Engineering*, 2(6): 263-268. https://doi.org/10.5923/j.ajbe.20120206.05
3. Delaine-Smith, R.M. & Reilly, G.C. 2012. Mesenchymal stem cell responses to mechanical stimuli. *Muscles Ligaments Tendons Journal*, 2(3): 169-180.
4. Fitzsimmons, R.E.B., Mazurek, M.S., Soos, A. & Simmons, C.A. 2018. Mesenchymal stromal/stem cells in regenerative medicine and tissue engineering. *Stem Cell International*, 2018: 8031718. https://doi.org/10.1155/2018/8031718
5. Friedenstein, A.J., Piatetzky Shapiro I.I. & Petrakova, K.V. 1966. Development in transplants of bone marrow cells. *Journal of Embryology and Experimental Morphology*, 16(3): 381-390.
6. Guilak, F., Cohen, D.M., Estes, B.T., Gimble, J.M., Liedtke, W. & Chen, C.S. 2009. Control of stem cell fate by physical interactions with the extracellular matrix. *Cell Stem Cell*, 5(1):17-26. https://doi.org/10.1016/j.stem.2009.06.016
7. Golub, E. & Boesze-Battaglia, K. 2007. The role of alkaline phosphatase in mineralization. *Current Opinion in Orthopaedics*, 18(5): 444-448. https://doi.org/10.1097/BCO.0b013e3282630851
8. Keating, A. 2017. The nomenclature of mesenchymal stem cells and mesenchymal stromal cells, pp. 8-10. In: Atkinson, K. (ed.). *The Biology and Therapeutic Application of Mesenchymal Cells.* New John Wiley & Sons, Jersey, 965 pp.
9. Kim, E.C., Leesungbok, R., Lee, S., Lee, H.W., Park, S.H., Mah, S.J. & Ahn, S.J. 2015. Effects of moderate intensity static magnetic fields on human bone marrow-derived mesenchymal stem cells. *Bioelectromagnetics*, 36(4): 267-276. https://doi.org/10.1002/bem.21903
10. Kotani, H., Kawaguchi, H., Shimoaka, T., Iwasaka, M., Ueno, S., Ozawa, H., Nakamura, K. & Hoshi, K. 2002. Strong static magnetic field stimulates bone formation to a definite orientation *in vitro* and *in vivo*. *Journal of Bone and Mineral Research*, 17(10): 1814-1821. https://doi.org/10.1359/jbmr.2002.17.10.1814
11. Lohmann, K.J. & Lohmann, C.M. 2019. There and back again: natal homing by magnetic navigation in sea turtles and salmons. *Journal of Experimental Biology*, 222 (Pt Suppl 1): jeb184077. https://doi.org/10.1242/jeb.184077
12. Marędziak, M., Tomaszewski, K., Polinceusz, P., Lewandowski, D. & Marycz, K. 2017. Static magnetic field enhances the viability and proliferation rate of adipose tissue-derived mesenchymal stem cells potentially through activation of the phosphoinositide 3-kinase/Akt (PI3K/Akt) pathway. *Electromagnetic Biology and Medicine*, 36(1): 45-54. https://doi.org/10.3109/15368378.2016
13. Markov, M.S. 2007. Magnetic field therapy: a review. *Electromagnetic Biology and Medicine*, 26(1): 1-23. https://doi.org/10.1080/15368370600925342
14. Markov, M.S. 2015. XXI$^{st}$ Century megnetotherapy. *Electromagnetic Biology and Medicine*, 34(3): 190-196. https://doi.org/10.3109/15368378.2015.1077338
15. Marycz, K., Kornicka, K. & Röcken, M. 2018. Static magnetic field (SMF) as a regulator of stem cell fate-new perspectives in regenerative medicine arising from an underestimated tool. *Stem Cell Reviews and Reports*, 14(6): 785-792. https://doi.org/10.1007/s12015-018-9847-4
16. Murayama, M. 1965. Orientation of sickled erythrocytes in a magnetic field. *Nature*, 206(982): 420-422. https://doi.org/10.1038/206420a0
17. Ogiue-Ikeda, M. & Ueno, S. 2004. Magnetic Cell Orientation Depending on Cell Type and Cell Density.

*IEEE Transections on Magnetics*, 40(4): 3024-3026. https://doi.org/10.1109/TMAG.2004.830453

18. Rajabzadeh, N., Fathi, E. & Farahzadi, R. 2019. Stem cell-based regenerative medicine. *Stem Cell Investigation*, 6(19). https://doi.org/10.21037/sci.2019.06.04
19. Sadri, M., Abdolmaleki, P., Behmanesh, M., Abrun, S., Beiki, B. & Samani, F.S. 2017. Static magnetic field effect on cell alignment, growth and differentiation in human cord-derived mesenchymal stem cells. *Cellular and Molecular Engineering*, 10(3): 249-262. https://doi.org/10.1007/s12195-017-0482-y
20. Silva, L.H., Silva, S.M., Lima, E.D., Silva, R.C., Weiss, D.J., Morales, M.M., Cruz, F.F. & Rocco, P.R.M. 2018. Effects of static magnetic fields on natural or magnetized mesenchymal stromal cells: Repercussions for magnetic targeting, *Nanomedicine*, 14(7): 2075-2085. https://doi.org/10.1016/j.nano.2018.06.002
21. Stefanita, C.G. 2012. Traditional Magnetism. pp. 1-38. In: Stefanita, C.G. (ed.). *Magnetism: Basic and Application*. Springer, London, 188 pp.
22. Suman, S., Domingues A, Ratajczak J. & Ratajczak MZ. 2019. Potential clinical applications of stem cells in regenerative medicine. *Advances in Experimental Medicine and Biology*, 1201:1-22. https://doi.org/10.1007/978-3-030-31206-0_1
23. Trohatou, O. & Roubelakis, M.G. 2017. Mesenchyal stem/stromal cells in regenerative medicine: past, present and future. *Cellular Programming*, 19(4): 217-224. https://doi.org/10.1089/cell.2016.0062
24. Yamamato, Y., Ohsaki, Y., Goto, T., Nakasima, A. & Lijima, T. 2003. Effects of static magnetic fields on bone formation in rat osteoblast cultures. *Journal of Dental Research*, 82(12): 962-966. https://doi.org/10.1177/154405910308201205
25. Yang, J., Zhang, J., Ding, C., Dong, D. & Shang, P. 2018. Regulation of osteoblast differentiation and iron content in MC3T3-E1 cells by static magnetic field with different intensities. *Biological Trace Element Research*, 184(1): 214-225. https://doi.org/10.1007/s12011-017-1161-5
26. Wang, X.B., Xiang, B., Deng, J., Freed, D.H., Arora, R. & Tian, G. 2016. Inhibition of viability, proliferation, cytokines secretion, surface antigen expression, and adipogenic and osteogenic differentiation of adipose-derived stem cells by seven-day exposure to 0.5 T static magnetic fields. *Stem Cells International*, 2016: 7168175. https://doi.org/10.1155/2016/7168175
27. Wills, B.A. & Finch, J.A. 2015. Magnetic and Electrical Separation. pp. 381-407. In: Wills BA, Finch JA (eds). *Wills' Mineral Processing Technology*. Elsevier, Butterworth-Heinemann, 512 pp.
28. Zhang, X., Yarema, K. & Xu, A. 2017a. Parameters of Magnetic Fields and Their Differential Biological Effects. 3-25. In: Zhang, X., Yarema, K. & Xu, A. (eds). *Biological Effects of Static Magnetic Fields.* Springer, Singapore, 172 pp.
29. Zhang, X., Yarema, K. & Xu, A. 2017b. Impact of Static Magnetic Fields (SMFs) on Cells. 81-131. In: Zhang, X., Yarema, K. & Xu, A. (eds). *Biological Effects of Static Magnetic Fields.* Springer, Singapore, 172 pp.

*http://dergipark.org.tr/trkjnat*
*Trakya University Journal of Natural Sciences, 22(1): 43-48, 2021*
*ISSN 2147-0294, e-ISSN 2528-9691*
*DOI: 10.23902/trkjnat.805545*

**Research Article**

# THE ANTI HRSV ACTIVITY OF *Ferula halophila* Peşmen AQUEOUS AND METHANOL EXTRACT BY MTT ASSAY

Hasan Hüseyin DOĞAN*, Rüstem DUMAN

Selçuk University, Science Faculty, Biology Department, Alaeddin Keykubat Campus, Konya, TURKEY

**Cite this article as:**

Doğan H.H. & Duman R. 2021. The Anti HRSV Activity of *Ferula halophila* Peşmen Aqueous and Methanol Extract by MTT Assay. *Trakya Univ J Nat Sci*, 22(1): 43-48, DOI: 10.23902/trkjnat.805545

Received: 05 October 2020, Accepted: 05 March 2021, Online First: 22 March 2021, Published: 15 April 2021

**Abstract:** The trend towards natural products in the world is increasing due to the increased drug resistance of infectious diseases, the high prices for drugs and the difficulty of access. Also, bacterial or viral diseases that are difficult to treat and need a long time for proper treatment cause important infections in people. Since effective drugs could not be developed for most viral infections, it is very important to find natural products against viruses to introduce them to the world of science. The antiviral activities of the aqueous and methanol extract from *Ferula halophila* Peşmen, an endemic species to Turkey, has been investigated against human respiratory syncytial virus (HRSV, ATCC-VR-26). The cytotoxic and antiviral properties of plant extracts were investigated in HRSV / HEp-2 cell systems, respectively by the colorimetric MTT assay.

In the study, the titer of RSV was used as 100 $TCID_{50}$ (50% tissue culture infective dose). While MNTC (Maximum non-toxic concentration) of methanol extract was 195.313 µg/mL and $CC_{50}$ (50% cytotoxic concentration) was 4366.22 µg/mL, it was determined as MNTC = 390.625 µg/mL and $CC_{50}$ = 4366.22 for aqueous extract. According to the results, methanol extract showed more toxicity than the aqueous extract. The MNTC of Ribavirin used as a positive control was determined as 0.98 µg/mL and $CC_{50}$ was 110.40 µg/mL.

As a result of the study, it was determined that the methanol extract was not effective, whereas the aqueous extract had a significant anti-HRSV activity with the values of 50.69 µg/mL $EC_{50}$ (50% Effective Concentration) and 97.54 Selectivity Index (SI). The $EC_{50}$ and SI values of Ribavirin were 2.39 µg/mL and 46.19, respectively.

According to the results, we can explain the presence of antiviral activity only in the aqueous extract and the absence in the methanol extract by the high toxicity of it and the insolubility of the antiviral compounds in the methanol extract.

**Özet:** Dünyada doğal ürünlere yönelik eğilim, enfeksiyöz hastalıkların ilaç direncindeki artış, yüksek ilaç fiyatları ve erişim zorluğu nedeniyle artmaktadır. Ayrıca, tedavisi zor ve uzun süren bakteriyal veya viral hastalıklar insanlar üzerinde önemli enfeksiyonlara neden olur. Çoğu viral enfeksiyon için etkili bir ilaç geliştirilemediğinden, virüslere karşı doğal ürünlerin bulunması ve bilim dünyasına tanıtılması çok önemlidir. Bu amaçla, Türkiye'ye endemik bir tür olan *Ferula halophila* Peşmen'den elde edilen su ve metanol ekstrelerinin antiviral aktiviteleri, insan solunum sinsityal virüsüne (HRSV, ATCC-VR-26) karşı araştırılmıştır. Çalışmada, bitki ekstrelerinin sitotoksik ve antiviral özellikleri sırasıyla, HRSV/HEp-2 hücre sistemlerinde kolorimetrik MTT deneyi ile araştırılmıştır. RSV'nin titresi 100 $DKID_{50}$ (%50 Doku kültürü infektif doz) olarak kullanılmıştır.

Metanol ekstresinin MNTC'u (Maksimum non toksik konsantrasyon) 195,313 µg/mL ve $CC_{50}$'u (%50 sitotoksik konsantrasyon) 4366,22 µg/mL, su ekstresinin ise MNTC'u 390,625 µg/mL ve $CC_{50}$ 4366,22 olarak belirlenmiştir. Sonuçlara göre metanol ekstresi su ekstresinden daha toksik özellik göstermiştir. Kontrol olarak kulllanılan Ribavirinin MNTC 0,98 µg/mL ve $CC_{50}$ ise 110,40 µg/mL olarak belirlenmiştir. Antiviral çalışma sonucunda metanol ekstresinin etkili olmadığı, buna karşın su ektresinin 50,69 µg/mL $EC_{50}$ (%50 etkili konsantrasyon) ve 97,54 SI (Seçicilik indeksi) değerleri ile önemli bir anti-HRSV aktivitesi olduğu belirlenmiştir. Ribavirinin $EC_{50}$ ve SI değerleri ise sırasıyla 2,39 ve 46,19 µg/mL dir. Elde edilen sonuçlara göre sadece su ekstresinde antiviral aktivitenin görülmesi ve metanol ekstresinde antiviral aktivitenin olmayışını, methanol ekstresinin toksitesinin yüksek olması ve antiviral özellikte olan bileşiklerin metanol ekstresinde çözünmemesiyle açıklayabiliriz.

***Edited by:***
*Hatice Korkmaz Güvenmez*

***Corresponding Author:***
*Hasan Hüseyin Doğan*
*hhuseyindogan@yahoo.com*

***ORCID iDs of the authors:***
*H.H.D. orcid.org/0000-0001-8859-0188*
*R.D. orcid.org/0000-0002-2320-7448*

***Key words:***
*Ferula halophila*
*Methanol and aqueous extract*
*Cytotoxicity*
*Antiviral activity*
*Human respiratory syncytial virus*

## Introduction

Respiratory syncytial virus (RSV) is a negative-stranded segmentless RNA virus belonging to the genus Pneumovirus of the family Paramyxoviridae (Falsey & Walsh 2000). RSV is recognized worldwide as one of the leading causes of lower respiratory tract disease in infants and children under the age of 5, and the estimated annual number of human respiratory syncytial virus (HRSV)-associated hospitalizations is 3.4 million with at least 66,000 deaths worldwide (Hall *et al.* 2009, Nair *et al.* 2010, Lambert *et al*. 2014).

The virus also causes acute respiratory diseases in the elderly (Collins & Melero 2011) and can be destructive in individuals with weakened immune systems (Dudas & Karron 1998). Although most individuals are infected with RSV at an early age of their lifes, susceptibility to recurrent RSV infections continues throughout whole life, also in older ages (Varga & Braciale 2013). RSV can infect the upper respiratory mucosa and may initially replicate in the nasopharynx. It is likely to spread rapidly to the lower respiratory tract by aspiration of secretions and causes morbidity and mortality mainly with the pathology of the lower respiratory tract. Therefore, the management of RSV infection requires an effective strategy to prevent viral infection of both the upper and the lower respiratory tracts (Collins & Crowe 2007). No licensed RSV vaccine has yet been developed, although the disease remains a common viral cause of serious respiratory disorders (Durbin & Karron 2003). Failure to develop specific therapeutic or safe and effective vaccines adversely affects the effort to reduce global mortality and morbidity caused by RSV infections.

Ribavirin (RBV) is known as the only drug approved for treatment of RSV infections, and immunoglobulin preparations are also used for prevention from RSV infections. However, none of these methods is cheap, they are difficult to implement (Kneyber *et al.* 2000, Pelaez *et al.* 2009) and all potential RSV vaccines as prophylactic and therapeutic candidates are currently under clinical trials (Lindsay *et al.* 2015).

The genus *Ferula* L. (*Apiaceae*) contains about 170 species generally growing in the arid regions of temperate Eurasia, the Canary Islands and North Africa (Downie *et al.* 2000). The gene centre of the genus is located in West and Central Asia (Drude 1898). Traditionally, some species of this genus are being used both in "the kitchen" and for "medical treatment". The genus is well known in Turkey and aerial or root parts of some species are used as food and aphrodisiac in some parts of the country (Baytop 1984). The exudates of *Ferula assa-foetida* L. grown in Iran are traditionally used as aphrodisiac and emmenagogue, in addition to their use in the treatment of some cases such as urinary and gastrointestinal diseases, respiratory infections and epilepsy (Samsam Shariat & Moattar 1990, Iranshahy & Iranshahi 2011). Coumarin and sesquiterpene coumarins isolated from members of the genus have been reported to have antiviral activity against various viruses such as influenza A virus (H1N1), human rhinoviruses (HRV), HIV, herpes simplex virus type 1 (HSV-1), and antibacterial, anti-ligaminal, anti-inflammatory and anti-tumour activities (Mohamed *et al.* 2006, Gliszczyńska & Brodelius 2012, Ghannadi *et al.* 2014, Duman 2016).

Considering the medical features mentioned above, *F. halophila* Peşmen, an endemic species for Turkey, has been chosen to determine its antiviral effects. Although several studies were performed on antiviral properties of extracts of some species of the genus against various viruses, no study was performed on antiviral effects on RSV. In the present study, we tested, cytotoxic and antiviral effects of methanol and aqueous extracts of *F. halophila* on HRSV cultured in HEP-2 human laryngeal epidermoid carcinoma cell line.

## Materials and Methods

### *Plant samples*

*Ferula halophila* samples were collected from the Cihanbeyli-Yavşan Salty area Konya province in Central Anatolia, Turkey, and the collected specimens were identified taxonomically by Dr. Osman TUGAY from Selçuk University, Faculty of Pharmacy. A voucher sample is stored at S.Ü. Kon-Fungarium, Konya/Turkey.

### *Cell and virus*

Human larynx epidermoid carcinoma cells [HEp-2; ATCC (the American Type Culture Collection) CCL 23] were used to culture human respiratory syncytial virus (HRSV Long strain: ATCC VR-26). Cells were propagated at 37°C under 5% $CO_2$ in Eagle's minimum essential medium (EMEM) supplemented with 10% foetal bovine serum (FBS, ATCC-30-2020), 10000 U/mL penicillin, 10 mg/mL streptomycin, and 25 µg/mL amphotericin B. HRSV is a medium-sized (120-200 nm) enveloped virus that contains a linear negative-sense RNA genome (must be converted to a positive RNA prior to translation). Virus (coded as ATCC-VR-26) was purchased from American Type Culture Collection (ATCC) and reproduced in Virology Laboratory of Science Faculty of Selçuk University. The virus was propagated on a 90% confluent cell monolayer in EMEM with 1% FBS and antibiotics as described above. Viral titer was determined by 50% tissue culture infectious dose ($TCID_{50}$) method and expressed as $TCID_{50}$ per 0.1 mL (Kaerber 1964). The virus was stored at -196°C until use.

### *Preparation of the extracts*

Dried aerial parts (body and leaves) of the plant were used for the experiments. Each 30 g sample in powder form was placed separately in 400 mL of methanol and 400 mL of sterile distilled water and extracted for 1 hour with an ultrasonicator at 45°C. Plant extracts were filtered through Whatman No: 1 filter paper, and then the solvents used were completely evaporated at 45°C under reduced pressure in a rotary evaporator (Heidolph Laboratory 4000, Germany). After evaporation, the plant extracts were lyophilized at -110°C under reduced pressure in the

lyophilizer (Labconco, USA). Each 1000 mg of the lyophilized extracts were dissolved in 10 mL of EMEM (serum-free) and stock solutions were prepared at a concentration of 100 mg/mL. The stock solutions were sterilized by a trough in 0.22 µm Millipore filter, then stored in 2 mL tubes and stored at +4°C until use. Ribavirin (RBV, R9644-10 mg, Sigma, USA), a drug approved for the treatment of HRSV infections in humans, was purchased. 10 mg ribavirin was dissolved in 5 mL of EMEM (serum-free). This 2 mg/mL stock concentration was filtered in 0.22 µm Millipore filter, then they were stored at -80°C or +4°C (When stored at +4°C, it was used within 1 week).

*Cytotoxicity assay*

The cytotoxic effects of methanol and aqueous extracts of *F. halophila* on HEp-2 cells, and RBV were determined by the ability to reduce Trypan blue dye and Tetrazolium salt (MTT) which was described by Ho *et al.* (2010). 96-well microtiter plates were used in the experiments. The 1st column was used as Negative control (Nc), the 2nd was used as Cell control (Cc), and serial dilutions according to log2 base for both extract solutions with a concentration of 100,000 µg/mL were used from 50,000 to 195.313 µg/mL. A suspension of HEp-2 at a concentration of $0.625 \times 10^5$ cells/mL was prepared with the cell growth medium, and 100 µL cell suspensions were seeded to all wells of the plate (6250 cells/well) except the 1st column and all 3 lower wells of columns 3-12 which was used to check whether the extracts had direct chemical interaction with MTT. After 24 hours of incubation at 37°C in 5% $CO_2$, each 100 µg/mL extracts were added on to wells and the plates were incubated for 48 hours. Then, the MTT assay was performed. Mean OD were read via an ELISA reader (Multiskan EX, Lab systems) at a test wavelength of 570 nm and a reference wavelength of 630 nm. The mean OD values of the extracts of the same concentration without cells were subtracted from the mean OD of the different extract concentrations in the cell-containing wells.

Maximum non-toxic concentrations (MNTCs) of the extracts were determined by comparing them with the OD of the Cc. These MNTCs were used to determine the antiviral activity of the extracts.

In determining the cytotoxic effects of RBV on HEp-2 cells, a solution of RBV was prepared at a concentration of 1,000 µg/mL in EMEM from the stock solution (2,000 µg/mL). Subsequent dilutions (from 500 to 1.95 µg/mL concentrations) were prepared from the base of log2. Then the same procedure which was used to determine the cytotoxic effects of the extracts was followed for RBV.

*Antiviral assay*

The anti-RSV activities of the extracts and RBV were evaluated by the MTT test (Andrighetti-Fröhmer *et al.* 2003, Shoemaker *et al.* 2004). A suspension of RSV at 100 tissue culture infective dose ($TCID_{50}$) was prepared with maintenance medium (EMEM with 1% FBS). Dilutions of the test samples (extracts and RBV) in 2 × MNTCs (MNTCs= 195.313 µg/mL for methanol, 390.625 µg/mL for aqueous and 0.98 µg/mL for ribavirin) were prepared using maintenance medium. Subsequently, two-fold dilutions with maintenance medium were prepared from these dilutions. $2.5 \times 10^4$ cells were seeded on the wells and incubated at 37ºC for 24 hours in a 5% $CO_2$ incubator. When the cells were confluent, the production medium in the wells was evacuated and each 100 µL of RSV suspension (containing 100 $TCID_{50}$) and each 100 µL of the extract samples were put in the wells, simultaneously. 100 µL of RSV suspension and 100 µL of maintenance medium were put into Virus Control (VC) wells. 200 µL of maintenance medium was added to the Ccwells. Plates were incubated for 2-5 days (more precisely, until 85-90% CPE was seen in VC wells) for the development of CPE at 37°C in 5% $CO_2$. When 85-90% CPE was observed in VC wells, the solutions were removed in the wells, and an MTT assay was performed. The protection percentages were calculated. The $EC_{50}$ value, which is defined as the concentration of extract (or RBV) that provides protection in 50% of the infected cells, was determined and the SI of the extracts (or RBV) was calculated.

*Statistical analysis*

Non-linear regression analysis in GraphPad Prism for Windows, version 5.03 (Graph Pad Software Inc., San Diego, CA, USA, 2005) was used to determine the 50% cytotoxic concentration ($CC_{50}$) and 50% effective concentration ($EC_{50}$) values. To calculate the percentage of cytotoxicity, the following formula was used, where A represents the Optic Dencity (OD) of the Cc and B represents the OD of the extract-treated cells (Andrighetti-Fröhmer *et al.* 2003);

$$\%\, Cytotoxicity = \frac{A - B}{A}\, x\, 100$$

The percentage of cell viability (cytotoxicity) was calculated as absorbance of sample/absorbance of control × 100. The selectivity index (SI) was calculated as $CC_{50}/EC_{50}$.

The protection percentages were calculated spectrophotometrically from the formula;

$$\%\, Protection = \frac{A - B}{C - B}\, x\, 100$$

A= absorbance of extract (or RBV) dilutions

B= absorbance of virus

C= absorbance of Cc

Experiments were done in triplicates.

**Results and Discussion**

*Virus Titration*

In the titration of RSV in HEp-2 cell culture by the microtitration method, the power of infectiousness was determined as $DCID_{50} = 10^{-4.5}/0.1$ mL at the end of the 5th

day. The CPEs of the virus in HEp-2 cells, and the appearance of uninfected HEp-2 cells (HEp-2 control) are shown in Figs 1-2.

*Cytotoxicity and Antiviral Assay Results*

The cytotoxic effect of the extracts and RBV on Hep-2 cells , were evaluated by colorimetric cell viability test. In the experiments, the non-toxic dose of the extracts and RBV on HEp-2 cells was determined. Then, starting from non-toxic doses, the protection percentages and SI of the extracts and RBV were determined. The MNTCs and $CC_{50}$ values of the methanol, aqueous extracts, and RBV against HEp-2 cells are shown in Table 1. Methanol extract is more toxic than aqueous extract (Fig. 3). The MNTCs of methanol was 195.313 µg/mL, while aqueous was 390.625 µg/mL, and for RBV was 0.98 µg/mL (Fig. 4). While methanol extract did not show any activity against RSV, on the contrary, the aqueous extract showed an important antiviral activity. The $EC_{50}$ value of aqueous extract was 50.69 µg/mL, while the SI value was 97.54 (Fig. 5). The $EC_{50}$ and SI values of RBV were 2.39 µg/mL and 46.19 µg/mL, respectively (Fig. 6).

In this study, the aqueous extract is even more effective than the standard drug RBV, whereas methanol extract was found to be ineffective against RSV.

Furthermore, it can be seen that the extracts are less toxic than RBV on HEp-2 cells, and $CC_{50}$ values of aqueous extract and RBV are higher than $EC_{50}$ values.

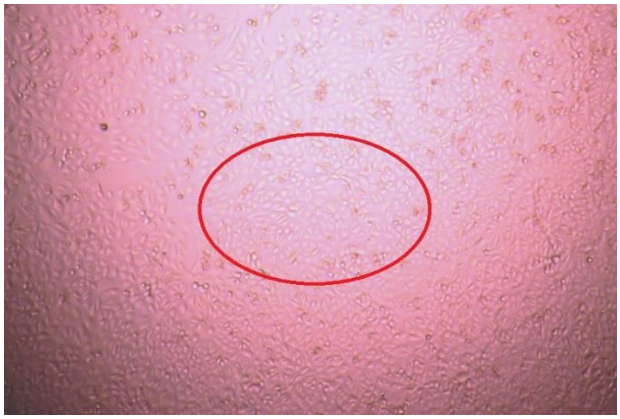

**Fig. 1.** View of HEp-2 cells (Original).

**Fig. 2.** CPE view of RSV in HEp-2 cells (Original).

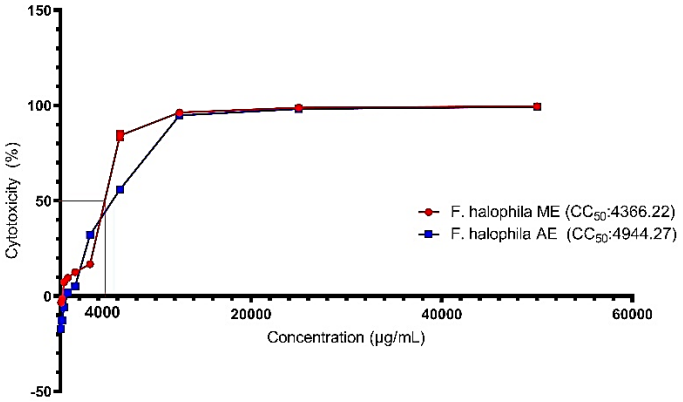


**Fig. 3.** Cytotoxicity of the extracts.

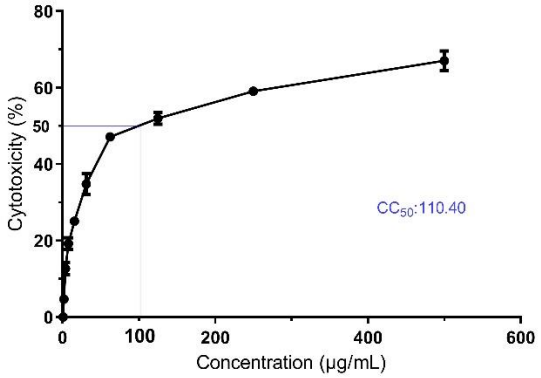


**Fig. 4.** Cytotoxicity of the ribavirin.

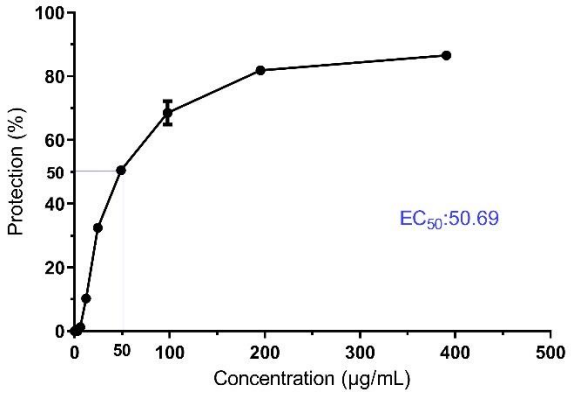


**Fig. 5.** Antiviral activity of the aqueous extract.

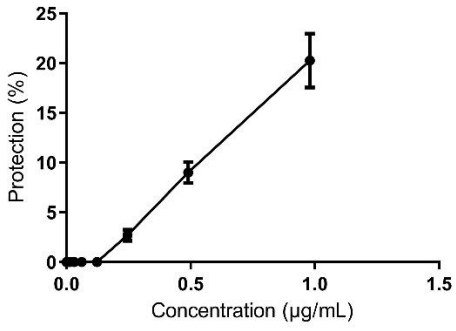


**Fig. 6.** Antiviral activity of ribavirin.

**Table 1.** Cytotoxicity and antiviral activity of methanol and aqueous extracts of *F. halophila* and RBV.

| Plant species | Extract type | Toxicity | | Antiviral activity | |
|---|---|---|---|---|---|
| | | MNTCs (µg/mL) | $CC_{50}$ (µg/mL) | $EC_{50}$ (µg/mL) | SI |
| ***Ferula halophila*** | Methanol | 195.313 | 4366.22 | – | – |
| | Aqueous | 390.625 | 4944.27 | 50.69 | 97.54 |
| | Ribavirin | 0.98 | 110.40 | 2.39 | 46.19 |

This is important for the reliability of an antiviral agent (Schinazi *et al.* 2009). Besides, Chattopadhyay *et al.* (2009) reported that if SI values are 10 or greater than 10, antiviral results determined at or above this SI value may indicate that the extracts may have potential antiviral activity. *Ferula* species are rich in biologically active compounds, some of which are coumarins, sesquiterpenes, sesquiterpene coumarins, sesquiterpene lactones, and daucan esters (Zhou *et al.* 2017). It was reported in many studies on phytochemicals that these secondary metabolites and extracts obtained from *Ferula* species can show anti-fertility, antifungal, anti-inflammatory, antispasmodic, antitumor, antiviral, antiulcerogenic, cancer chemopreventive, digestive enzyme inhibition and hypotensive effects (Iranshahy & Iranshahi 2011). *Ferula* genus consists of 170 species in a wide region extending from Central Asia to the Mediterranean part (Mozaffarian 1996, Downie *et al.* 2000), and is represented in Turkey with 18 species of which 9 are endemic for the country (Davis 1972). Different parts of *Ferula* species are used in the treatment of various diseases such as neurological diseases, inflammations, dysentery, digestive system disorders, rheumatism, headache, arthritis and dizziness (Tamemoto *et al.* 2001). The anti-inflammatory, cytotoxicity and P-gp inhibitor, cancer chemo-preventive, antibacterial and anti-leishmanial activities of the components obtained from the genus *Ferula* are summarized (Nazari & Iranshahi 2011).

Also, extracts, pure compounds and essential oils obtained from different *Ferula* species have been reported antiviral activities against DNA and RNA viruses such as influenza A (H1N1) (Lee *et al.* 2009), hepatitis B (Zhai *et al.* 2012), HSV-1 (Mohamed *et al.* 2006, Ghannadi *et al.* 2014, Duman 2016). Lee *et al.* (2009) isolated 11 sesquiterpene coumarins from *F. assa-foetida* extract, and these sesquiterpene coumarins were effective against influenza A (H1N1) virus at $EC_{50}$ values ranging from 0.26-0.99 µg/mL. This result is more effective than the traditional antiviral agent amantadine ($EC_{50}$ 0.92 µg/mL) used against H1N1 virus.

The basic contents of essential oils obtained by hydro-distillation from dried roots of *F. hormonis* Boiss. were analysed by Gas Chromatography-Mass Spectroscopy (GC-MS) and the anti-HSV-1 activity of the essential oil was evaluated with the plaque inhibition test. The results showed that the plaque inhibition percentage of essential oil against HSV-1 was 81.4 (Mohamed *et al.* 2006).

In a study evaluating the anti-HSV-1 activities of sesquiterpene coumarins (badrakemin acetate, kellerin (2) and samarcandin diastereomer) isolated from the gum resin of *F. assa-foetida*, it has been shown that kellerin could significantly inhibit the cytopathic effects and reduce the viral titre of theHSV-1 DNA viral strain KOS at concentrations of 10, 5 and 2.5 µg/mL (Ghannadi *et al.* 2014). Antiviral activity of the methanol and water extracts of *F. halophila was investigated against* HSV-1(strain HF, ATCC VR-260) by the colorimetric XTT assay *in vitro* HSV-1/Vero cell systems by Duman (2016). According to his results, $EC_{50}$ and SI values for methanol extract were 1035.29 µg/mL and 35.56, respectively, and $EC_{50}$ and SI values for water extract were 264.45 µg/mL and 130.81, respectively. Similarly, $EC_{50}$ and SI of aqueous extract ($EC_{50}$: 50.64, SI: 97) in the present study are higher than methanol extract. According to Duman (2016) and our results, we can say that aqueous extracts are more effective than methanol extracts. Several compounds, including glucuronic acid, galactose, arabinose, and rhamnose (Kapoor 1990), sulfur-containing derivatives (Kajimoto *et al.* 1998), coumarins (Iranshahi *et al.* 2004), sesquiterpenes (Gonzalez & Barrera 1995), sesquiterpene coumarins (Ahmed 1999, Ahmed *et al.* 2001), sesquiterpene lactones, and daucane esters are important in various biological activities of *Ferula* species. Among these compounds, sesquiterpene coumarins are very important because of their wide range and promising biological properties, particularly their antiviral properties. Indeed, it has been shown that sesquiterpene coumarins obtained from *F. assa-foetida* have significant antiviral activity against HSV-1 KOS strain (Ghannadi *et al.* 2014).

According to the current literature, there is only one study on the phytochemical profile of *F. halophila* (Zengin *et al.* 2018), and there are no studies on anti-RSV activity. Zengin *et al.* (2018) studied acetone, chloroform, and methanol extracts of *F. halophila* on diabetes (α-amylase, α-glucosidase), cognitive functions [acetyl cholinesterase (AChE), butyrylcholinesterase (BChE)], inhibitor effects against hyperpigmentation (tyrosinase) related enzymes and mutagenic/antimutagenic activities. They also detected its phytochemical profiles by LC-MS/MS (Liquid Chromatography-Mass/Mass Spectrophotometer). According to their results, total phenolic contents for acetone, methanol and chloroform extracts of *F. halophila* were found as 55.22, 48.06, andb20.66 mg GAE/g, respectively, while total flavonoid contents for the same extracts were 34.52, 24.13, and 8.61

mg/g, respectively. Many phenolic agents, especially flavonoids, are known to have antiviral activity against different types of viruses, including RSV (Naithani *et al.* 2008, Li *et al.* 2014).

However, it was determined that *F. halophila* methanol extract did not have antiviral activity against RSV, whereas the aqueous extract of the same plant had significant antiviral activity. This may be due to the presence of the compound or compounds that are soluble in water, which are insoluble in the methanol extract.

## Conclusion

In this study, anti-RSV activities of methanol and aqueous extracts of *F. halophila* were investigated, and aqueous extract exhibited the highest antiviral effect. To find the compound that causes antiviral activity, it is necessary to analyse the aqueous extract in the following steps and to renew the antiviral tests. In this way, the active substance or substances would be determined and they would be used as new antiviral drugs. However, the methanol extract did not show any antiviral effect. Due to the high toxicity of the methanol extract on HEp-2 cells, the use of lower concentrations in the antiviral test might have reduced the antiviral effect, or the antiviral compounds had not been completely dissolved in the methanol extract.

**Ethics Committee Approval:** Since it was a systematic review, its approval to the ethics committee was not required.

**Author Contributions:** Concept: H.H.D, R.D., Design: H.H.D, R.D., Execution: H.H.D, R.D., Material supplying: H.H.D, R.D., Data acquisition: H.H.D, R.D., Data analysis/interpretation: H.H.D, R.D., Manuscript writing: H.H.D, R.D., Critical revision: H.H.D, R.D.

**Conflict of Interest:** The authors have no conflicts of interest to declare.

**Funding:** This work was supported by Selçuk University, Scientific Research Projects Coordinating Office, Project Number: BAP/17401079.

## References

1. Ahmed, A.A. 1999. Sesquiterpene coumarins and sesquiterpenes from *Ferula sinaica*. *Phytochemistry*, 50: 109-112.
2. Ahmed, A.A., Abd El-Razek, M.H., Nassar, M.I., Izuma, S., Ohta, S. & Hirata, T. 2001. Sesquiterpene coumarins from the roots of *Ferula assa-foetida*. *Phytochemistry*, 58: 1289-1295.
3. Andrighetti-Fröhmer, C.R., Antonio, R.V., Greczynski-Pasa, T.B., Barardi, C.R.M. & Simões, C.M.O. 2003. Cytotoxicity and potential antiviral evaluation of violacein produced by *Chromobacterium violaceum*. *Memórias do Instituto Oswaldo Cruz*, 98: 843-848.
4. Baytop, T. 1984. *Türkiye'de Bitkilerle Tedavi*. İstanbul Üniversitesi Eczacılık Fakültesi Yayınları No: 3255, İstanbul, 371 pp.
5. Chattopadhyay, D., Chawla-Sarkar, M., Chatterjee, T., Dey, R.S., Bag, P., Chakraborti, S. & Khan, M.T.H. 2009. Recent advancements for the evaluation of antiviral activities of natural products. *New Biotechnol*, 25: 347-368.
6. Collins, P.L. & Crowe, J.E. 2007. Respiratory syncytial virus and metapneumovirus. pp: 1601-1646. In: Knipe D.M., Howley P.M., Griffin D.E., Martin M.A., Lamb R.A., Roizman B., Straus S.E. (eds.). *Fields Virology*. Lippincott Williams & Wilkins, Philadelphia, 2501 pp.
7. Collins, P.L. & Melero, J.A. 2011. Progress in understanding and controlling respiratory syncytial virus: still crazy after all these years. *Virus Research*, 162: 80-99.
8. Davis, P.H. 1972. *Flora of Turkey and the East Aegean Islands* Vol: 4. Edinburgh University Press, Edinburgh, 657 pp.
9. Downie, S.R., Watson, M.F., Spalik, K. & Katz-Downie D.S. 2000. Molecular systematics of old World 2. Apioideae (Apiaceae): relationships among some members of tribe Peucedaneae sensu lato, the placement of several island-endemic species, and resolution within the apioid superclade. *Canadian Journal of Botany*, 78: 506-528.
10. Drude, O. 1898. *Ferula* L. In A. Engler (Ed.), *Die natürlichen Pflanzenfamilien*, Wilhelm Engelmann, Leipzig, Vol. 3(8): 228-232.
11. Dudas, R.A. & Karron R.A. 1998. Respiratory syncytial virus vaccines. *Clinical Microbiology Reviews*, 11(3): 430-439.
12. Duman, R. 2016. Antiviral activity of *Ferula halophila* Peşmen against herpes simplex virus type 1 (HSV-1). *International Journal of Scientific and Technological Research*, 2(4): 1-9.
13. Durbin, A.P & Karron, R.A. 2003. Progress in the development of respiratory syncytial virus and parainfluenza virus vaccines. *Clinical Infectious Diseases*, 37(12): 1668-1677.
14. Falsey, A.R. & Walsh, E.E. 2000. Respiratory syncytial virus infection in adults. *Clinical Microbiology Reviews*, 13(3): 371-384.
15. Ghannadi, A., Fattahian, K., Shokoohinia, Y., Behbahani, M. & Shahnoush, A. 2014. Anti-viral evaluation of sesquiterpene coumarins from *Ferula assa-foetida* against HSV-1. *Iranian Journal of Pharmaceutical Research*, 12(2): 523-530.
16. Gliszczyńska, A. & Brodelius, P.E. 2012. Sesquiterpene coumarins. *Phytochemistry*, 11(1): 77-96.
17. Gonzalez, A.G. & Barrera, J.B. 1995. Chemistry and the sources of mono- and bicyclic sesquiterpenes from *Ferula* species. *Progress in the Chemistry of Organic Natural Products*, 64: 1-92.
18. Hall, C.B., Weinberg, G.A., Iwane, M.K., Blumkin, A.K., Edwards, K.M., Staat, M.A., Auinger, P., Griffin, M.R., Poehling, K.A., Erdman, D., Grijalva, C.G., Zhu, Y. &

Szilagyi, P. 2009. The burden of respiratory syncytial virus in young children. *The New England Journal of Medicine*, 360(6): 588-598.

19. Ho, W.S., Xue, J.Y., Sun, S.S., Ooi, V.E. & Li, Y.L. 2010. Antiviral activity of daphnoretin isolated from *Wikstroemia indica*. *Phytotherapy Research*, 24(5): 657-661.

20. Iranshahi, M., Amin, G. & Shafiee, A. 2004. A new coumarin from *Ferula persica*. *Pharmaceutical Biology*, 42: 440-442.

21. Iranshahy, M. & Iranshahi, M. 2011. Traditional uses, phytochemistry and pharmacology of Asafoetida (*Ferula assa-foetida* oleo-gum-resin)-A review. *Journal of Ethnopharmacology*, 134(1): 1-10.

22. Kaerber, G. 1964. Diagnostic procedures for virus and rickettsial disease. *Public Health Association*, 3: 48-50.

23. Kajimoto, T., Yahiro, K. & Nohara, T. 1998. Sesquiterpenoid and disulphide derivatives from *Ferula assa-foetida*. *Phytochemistry*, 28: 1761-1763.

24. Kapoor, L.D. 1990. *Handbook of Ayurvedic Medicinal Plants*. CRC Press, Boca Raton, FL, 424 pp.

25. Kneyber, M.C.J., Mou, H.A. & Groot, R.D. 2000. Treatment and prevention of respiratory syncytial virus infection. *European Journal of Paediatrics*, 159: 339-411.

26. Lambert, L., Sagfors, A.M., Openshaw, P.J. & Culley, F.J. 2014. Immunity to RSV in early-life. *Frontiers in Immunology*, 5: 466.

27. Lee, C.L., Chiang, L.C., Cheng, L.H., Liaw, C.C., El-Razek, M.H.A., Chang, F.R. & Wu, Y.C. 2009. Influenza A (H1N1) antiviral and cytotoxic agents from *Ferula assa-foetida*. *Journal of Natural Products*, 72: 1568-1572.

28. Li, Y., Ooi, L.S., Wang, H., But, P.P. & Ooi, V.E. 2004. Antiviral activities of medicinal herbs traditionally used in southern mainland China. *Phytotherapy Research*, 18: 718-722.

29. Lindsay, B., Helen, G., Michael, D. & Ultan, F.P. 2015. Respiratory syncytial virus, an ongoing medical dilemma: an expert commentary on respiratory syncytial virus prophylactic and therapeutic pharmaceuticals currently in clinical trials. *Influenza and other Respiratory Viruses*, 9(4): 169-178.

30. Mohamed, S.M., Ibrahim, N.A., Ali, M.A. & Faraid, M.A. 2006. Chemical composition, antiviral and antimicrobial activities of the essential oils of *Ferula hormonis*, *Plectranthus coleoides* and *Magnolia grandiflora*. *Planta Medica*, 72: 113.

31. Mozaffarian, V. 1996. *A Dictionary of Iranian Plant Names*. Farhang Moaser Publications, Tahran, 70 pp.

32. Nair, H., Nokes, D.J., Gessner, B.D., Dherani, M., Madhi, S.A., Singleton, R.J., O'Brien, K.L., Roca, A., Wright, P.F., Bruce, N., Chandran, A., Theodoratou, E., Sutanto, A., Sedyaningsih, E.R., Ngama, M., Munywoki, P.K., Kartasasmita, C., Simões, E.A., Rudan, I., Weber, M.W. & Campbell, H. 2010. Global burden of acute lower respiratory infections due to respiratory syncytial virus in young children: a systematic review and meta-analysis. *Lancet*, 375 (9725): 1545-1555.

33. Naithani, R., Huma, L.C., Holland, L.E., Shukla, D., Mccormick, D.L., Mehta, R.G. & Moriarty, R.M. 2008. Antiviral activity of phytochemicals: A comprehensive review. *Mini-Reviews in Medicinal Chemistry*, 8: 1106-1133.

34. Nazari, Z.E. & Iranshahi, M. 2011. Biologically active sesquiterpene coumarins from *Ferula* species. *Phytotherapy Research*, 25: 315-323.

35. Pelaez, A., Lyon, G.M., Force, S.D., Ramirez, A.M., Neujahr, D.C., Foster, M., Naik, P.M., Gal, A.A., Mitchell, P.O. & Lawrence E.C. 2009. Efficacy of oral ribavirin in lung transplant patients with respiratory syncytial virus lower respiratory tract infection. *The Journal of Heart and Lung Transplantation*, 28(1): 67-71.

36. Samsam Shariat, S.H. & Moattar F. 1990. *Medicinal Plants and Natural Products*, Mashal Publications, Isfahan. p. 431-433.

37. Schinazi, R.F., Coats, S.J., Bassit, L.C., Lennerstrand, J., Nettles, J.H. & Hurwitz S.J. 2009. Approaches for the development of antiviral compounds: the case of hepatitis C virus. *Handbook of Experimental Pharmacology*, 189: 25-51.

38. Shoemaker, M., Cohen, I. & Campbell M. 2004. Reduction of MTT by aqueous herbal extracts in the absence of cells. *Journal of Ethnopharmacology*, 93(2-3): 381-384.

39. Tamemoto, K., Takaishi, Y., Chen, B., Kawazoe, K., Shibata, H., Higuti, T., Honda, G., Ito, M., Takeda, Y., Kodzhimatov, O.K. & Ashurmetov, O. 2001. Sesquiterpenoids from the fruits of *Ferula kuhistanica* and antibacterial activity of the constituents of *F. kuhistanica*. *Phytochemistry*, 58: 763-767.

40. Varga, S.M. & Braciale, T.J. 2013. The adaptive immune response to respiratory syncytial virus. *Current Topics in Microbiology and Immunology*, 372: 155-171.

41. Zengin, G., Uysal, A., Diuzheva, A., Gunes, E., Jekő, J., Cziáky, Z., Picot-Allain, C.M.N. & Mahomoodally, M.F. 2018. Characterization of phytochemical components of *Ferula halophila* extracts using HPLC-MS/MS and their pharmacological potentials: a multi-functional insight. *Journal of Pharmaceutical and Biomedical Analysis*, 160: 374-382.

42. Zhai, L.L., Liu, T., Xie, H.Q., Xie, Y.H. & Mu, Q. 2012. Inhibition effects on Hepatitis B virus replication by hydrophobic extracts from *Ferula ferulaeoides* (Steud.) Korov. *Journal of Medicinal Plants Research*, 6(8): 1486-1488.

43. Zhou, Y., Xin, F., Zhang, G., Qu, H., Yang, D. & Han, X. 2017. Recent advances on bioactive constituents in *Ferula*. *Drug Development Research* 78(7): 321-331.

*http://dergipark.org.tr/trkjnat*
*Trakya University Journal of Natural Sciences, 22(1): 49-58, 2021*
*ISSN 2147-0294, e-ISSN 2528-9691*
*DOI: 10.23902/trkjnat.835403*

**Research Article**

# THE MICROBIAL COMMUNITY COMPOSITION OF AN ANAEROBIC REACTOR IN A SUGAR INDUSTRY WASTEWATER TREATMENT PLANT-FROM CLASSICAL TO NEW APPROACHES

Nilgün POYRAZ

Department of Biology, Faculty of Science and Humanities, Kütahya Dumlupınar University, Kütahya, TURKEY, e-mail: nilgun.kavak@dpu.edu.tr

**Cite this article as:**

Poyraz N. 2021. The microbial community composition of an anaerobic reactor in a sugar industry wastewater treatment plant-from classical to new approaches. *Trakya Univ J Nat Sci*, 22(1): 49-58, DOI: 10.23902/trkjnat.835403

Received: 03 December 2020, Accepted: 22 March 2021, Online First: 02 April 2021, Published: 15 April 2021

**Abstract:** In this study, the microbial characteristics of the anaerobic reactor of a sugar industry wastewater treatment plant were analyzed using cloning, FISH (Fluoresan in situ hybridization) and metagenomic analysis. Samples were obtained from seven different ports of the reactor on the 148$^{th}$ day of operation. The temperature was maintained at mesophilic conditions. The system's pH range was operated at 6.8. The cloning results showed that most of the bacterial clones belonged to uncultured members of the Bacteria domain. Many archaeal clones were related to uncultured Archaea and *Methanosarcina*. The FISH method was applied to determine the microbial composition of the samples, which showed that bacterial and archaeal species had nearly equal rates. Rod-shaped cells, long bacilli, coccus and long chains were detected in the samples.
After metagenomic analysis, in all samples, Archaea domain members ranged between 60-36% and Bacteria domain members ranged between 58-31%. At the phylum level, in all samples, Euryarchaeota was the most dominant phylum. Proteobacteria (14.8-21.97%) and Actinobacteria (5.53-15.94%) phyla were high in rate. Furthermore, members of Spirochaeotes (0.63-4.82%) and Bacteroidetes (1.72-2.38%) were analyzed in the samples. This study revealed both bacterial and archaeal populations in the reactor of high-concentration organic sugar wastewater. These results will help in the development of more efficient anaerobic treatment systems.

***Edited by:***
*Beata Zimowska*

***ORCID iD of the author:***
*orcid.org/0000-0002-5861-7922*

***Key words:***
*Anaerobic reactor*
*16S rRNA gene cloning*
*FISH*
*Microbial diversity*
*Metagenomic analysis*

**Özet:** Çalışmada bir şeker endüstrisi atık su arıtma tesisinin anaerobik reaktörünün mikrobiyal özellikleri klonlama, FISH (Floresan in situ hibridizasyon) ve metagenomik analiz kullanılarak analiz edilmiştir. Örnekler 148. operasyon gününde reaktörün yedi farklı girişinden alınmıştır. Sıcaklık mezofilik koşullarda tutulmuştur. Sistem 6,8 pH aralığında çalışmıştır. Klonlama sonuçları, bakteri klonlarının çoğunun kültüre alınmamış Bacteria üyelerine ait olduğunu göstermiştir. Birçok arkeal klon, kültüre alınmamş Archaea ve *Methanosarcina* ile ilişkilidir. FISH yöntemi de örneklerin mikrobiyal kompozisyonunu belirlemek için uygulanmıştır. Elde edilen sonuçlar bakteriyel ve arkel türlerin neredeyse eşit oranlarda bulunduğunu göstermiştir. Örneklerde çubuk şeklindeki hücreler, uzun basiller, koklar ve uzun zincirler tespit edilmiştir.
Metagenomik analiz sonuçları değerlendirildiğinde ise, tüm örneklerde, Archaea domaini üyelerinin %60-36 oranları arasında ve Bakteri domaini üyelerinin ise %58-31 oranları arasında bulunduğu belirlenmiştir. Filum düzeyinde, tüm örneklerde Euryarchaeota filumunun en baskın filum olduğu saptanmıştır. Proteobacteria (%14,8-21,97) ve Actinobacteria (%5,53-15,94) filumlarının da yüksek oranda olduğu görülmüştür. Ayrıca örneklerde Spirochaeotes (%0,63-4,82) ve Bacteroidetes (%1,72-2,38) üyeleri analiz edilmiştir. Bu çalışma, yapılan analizler ile yüksek konsantrasyonlu organik şeker atıksu reaktöründe hem bakteriyel hem de arkael popülasyonları ortaya çıkarmıştır. Bu sonuçlar, daha verimli anaerobik arıtma sistemlerinin geliştirilmesine yardımcı olacaktır.

## Introduction

The first modern wastewater plant in the world was built in Hamburg in 1842, and 12 years later, in 1855, the first sewer was built in Chicago. The treatment plant was constructed after 1870. In the middle of the 20$^{th}$ century, regulations came into force, and the Federal Water Pollution and Control Law was created in America in 1948 (Yıldız *et al*. 2013). The increasing amount of wastewater accelerated the development of more serious discharge arrangements and alternative methods for biological wastewater treatment. The increase in research

on biofilm systems in the 1980s led to the development of innovative and flexible processes.

Waterborne disease outbreaks, eutrophication and micro-pollutants, combined with underdeveloped infrastructure and poor economy make the issues associated with the disposal and treatment of wastewater even more serious. Therefore, research should be conducted to develop efficient, low-cost and low-maintenance systems (Andersson 2009).

Anaerobic treatment technology refers to the biological treatment of organic wastes and wastewater without oxygen, and with the use of this technology, operating costs are reduced and biogas (methane) is produced from organic wastes as an alternative energy source (Narihiro & Sekiguchi 2007). The greatest application of this technology is as a sludge digester, which is widely used in municipal wastewater treatment plants. Conversion of organic substances to biogas anaerobically is a complex multi-stage process involving interactions between many different types of bacteria and archaea. Microbial processes, each performed by a certain group of microorganisms, can be defined as hydrolysis, acidogenesis, acetiogenesis and methanogenesis (Venkiteshwaran *et al*. 2015).

However, it is important to ensure and maintain a balanced reaction rate between steps or groups to ensure a fast and stable treatment. Microbial diversity and activity information is also important for proper application and selection of a vaccine mud. The microbial community structure in the anaerobic digester is affected by many environmental parameters (Chen *et al*. 2008). Due to these reasons, one of the most advanced technological areas in recent years is the microbiology of anaerobic treatment processes. In order to better control the biological processes, detailed information about the ecology and function of microbial communities in these processes is required. Detailed structures of community compositions can be revealed through culture-independent analyses that target the 16S rRNA gene.

In the present study, sugar industry wastewater containing high concentrations of hydrocarbon and sugar was used. In addition to traditional methods such as FISH (Fluoresan in situ hybridization) and cloning, 16S rRNA gene-targeted metagenomic studies were applied to determine the microbial diversity of the facility and carry out an analysis of wastewater microbial diversity based on modern methods.

## Materials and Methods

*Sampling*

Since the beet sugar factory treatment plant is an anaerobic feature, anaerobic sludge samples were obtained from 7 different ports of an upstream anaerobic sludge blanket reactor (UASB) on the 148$^{th}$ day of operation from facility in Eskisehir. Samples were collected in 5 L sterile bottles and transferred to the laboratory within 1 hour.

*Determination of the physical and chemical parameters of the samples*

Temperature, pH and element concentrations of the samples were measured. Some element contents of water samples were determined by the ICP-OES device (Perkin Elmer) within the Anadolu University Plant Medicine and Scientific Research Center (BİBAM). The optical emission spectrometry was determined with Optima 4300 DV device, and the pH was measured with a pH meter (Mettler Toledo).

*Total DNA extraction from samples*

DNA extraction was performed for all samples of the reactor. For efficient and high-quality DNA extraction, the protocol proposed by Singka *et al*. (2012) was used with small modifications. In addition to the lysis step with glass beads, lysozyme (3 mg/ml) was added and incubated at 37°C for 15 minutes in a shaking incubator at 150 rpm. Then, proteinase K (150 mg/ml) and 10% sodium dodecyl sulfate (SDS) were added and incubated at 37°C for 40 minutes in the shaking incubator. After extraction, the DNA was checked by gel electrophoresis and Nanodrop (between 1.8-2.0 in 260-280 nm, more than 1.7 in 260-230 nm).

*Amplification by PCR for 16S rRNA gene*

PCR reaction was established using archaea- and bacteria-specific primers from Total DNA. To establish a PCR reaction, bacteria-specific 27F (5'AGAGTTTGATCATGGCTCAG-3') and 21F (5′-TCCGGTTGATCCYGCCGG-3′) were used for Archaea as the forward primer and 1492R (5'-GGTTACCTTGTTACGACTT3') (Lane *et al*. 1985) was used for both Archaea and Bacteria. Bacter 50 program was used for 16S rRNA amplification of bacteria and Archaea members. The reaction conditions of the Bacter 50 program were a cycle of 94°C for 3 min, 30 cycles of 94°C for 15 s, 55°C for 30 s, and 72°C for 2 min, as well as an extension step of 7 min at 72°C. Applied Biosystems® Thermal Cycler was used for the reactions. In all studies, both positive and negative control reactions were prepared. The obtained PCR products were controlled by applying 5V/cm current in 1X TAE (Tris-Acetic acid-EDTA) buffer to 1% agarose gel (Mutlu & Güven, 2015).

*16S rRNA cloning*

The ligation of the 16S rRNA gene region to the vector system was performed using the T4 DNA Ligase enzyme according to the conditions specified in the TA cloning kit (Invitrogen) protocol. After all the components were added, it was incubated overnight at 14°C. The samples obtained after ligation were placed on ice, and a 50 µl vial containing the competent cells was opened on ice and 2 µl of the ligation reaction was added to them. The vials were incubated on ice for 30 minutes and then kept at 42°C for 30 seconds. The cells were quickly transferred to ice. Then, 250 µl of SOC medium was added to the samples and incubated at 37°C for 60 minutes at 225 rpm in a shaking incubator. 10-200 µl was taken from each prepared transformation vial and cultivated in LB Agar Petri plates containing 100 µg/ml ampicillin and X-gal and kept in the

incubator at 37°C overnight. Then, white colonies were selected from the Petri dishes. The white colonies and blue colonies were selected according to the X-gal degradation and fragmentation. The glycerol stock was prepared to be stored at -80°C from the selected white colonies.

Plasmid isolation was performed using the plasmid isolation kit from the obtained white colonies. If the insert was on vector, positive clones were screened for by amplified rDNA restriction analysis (ARDRA) (Vaneechoutte *et al*. 1992) with the enzymes *Hinf*I and *Mbo*I (New England Biolabs) for different patterns. Clones with different restriction patterns were selected for sequencing and sent to sequence analysis using M13 forward and reverse primers. The chromatogram results from the sequence analysis were displayed with the programs BioEdit and Chromas Lite, and the sequences were compared with data in NCBI BLAST and 16S rRNA databases to match the species with the highest similarity. The accession numbers were obtained from NCBI for 16S rRNA sequence regions for all the clones obtained, and their records were provided to the gene bank.

Phylogenetic trees were constructed using the MEGA X program (Kumar *et al*. 2018) and the Nearest-Neighbor-Interchange (NNI) method (Saitou & Nei 1987). The bootstrap method (1000 replicates) was used for evaluation of the validity of the tree topology. The Jukes-Cantor algorithm was chosen for calculation of the distance matrix (Jukes & Canthor 1969).

*Microbial community analysis with FISH method*

The FISH technique was applied to determine the microbial composition of the samples. For this purpose, the protocols of Amann *et al*. (1995) and Daims *et al*. (2005) were modified and used. First, the fixation process was applied to the wastewater samples. The fixed samples were homogenized and then vortexed. Samples of different volumes were taken, and 10 ml of 1X PBS was added, after which the mixture was passed through a 0.2 µm pore diameter GTTP Isopore (Millipore) filter. To wash the filter, it was passed through a 1X 10 ml PBS filter again (Aman *et al*. 1995). An in situ hybridization buffer was prepared for the hybridization of the fixed and filtered samples. A mixture of 18 µl *in situ* hybridization buffer for reaction and 2 µl probe at 50 ng/µl concentration from ARC344 for Archaea and EUB338 for Bacteria were mixed. In addition, specific probes (Methanomicrobiales inclusive for Methanosarcinaceae specific MG1200) (CGGATAATTCGGGGCATGCTG) were used for specific groups (Raskin *et al*. 1994) The samples were horizontally placed in a hybridization oven (Biometra OV3) for hybridization and incubated for 3 hours at 46°C. They were washed to remove unbound probes after hybridization (Aman *et al*. 1995). After the filters were dried, they were stained with DAPI (4',6'-diamidino-2-phenylindole-dihydrochloride) and examined under an epifluorescent microscope (Leica DM6000B) at 100X lens (Daims *et al*. 2005).

*Metagenomic analysis*

For this purpose, total genomic DNA extraction was performed on the samples to be analyzed, and DNA concentration was measured in NanoDrop in order to determine the DNA quality. After total nucleic acid extraction, DNA amplification, amplicon library construction, and next-generation sequencing studies were performed for highly efficient gene sequencing based on 16S rDNA from extracts. GATC Biotech provided support for these analyses. For genomic DNA amplification, a barcode primer set according to the protocols was used, adapted to the Illumina device. The NCBI database was used for taxonomic profiling and KEGG functional profiling of microbial communities was used for the integrated gene catalogue of the human gut microbiome (IGC). Estimation of diversity indices and community composition were performed QIIME (Quantitative Insights into Microbial Ecology) and R software (Caporaso *et al*. 2010, Oksanen 2013).

## Results

*Physicochemical parameters of samples*

The sample collection was carried out from the bottom port (1M-2M…) to the upper port (7H2) of the reactor. Samples were taken on the 148$^{th}$ operation day of the reactor. The system's temperature was adjusted to mesophilic value of 34.0 ± 1°C controlling the temperature panel. The overall system's average pH range was at 6.8. The pH values of samples from the lower part to the upper part were measured as 6.88, 6.89, 7.16, 7.11, 7.84, 7.20 and 6.92, respectively. $Mg^{+2}$ and $Ca^{+2}$ concentrations were high. The $Mg^{+2}$ contents of samples from the lower part to the upper part were determined as 341.1, 302.9, 272.1, 292.3, 337.7, 287.3, 324.2, 348.1 and 341.4 ppm, respectively. The $Ca^{+2}$ contents of samples from the lower part to the upper part were determined as 309.8, 179.21, 186.6, 159.08, 315.0, 207.5, 425.9, 320.4 and 113.0 ppm, respectively. The obtained samples were stored at -20°C within 60 minutes and samples were kept frozen until DNA extraction.

*16S rRNA cloning*

Using ARDRA, 189 Archaea clones and 282 Bacteria clones were analyzed, which yielded 12 different patterns for Archaea and 25 different patterns for Bacteria. At least 76 clones from the restriction pattern were chosen for sequencing.

Environmental 16S rRNA gene sequences from the samples were stored in the GenBank with these accession numbers MT322876-MT322913, MT325975-MT325986 and MT325989-MT326014. Most of the bacterial clones were related to uncultured Bacteria. Many archaeal clones were related to uncultured Archaea and *Methanosarcina*. For phylogenetic analysis, the maximum-likelihood treeing algorithm in the MEGA X program was used. The phylogenetic trees for Bacteria and Arhaea, constructed based on partial 16S rRNA sequences, were shown in Fig. 1 and 2.

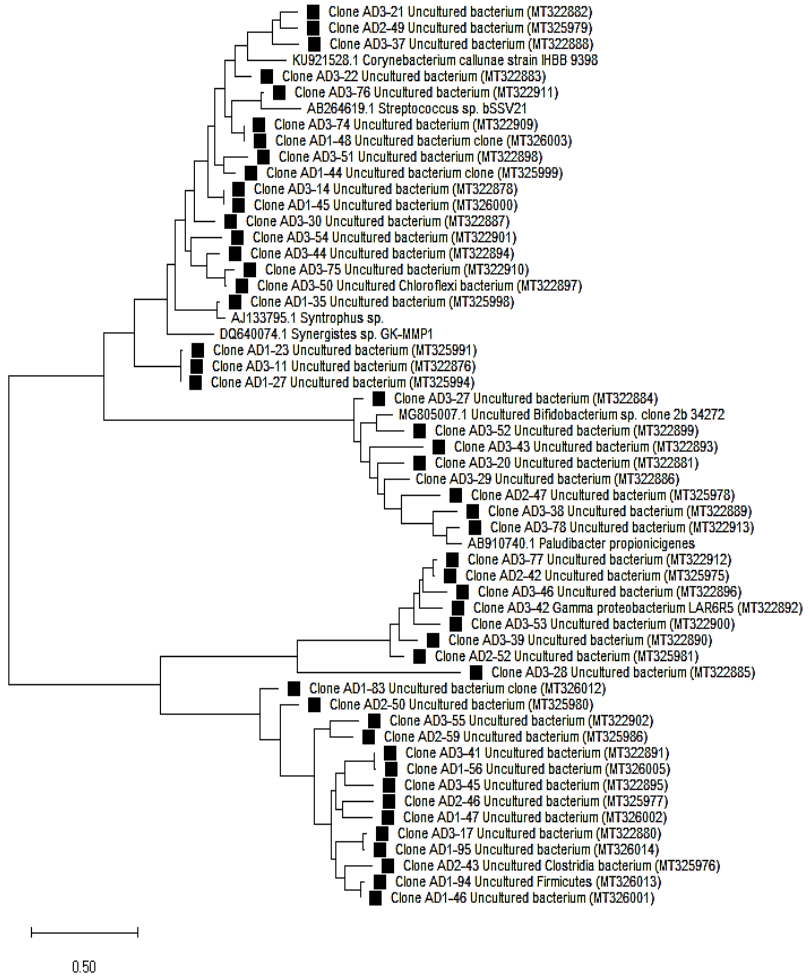


**Fig. 1.** Phylogenetic tree based on 16S rRNA gene sequences from clones belonging to Bacteria (indicated by squares). The scale bar represents the expected number of substitutions per site. Bootstrap support values below 50% were not included in the figure.

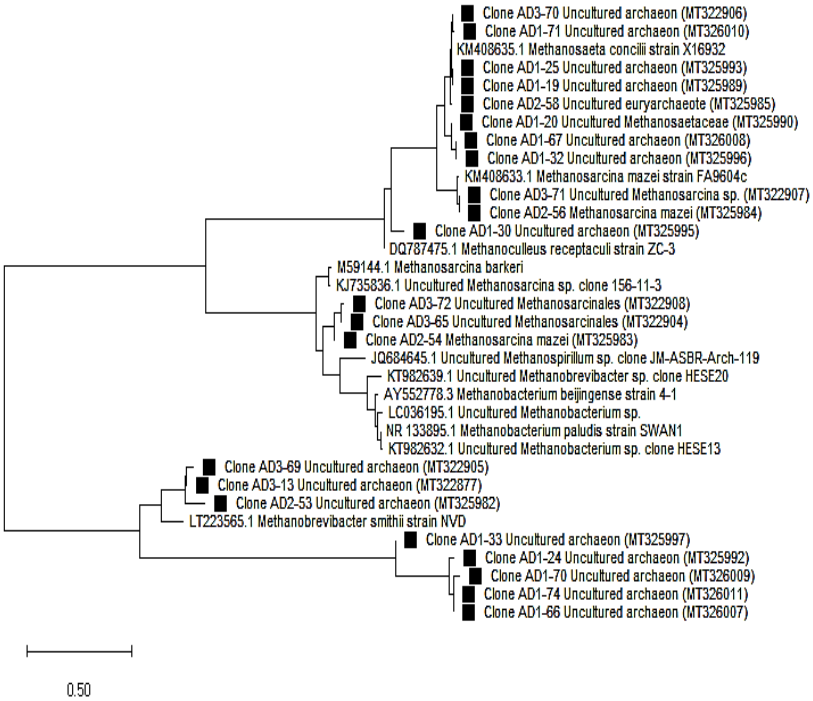


**Fig. 2.** Phylogenetic tree based on 16S rRNA gene sequences from clones belonging to Archaea (indicated by squares). The scale bar represents the expected number of substitutions per site. Bootstrap support values below 50% were not included in the figure.

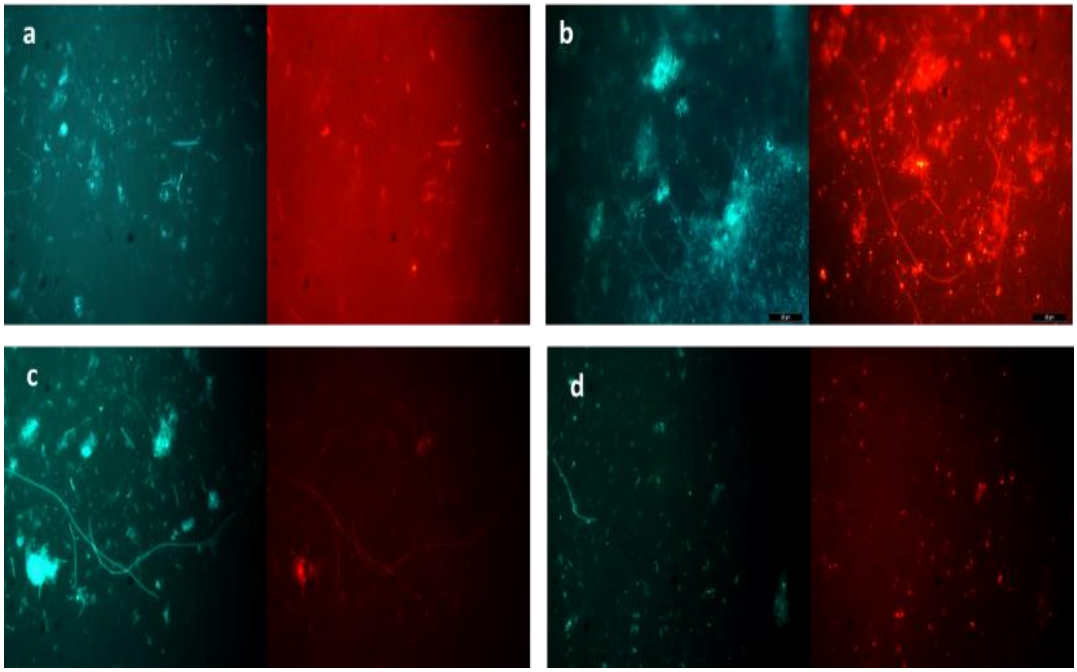


**Fig. 3.** Images of the samples' microbiota (a-d). DAPI staining is shown on the left, and hybridization signals with FISH probes Arc344 (a, b), MG1200 (c) and Eub338 (d) on the right. Image sources were 3M (a), 2M (b) and 5M samples (c, d).

*FISH results*

The FISH analysis of the samples showed that bacterial and archaeal species had nearly equal rates. Rod-shaped cells, long bacilli, coccus and long chains were detected in the samples (Fig. 3).

Positive signals were received as a result of hybridizations with ARC 344, EUB338, and MG1200 probes. Total cell number calculations concluded that microbial cells in the samples was very high; total cells were nearly $10^{10}$-$10^{11}$ cells mL. The concentrations of bacteria for the seven samples ranged between $2.68\times10^{10}\pm4.29\times10^{9}$ and $5.07\times10^{10}\pm7.20\times10^{9}$ cells per mL of samples (Table 1). When compared with the total cell counts determined by DAPI staining, the ratio of bacteria varied between roughly 48% and 60% of the total cell numbers. Archaeal cells ranged between $2.45\times10^{10}\pm4.02\times10^{9}$ and $3.99\times10^{10}\pm1.05\times10^{10}$ cells per ml of samples. The percentage of archaea ranged between 38% and 52% of the total cell numbers. The concentrations of Methanomicrobiales, inclusive of Methanosarcinaceae cells, were between $1.78\times10^{10}\pm4.44\times10^{9}$ and $2.91\times10^{10}\pm3.60\times10^{9}$. This archaeal group was dominant, containing 22-37% of the total archaeal population. The high percentages of standard deviations in the results may be due to high background fluorescence in the samples, affecting the correct probe signal acquisition.

**Table 1.** Cell counts with DAPI, % Archaea, and Bacteria with FISH probes.

| SAMPLE | DAPI counts/ml (mean SD) | EUB338 counts/ml (mean SD) (%) | ARC 344 counts/ml (mean SD) (%) | MG1200 counts/ml (mean SD) (%) |
|---|---|---|---|---|
| **1M** | $6.64\times10^{10}\pm8.32\times10^{9}$ | $3.24\times10^{10}\pm2.12\times10^{9}$ (48%) | $3.53\times10^{10}\pm4.78\times10^{9}$ (52%) | $2.22\times10^{10}\pm8.50\times10^{8}$ (33%) |
| **2M** | $7.97\times10^{10}\pm4.82\times10^{9}$ | $4.57\times10^{10}\pm6.52\times10^{9}$ (53%) | $3.99\times10^{10}\pm1.05\times10^{10}$ (47%) | $2.91\times10^{10}\pm3.60\times10^{9}$ (34%) |
| **3M** | $1.03\times10^{11}\pm2.57\times10^{10}$ | $3.52\times10^{10}\pm2.71\times10^{9}$ (51%) | $3.36\times10^{10}\pm5.29\times10^{8}$ (49%) | $2.13\times10^{10}\pm5.77\times10^{8}$ (31%) |
| **4M** | $9.89\times10^{10}\pm2.35\times10^{10}$ | $5.07\times10^{10}\pm7.20\times10^{9}$ (60%) | $3.36\times10^{10}\pm3.07\times10^{9}$ (40%) | $1.87\times10^{10}\pm5.35\times10^{9}$ (22%) |
| **5M** | $6.57\times10^{10}\pm1.53\times10^{9}$ | $2.68\times10^{10}\pm4.29\times10^{9}$ (52%) | $2.45\times10^{10}\pm4.02\times10^{9}$ (48%) | $1.88\times10^{10}\pm4.90\times10^{9}$ (37%) |
| **6M** | $6.99\times10^{10}\pm1.47\times10^{10}$ | $4.69\times10^{10}\pm3.48\times10^{9}$ (62%) | $2.85\times10^{10}\pm1.07\times10^{10}$ (38%) | $1.83\times10^{10}\pm1.91\times10^{9}$ (24%) |
| **7H2** | $7.09\times10^{10}\pm1.35\times10^{10}$ | $3.73\times10^{10}\pm4.58\times10^{8}$ (60%) | $2.48\times10^{10}\pm1.55\times10^{9}$ (40%) | $1.78\times10^{10}\pm4.44\times10^{9}$ (29%) |

*Metagenomic analysis*

After analyzing the samples, microbial diversity and loading showed some differences. In all samples, Archaea members ranged between 60-36%, and Bacteria members ranged between 58-31%. At the phylum level, in all samples, Euryarchaeota was the most dominant phylum; 1M, 2M, 4M, and 7H2 had more than 50% of it. Proteobacteria (between 14.8-21.97%) and Actinobacteria (between 5.53-15.94%) phyla had a high rate. Members of Spirochaeotes (between 0.63-4.82%) and Bacteroidetes (between 1.72-2.38%) were also analyzed in the samples. At the genus level, there were some differences. *Methanosaeta* was the most dominant genus in sample 1M (55.75%) and sample 7H2 (60.48%), while *Methanosarcina* was the most dominant genus in other samples. Nearly half of the community structures of 3M, 4M, and 6M consisted of *Methanosarcina* members. Members of *Corynebacterium*, *Serratia*, *Streptococcus*, *Bifidobacterium*, *Spharochaeta*, *Clostridium*, *Acinetobacter*, and *Pseudomonas* were detected in the samples. At the species level, *Methanosaeta concilii* was dominant in the samples (Fig. 4). *Corynebacterium callunae* was also dominant. The frequency was nearly the same in samples 2M, 3M, 4M, 5M, and 6M. The other species found were *Methanosarcina vacuolata*, *Serratia marcescens*, *Methanosarcina* sp., and *Methanosarcina barkeri*. In sample 7H2, *Streptococcus agalacticae* and *Serratia marcescens* were detected. Members of *Clostridium saccharoperbutylacetonicum* were observed in samples 5M and 6M (Fig. 4).

The diversity index is a quantitative measure that shows many different species in a dataset as well as the distribution of these species. It increases when the number of species increases and when all species are present at nearly the same level. The diversity indices were calculated using the vegan package in R and QIIME softwares (Table 2).

*Global gene functional profiles*

To detect of the functional profiling of the anaerobic sludge samples, the total reads were consolidated based on the categories of the KEGG database. KEGG analysis showed that 9.70-10.91% of the total reads were related to genetic information processing, 5.20-6.57% were assigned to replication and repair, 3.99-6.41% were related to carbohydrate metabolism, and 4.69-5.11% corresponded to cellular processes and signaling in anaerobic digestion sludge (Fig. 5).

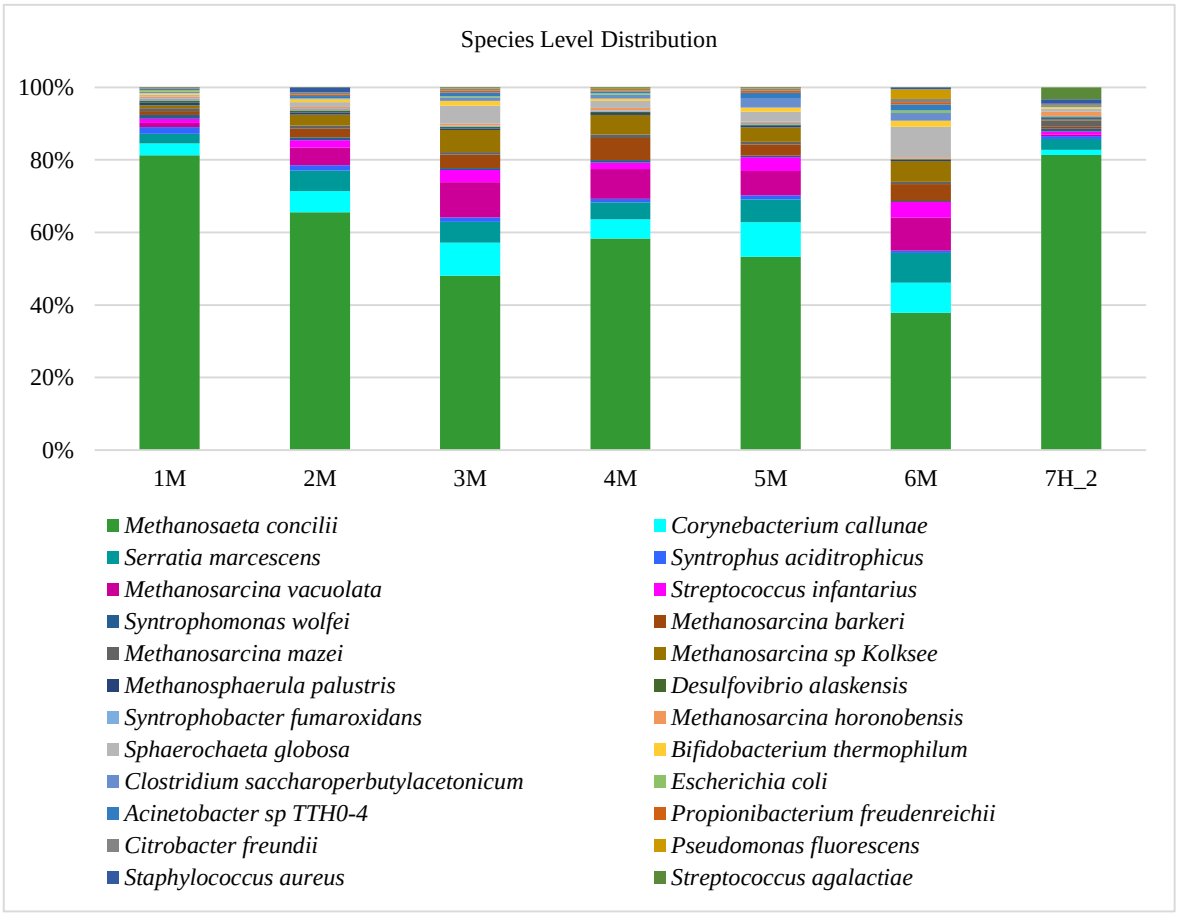


**Fig. 4.** Species level distribution of samples.

**Table 2.** Diversity indices of the microbial communities of the samples

| Sample | Simpson | Shannon | InvSimpson | Alpha | SpeciesNo | Evenness |
|---|---|---|---|---|---|---|
| **1M** | 0.660822175 | 3.228583887 | 2.94830595 | 247.0938675 | 1826 | 0.429911 |
| **2M** | 0.784162313 | 3.723042476 | 4.633111177 | 247.7199183 | 1830 | 0.495608 |
| **3M** | 0.88338962 | 4.170978223 | 8.575565914 | 247.7199183 | 1830 | 0.555237 |
| **4M** | 0.825997654 | 3.846167703 | 5.747048941 | 247.5633824 | 1829 | 0.512036 |
| **5M** | 0.861639717 | 4.076570752 | 7.227507625 | 247.5633824 | 1829 | 0.542709 |
| **6M** | 0.921908257 | 4.361425656 | 12.80545119 | 247.5633824 | 1829 | 0.580631 |
| **7H2** | 0.596514623 | 2.76219843 | 2.478404567 | 246.9373935 | 1825 | 0.367835 |

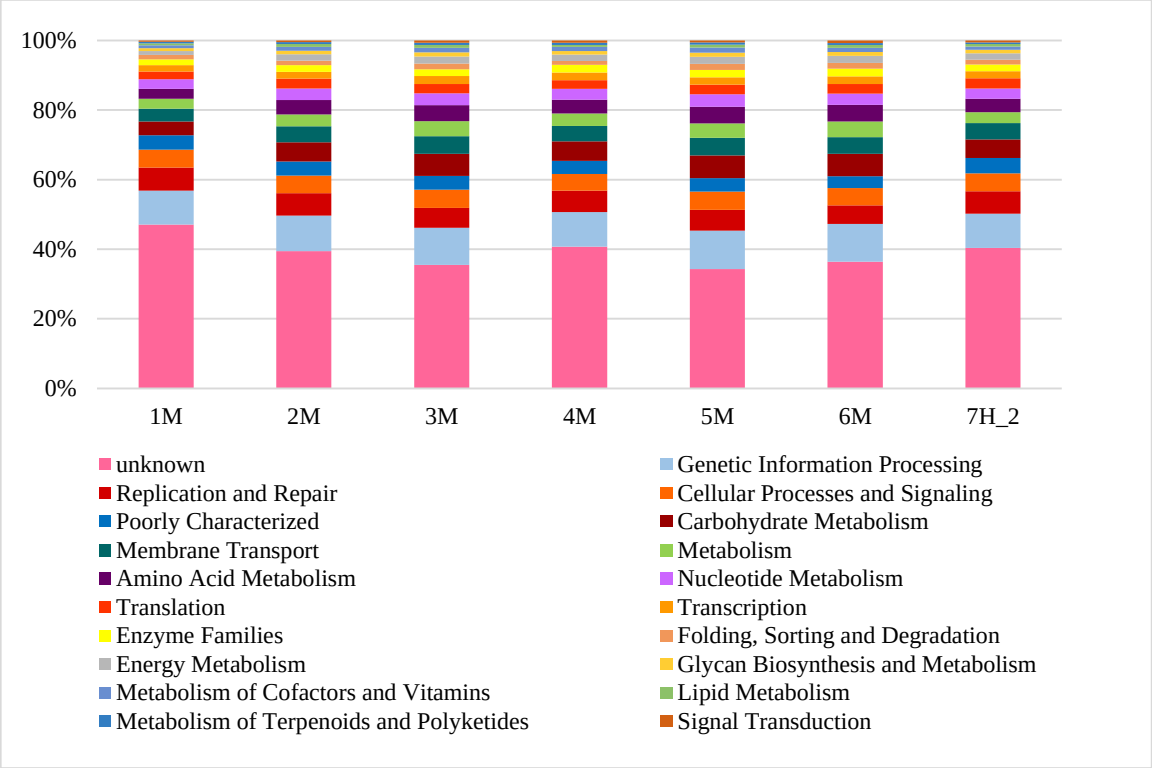


**Fig. 5.** Functional gene categories of the samples.

## Discussion

Anaerobic digestion contains highly complex microbial communities that convert substrates into methane-containing biogas for renewable energy. These microbial communities play critical roles in excess sludge treatment, particularly in determining sludge reduction performance and methane production efficiency. Anaerobic digestion process is accomplished through a series of processes based on the interaction of bacteria and archaea, and it is important to minimize changes in microorganism dynamics and distribution during methane production and to monitor changes to maintain stable performance (Nakasaki *et al.* 2015). Therefore, the relationship between the microbial community structure and function needs to be understood well.

For the analysis of a wide variety of environmental samples such as water and wastewater systems and anaerobic systems, traditional methods such as ARDRA (16S-RFLP), t-RFLP, DGGE, gene cloning based on the comparison and amplification of rRNA sequences gene and FISH have been applied.

Analysis techniques based on nucleic acid have been developed to explain the structure of the community without developing microorganisms in the culture medium (Gilbride *et al*. 2006, Nayak *et al*. 2009, Vanwonterghem *et al*. 2014).

In this study, we applied both traditional methods (FISH and cloning) and metagenomic approaches. The cloning results showed that most of the bacterial clones were related to uncultured members of the Bacteria domain. Many archaeal clones were related to uncultured Archaea and *Methanosarcina*. Cloning and sequencing of the 16S rRNA gene has often been applied to explain the full structure of a microbial community. However, there are microbial clones that are very difficult to classify phylogenetically, and most of the clones are closely related to uncultured strains. There may be some errors in detecting the microorganism community by gene cloning. Since different cells have different 16S rRNA gene copies, inappropriate primer clusters can cause problems in differentiating some microbial species. Thus, many methods have been used in our study to reduce errors. Moreover, clone library sequencing of the 16S rRNA

gene for microbial ecology studies may lead to overestimation or underestimation of the number and diversity of microorganisms due to deviations in amplification (Ye *et al*. 2012, Aird *et al*. 2011, Gao *et al*. 2012).

FISH was also applied, but in wastewater samples, there are humic acids, metals, colloids, and organic and inorganic substances, all which can affect the penetration of the probes into the cells. Thus, samples need pre-treatment steps. These steps may change the results of bacterial and archaeal numbers. We found that bacterial and archaeal species were of nearly equal rates in the samples. In a similar study, Khan *et al*. (2019) detected specific groups of bacteria in the anaerobic digester sludge samples. The number of cells hybridized by the probe EUBmix ranged between 54-89%, and there were different morphologies like cocci, rods, and filaments.

Metagenomic approaches include the analysis of all the genomes of the members of a microbial community. Cloning and genome analysis are conducted without cultivating the organisms in the community. This provides an additional tool for studying non-cultured species. Therefore, the new generation of high-throughput sequencing provides a powerful tool to study the microbial community structure (Albertsen *et al*. 2013, Bragg & Tyson 2014). Thus, in our study, microbial communities in an anaerobic reactor were analyzed using both traditional and modern methods to show the species structure and relations between microorganisms. The use of NGS facilitated detailed analyses of both archeal and bacterial community structures.

When previous studies were evaluated, more than 20 methanogenic bacterial phyla were detected in anaerobic waste and wastewater sludges. The 16S rRNA gene clones' sequencing results concluded various prokaryotic taxa such as Proteobacteria (especially Deltaproteobacteria class), Chloroflexi, Firmicutes, Spirochaetes, and Bacteroidetes. Similarly, clones in the Archaea domain in the classes Methanomicrobia, Methanobacteria, and Thermoplasmata were typical of the clones found in such muds (Narihiro & Sekiguchi 2007). Microbial diversity in full-scale biogas production reactors has been reported using metagenomic studies. In most studies, the results were similar. Guo *et al*. (2015) determined that in anaerobic sludge, Bacteria members were dominant (93%), while Archaea members made up 5.6% of it. It was determined that the most abundant bacterial populations were members of Proteobacteria, Firmicutes, Bacteroidetes, and Actinobacteria at phylum level. The largest class in the Euryarchaeota phylum is Methanomicrobia. It was stated that the predominance of Methanomicrobia was associated with the discovery of *Methanosaeta* and *Methanosarcina*. When our results were compared with this study for functional analysis, it was concluded that a large number of the reads belonged to metabolism. In the category of metabolism, energy production and conversion, amino acid transport and metabolism, and carbohydrate transport and metabolism were dominant. In our study, the total reads were related to genetic information processing, replication, and repair. 3.99-6.41% of the reads were related to carbohydrate metabolism. These results can be used for detecting pathways for the conversion of activated sludge into methane (Guo *et al*. 2015).

In another study, the microbial structure of cassava alcohol wastewater plant was analyzed with the clone libraries by using 16S rRNA gene. Most bacterial OTUs were identified as phyla of Firmicutes, Chloroflexi, Proteobacteria and Bacteroidetes. Methanosaeta, Methanobacterium, Methanomethylovorans and Methanosarcina were the most abundant archaeal groups (Gao *et al*. 2012). However, in our study, Bacteria and Archaea members had nearly equal rates. To summarize, 30315, 32316, 35562, 21255, 28716, 19821 and 27812 sequences were analyzed, respectively, and the microbial community structure was revealed at species and genus levels. The Shannon, Simpson, and Evenness indices changed between 2.76-4.36, 0.59-0.92 and 0.36-0.58, respectively. The calculation of these diversity indices yielded higher diversity values. Between 36-60% of the identified sequences belonged to Archaea, while 31-58% belonged to Bacteria. Euryarchaeota was the most dominant phylum, with nearly 50% rate of the total sequences. The dominant orders were acetotrophic Methanosaeta and Methanosarcina. In Bacteria, the dominant genera were *Corynebacterium*, *Serratia*, *Streptococcus*, *Bifidobacterium*, *Sphaerochaeta*, *Clostridium*, *Acinetobacter* and *Pseudomonas*. The most dominant species detected were *Methanosaeta concilii* and *Methanosarcinia vacuolata* in Archaea and *Corynebacterium callunae* in Bacteria. In the study conducted by Ambuchi *et al.* (2016), 31 phyla were detected, similar to our study. The predominant microbial community phyla belonged to Chloroflexi (27.71%), Euryarchaeota (60.48%) and Firmicutes (44.24%) in the bottom, middle, and upper samples, respectively. These results revealed that the archaeal community members were dominant in almost all parts. The hydrogenotrophic methanogens in the reactor belonged to members of the *Methanospirillum* and *Metanocella* genus, but their abundance was very low. However, aceticlastic methanogens of the genus *Methanosaeta* were predominantly abundant in all parts of the reactor. Moreover, members of *Methanosarcina* were obtained in low rates (Ambuchi *et al*. 2016).

The number of Methanosarcinales is usually more than that of Methanomicrobiales in the methane fermentation process (Tabatabaei *et al.* 2010). The groups of acetotrophic, hydrogenotrophic, and methylotropic Archaea are in balance in the anaerobic system and have an equal role in the production of methane when the organic load is low. *Methanosaeta* sp. is predominant during the fermentation of organically rich substrates such as polysaccharides and protein rich granules in the up-flow UASB (Amin & Vriens 2014). However, environmental parameters affect the structure of the

microbial community in the anaerobic digester. Environmental parameters are especially important for methanogenesis. Compared to bacteria, methanogens have a lower growth rate and are susceptible to environmental degradation, such as pH drop and high amounts of essential fatty acid and ammonia. Environmental parameters such as pH, temperature, substrate concentration and the formation of toxic or inhibitory compounds can alter the balance in the methanogenic community structure and affect the overall treatment process. (Chen *et al*. 2008). Reducing the temperature to psychrophilic values can change the structure of the microbial community from acetoclastic to hydrogenotrophic methanogens. If changes in the amount and content of the substrate occur, it can affect the methanogenic community and activity. Different substrate types can cause different methanogenic communities to form (Lee *et al*. 2009).

## Conclusion

This study revealed the detailed microbial community structure of an anaerobic digester by applying cloning, FISH and metagenomic analysis. The taxonomic analysis showed that the Euryarchaeota phylum was the most dominant in archaeal populations, while Proteobacteria, Actinobacteria, Spirochaeotes and Bacteroidetes were the most abundant bacterial populations in the anaerobic digestion sludge. The results showed that acetoclastic methanogenes such as *Methanosaeta* and *Methanosarcina* were predominant in the anaerobic reactor, and it was concluded that acetoclastic methanogenesis may be dominant. The anaerobic digestion system has problems due to overloading, particularly in the presence of high-strength organic wastewater such as molasses, which causes the degradation of system performance. These results will help facilitate the development of more efficient anaerobic treatment systems.

## Acknowledgement

I would like to thank Prof. Dr. Mehmet Burcin MUTLU (Eskişehir-Turkey) for his scientific comments on this work.

**Ethics Committee Approval:** Since the article does not contain any studies with human or animal subject, its approval to the ethics committee was not required.

**Conflict of Interest:** The authors have no conflicts of interest to declare.

**Funding:** The author declared that this study has received no financial support.

## References

1. Aird, D., Ross, M. G., Chen, W. S., Danielsson, M., Fennell, T., Russ, C., Jaffe B.D., Nusbaum C. & Gnirke, A. 2011. Analyzing and minimizing PCR amplification bias in Illumina sequencing libraries. *Genome Biology*, 12(2): 1-14. https://doi.org/10.1186/gb-2011-12-2-r18
2. Albertsen, M., Hugenholtz, P., Skarshewski, A., Nielsen, K.L., Tyson, G.W. & Nielsen, P.H. 2013. Genome sequences of rare, uncultured bacteria obtained by differential coverage binning of multiple metagenomes. *Nature Biotechnology*, 31(6): 533-538. https://doi.org/10.1038/nbt.2579
3. Amann, R.I., Ludwig, W. & Schleifer, K.H. 1995. Phylogenetic identification and in situ detection of individual microbial cells without cultivation. *Microbiological Reviews*, 59(1): 143-169. https://doi.org/10.1128/MMBR.59.1.143-169.1995
4. Ambuchi, J.J., Liu, J., Wang, H., Shan, L., Zhou, X., Mohammed, M.O. & Feng, Y. 2016. Microbial community structural analysis of an expanded granular sludge bed (EGSB) reactor for beet sugar industrial wastewater (BSIW) treatment. *Applied Microbiology and Biotechnology*, 100(10): 4651-4661. https://doi.org/10.1007/s00253-015-7245-2
5. Amin, G.A. & Vriens, L. 2014. Optimization of up-flow anaerobic sludge blanket reactor for treatment of composite fermentation and distillation wastewater. *African Journal of Biotechnology*, 13(10): 1136-1142. https://doi.org/10.5897/AJB2013.12228
6. Andersson, S. 2009. Characterization of bacterial biofilms for wastewater treatment (Doctoral dissertation, Kungliga Tekniska Högskolan). *KTH, School of Biotechnology, Environmental Microbio*logy, Stockholm, Swedish.
7. Bragg, L. & Tyson, G.W. 2014. Metagenomics using next-generation sequencing. In: Environmental microbiology: methods and protocols, *vol. 1096. 2nd ed, Paulsen IT.*, Holmes AJ, (eds.). New York City: Humana Press; 183-201. https://doi.org/10.1007/978-1-62703-712-9_15
8. Caporaso, J. G., Kuczynski, J., Stombaugh, J., Bittinger, K., Bushman, F. D., Costello, E. K., & Knight, R. 2010. QIIME allows analysis of high-throughput community sequencing data. *Nature Methods*, 7(5): 335-336. https://doi.org/10.1038/nmeth.f.303
9. Chen, Y., Cheng, J.J. & Creamer, K.S. 2008. Inhibition of anaerobic digestion process: a review. *Bioresource Technology*, 99(10): 4044-4064. https://doi.org/10.1016/j.biortech.2007.01.057
10. Daims, H., Stoecker, K. & Wagner, M. 2005. Fluorescence *in situ* hybridization for the detection of prokaryotes. In Molecular Microbial Ecology: 208-228. Osborn, A.M., Smith, C.J., (eds.) Taylor & Francis, Abingdon, UK.
11. Gao, R., Cao, Y., Yuan, X., Zhu, W., Wang, X. & Cui, Z. 2012. Microbial diversity in a full-scale anaerobic reactor treating high concentration organic cassava wastewater. *African Journal of Biotechnology*, 11(24): 6494-6500. https://doi.org/10.5897/AJB11.3142
12. Gilbride, K.A., Lee, D.Y. & Beaudette, L.A. 2006. Molecular techniques in wastewater: understanding microbial communities, detecting pathogens, and real-time process control. *Journal of Microbiological Methods*, 66(1): 1-20. https://doi.org/10.1016/j.mimet.2006.02.016

13. Guo, J., Peng, Y., Ni, B.J., Han, X., Fan, L. & Yuan, Z. 2015. Dissecting microbial community structure and methane-producing pathways of a full-scale anaerobic reactor digesting activated sludge from wastewater treatment by metagenomic sequencing. *Microbial cell factories*, 14(1): 33-44. https://doi.org/10.1186/s12934-015-0218-4

14. Jukes, T.H. & Cantor, C.R. 1969. Evolution of protein molecules. Mammalian protein metabolism, Munro, H.N. (ed.). New York: Academic Press. 3: 21-132. https://doi.org/10.1016/B978-1-4832-3211-9.50009-7

15. Khan, M.A., Ashar, N.N., Ganesh, A.G., Rais, N., Faheem, S.M. & Khan, S.T. 2019. Bacterial Community Structure in Anaerobic Digesters of a Full Scale Municipal Wastewater Treatment Plant–Case Study of Dubai, United Arab Emirates. *Journal of Sustainable Development of Energy, Water and Environment Systems*, 7(3): 385-398. https://doi.org/10.13044/j.sdewes.d6.0222

16. Kumar, S., Stecher, G., Li, M., Knyaz, C. & Tamura, K. 2018. MEGA X: molecular evolutionary genetics analysis across computing platforms. *Molecular Biology and Evolution*, 35(6): 1547-1549. https://doi.org/10.1093/molbev/msy096

17. Lane, D.J., Pace, B., Olsen, G.J., Stahl, D.A., Sogin, M.L. & Pace, N.R. 1985. Rapid determination of 16S ribosomal RNA sequences for phylogenetic analyses. *Proceedings of the National Academy of Sciences*, 82(20): 6955-6959. https://doi.org/10.1073/pnas.82.20.6955

18. Lee, C., Kim, J., Hwang, K., O'Flaherty, V. & Hwang, S. 2009. Quantitative analysis of methanogenic community dynamics in three anaerobic batch digesters treating different wastewaters. *Water Research*, 43(1): 157-165. https://doi.org/10.1016/j.watres.2008.09.032

19. Mutlu, M.B. & Güven, K. 2015. Bacterial diversity in Çamaltı saltern, Turkey. *Polish Journal of Microbiology*, 64(1): 37-45. https://doi.org/10.33073/pjm-2015-005

20. Nakasaki, K., Kwon, S.H. & Takemoto, Y. 2015. An interesting correlation between methane production rates and archaea cell density during anaerobic digestion with increasing organic loading. *Biomass and Bioenergy*, 78: 17-24. https://doi.org/10.1016/j.biombioe.2015.04.004

21. Narihiro, T. & Sekiguchi, Y. 2007. Microbial communities in anaerobic digestion processes for waste and wastewater treatment: a microbiological update. *Current Opinion in Biotechnology*, 18(3): 273-278. https://doi.org/10.1016/j.copbio.2007.04.003

22. Nayak, B.S., Levine, A.D., Cardoso, A. & Harwood, V.J. 2009. Microbial population dynamics in laboratory-scale solid waste bioreactors in the presence or absence of biosolids. *Journal of Applied Microbiology*, 107(4): 1330-1339. https://doi.org/10.1111/j.1365-2672.2009.04319.x

23. Oksanen, J. 2013. Vegan: ecological diversity. *R Project*, 368 pp.

24. Raskin, L., Stromley, J.M., Rittmann, B.E. & Stahl, D.A. 1994. Group-specific 16S rRNA hybridization probes to describe natural communities of methanogens. *Applied and Environmental Microbiology*, 60(4): 1232-1240. https://doi.org/10.1128/AEM.60.4.1232-1240.1994

25. Saitou, N. & Nei, M. 1987. The neighbor-joining method: a new method for reconstructing phylogenetic trees. *Molecular Biology and Evolution*, 4(4): 406-425.

*26.* Singka, D., Kumdhitiahutsawakul, L., Rekkriangkrai, P. & Pathom-Aree, W. 2012. A simple method for DNA extraction from activated sludge. *Chiang Mai Journal of Science*, 39(1): 111-118.

27. Tabatabaei, M., Rahim, R.A., Abdullah, N., Wright, A.D.G., Shirai, Y., Sakai, K., Sulaiman, A. & Hassan, M.A. 2010. Importance of the methanogenic archaea populations in anaerobic wastewater treatments. *Process Biochemistry*, 45(8): 1214-1225. https://doi.org/10.1016/j.procbio.2010.05.017

28. Vaneechoutte, M., Rossau, R., De Vos, P., Gillis, M., Janssens, D., Paepe, N., De Ruck, A., Fiers, T., Claeys, G. & Kersters, K. 1992. Rapid identification of bacteria of the Comamonadaceae with amplified ribosomal DNA-restriction analysis (ARDRA). *FEMS Microbiology Letters*, 93(3): 227-233. https://doi.org/10.1111/j.1574-6968.1992.tb05102.x

29. Vanwonterghem, I., Jensen, P.D., Ho, D.P., Batstone, D.J. & Tyson, G.W. 2014. Linking microbial community structure, interactions and function in anaerobic digesters using new molecular techniques. *Current Opinion in Biotechnology*, 27: 55-64. https://doi.org/10.1016/j.copbio.2013.11.004

30. Venkiteshwaran, K., Bocher, B., Maki, J. & Zitomer, D. 2015. Relating anaerobic digestion microbial community and process function. *Microbiology Insights*, 8(2): 37-44. https://doi.org/10.4137/MBI.S33593

31. Ye, L., Zhang, T., Wang, T. & Fang, Z. 2012. Microbial structures, functions, and metabolic pathways in wastewater treatment bioreactors revealed using high-throughput sequencing. *Environmental Science and Technology*, 46(24): 13244-13252. https://doi.org/10.1021/es303454k

32. Yıldız, S., Namal, O.Ö. & Çekim, M. 2013. Atık su arıtma teknolojilerindeki tarihsel gelişimler. *Selçuk Üniversitesi Mühendislik, Bilim ve Teknoloji Dergisi*, 1(1): 55-67 (In Turkish).

*http://dergipark.org.tr/trkjnat*
*Trakya University Journal of Natural Sciences, 22(1): 59-65, 2021*
*ISSN 2147-0294, e-ISSN 2528-9691*
*DOI: 10.23902/trkjnat.815752*

**Research Article**

# PHENOLOGICAL CYCLE AND DIURNAL VARIATION EFFECTS ON THE VOLATILE OIL CHARACTERISTICS OF SAGE (*Salvia officinalis* L.)

Amir SOLTANBEIGI[1*], Elnaz SAMADPOURRIGANI[2]

[1] Department of Basic Pharmaceutical Sciences, Faculty of Pharmacy, Afyonkarahisar Health Sciences University, Afyonkarahisar, TURKEY

[2] Ambaryolu St. Apt. 15, Afyonkarahisar, TURKEY.

**Cite this article as:**

Soltanbeigi A. & Samadpourrigani E. 2021. Phenological cycle and diurnal variation effects on the volatile oil characteristics of sage (*Salvia officinalis* L.). *Trakya Univ J Nat Sci*, 22(1): 59-65, DOI: 10.23902/trkjnat.815752

Received: 24 October 2020, Accepted: 26 March 2021, Online First: 07 April 2021, Published: 15 April 2021

**Abstract:** This study was carried out to evaluate the effects of phenological and diurnal variation on volatile oil content and quality of *Salvia officinalis* L. (Lamiaceae) cultivated in Afyonkarahisar/Turkey. The harvesting times based on ontogeny were the pre-flowering, flowering and post-flowering stages. The harvesting took place three times a day, at 6:00 a.m., 2:00 and 8:00 p.m. The results showed that the highest volatile oil was obtained at 8:00 p.m. of the flowering stage (2.05%). In general, the best harvesting time was the flowering stage and the last hours of the day. The synthesis of volatile oil was almost the same at other phenological stages. The amount of volatile oil increased at the sunset time of the day in all studied stages. Among the identified of *S. officinalis* volatile oil compounds, oxygenated monoterpenes were the largest chemical group (52.8-68.6%). α-Thujone (13.0-35.8%) was the major compound of the most samples. The highest and lowest values of this compound were observed in the post-flowering and flowering stages, respectively. The other main compounds were camphor (7.0-20.2%), 1,8-cineole (6.9-14.1%), borneol (2.8-15.8%) and veridiflorol (4.5-12.3%). The effects of climatic factors such as day length, insolation, temperature and plant growth stage affected the quantity and quality of volatile oil content of *S. officinalis*. The results showed that the best harvesting time for *S. officinalis* for volatile oil content is 8:00 p.m. at the flowering stage in Afyonkarahisar climatic conditions. The volatile oil compositions of the plant varied widely at different harvest times (ontogeny and diurnal).

**Özet:** Bu çalışmada Afyonkarahisar'da yetiştirilen *Salvia officinalis* L. (Lamiaceae) uçucu yağ oranı ve kalitesi üzerindeki fenolojik evre ve diurnal varyabilite etkileri araştırılmıştır. Ontogenetik varyabiliteye dayalı hasat zamanları çiçeklenme öncesi, çiçeklenme dönemi ve çiçeklenme sonrası olarak belirlenmiştir. Diurnal varyabilite olarak hasat saatleri 06:00, 14:00 ve 20:00 ayarlanmıştır. Sonuçlara göre en yüksek uçucu yağ çiçeklenme döneminde ve saat 20:00'de (%2,05) elde edilmiştir. En iyi hasat zamanı çiçeklenme dönemi ve günün son saatleri olarak saptanmıştır. Diğer fenolojik evrelerde uçucu yağ sentezi neredeyse aynı oranda bulunmuştur. Ayrıca, çalışılan tüm evrelerde uçucu yağ içeriği günün son saatlerine doğru artmıştır. *Salvia officinalis* uçucu yağının tanımlanan bileşikleri arasında oksijenli monoterpenler en büyük kimyasal gruba sahip olmuştur (%52,8-68,6). α-Thujone (%13,0-35,8) deneme örneklerinin çoğunda ana bileşik olarak belirlenmiştir. Bu bileşiğin en yüksek ve en düşük değerleri sırasıyla çiçeklenme sonrası ve çiçeklenme aşamalarında gözlenmiştir. Camphor (%7,0-20,2), 1,8-sineol (%6,9-14,1), borneol (%2,8-15,8) ve veridiflorol (%4,5-12,3) diğer önemli bileşikler olarak tanımlanmıştır. *Salvia officinalis* uçucu yağının miktarı ve kalitesi üzerinde gün uzunluğu, güneşlenme, sıcaklık gibi iklim faktörleri ve bitki büyüme evresi etkileri belirgin bir şekilde ortaya çıkmıştır. Bu çalışmanın sonuçları doğrultusunda, *S. officinalis*'in en uygun hasat zamanı Afyonkarahisar koşullarında çiçeklenme dönemi ve saat 20:00 olarak belirlemiştir. Bitkinin uçucu yağ bileşenleri, farklı hasat zamanlarında (ontogenetik ve diurnal) geniş değişim göstermiştir.

***Edited by:***
*Mehmet Bora Kaydan*

***Corresponding Author:***
*Amir Soltanbeigi*
*amir.soltanbeigi@afsu.edu.tr*

***ORCID iDs of the authors:***
*AS. orcid.org/0000-0002-7891-0491*
*ES. orcid.org/0000-0003-3768-8147*

***Key words:***
*Diurnal*
*Essential oil*
*GC-MS*
*Ontogeny*
*Salvia officinalis*

## Introduction

*Salvia officinalis* L. (common sage), as a woody perennial herb, is one of the most important commercial species of the genus *Salvia* which includes nearly 1000 species throughout the Old and New Worlds (Lakušić *et al.* 2013). *Salvia officinalis* is native to the Mediterranean region but does not exist naturally in Turkey (Sönmez &

Bayram 2017). The cultivation of *S. officinalis* has recently become common in different regions of Turkey. This plant has anti-oxidant, anti-diabetic, anti-inflammatory, anti-bacterial, anti-viral, anti-fungal, anti-anxiety, memory-improving and hypoglycemic activities and there exist reports on its protective effects against Alzheimer, cardiovascular diseases and cancer (Grdiša *et al.* 2015, Miraj & Kiani 2016). It is also used as a diuretic, a local anesthetic for the skin, a styptic, traditionally (Bozin *et al.* 2007). The extensive therapeutic properties of *S. officinalis* are mainly related to bioactive compounds, especially its volatile oils (VOs) (Rguez *et al.* 2018). Camphor (23.6-32.5%), α-thujone (11.3-28.5%), 1,8-cineole (7.9-9.5%), camphene (6.2-8.6%), β-thujone (4.6-10.5%), α-pinene (3.2-5.9%), borneol (3.1-4.2%), β-pinene (2.3-2.7%), viridiflorol (2.5-3.9%), α-humulene (1.9-3.1%) and manool (1.0-2.9%) were determined as the major chemical components of *S. officinalis* (Katar *et al.* 2019).

The production of secondary metabolites in plants as bioactive chemicals is a natural response to biotic and abiotic stresses that improve plant resistance to adverse conditions (Ramakrishna & Ravishankar 2011). The biosynthesis of secondary metabolites in terms of quality and quantity, although controlled genetically, is strongly affected by the climatic conditions, environment organisms, applied agro-techniques, harvesting time and post-harvesting processing (Miguel *et al.* 2004, Soltanbeigi & Sakartepe 2020). In other words, the volatile oil synthesis depends on the interaction between genetic, ontogenesis and physiological state of the plant with environmental conditions. The regulation of the volatile compounds is further complicated by dynamic differential components of abiotic factors such as edaphic properties, moisture, temperature and light intensity (Lee & Ding 2016). Ontogeny acts as a timeline for plant growth, which has a major role in determining the maximum accumulation time of volatile oils (Verma *et al.* 2012). The accumulation pattern of secondary metabolites in plants is characterized by diurnal fluctuation due to enzymatic activities, temperature and light (Asghari *et al.* 2014). Knowledge of factors that increase the quality and quantity in agro-ecosystems is necessary. These factors largely depend on the type of plant that can be considered to achieve cultivation aim. Therefore, methods that can produce a healthy medicinal plant with more effective substances may be needed (Azarnivand *et al.* 2010). Since climatic conditions cannot be controlled and managed, planting time, agronomic practices and especially harvesting time are the most critical factors in the optimal production of volatile oil and its quality (Lakušić *et al.* 2013, Katar *et al.* 2019).

This study aimed to determine the appropriate harvest time for *S. officinalis* in terms of ontogenetic and diurnal variability in Afyonkarahisar climate conditions.

## Materials and Methods

### *Plant Material, Location*

The plant material was 3-year-old *Salvia officinalis*. The samples were obtained from an ongoing study in Afyonkarahisar Medicinal and Aromatic Plants Centre (38° 46' N, 30° 30' E) located in Turkey's inner Aegean region. The region is characterized as a transitional climate zone affected by three main climatic conditions seen in the Mediterranean (South), Central Anatolia (East) and Aegean (West) regions. The climate of the experimental location is harsh, with moderate rainy. Most precipitation occurs in winter and spring. Summers are hot and dry and winters are cold and snowy. Some meteorological data during the sampling season are given in Table 1 and some physico-chemical properties of the soil of the sampling area are given in Table 2.

### *Treatments*

Plants allocated for sampling were grown following sustainable farming methods. Samples were taken at three different growth and developmental stages (ontogenetic variability) and three different hours of the day (diurnal variability). The pre-flowering (1 June), full flowering (24 July) and post-flowering (29 August) stages were chosen for ontogenetic variability samples. The hours for diurnal diversity were 6:00 a.m., 2:00 p.m. and 8:00 p.m. The plant samples were cut from 5-8 cm and were separated to leaves and stems. The leaves were dried at 37°C in a cabinet type dryer for 72 hours.

**Table 1.** Some local meteorological data of the experimental field in 2019.

| Months | Min. Temperature (°C) | Max. Temperature (°C) | Mean Temperature (°C) | Precipitation (mm) | Relative humidity (%) | Exposure to sun rays (h) |
|---|---|---|---|---|---|---|
| **January** | -1.5 | 5.2 | 1.6 | 58.7 | 78.7 | 72.3 |
| **February** | 0.3 | 8.5 | 4 | 35.3 | 71.3 | 104.5 |
| **March** | 1.4 | 12.8 | 6.8 | 10.9 | 58 | 185.2 |
| **April** | 4.3 | 15.2 | 9.5 | 21.3 | 61.5 | 150.8 |
| **May** | 10.4 | 23.2 | 16.7 | 44.1 | 53.5 | 249.1 |
| **June** | 14.5 | 26.7 | 20.5 | 78.4 | 58.3 | 232.3 |
| **July** | 14.9 | 28.5 | 21.9 | 29.1 | 49.1 | 325.3 |
| **August** | 16.2 | 29.5 | 22.8 | 4.5 | 47.4 | 286.7 |
| **September** | 12 | 26.8 | 19.4 | 2.7 | 48.1 | 270.1 |

Turkish State Meteorological Service

**Table 2.** The values of some physico-chemical properties of the experimental soil.

| Properties | (%) | Elements | (ppm) |
|---|---|---|---|
| Organic matter content | 1.84 | Ca | 3287 |
| Total N | 0.14 | Mg | 577 |
| Sand | 46.41 | K | 783 |
| Clay | 32.98 | Na | 80 |
| Dust | 20.61 | Fe | 0.21 |
| Lime | 3.14 | P | 109 |
| Field capacity | 27.43 | Cu | 2.3 |
| Wilting point | 17.01 | Zn | 0.17 |
| Available moisture | 10.41 | Mn | 1.91 |

Soil class: Sandy clay; EC (mS $cm^{-1}$): 0.19; pH: 8.37

*Volatile oil isolation*

For VO isolation, 50 grams of dry leaves were subjected to hydro-distillation with distilled water (1:10) by a neo-Clevenger type apparatus for three hours in 3 replications. The VO content was determined volumetrically (mL 100 $gr^{-1}$). After decantation, the VO samples were dried over anhydrous sodium sulfate and kept in amber vials at -4°C.

*Identification of chemical compounds*

The chromatographic analysis was conducted by a gas chromatography (GC) system (Agilent 7890B-USA) equipped with a flame ionization detector (FID) and coupled to a mass spectrometry detector (MSD) (Agilent 5977A-USA) under electron impact ionization (70 eV). The MS scan range was 50-550 atomic mass units (AMU). The column for the separation of the compounds was HP-Innowax (Agilent 19091N-116: 60 m × 0.320 mm internal diameter and 0.25 µm film thickness). The carrier gas was helium at a flow rate of 1.3 mL $min^{-1}$. The detector, injector and ion source temperatures were 270°C, 250°C and 230°C, respectively. Injection volume was set at 1 µL (20 µL VO was diluted in 1 mL n-Hexane) in split mode (40:1). The samples were analyzed with the column held initially at 70°C for 5 min hold time. Then, the temperature was raised to 160°C with a 3°C $min^{-1}$ heating ramp and 5 min hold time. Eventually, the temperature reached to 250°C with a 6°C $min^{-1}$ heating ramp and 5 min hold time. For accurate determination of chemical compounds, the retention indices (RI) were calculated by injecting $C_7$-$C_{30}$ n-alkanes (Sigma-Aldrich-USA) to (GC/FID) system (Agilent 7890B-USA) under the same conditions of the VO analyses. The identifications of the VO components were performed by comparing retention indices, mass spectra by the computer library database of US National Institute of Standards and Technology (NIST), Wiley libraries, other published mass spectra data (Adams 2007) and our database. Relative abundance (% area) was calculated based on the ratio between each compound's peak area and the sum of areas of all compounds. No response factors were calculated.

## Results and Discussions

The distillation step revealed that the samples' VO content varied by different growth stages and different hours of the day (1.0-2.05 mL $100gr^{-1}$). In terms of ontogenetic variability, the maximum VO contents was obtained from samples taken in the full flowering stage (1.4-2.05 mL $100gr^{-1}$). The VO content VO increased diurnally in all three stages of the harvests as hours progressed during the day (1.3-2.05 mL $100gr^{-1}$) (Table 3). Although genetics is considered to be the crucial determinant of quantity and quality (Lee & Ding 2016), it is inferred that in addition to agricultural practices, plant age, day length, light intensity, day and night temperature changes and relative humidity affect the VO content (Soltanbeigi 2020). Based on European Pharmacopoeia (2005) standards, the minimum VO content of *S. officinalis* should not be less than 1.5% in dried leaves. According to Paulus *et al.* (2019), the sunlight (quality, intensity and duration) has the most effect on VO synthesis. The flowering stage in this study coincided with July, when the plants received most of the light intensity (Table 1). Ben-Farhat *et al.* (2016) showed that the best time to harvest *S. officinalis* is the flowering stage (1.49%) in terms of VO content. Besides, the process of biosynthesis of VOs in plants takes place only in very young cells. Since the accumulation of VO is directly related to leaf ontogeny, its synthesis rate is rapid in the early stages of leaf growth. With increasing leaf weight, its VO content remains almost constant (Nurzyńska-Wierdak *et al.* 2012). Ramezani *et al.* (2009) indicated the temperature variation during the day has more effect on VO accumulation. More recently, Rguez *et al.* (2018) reported an increase in *S. officinalis* VO content from morning to afternoon (7 a.m.: 0.78%, 12 noon: 0.93% and 5 p.m.: 1.1%).

A total of 44 components were obtained as a result of GC-MS analyses (Table 3). The highest number of components was found at 2:00 p.m. sample related to the pre-flowering stage. The least component was obtained at 2:00 p.m. in the full flowering stage. Some components were not found in different growth stages and different times of the day. For instance, tricyclene, sabinene and 1-octen-3-ol were not found in the pre-flowering samples, sabinyl acetate, alloaromadendrene and (+)-spathulenol were not detected in the pre-flowering and flowering stages, cis-Ocimene, α-copaene, linalool and propanal, 2-methyl-3-phenyl- did not appear in the flowering and post-flowering stages. Aromadendrene and γ-cadinene were not identified in the flowering and post-flowering stages, respectively.

Oxygenated monoterpenes were the main chemical group at different phenological stages with a considerable difference (52.8-68.6%) (Table 3). The highest accumulation of oxygenated monoterpenes occurred in the post-flowering stage, followed by flowering and pre-flowering stages, respectively. In other words, with the aging of the plants, the amounts of oxygenated monoterpenes increased. Although the highest level of oxygenated monoterpenes was observed at 8:00 p.m. of

the pre-flowering stage, this group's amounts were higher in the morning harvests (6:00 a.m.) of flowering and post-flowering stages. This group was followed by hydrocarbon sesquiterpenes (6.6-19.6%), hydrocarbon monoterpenes (4.7-14.3%), oxygenated sesquiterpenes (7.0-13.6%), oxygenated diterpenes (2.1-6.5%) and esters (0.6-4.5%). The highest level of hydrocarbon monoterpenes was observed in the flowering and post-flowering stages. This group lacked specific behavior in terms of diurnal changes. However, the total amount of monoterpenes (oxygenated monoterpenes + hydrocarbon sesquiterpenes) in VO was highest at 6:00 a.m. Levels of both oxygenated sesquiterpenes and sesquiterpene hydrocarbons decreased with the aging of the plants. This state was in contrast to monoterpene's behavior. Epimanool, as a labdane diterpenoid, was the only oxygenated diterpene in VO samples of *S. officinalis*. The highest amounts of this composition were identified in the pre-flowering stage. As the hour progresses during the day, the values of this compound increased in all three phenological stages. Also, the highest accumulation of esters was in the flowering stage (Table 3). According to Piccaglia *et al.* (1997) low light and low temperatures at harvest time are likely to cause internal conversions between monoterpenes and sesquiterpenes. Increased oxygenated monoterpenes of *S. officinalis* VO in the post-flowering stage (fruiting) have been reported by Ben-Farhat *et al.* (2016) and Mirjalili *et al.* (2006). In the study of Lakušić *et al.* (2013) on *S. officinalis*, the total monoterpene compounds increased in the warm months of the year and at the same time, the sesquiterpene compounds decreased, as in the case of our findings. The amount of monoterpene hydrocarbons at the flowering stage was also reported to be higher than at other phenological stages (Mirjalili *et al.* 2006), similar to our findings, but the sum of monoterpenes was higher in the flowering stage. Rguez *et al.* (2018) indicated that the amount of oxygenated monoterpenes in the late afternoon hours of the day (5:00 p.m.) was at the highest level and monoterpene hydrocarbons were at the lowest level. But the sum of these two groups increased as the hour progresses during the day.

Except for the samples taken at 2:00 p.m. and 8:00 p.m. in the flowering stage, α-thujone (13.0-35.8%) was identified as the major compound of *S. officinalis* VO. The lowest (13.0%) and highest (35.8%) content of α-thujone was found at 8:00 p.m. in the flowering stage and 2:00 p.m. in the post-flowering samples, respectively. In terms of ontogenetic variation, the highest α-thujone content was in the after-flowering stage (32.3-38.8%). The pre-flowering and flowering stages followed the post-flowering stage. The highest α-thujone in the pre-flowering and flowering stages were recorded at 6:00 a.m. (23.8 and 19.2%) (Table 3). According to the observations of Mirjalili *et al.* (2006) and Ben-Farhat *et al.* (2016), the maximum amount of α-thujone was in the post-flowering stage (fruiting stage) and the lowest level was in the flowering stage. Katar *et al.* (2019) also reported the highest amounts of this compound in the full-flowering and fruiting-set stages. As the aging of *S. officinalis*, α-thujone biosynthesis accelerates, which almost coincides with the warmer months of the year (Lakušić *et al.* 2013). A study that examined diurnal variations in *S. officinalis* VO compositions, α-thujone showed no clear response to hour changes (Rguez *et al.* 2018).

The other main constituents identified were camphor (7.0-20.2%), 1,8-cineole (6.9-14.1%), borneol (2.8-15.8%) and veridiflorol (4.5-12.3%). The highest camphor content was found at 2:00 p.m. sample in the flowering stage (20.2%), and the lowest content was seen at 6:00 a.m. of pre-flowering. Although this compound's highest and lowest values were observed at 2:00 p.m. and 6:00 a.m. samples in the flowering and pre-flowering stages, this was not the case in the post-flowering stage. According to α-thujone and camphor action, it was observed that with the raising of α-thujone content, the content of camphor decreased in each growth stage. The highest content of 1,8-cineole (14.1%) was found in the pre-flowering stage. The highest values of this component were detected at 6:00 a.m. samples in all three growth stages. Besides, as the plants got older, 1,8-cineole biosynthesis was adversely affected. The greatest formation of borneol occurred during the flowering stages (10.2-15.8%). An increase was observed in the content of this compound from early morning hours to sunset. The highest and lowest contents of veridiflorol were identified at 2:00 p.m. sample of pre-flowering and the 6:00 a.m. sample of post-flowering, respectively. Veridiflorol contents decreased with plant aging. The other important compounds of *S. officinalis* VO were α-pinene (0.6-4.2%), camphene (1.0-5.2%), β-pinene (0.7-2.6%), β-thujone (1.1-4.9%), caryophyllene (2.1-8.6%), α-humulene (3.3-10.9%), and epimanool (2.1-6.5%). α-Pinene and camphene had higher contents in the post-flowering and flowering stages, respectively. β-thujone was found in minimal quantities during the flowering stage. The highest contents for caryophyllene, α-humulene and epimanool were seen in the post-flowering stage. However, these components do not have clear action in terms of diurnal variability.

According to the current findings, the chemical components of plant VO were not stable during the growing season and at different times of the day. In addition to the genetic makeup of the plants (Sedlakova *et al.* 2003), the climatic conditions, agronomic management, harvesting time and post-harvest processing affect the synthesis of secondary metabolites (Özgüven *et al.* 2008). The variation in the amounts of constituents could be due to seasonal changes and climate changes during the day (Bouaziz *et al.* 2009). In addition, day length (presence of light) and solar intensity cause the plant's photochemical reaction and change in the accumulation of secondary metabolites and their constituents (Ben-Taarit *et al.* 2010). According to Bradley (2006), the main compounds of the *S. officinalis* are α-thujone (10-60%), β-thujone (4-36%), camphor (5-20%), 1,8-cineole (1-15%). Cis-thujone (18-43%), trans-thujone (3-8.5%), camphor

**Table 3.** The content and chemical characteristics of *Salvia officinalis* volatile oil affected by phenological cycle and diurnal variation.

| RI* | Compounds (%) | Pre-flowering Stage | | | Flowering Stage | | | Post-flowering Stage | | |
|---|---|---|---|---|---|---|---|---|---|---|
| | | 6:00 a.m. | 2:00 p.m. | 8:00 p.m. | 6:00 a.m. | 2:00 p.m. | 8:00 p.m. | 6:00 a.m. | 2:00 p.m. | 8:00 p.m. |
| 940 | cis-Salvene | 0.31 | 0.16 | 0.08 | 0.35 | 0.12 | 0.18 | 0.4 | 0.11 | 0.37 |
| 1015 | Tricyclene | | | | 0.11 | 0.15 | 0.18 | 0.14 | 1.54 | 0.12 |
| 1028 | α-Pinene | 2.72 | 1.27 | 0.67 | 2.31 | 2.25 | 2.76 | 4.2 | 3.53 | 3.7 |
| 1074 | Camphene | 1.03 | 1.64 | 1.25 | 4.67 | 4.4 | 5.29 | 4.03 | 2.02 | 3.61 |
| 1117 | β-Pinene | 1.58 | 2.04 | 0.79 | 2.39 | 1.91 | 2.67 | 1.41 | 0.91 | 1.42 |
| 1129 | Sabinene | | | | 0.16 | 0.14 | 0.14 | 0.13 | | 0.15 |
| 1168 | β-Myrcene | 0.55 | 0.51 | 0.23 | 0.71 | 0.58 | 0.58 | 0.71 | 0.57 | 0.7 |
| 1188 | α-Terpinene | 0.19 | 0.12 | 0.05 | 0.15 | | 0.12 | 0.16 | 0.17 | 0.16 |
| 1207 | Limonene | 0.77 | 0.89 | 0.59 | 1.48 | 1.65 | 1.74 | 1.49 | 1.07 | 1.39 |
| 1218 | 1,8-Cineole | 14.15 | 13.86 | 13.39 | 13.72 | 7.07 | 7.32 | 8.3 | 6.99 | 8.3 |
| 1240 | cis-Ocimene | 0.97 | 0.71 | 0.51 | | | | | | |
| 1254 | γ-Terpinene | 0.44 | 0.3 | 0.13 | 0.34 | 0.22 | 0.22 | 0.33 | 0.4 | 0.34 |
| 1257 | trans-β-Ocimene | 0.22 | 0.15 | 0.13 | | | | | | |
| 1281 | o-Cymene | 0.17 | 0.1 | 0.11 | 0.19 | 0.13 | 0.14 | 0.54 | 0.55 | 0.54 |
| 1292 | α-Terpinolene | 0.23 | 0.24 | 0.2 | 0.29 | 0.38 | 0.36 | 0.2 | 0.16 | 0.18 |
| 1442 | α-Thujone | 23.83 | 15.78 | 16.22 | 19.22 | 14.98 | 13.04 | 32.73 | 35.8 | 32.32 |
| 1449 | 1-Octen-3-ol | | | | 0.21 | 0.19 | 0.18 | 0.05 | 0.21 | 0.21 |
| 1460 | β-Thujone | 4.75 | 3.15 | 4.91 | 2.74 | 1.44 | 1.15 | 3.03 | 3.8 | 3.03 |
| 1471 | cis-Sabinene hydrate | 0.15 | 0.22 | 0.18 | 0.25 | 0.26 | 0.2 | 0.15 | | 0.19 |
| 1510 | α-Copaene | 0.07 | 0.12 | 0.11 | | | | | | |
| 1543 | Camphor | 7.01 | 10.05 | 9.35 | 15.05 | 20.26 | 19.27 | 19.22 | 12.1 | 14.43 |
| 1547 | Linalool | 0.39 | 0.45 | 0.44 | | | | | | |
| 1556 | trans-Sabinene hydrate | 0.11 | 0.12 | 0.12 | 0.19 | 0.22 | 0.18 | 0.16 | | 0.19 |
| 1598 | (-)-Bornyl acetate | 0.65 | 1.03 | 2.65 | 2.58 | 4.53 | 3.66 | 1.03 | 0.89 | 0.94 |
| 1615 | 4-Terpineol | 0.17 | 0.22 | 0.17 | 0.38 | 0.33 | 0.39 | 0.44 | 0.64 | 0.43 |
| 1623 | Caryophyllene | 8.14 | 8.63 | 6.61 | 4.94 | 3.37 | 3.57 | 2.1 | 2.91 | 2.42 |
| 1633 | Aromadendrene | | 0.15 | 0.12 | | | | 0.3 | 0.35 | |
| 1664 | Sabinyl acetate | | | | | | | 0.14 | 0.29 | 0.11 |
| 1672 | Alloaromadendrene | | | | | | | | 0.12 | 0.25 |
| 1683 | α-Terpineol | 0.23 | 0.37 | 0.31 | 0.29 | 0.28 | 0.26 | 0.22 | 0.21 | 0.21 |
| 1697 | α-Humulene | 10.91 | 7.65 | 7.55 | 3.8 | 4.2 | 4.52 | 3.3 | 4.16 | 3.4 |
| 1709 | α-Amorphene | 0.41 | 1.04 | 0.56 | 1.05 | 1.17 | 1.18 | 0.94 | 0.88 | 0.87 |
| 1716 | Borneol | 2.8 | 8.3 | 11.66 | 10.27 | 15.16 | 15.88 | 3.99 | 3.81 | 5.71 |
| 1777 | γ-Cadinene | 0.2 | 0.3 | 0.18 | 0.15 | 0.09 | 0.11 | | | |
| 1805 | Myrtenol | 0.21 | 0.1 | 0.14 | 0.16 | 0.23 | 0.24 | 0.38 | 0.36 | 0.31 |
| 1809 | Propanal, 2-methyl-3-phenyl- | 0.18 | 0.25 | 0.1 | | | | | | |
| 2024 | Caryophyllene oxide | 0.47 | 0.48 | 0.31 | 0.8 | 0.78 | 0.7 | 0.86 | 1.2 | 1.19 |
| 2055 | Humulene oxide | 0.19 | 0.09 | 0.14 | 0.09 | 0.11 | 0.1 | 0.16 | 0.23 | 0.18 |
| 2080 | Humulene oxide II | 0.91 | 0.6 | 0.64 | 0.65 | 0.79 | 0.77 | 1.13 | 1.82 | 1.33 |
| 2112 | Veridiflorol | 8.56 | 12.31 | 11.83 | 7.62 | 7.9 | 7.85 | 4.52 | 5.47 | 5.8 |
| 2146 | (+)-Spathulenol | | | | | | | 0.19 | 0.28 | 0.21 |
| 2216 | m-Eugenol | 0.21 | 0.12 | 0.24 | | | 0.16 | | 0.31 | 0.2 |
| 2319 | α-Caryophylladienol | 0.22 | 0.17 | 0.19 | 0.21 | 0.24 | 0.18 | 0.2 | 0.33 | 0.28 |
| 2679 | Epimanool | 4.94 | 5.58 | 6.51 | 2.16 | 4.16 | 4.41 | 2.43 | 4.04 | 4.18 |
| **Volatile oil content (mL 100gr$^{-1}$)** | | 1 | 1.1 | 1.3 | 1.4 | 1.8 | 2.05 | 0.85 | 1.05 | 1.3 |
| **Grouped compounds (%)** | | | | | | | | | | |
| Oxygenated monoterpenes | | 54.29 | 52.87 | 57.22 | 62.47 | 60.41 | 58.26 | 68.68 | 65.21 | 65.54 |
| Monoterpene hydrocarbons | | 9.19 | 8.14 | 4.74 | 13.17 | 11.92 | 14.37 | 13.73 | 11.02 | 12.67 |
| Oxygenated sesquiterpenes | | 10.35 | 13.64 | 13.1 | 9.36 | 9.82 | 9.59 | 7.06 | 9.35 | 8.99 |
| Sesquiterpene hydrocarbons | | 19.64 | 17.99 | 15.12 | 9.93 | 8.83 | 9.37 | 6.64 | 8.43 | 6.93 |
| Oxygenated diterpene | | 4.94 | 5.58 | 6.51 | 2.16 | 4.16 | 4.41 | 2.43 | 4.04 | 4.18 |
| Esters | | 0.65 | 1.03 | 2.65 | 2.58 | 4.53 | 3.66 | 1.16 | 1.18 | 1.06 |
| **Total** | | 99.06 | 99.24 | 99.35 | 99.66 | 99.67 | 99.65 | 99.7 | 99.22 | 99.37 |

* Retention indices (RI) calculated against n-alkanes (C7-C30) on HP-Innowax column

(4.5-24.5%), 1,8-cineole (5.5-13%), a-humulene (0-12%), a-pinene (1-6.5%), camphene (1.5-7%), limonene (0.5-3%), linalool, and bornyl acetate (2.5% maximum) have also been suggested as major *S. officinalis* compounds (ISO 9909).

The amounts of the major constituents of current findings such as α-thujone (13-35.8%), camphor (7-20.2%) and 1,8-cineole (6.9-14.15%) were largely within the range of the proposed standards. Most of the compounds found in the present study have been reported in other studies on *S. officinalis* with different amounts (Mirjalili *et al.* 2006, Ben-Farhat *et al.* 2016, Rguez *et al.* 2018, Katar *et al.* 2019).

## Conclusion

In this study, the influence of phenological cycle and diurnal variation were investigated on the content and chemical properties of VOs of *S. officinalis* sampled in Afyonkarahisar/Turkey. The quantity and quality of plant VOs were significantly affected by harvesting times. Based on the obtained results, the highest synthesis of VO occurred in the full flowering stage and at 8:00 p.m. The VO compositions of the plant varied widely at different growing stages and harvesting times (ontogeny and diurnal). The effects of climatic factors such as day length, insolation, temperature and also plant growth stage on these changes were evident. Knowing the agronomic and chemical properties and accurately determining the biologically active compounds of medicinal plants at different growth stages provide a clear perspective for their purposeful use including cosmetic, medicine and food industries. Extensive research is being conducted on adaptation of *S. officinalis*, including the effects of optimal planting time, density, nutrition and irrigation on the quantity and quality of the plant under the climatic conditions of Afyonkarahisar.

## Acknowledgement

We would like to show our gratitude to the director, researchers and technicians of Afyonkarahisar Medicinal and Aromatic Plants Center affiliated to the General Directorate of Forestry (Turkey) for sharing their experiences with us during this study.

**Ethics Committee Approval:** Since it was a systematic review, its approval to the ethics committee was not required.

**Author Contributions:** Concept: A.S., E.S., Desing: A.S., Execution: A.S., E.S., Material Supplying: A.S., E.S., Data Acquisition/interpretatition: A.S., E.S., Writing: A.S., E.S., Critical Review: A.S.

**Conflict of Interest:** The authors have no conflicts of interest to declare.

**Funding:** The authors received no financial support for this research.

## References

1. Adams, R.P. 2007. *Identification of essential oil components by gas chromatography/mass spectrometry*, 4th ed. Allured Publishing Co., Carol Stream, 804 pp.
2. Asghari, G., Gholamali, H., Mahmoudi, Z. & Asghari M. 2014. Diurnal variation of essential of the oil components of *Pycnocycla spinosa* Decne. ex Boiss. *Jundishapur Journal of Natural Pharmaceutical Products*, 9(1): 35-38. https://doi.org/10.17795/jjnpp-12229
3. Azarnivand, H., Ghavam Arabani, M., Sefidkon, F. & Tavili, A. 2010. The effect of ecological characteristics on quality and quantity of the essential oils of *Achillea millefolium* L. subsp. *millefolium*. *Iranian Journal of Medicinal and Aromatic Plants*, 25(4): 556-571.
4. Ben-Farhat, M., Jordán, M.J., Chaouch-Hamada, R., Landoulsi, A. & Sotomayor, J.A. 2016. Phenophase effects on sage (*Salvia officinalis* L.) yield and composition of essential oil. *Journal of Applied Research on Medicinal and Aromatic Plants*, 3(3): 87-93. https://doi.org/10.1016/j.jarmap.2016.02.001
5. Ben-Taarit, M., Msaada, K., Hosni, K., Chahed, T. & Marzouk, B. 2010. Essential oil composition of *Salvia verbenaca* L. growing wild in Tunisia. *Journal of Food Biochemistry*, 34(1): 142-151. https://doi.org/10.1111/j.1745-4514.2009.00270.x
6. Bouaziz, M., Yangui, T., Saya, S. & Dhouib, A. 2009. Disinfectant activities of essential oils from *Salvia officinalis L* cultivated in Tunisia. *Food and Chemical Toxicology*, 47(11): 2755-2760. https://doi.org/10.1016/j.fct.2009.08.005
7. Bozin, B., Mimica-Dukic, N., Samojlik, I. & Jovin, E. 2007. Antimicrobial and antioxidant properties of rosemary and sage (*Rosmarinus officinalis* L. and *Salvia officinalis* L., Lamiaceae) essential oils. *Journal of Agricultural and Food Chemistry*, 55(19): 7879-7885. https://doi.org/10.1021/jf0715323
8. Bradley, P.R. 2006. *British herbal compendium: a handbook of scientific information on widely used plant drugs.* British Herbal Medicine Association, Exeter. 409 pp.
9. European Pharmacopoeia, 2005. 5th ed, version 5.1. EDQM, Strasbourg.
10. Grdiša, M., Jug-Dujaković, M., Lončarić, M., Carović-Stanko, K., Ninčević, T., Liber, Z., Radosavljević, I. & Šatović, Z. 2015. Dalmatian sage (*Salvia officinalis* L.): A review of biochemical contents, medical properties and genetic diversity. *Agriculturae Conspectus Scientificus*, 80(2): 69-78.
11. ISO 9909, 1997. International Organization for Standardization. Oil of Dalmatian Sage (*Salvia officinalis* L.), Geneva (Switzerland).
12. Katar, N., Aydin, D. & Katar, D. 2019. Determination of the effect of different drying temperatures on the content and chemical composition of essential oil of sage (*Salvia officinalis*). *Biological Diversity and Conservation*, 12(1): 122-127. https://doi.org/10.5505/biodicon.2019.66376
13. Lakušić, B.S., Ristić, M.S., Slavkovska, V.N., Stojanović, D.L.J. & Lakušić, D.V. 2013. Variations in essential oil yields and compositions of *Salvia officinalis* (Lamiaceae)

at different developmental stages. *Botanica Serbica*, 37(2): 127-139.

14. Lee, Y.L. & Ding, P. 2016. Production of essential oil in plants: Ontogeny, secretory structures and seasonal variations. *Pertanika Journal of Scholarly Research Reviews*, 2(1): 1-10.

15. Miguel, M.G., Guerrero, C., Rodrigues, H., Brito, J.C., Duarte, F., Venancio, F. & Tavares, R. 2004. Main components of the essential oils from wild Portuguese *Thymus mastichina* (L.) L. ssp. *mastichina* in different developmental stages or under culture conditions. *Journal of Essential Oil Research*, 16(2): 111-114. https://doi.org/10.1080/10412905.2004.9698665

16. Miraj, S. & Kiani, S. 2016. A review study of therapeutic effects of *Salvia officinalis* L. *Der Pharmacia Lettre*, 8(6): 299-303.

17. Mirjalili, M.H., Salehi, P., Sonboli, A. & Vala, M.M. 2006. Essential oil variation of *Salvia officinalis* aerial parts during its phonological cycle. *Chemistry of Natural Compounds*, 42(1): 19-23. https://doi.org/10.1007/s10600-006-0027-4

18. Nurzyńska-Wierdak, R., Bogucka-Kocka, A., Kowalski, R. & Borowski, B. 2012. Changes in the chemical composition of the essential oil of sweet basil (*Ocimum basilicum* L.) depending on the plant growth stage. *Chemija*, 23(3): 216-222.

19. Özgüven, M., Şener, B., Orhan, I., Sekeroğlu, N., Kırpık, M. & Kartal, M. 2008. Effects of varying nitrogen doses on yield: yield components and artemisinin content of *Artemisia annua*. *Industrial Crops and Products*, 27(1): 60-64. https://doi.org/10.1016/j.indcrop.2007.07.012

20. Paulus, D., Valmorbida, R., & E.P. Ramos, C. 2019. Productivity and chemical composition of the essential oil of *Ocimum* × *citriodorum* Vis. according to ontogenetic and diurnal variation. *Journal of Applied Research on Medicinal and Aromatic Plants*, 12: 59-65. https://doi.org/10.1016/j.jarmap.2018.12.004

21. Piccaglia, R., Marotti, M. & Dellacecca, V. 1997. Effect of planting density and harvest date onyield and chemical composition of sage oil. *Journal of Essential Oil Research*, 9(2): 187-191. https://doi.org/10.1080/10412905.1997.9699457

22. Ramakrishna, A. & Ravishankar, G.A. 2011. Influence of abiotic stress signals on secondary metabolites in plants. *Plant Signaling & Behavior*, 6(11): 1720-1731. https://doi.org/10.4161/psb.6.11.17613

23. Ramezani, S., Rahmanian, M., Jahanbin, R., Mohajeri, F., Rezaei, M.R. & Solaimani B. 2009. Diurnal changes in essential oil content of coriander (*Coriandrum sativum* L.) aerial parts from Iran. *Research Journal of Biological Sciences*, 4(3): 277-281.

24. Rguez, S., Msaada, K., Daami-Remadi, M., Chayeb, I., Bettaieb Rebey, I., Hammami, M., Laarif, A. & Hamrouni-Sellami, I. 2018. Chemical composition and biological activities of essential oils of *Salvia officinalis* aerial parts as affected by diurnal variations. *Plant Biosystems*, 153(2): 264-272. https://doi.org/10.1080/11263504.2018.1473305

25. Sedlakova, J., Kocourkova, B., Lojkova, L. & Kuban, V. 2003. The essential oil content in caraway species (*Carum carvi* L.). *Horticultural Science*, 30(2): 73-79. https://doi.org/10.17221/3818-HORTSCI

26. Soltanbeigi, A. 2020. Qualitative variations of lavandin essential oil under various storage conditions. *Journal of Essential Oil Bearing Plants*, 23(6): 1237-1252. https://doi.org/10.1080/0972060X.2020.1871076

27. Soltanbeigi, A. & Sakartepe, E. 2020. Chemical specification of Wild *Salvia tomentosa* Mill. collected From Inner Aegean Region of Turkey. *Journal of Medicinal and Spice Plants*, 24(1): 31-35.

28. Sönmez, C. & Bayram, E. 2017. The influences of different water and nitrogen application on some yield parameters and antioxidant activity in sage (*Salvia officinalis* L.). *Turkish Journal of Field Crops*, 22(1): 96-103. https://doi.org/10.17557/tjfc.311012

29. Verma, R.S., Padalia, R.C. & Chauhan, A. 2012. Variation in the volatile terpenoids of two industrially important basil (*Ocimum basilicum* L.) cultivars during plant ontogeny in two different cropping seasons from India. *Journal of Agricultural and Food Chemistry*, 92(3): 626-631. https://doi.org/10.1002/jsfa.4620

*http://dergipark.org.tr/trkjnat*
*Trakya University Journal of Natural Sciences, 22(1): 67-76, 2021*
*ISSN 2147-0294, e-ISSN 2528-9691*
*DOI: 10.23902/trkjnat.817451*

**Research Article**

# PRODUCTION OF *Candida* BIOMASSES FOR HEAVY METAL REMOVAL FROM WASTEWATERS

Gülşah MERSİN[1*], Ünsal AÇIKEL[2]

[1] Uşak University, Technology Transfer Office, Project Support Unit, Rectorate Ground Floor Office No: 106, 64000, Uşak, TURKEY
[2] Cumhuriyet University, Faculty of Engineering, Chemical Engineering Department, 58140, Sivas, TURKEY

**Cite this article as:**
Mersin G., Açıkel Ü. 2021. Production of *Candida* biomasses for heavy metal removal from wastewaters. *Trakya Univ J Nat Sci*, 22(1): 67-76, DOI: 10.23902/trkjnat.817451

Received: 28 October 2020, Accepted: 06 April 2021, Online First: 11 April 2021, Published: 15 April 2021

**Abstract:** Yeasts can accumulate heavy metals and grow in acidic media. In the present study, it was shown that *Candida* yeasts in an aqueous solution accumulate single Cu(II) and Ni(II) cations. The effect of heavy metal ions on the specific growth rate of biomasses and the uptake of metal ions during the growth phase was investigated in a batch system. Bioaccumulation efficiency decreased with increasing metal ion concentrations at constant sucrose concentrations. Both the specific growth rate and the biomass concentration were more inhibited in the bioaccumulation media containing Ni(II) ions singly as compared with the bioaccumulation media containing Cu(II) ions singly. The maximum specific growth rate and the saturation constant of yeasts were examined with a double-reciprocal form of Monod equation. Metal uptake performance decreased from 81.68% to 46.28% with increasing Ni(II) concentration from 25 mg/L to 250 mg/L for *Candida lipolytica*. *Candida* biomasses may be an alternative way of removal of heavy metals from wastewaters and may constitute a sample to produce new biomass. The study showed that *Candida* yeasts can be used as economical biomass due to their metal resistance and efficient production.

**Özet:** Mayalar, asidik ortamda büyüyebilir ve ağır metalleri biriktirebilir. Bu çalışma, *Candida* türü mayaların sulu çözeltilerden tekli Cu(II) ve Ni(II) katyonlarını biriktirdiğini göstermiştir. Ağır metal iyonlarının, biyokütlelerin spesifik büyüme hızı ve büyüme periyodu boyunca metal iyonlarını giderimi üzerindeki etkisi, bir kesikli sistemde araştırılmıştır. Sabit sakaroz derişiminde, metal iyonu derişimi arttıkça, biyobirikim verimi azalmıştır. Hem spesifik büyüme hızı hem de biyokütle konsantrasyonu, tek başına Cu(II) iyonları içeren biyoakümülasyon ortamına kıyasla Ni(II) iyonları içeren biyoakümülasyon ortamında daha fazla inhibe edilmiştir. Mayaların maksimum özgül büyüme hızı ve doygunluk sabiti, Monod denkleminin çift-karşılıklı formu ile incelenmiştir. *Candida lipolytica*'nın metal giderim performansı Ni(II) derişiminin 25 mg/L'den 250 mg/L'ye çıkmasıyla % 81,68'den % 46,28'e düşmüştür. *Candida* biyokütleleri, ağır metallerin atık sulardan gideriminde alternatif bir yol olabilir ve yeni biyokütle üretimi için bir örnek oluşturabilir. Bu çalışma, *Candida* mayalarının, metal direnci ve verimli üretimleri nedeniyle ekonomik biyokütle olarak kullanılabileceğini göstermektedir.

***Edited by:***
*Bülent Yorulmaz*

****Corresponding Author:***
*Gülşah Mersin*
*gulsah.mersin@gmail.com*

***ORCID iDs of the authors:***
*GM. orcid.org/0000-0002-2852-6114*
*ÜA. orcid.org/0000-0003-4969-8502*

***Key words:***
*Bioaccumulation*
*Heavy metal cations*
*Wastewater*
*Candida*
*Biomass*

## Introduction

Clean water plays a vital role in living organisms. Industrial activities cause water contamination due to chemical, physical and biological components in water bodies. One of the important sources of water contamination is heavy metals. The presence of heavy metals in the environment may cause significant hazards to both animals and humans. Even in trace amounts, heavy metals play a vital role in human metabolic systems, and high concentrations of trace elements are toxic, and they cause physiological and neurological hazards (Tchounwou *et al.* 2012). Several methods are used for the treatment of wastewater effluents. These methods include chemical precipitation, ion exchange, adsorption, membrane filtration, reverse osmosis, solvent extraction etc. (Wolowiec *et al.* 2019). Some adsorbents such as clay, zeolite, fly ash, agro wastes, and chitin have been reported as low-cost for the removal of contaminations from aqueous solutions. Biomass can be derived from both vegetables and animals, either living or dead, and is used as an adsorbent to efficiently remove heavy metals from wastewaters. Biomasses have some advantages such as high efficiency, minimal sludge formation, regeneration, and no additional supplementary of nutrients (Tripathi & Ranjan 2015). Yeasts which are used

in the enzymatic industry and medicine can survive in a medium containing low or high concentrations of heavy metals (Cottet *et al.* 2020). One of the most important microbial source for biosorption of heavy metals is *Candida* species (Luna *et al.* 2016), which were shown to play an important role in the accumulation of metal ions (Honfi *et al.* 2016, Luk *et al*. 2017). Metal uptake capacity of *Candida* species under various experimental conditions depends on the metal type and the yeast species itself (Legorreta-Castañeda *et al.* 2020). Bioaccumulation, which contains some processes as complex formation, ion transfer, adsorption, and chelation is applied to eliminate toxic effects of heavy metals as a cheap, efficient, and green technology (Redha 2020, Fadel *et al.* 2017). The biosorption of metals is affected by several factors such as pH, temperature, concentration, type of biomass, contact time, and type of metal ions in solution. Bioaccumulation based on the accumulation of metals in living microorganisms is metabolism dependent (Açıkel & Alp 2009). The bioaccumulation of heavy metals by living cells contains two stages. The first step is very fast due to surface adsorption carried out on the surface of the microorganism with physical adsorption and ion exchange. The second step is the intracellular metal uptake stage which occurs slower due to the metabolic activity of microorganisms (Podder & Majumder 2019). Bioaccumulation has been investigated in many studies for the removal of heavy metals from wastewaters. Cd(II) removal by *Candida tropicalis*, Cu(II) removal by *C. utilis*, Pb(II) removal by *C. albicans* can be given as examples (Gönen & Aksu 2008, Baysal *et al*. 2009, Rehman & Anjum 2011). In the bioaccumulation process, high concentrations of heavy metals may interact with microorganisms which would result in prolonged lag time and reduced growth rate. Therefore, microbial growth kinetics are affected by heavy metals. Nickel is a trace element necessary for microbial growth, but it may cause oxidative stress and disruption of the cell membrane when in higher concentrations, (Fashola *et al.* 2016). Cu(II) is one of the most stable metals and shows a high affinity for metalloproteins in cells (Waldron & Robinson 2009). Some microorganisms use Cu as a catalyzer for electron transfer reactions in cell metabolism. Microorganisms have different metal-binding proteins due to their nature (Dupont *et al.* 2011). Mathematical description of the growth kinetics can be explained by the Monod equation (Şengör *et al.* 2009), which is widely used to describe the empirical microbial growth of microorganisms as a simple model (1).

$$\mu = \frac{\mu_{max} S}{K_s + S} \qquad (1)$$

Where $\mu_{max}$ is the maximum growth rate when there is enough substrate supplied to the cell and the value exceeds the limiting substrate concentration, $S>K_s$. The constant $K_s$ is the saturation constant or half of the velocity constant and is equal to the concentration of the rate-limiting substrate when the specific growth rate is equal to one-half of the maximum specific growth rate (Monod 1949, Liu 2007). Microorganism cell consists of an outer cover called a cell wall and contains a variety of functional sites such as amines, phosphates, sulfates, phenols, and hydroxyls with the ability for adsorption of metal ions (Javanbakht *et al.* 2013, Cottet *et al.* 2020). Metal ion adsorption by microorganisms is calculated by the mass balance equation (2).

$$q_e = \frac{(C_o - C_e)V}{m} \qquad (2)$$

Where $q_e$ is metal ion uptake per unit mass of biomass at equilibrium (mg/g biomass), $C_e$ is the metal ion concentration in solution at equilibrium (mg/L), $C_o$ is the initial metal ion concentration in solution (mg/L), $V$ is volume of the initial metal ion's solution (L), and $m$ is the mass of biomass (g) (Zha *et al*. 2020).

In this study, bioaccumulation, and growth properties of *Candida* biomasses for the uptake of Cu(II) and Ni(II) ions were investigated as a function of molasses sucrose and metal ion concentrations. Molasses sucrose was used as the main carbon source. The inhibition effects of metal ions on specific growth rates were examined. The results showed that *Candida* species can be used as a biosource for efficient removal of heavy metals from aqueous solutions at low costs.

## Materials and Methods

*Candida membranafiens (C. membranafiens*-ATCC® 201377™), *C. utilis* (*C. utilis*-ATCC® 9950), *C. tropicalis (C. tropicalis*-ATCC® 13803™) and *C. lipolytica* (*C. lipolytica*-ATCC® 9733™) were obtained from the Biology Department of Ankara University. $(NH_4)_2SO_4$ and $K_2PO_4$ were purchased from Sigma-Aldrich Company. Molasses sucrose was supplied from a sugar factory in Ankara (Turkey). Molasses consisting of 47-48% sugar was used as the sole carbon source for the growth of the microorganisms. Total sugars constitute of the system included approximately 50% (w/w) of molasses, ash 11% (w/w), and total nitrogen compounds 7-8% (w/w). Non-sugar part of molasses contained minerals and trace elements such as $K^+$, $Na^+$, $Ca^{2+}$, $Mg^{2+}$, $Fe^{2+}$, $Cl^-$, $SO_4^-$, $PO_4^-$, $NO_3^-$ and metal oxides (as ferric 0.4-2.7%) (Açıkel & Alp 2009).

*Microorganism growth and bioaccumulation media*

Yeasts were grown in aqueous media containing (1-10 g/L) molasses sucrose, (1 g/L) $(NH_4)_2SO_4$ and (1 g/L) $K_2PO_4$ at 25 °C (pH: 4.0). The growth and cultivation media were sterilized in an autoclave operating at 121°C at 0.99 bar for 15 minutes. Subcultures were grown for 4 days at a rotating speed of 150 rpm. 1 g/L Cu(II) and Ni(II) stock solutions were prepared by diluting Cu $(NO_3)_2.3H_2O$ and Ni $(NO_3)_2.6H_2O$ in distilled water. The pH of the working solutions was adjusted to desired value by adding 0.1 N NaOH and $HNO_3$ (pH: 4.0). The yeasts were adapted to the metal ions in culture medium by exposing them to single Cu(II) and Ni(II) ions during the growth phase to increase their metal resistance. The resistance to Cu(II) and Ni(II) ions was investigated as functions of initial metal ion and molasses sucrose

concentrations and the yeasts were adapted to higher metal ion concentrations after the first inoculation. Each yeast was adapted to each metal ion in its culture medium. Adapted yeasts were obtained from subcultures with different concentrations of metal ions in the range of 25-250 mg/L in varying concentrations from 1 g/L to 20 g/L for molasses. Yeast cultures which were resistant to 25 mg/L Cu(II) and Ni(II) ions at 10 g/L molasses sucrose concentration was used for further inoculation. 1 mL culture medium was used to inoculate the next culture medium containing 50 mg/L Cu(II) and Ni(II) ions at the same molasses sucrose concentration when growth culture reached to the exponential growth phase. Adaptation experiments by *Candida* species were carried out in 250 mL flask with 100 mL working volume.

*Analytical procedure*

5 mL samples were centrifuged at 3000xg for 5 min and the supernatant fluid was analyzed for metal ions. The precipitated cells were used for determination of the dry weight of the biomass and the biomass concentration. Yeast pellets were dried until constant mass at 60°C for 24 h. The amount of total metal ions was calculated from the calibration graph. Microorganism concentration was measured at 360 nm using a calibration curve relating the wet weight of the biomass to the dry weight of the biomass at 25°C. Residual metal concentrations were measured at 460 nm and 340 nm for Cu(II) and Ni(II), respectively by using Sodium diethyldithiocarbamate as the complexing agent (Sandell, 1950).

*Abbrevations*

$\mu$ : Specific growth rate of yeast ($h^{-1}$)

$\mu_{max}$ : Maximum specific growth rate ($h^{-1}$)

$C_{iCu}$ : Initial Cu(II) ion concentration (mg/L)

$C_{iNi}$ : Initial Ni(II) ion concentration (mg/L)

$C_{ac,Cu}$ : Bioaccumulated Cu(II) ion concentration at any time (mg/L)

$C_{ac,Ni}$ : Bioaccumulated Cu(II) ion concentration at any time (mg/L)

$K_s$ : Saturation constant (g/L)

$q_{Cu}$ : Specific Cu(II) uptake defined as bioaccumulated Cu(II) ion quantity per gram of dried yeast at the end of microbial growth (mg/g)

$q_{Ni}$ : Specific Ni(II) uptake defined as bioaccumulated Ni(II) ion quantity per gram of dried yeast at the end of microbial growth (mg/g)

$S_o$ : Initial sucrose concentration (g/L)

S : Sucrose concentration (g/L)

T : Temperature (°C)

t : Reaction time (h)

X : Dried yeast concentration in feed medium at any time (g/L)

$X_{max}$ : Maximum dried yeast concentration (g/L)

## Results and Discussions

Microorganism growth and bioaccumulation properties were investigated as functions of initial metal ion and molasses sucrose concentrations at pH: 4.0 and 25°C. The uptake yield (uptake %) was described as the ratio of bioaccumulated concentration of metal ion at the end of growth to the initial metal ion concentration. The results were expressed as the units of bioaccumulated metal ion concentration ($C_{ac,m}$: mg/L) and specific metal ion uptake determined as the amount of metal ion per unit of dry weight of cells ($q_m$: mg/g), dried cell concentrations at any time (X: g/L), specific growth rate of yeast ($\mu$: $h^{-1}$). The specific growth rate of *Candida* yeasts was determined from the slope of ln X versus time plot at the exponential growth phase. The results indicated that biomass concentration was related to the metal concentrations in fermentation medium and the physiological properties of the yeasts. The ability of metal uptake by metal adapted yeasts were different due to the physiological properties of the yeasts. All experiments were conducted at 25°C. The effect of temperature on metal bioaccumulation depends on cellular metabolism. Uptake capacity of heavy metals by microorganisms decreased at low temperatures whereas high temperatures could damage cells and reduced uptake levels (Brady & Duncan 1994).

*Effect of initial pH on microbial growth*

Effect of initial pH on specific growth rate and maximum microorganism concentrations of *Candida* yeasts was examined in the pH range of 2.0-5.0 at 10 g/L molasses sucrose concentration. Maximum specific growth rate and microorganism concentrations were obtained at pH: 4.0. Initial pH was a major factor in the quantity of metal ion bioaccumulation. All *Candida* species showed growth at pH: 2.0-5.0. The highest value of specific growth rate and microorganism concentration was found as 0.308 $h^{-1}$ and 3.111 g/L respectively using *C. lipolytica* in metal free media (Table 1). Bioaccumulation experiment was conducted at pH: 4.0 which showed maximum growth.

*Effect of initial sucrose concentration on microbial growth*

The effect of initial sucrose concentration on growth rates of *Candida* yeasts in metal-free media was investigated in the sucrose concentration range of 1.0-20.0 g/L, at pH: 4.0 and 25°C. The relationship of specific growth rate to substrate concentration was explained with saturation kinetics. It was observed that the specific growth rate and biomass concentration increased with increasing initial sucrose concentration up to 20.0 g/L. Microorganism concentration increased from 1.52 g/L to 3.48 g/L with an increase in the initial sucrose concentration from 1.0 to 20.0 g/L for *C. lipolytica* in metal-free media (Fig. 1). Lower growth performance among the yeast cells was seen using *C. utilis.* We have found that molasses was a suitable carbon source for fermentation medium of *Candida* species. It was also reported in previous studies that molasses could be used as feasible and economical for microbial growth (Aksu & Dönmez 2000, Açıkel & Alp 2009, Evirgen & Sağ Açıkel 2014).

*Effect of initial metal ion concentrations on growth of Candida species*

The effect of initial Cu(II) and Ni(II) ion concentrations on microbial growth of *Candida* species were examined at different Cu(II) and Ni(II) ion concentrations. The metal ion concentrations in the fermentation the medium varied in the range of 25-250 mg/L for Cu(II) and Ni(II). The range of molasses sucrose concentrations of prepared fermentation media varied between 1 and 20 g/L. Both metal ions inhibited specific growth rates and biomass concentrations for all yeasts. We found that the inhibition effect of Ni(II) ions on specific growth rate and microorganism concentration was higher than Cu(II) ions for all yeasts. *Candida lipolytica* showed the highest specific growth rate and microorganism concentration among the yeasts in metal media. Maximum specific growth rate significantly decreased from 0.302 $h^{-1}$ to 0.278 $h^{-1}$ with an increase in the initial Ni(II) concentration from 100 to 200 mg/L for *C. utilis*. Inhibition kinetics was determined using the double reciprocal plot of the Monod equation. When initial Cu(II) and Ni(II) ion concentrations were increased in the range of 25-250 mg/L, the maximum specific growth rate ($h^{-1}$) of the yeasts decreased whereas saturation constants ($K_s$) increased (Table 2).

**Table 1**. Effect of initial pH on the maximum specific growth rate, maximum dried microorganism concentration in metal-free medium (So: 10 g/L; T:25°C).

| pH | *C. membranaefaciens* | | *C. utilis* | | *C. tropicolis* | | *C. lipolytica* | |
|---|---|---|---|---|---|---|---|---|
| | $\mu_{max}$ ($h^{-1}$) | $X_{max}$ (g/L) | $\mu_{max}$ ($h^{-1}$) | $X_{max}$ (g/L) | $\mu_{max}$ ($h^{-1}$) | $X_{max}$ (g/L) | $\mu_{max}$ ($h^{-1}$) | $X_{max}$ (g/L) |
| **2** | 0.198 | 2.001 | 0.177 | 1.985 | 0.206 | 2.112 | 0.211 | 2.223 |
| **3** | 0.241 | 2.552 | 0.222 | 2.443 | 0.253 | 2.601 | 0.261 | 2.751 |
| **4** | 0.253 | 2.854 | 0.238 | 2.658 | 0.289 | 2.999 | 0.308 | 3.111 |
| **5** | 0.251 | 2.851 | 0.235 | 2.651 | 0.279 | 2.995 | 0.306 | 3.005 |

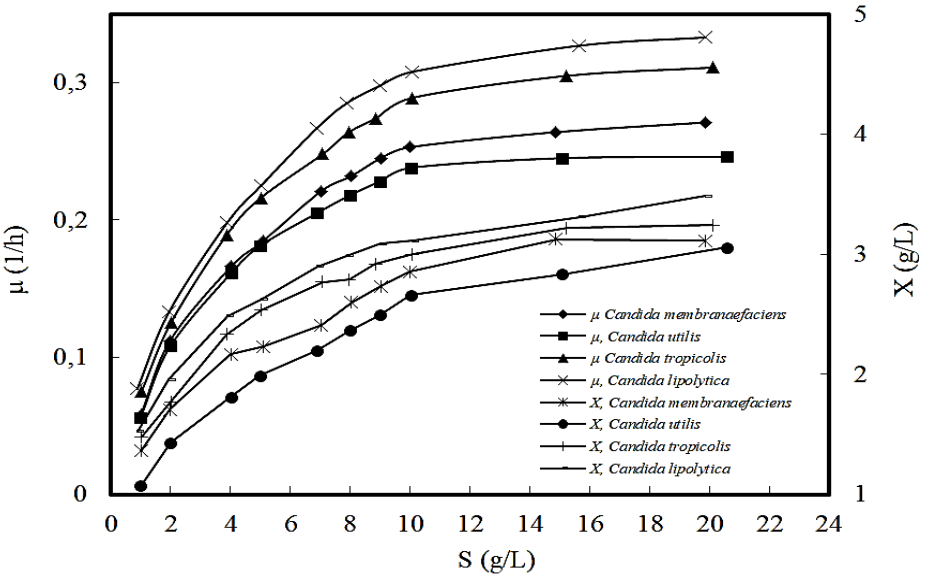


**Fig. 1.** Effect of initial sucrose concentration on specific growth rate and microorganism concentration for *Candida lipolytica*, *Candida utilis*, *Candida tropicalis* and *Candida membranaefaciens* (pH: 4.0; SR: 150 rpm; T: 25ºC).

**Table 2.** Comparison of the maximum specific growth rates and the saturation constants in the presence of increasing concentrations of single Cu(II) and Ni(II) ions (So: 1-20 g/L; pH: 4, T: 25°C; SR: 150 rpm.

| **Metal Ion** | | ***C. membranefeciens*** | | ***C. utilis*** | | ***C. tropicalis*** | | ***C. lipolytica*** | |
|---|---|---|---|---|---|---|---|---|---|
| **$C_{iCu}$ (mg/L)** | **$C_{iNi}$ (mg/L)** | **$\mu_{max}$ ($h^{-1}$)** | **$K_s$ (g/L)** | **$\mu_{max}$ ($h^{-1}$)** | **$K_s$ (g/L)** | **$\mu_{max}$ ($h^{-1}$)** | **$K_s$ (g/L)** | **$\mu_{max}$ ($h^{-1}$)** | **$K_s$ (g/L)** |
| 25.0 | 0.0 | 0.354 | 5.399 | 0.341 | 5.805 | 0.374 | 4.555 | 0.422 | 5.080 |
| 100.0 | 0.0 | 0.337 | 5.354 | 0.341 | 6.472 | 0.363 | 4.677 | 0.388 | 4.568 |
| 200.0 | 0.0 | 0.336 | 6.586 | 0.299 | 6.033 | 0.338 | 4.887 | 0.378 | 5.378 |
| 250.0 | 0.0 | 0.310 | 6.771 | 0.285 | 6.519 | 0.313 | 4.984 | 0.335 | 4.920 |
| 0.0 | 25.0 | 0.346 | 5.725 | 0.319 | 5.600 | 0.352 | 4.243 | 0.345 | 4.473 |
| 0.0 | 100.0 | 0.333 | 5.718 | 0.302 | 5.408 | 0.356 | 5.013 | 0.395 | 5.268 |
| 0.0 | 200.0 | 0.309 | 7.004 | 0.278 | 6.374 | 0.309 | 5.111 | 0.328 | 4.918 |
| 0.0 | 250.0 | 0.267 | 6.265 | 0.264 | 7.196 | 0.284 | 5.269 | 0.317 | 5.796 |

*Candida utilis* was sensitive to high concentrations of Cu(II) with an extension in lag phase duration, correlated with a decrease in yeast production. The increase of Cu(II) and Ni(II) concentrations led to a drastic decrease in microbial growth for *C. utilis*. *Candida lipolytica* was highly resistant to Cu(II) when compared with three other yeasts. The increase in Cu(II) concentration also caused a decrease in biomass production. For instance, microorganism concentrations were found as 2.854 g/L, 2.658 g/L, 2.999 g/L and 3.111 g/L for *C. membranaefaciens*, *C. utilis*, *C. tropicalis* and *C. lipolytica*, respectively, in the metal-free media (Table 1). Biomass concentrations decreased as 2.666 g/L, 2.456 g/L, 2.831 g/L and 2.968 g/L for *C. membranaefaciens*, *C. utilis*, *C. tropicalis* and *C. lipolytica*, respectively, at 100 mg/L Cu(II) concentration (Table 3). The decrease in biomass concentration was found higher for fermentation medium containing 100 mg/L Ni(II). When initial Ni(II) concentration was 100.0 mg/L, microorganism concentrations were found as 2.574 g/L, 2.371 g/L, 2.735 g/L and 2.868 g/L for *C. membranaefaciens*, *C. utilis*, *C. tropicalis* and *C. lipolytica*, respectively (Table 3).

*Bioaccumulation experiments*

The combined effect of heavy metals and molasses sucrose on the bioaccumulation properties of adapted *Candida* yeasts was investigated. Initial metal ion concentration in the fermentation medium varied in the range 25-250 mg/L for Cu(II) and Ni(II) at changing sucrose concentrations in the range of 1-20 g/L. We found that bioaccumulated Cu(II) and Ni(II) ions and microbial growth increased with increasing initial molasses sucrose concentrations for all *Candida* yeasts. The uptake performance of Cu(II) ions was higher than Ni(II), and *C. lipolytica* showed the maximum removal efficiency in a medium containing both single metal ions. An increase in sucrose concentration significantly increased the growth and metal uptake capacity of the microorganisms. The amount of Cu(II) and Ni(II) ions uptake per gram dry microorganism increased with increasing the initial metal concentrations up to 250 mg/L. We found that microbial growth was supported by increasing initial sucrose concentrations in metal- stressed fermentation media. In other words, bioaccumulation of Cu(II) and Ni(II) ions by *Candida* species was metabolism dependent. Specific Cu(II) uptake was determined as 31.77 mg/g, 29.71 mg/g, 33.04 mg/g, and 34.39 mg/g for *C. membranaefaciens*, *C. utilis*, *C. tropicalis*, *C. lipolytica*, respectively, at fermentation media containing 10 g/L constant sucrose and 200 mg Cu(II) mg/L (Fig. 4). At the same conditions, the specific Ni(II) uptake significantly decreased for all yeasts in medium containing Ni(II) ions when compared to Cu(II) ions. For example, the specific growth rates were obtained in a medium containing 200 mg Ni(II)/L and 10 g/L sucrose were determined as 25.96 mg/g, 24.76 mg/g, 26.13 mg/g, and 28.80 mg/g for *C. membranaefaciens*, *C. utilis*, *C. tropicalis*, *C. lipolytica*, respectively (Fig. 5). Although removal efficiency increased with increasing initial sucrose concentration for all yeasts, it decreased with increasing initial metal ion concentrations. Uptake efficiency significantly decreased from 88.80% to 56.44% with an increase in the initial Cu(II) concentration from 25 to 200 mg/L for *C. lipolytica* at 20 g/L constant sucrose concentration (Table 4). This decrease may result from metal-binding sites on yeast surfaces. It was reported that binding sites were occupied first rapidly, then decreased with increasing metal concentrations (Honfi *et al.* 2016).

The bioaccumulated Cu(II) concentrations were higher than bioaccumulated Ni(II) concentrations in growth media containing 25 mg/L single Cu(II) and Ni(II) ions (Figs 2, 3).

The intolerance of living cells to high metal concentrations limits bioaccumulation process, but living cells have the potential genetic recombination to improve the metal-adapted strain (Malik 2004). Heavy metal bioaccumulation capacity of *Candida* species was strongly pH-dependent due to changing solution chemistry and active functional groups on the biomass. Due to the Ni(II) inhibition effect, metal uptake performance decreased from 81.68% to 46.28% with increasing Ni(II) concentration from 25 to 250 mg/L for *C. lipolytica*. According to Gönen and Aksu (2008), *C. utilis* accumulated toxic heavy metals. The uptake efficiency of Cu(II) by *C. utlis* was observed as 27.0% in a growth medium containing 11.2 g/L sucrose and 101.3 mg/L Cu(II) ions (Gönen & Aksu 2008). Pawan and Devi (2018) investigated bioaccumulation of Ni(II), Zn(II), Cr(VI) by *Aspergillus awamori*, *A. flavus* and *A. niger* and found that *A. niger* was a highly tolerant strain. Maximum dry weight of *A. flavus* was found as 12.31 g/L for Ni(II) in medium containing 100 mg/L initial broth concentration (Pawan & Devi 2018). Rehman and Anjum (2010) reported that *Candida tropicalis* was a metal-resistant yeast. They reported that *C. tropicalis* bioaccumulated 64% copper from industrial wastewater after 4 days (Rehman & Anjum 2010).

**Table 3.** Comparison of decrease in maximum dried microorganism concentrations obtained in the metal-free fermentation media with Cu(II) and Ni(II) ions present as the single metal at 100 and 250 mg/L (So: 10 g/L; pH: 4, T: 25°C; SR: 150 rpm).

| Metal Ion | | *C. membranefeciens* | | *C. utilis* | | *C.tropicalis* | | *C. lipolytica* | |
|---|---|---|---|---|---|---|---|---|---|
| $C_{iCu}$ (mg/L) | $C_{iNi}$ (mg/L) | $X_{max}$ (g/L) | Decrease % | $X_{max}$ (g/L) | Decrease % | $X_{max}$ (g/L) | Decrease % | $X_{max}$ (g/L) | Decrease % |
| 100.0 | 0.0 | 2.666 | 2.4 | 2.456 | 7.6 | 2.831 | 5.6 | 2.968 | 4.6 |
| 250.0 | 0.0 | 2.335 | 14.5 | 2.148 | 19.2 | 2.483 | 17.2 | 2.607 | 16.2 |
| 0.0 | 100.0 | 2.574 | 5.8 | 2.371 | 10.8 | 2.735 | 8.8 | 2.868 | 7.8 |
| 0.0 | 250.0 | 2.175 | 20.4 | 1.199 | 54.9 | 2.315 | 22.8 | 2.432 | 21.8 |

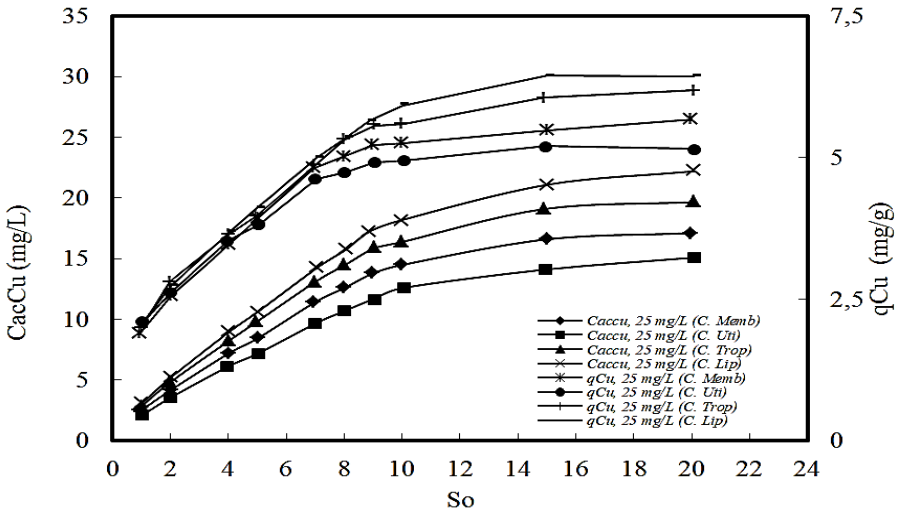


**Fig. 2.** Effect of initial sucrose concentration on the bioaccumulated Cu(II) ion quantity per unit weight of dried biomass and specific Cu(II) uptake in the presence of 25 mg/L Cu(II) (pH: 4.0; SR: 150 rpm; T: 25°C).

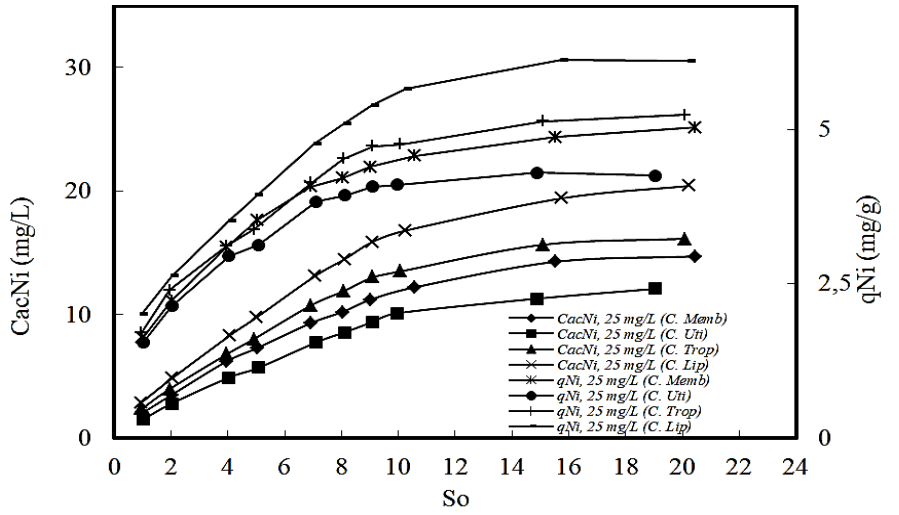


**Fig. 3**. Effect of initial sucrose concentration on the bioaccumulated Ni(II) ion quantity per unit weight of dried biomass and specific Ni(II) uptake in the presence of 25 mg/L Ni(II) (pH: 4.0; SR: 150 rpm; T:25°C).

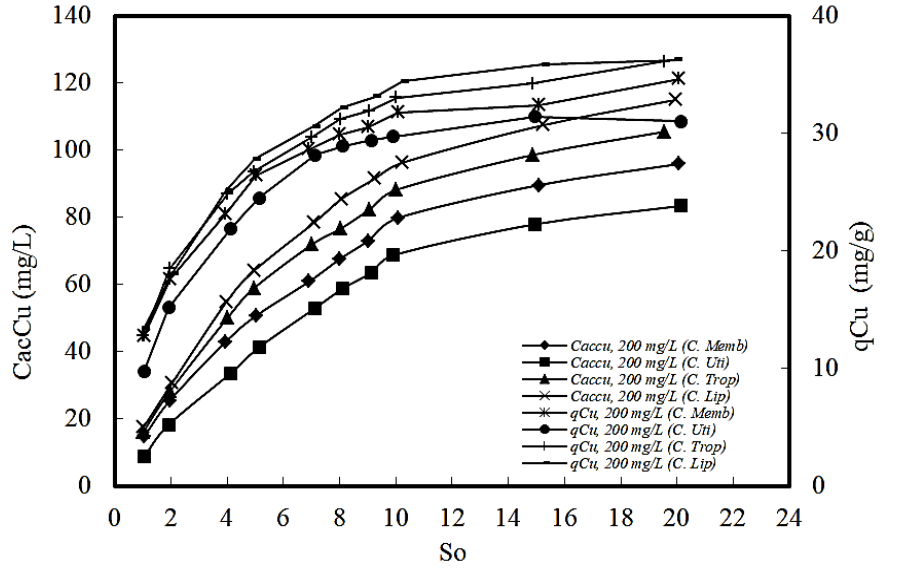


**Fig. 4.** Effect of initial sucrose concentration on the bioaccumulated Cu(II) ion quantity per unit weight of dried biomass and specific Cu(II) uptake in the presence of 200 mg/L Cu(II) (pH: 4.0; SR: 150 rpm; T: 25°C).

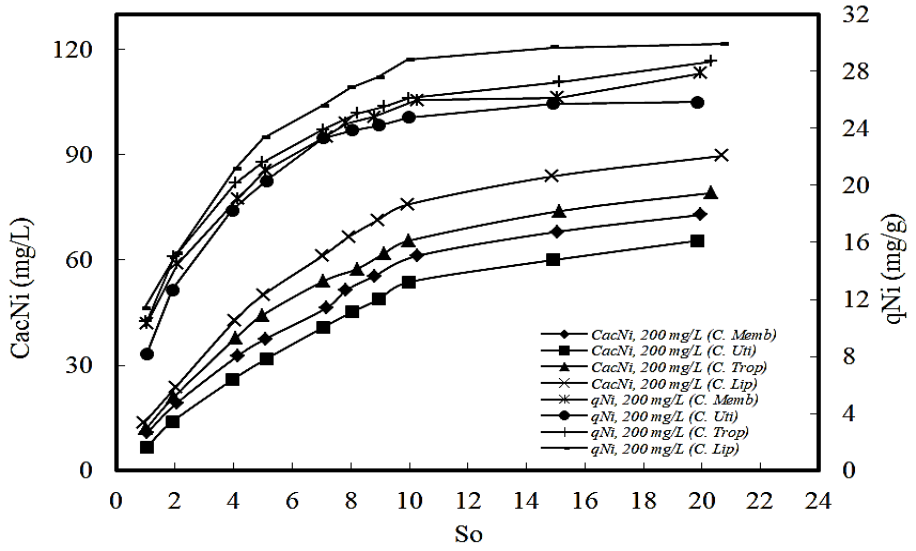


**Fig. 5.** Effect of initial sucrose concentration on the bioaccumulated Ni(II) ion quantity per unit weight of dried biomass and specific Ni(II) uptake in the presence of 200 mg/L Ni(II) (pH: 4.0; SR: 150 rpm; T: 25°C).

**Table 4.** Comparison of the bioaccumulated Cu(II) and Ni(II), the Cu(II) and Ni(II) metal ion bioaccumulation efficiency in the fermentation media containing single Cu(II) and Ni(II) ions (pH: 4.0; T: 25°C; SR: 150 rpm.

| **Yeast** | | ***C. membranaefaciens*** | | ***C. utilis*** | | ***C. tropicolis*** | | ***C.lipolytica*** | |
|---|---|---|---|---|---|---|---|---|---|
| **$S_i$ (g/L)** | **$C_{i,Cu}$ (mg/L)** | **$C_{ac,Cu}$ (mg/L)** | **Uptake (%)** | **$C_{ac,Cu}$ (mg/L)** | **Uptake (%)** | **$C_{ac,Cu}$ (mg/L)** | **Uptake (%)** | **$C_{ac,Cu}$ (mg/L)** | **Uptake (%)** |
| 1 | 25 | 2.50 | 10.00 | 2.13 | 8.52 | 2.88 | 11.52 | 3.13 | 12.52 |
| 10 | | 14.50 | 58.00 | 12.60 | 50.40 | 16.40 | 65.60 | 18.20 | 72.80 |
| 20 | | 17.10 | 68.40 | 15.1 | 60.4 | 19.67 | 78.68 | 22.20 | 88.80 |
| 1 | 100 | 6.88 | 6.88 | 5.50 | 5.50 | 7.56 | 7.56 | 8.70 | 8.70 |
| 10 | | 46.80 | 46.80 | 38.40 | 38.40 | 51.48 | 51.48 | 59.20 | 59.20 |
| 20 | | 58.47 | 58.47 | 46.77 | 46.77 | 64.31 | 64.31 | 73.96 | 73.96 |
| 1 | 200 | 14.60 | 7.30 | 8.65 | 23.38 | 16.06 | 8.03 | 17.51 | 8.75 |
| 10 | | 79.80 | 39.90 | 68.70 | 20.67 | 88.20 | 44.10 | 96.30 | 48.15 |
| 20 | | 95.88 | 47.94 | 83.37 | 34.35 | 105.46 | 52.73 | 114.96 | 57.48 |
| 1 | 250 | 11.60 | 4.64 | 8.50 | 3.40 | 15.20 | 6.08 | 16.42 | 6.56 |
| 10 | | 94.81 | 37.92 | 79.01 | 31.60 | 104.29 | 41.71 | 112.60 | 45.04 |
| 20 | | 115.05 | 46.02 | 95.88 | 38.35 | 126.56 | 50.62 | 141.10 | 56.44 |
| **$S_o$ (g/L)** | **$C_{i,Ni}$ (mg/L)** | **$C_{ac,Ni}$ (mg/L)** | **Uptake (%)** | **$C_{ac,Ni}$ (mg/L)** | **Uptake (%)** | **$C_{ac,Ni}$ (mg/L)** | **Uptake (%)** | **$C_{ac,Ni}$ (mg/L)** | **Uptake (%)** |
| 1 | 25 | 2.04 | 8.16 | 1.51 | 6.04 | 2.36 | 9.44 | 2.88 | 11.52 |
| 10 | | 12.20 | 48.80 | 10.10 | 40.40 | 13.50 | 54.00 | 16.8 | 67.20 |
| 20 | | 14.71 | 58.84 | 12.08 | 48.32 | 16.13 | 64.52 | 20.42 | 81.68 |
| 1 | 100 | 5.84 | 5.84 | 4.47 | 4.47 | 6.50 | 6.50 | 7.39 | 7.39 |
| 10 | | 39.70 | 39.70 | 31.20 | 31.20 | 44.30 | 44.30 | 50.70 | 50.70 |
| 20 | | 49.70 | 49.70 | 38.80 | 38.80 | 55.31 | 55.31 | 62.86 | 62.86 |
| 1 | 200 | 10.80 | 5.40 | 6.66 | 3.33 | 12.05 | 6.02 | 13.65 | 6.82 |
| 10 | | 61.20 | 30.60 | 53.70 | 26.85 | 65.50 | 32.75 | 75.80 | 37.90 |
| 20 | | 72.87 | 36.43 | 65.50 | 32.75 | 79.10 | 39.55 | 89.67 | 44.83 |
| 1 | 250 | 8.82 | 3.52 | 6.63 | 2.65 | 10.50 | 4.20 | 13.46 | 5.38 |
| 10 | | 72.20 | 28.88 | 62.10 | 24.84 | 79.26 | 31.70 | 92.33 | 36.93 |
| 20 | | 87.44 | 34.97 | 78.70 | 31.48 | 96.18 | 38.47 | 115.70 | 46.28 |

The physiological and biochemical properties of microorganisms can be changed by the presence of heavy metals. Heavy metals such as copper (Cu(I) and Cu(II)) carry soluble electrons and can catalyze Fenton and Haber-Weiss reactions. Cytoplasmic molecules in microorganisms can cause serious damage to DNA, lipids and other proteins (Giner-Lamia *et al*. 2014). Heavy metal can cause ion imbalance by binding to the cell surface and entering through ion channels or transmembrane carriers (Chen *et al*. 2014). High vitamin and mineral contents of molasses sucrose stimulate microorganisms growth (Razack *et al.* 2013). The structure of metal-binding agents (homopolysaccharides, single saccharides, and acid components) in microorganisms and their distributions in the cell wall determine the metal accumulation capacity (Raspor & Zupan 2006). Heavy

metal cations can interact with some cations on the cell wall. The cell wall and heavy metal interactions may inhibit the function of physiological cations in the cell structure. As a result of this inhibition, oxidative stress occurs in the cell. For example, Fe, Zn, and Ca affect the uptake and toxicity of heavy metals in microorganisms. Ca and Fe ions reduce the uptake of Cd (Volland *et al.* 2014). Metal uptake is mainly related to the concentrations of metals in solution (Modak & Natarajan 1995). Also, intercellular electrostatic interactions in cells play an important role in metal uptake capacity. At a certain equilibrium, biomass adsorbs more metal ions at lower cell concentrations (Gourdon *et al.* 1990). The inhibition effect of heavy metals on microorganism growth depends on the total metal ion concentration, the chemical structure of the metal, and redox potential of metal. Environmental factors such as temperature, pH, organic acids, and humic acids can alter the conversion, transport, valence of heavy metals, and the resistance of microorganisms to heavy metals.

## Conclusion

In the present study, microbial growth and bioaccumulation properties of *Candida* biomasses were investigated as a function of molasses sucrose and metal ion concentrations in a batch reactor. Optimum pH was found 4.0 for each yeast and all experiment conducted at this pH value. Biomass concentrations and specific growth rates increased with increasing initial sucrose concentration in metal and metal-free media. Both Cu(II) and Ni(II) inhibited specific growth rates and the contribution of Cu(II) inhibition was lower than Ni(II). Thus, the maximum specific growth rates of yeasts decreased with increasing initial metal ion concentrations. The saturation constants were determined in both metal and metal-free fermentation medium. Saturation constants and the amounts of Cu(II) and Ni(II) ions uptake per gram dry biomass increased with the increase of the initial concentration of heavy metals ions. The removal efficiency of Cu(II) ions was higher than Ni(II), and *Candida lipolytica* showed maximum uptake efficiency in fermentation medium containing Cu(II) and Ni(II) ions. Results showed that bioaccumulation of Cu(II) and Ni(II) ions by *Candida* biomass was metabolism dependent. *Candida* biomasses showed different bioaccumulative capacities for the same metal ions. The yeast surface properties and cell wall components may change affinity and cell-metal interaction. In addition, environmental conditions can affect the accumulation capacity of yeasts. Although Cu(II) and Ni(II) have similar chemical properties, genetic differences of yeasts and the chemical nature of metals caused differences in bioaccumulation performances. This study showed that *Candida* biomasses are useful for removal Cu(II) and Ni(II) ions from aqueous solutions. The comparison of bioaccumulation properties of Candida yeasts may help to an effective selection of *Candida* strains for water treatments.

**Ethics Committee Approval:** Since the article does not contain any studies with human or animal subject, its approval to the ethics committee was not required.

**Author Contributions:** Execution: G.M., Data analysis/interpretation: Ü.A., Writing: G.M., Critical Review: Ü.A.

**Conflict of Interest:** The authors have no conflicts of interest to declare.

**Funding:** This research was supported by Cumhuriyet University Scientific Research Projects Unit (Project Number: BAP- M-354).

## References

1. Açikel, U. & Alp, T. 2009. A study on the inhibition kinetics of bioaccumulation of Cu(II) and Ni(II) ions using *Rhizopus delemar*. *Journal of Hazardous Materials*, 168(2-3): 1449-1458. https://doi.org/10.1016/j.jhazmat.2009.03.040
2. Aksu, Z. & Dönmez, G. 2000. The use of molasses in copper (II) containing wastewaters: effects on growth and copper (II) bioaccumulation properties of *Kluyveromyces marxianus*. *Process Biochemistry*, 36(5): 451-458. https://doi.org/10.1016/S0032-9592(00)00234-X
3. Baysal, Z., Çinar, E., Bulut, Y., Alkan, H. & Dogru, M. 2009. Equilibrium and thermodynamic studies on biosorption of Pb(II) onto *Candida albicans* biomass. *Journal of Hazardous Materials*, 161(1): 62-67. https://doi.org/10.1016/j.jhazmat.2008.02.122
4. Brady, D. & Duncan, J.R. 1994. Bioaccumulation of metal cations by *Saccharomyces cerevisiae*. *Applied Microbiology and Biotechnology*, 41: 149-154. https://doi.org/10.1007/BF00166098
5. Chen, S., Yin, H., Ye, J., Peng, H., Liu, Z., Dand, Z. & Chang, J. 2014. Influence of co-existed benzo[a]pyrene and copper on the cellular characteristics of Stenotrophomonas maltophilia during biodegradation and transformation. *Bioresource Technology*, 158: 181-187. https://doi.org/10.1016/j.biortech.2014.02.020
6. Cottet, C., Ramirez-Tapias, Y.A., Delgado, J.F., de la Osa, O., Salvay, A.G. & Peltzer, M.A. 2020. Biobased Materials from Microbial Biomass and Its Derivatives. *Materials*, 13(6): 1263. https://doi.org/10.3390/ma13061263
7. Dupont, C.L., Grass, G. & Rensing, C. 2011. Copper toxicity and the origin of bacterial resistance-New insights and applications. *Metallomics*, (3): 1109-1118. https://doi.org/10.1039/c1mt00107h
8. Evirgen, O.A. & Sag Acikel, Y. 2014. Simultaneous copper bioaccumulation, growth and lipase production of *Rhizopus delemar* in molasses medium: optimisation of environmental conditions using RSM. *Chemistry and Ecology*, 30(1): 39-51. https://doi.org/10.1080/02757540.2013.827670
9. Fadel M., Hassanein, N.M., Elshafei, M.M., Mostafa, A.H., Ahmed, M.A. & Khater, H.M. 2017. Biosorption of manganese from groundwater by biomass of

*Saccharomyces cerevisiae*. *HBRC Journal*. 13(1): 106-113. https://doi.org/10.1016/j.hbrcj.2014.12.006

10. Fashola, M.O., Ngole-Jeme, V.M. & Babalola, O.O. 2016. Heavy metal pollution from gold mines: Environmental effects and bacterial strategies for resistance. *International Journal of Environmental Research and Public Health*, (13): 1047. https://doi.org/10.3390/ijerph13111047

11. Giner-Lamia, J., L´opez-Maury, L., Florencio, F.J. & Janssen, P.J. 2014. Global transcriptional profiles of the copper responses in the *cyanobacterium synechocystis sp.* PCC 6803. *PLOS ONE*, 9 (9): e108912. https://doi.org/10.1371/journal.pone.0108912

12. Gönen, F. & Aksu, Z. 2008. Use of response surface methodology (RSM) in the evaluation of growth and copper(II) bioaccumulation properties of *Candida utilis* in molasses medium. *Journal of Hazardous Materials*, 154(1-3): 731-738. https://doi.org/10.1016/j.jhazmat.2007.10.086

13. Gourdon, R., Bhende, S., Rus, E. & Sofer, S.S. 1990. Comparison of cadmium biosorption by Gram-positive and Gram-negative bacteria from activated sludge. *Biotechnology Letters*, 12: 839-842. https://doi.org/10.1007/BF01022606

14. Honfi, K., Tálos, K., Kőnig-Péter, A., Kilár, F. & Pernyeszi, T. 2016. Copper(II) and Phenol Adsorption by Cell Surface Treated *Candida tropicalis* Cells in Aqueous Suspension. *Water, Air & Soil Pollution*, 227: 1-14. https://doi.org/10.1007/s11270-016-2751-0

15. Javanbakht, V., Alavi, S.A. & Zilouei, H. 2013. Mechanisms of heavy metal removal using microorganisms as biosorbent. *Water Science and Technology*, 69(9): 1775-1787. https://doi.org/10.2166/wst.2013.718

16. Legorreta-Castañeda, A.J., Lucho-Constantino, C.A., Beltrán-Hernández, R.I., Coronel-Olivares, C. & Vázquez-Rodríguez, G.A. 2020. Biosorption of Water Pollutants by Fungal Pellets. *Water*, 12(4): 1155-1193. https://doi.org/10.3390/w12041155

17. Liu, Y. 2007. Overview of some theoretical approaches for derivation of the Monod equation. *Applied Microbiology and Biotechnology*, 73: 1241-1250 https://doi.org/10.1007/s00253-006-0717-7

18. Luk, C.H.J., Yip, J., Yuen, C.W.M., Pang, S.W., Lam, K.H. & Kan, C.W. 2017. Biosorption Performance of Encapsulated *Candida krusei* for the removal of Copper(II). *Scientific Reports*, 7: 1-9. https://doi.org/10.1038/s41598-017-02350-7

19. Luna, J.M., Rufino, R.D. & Sarubbo, L.A. 2016. Biosurfactant from *Candida sphaerica* UCP0995 exhibiting heavy metal remediation properties. *Process Safety and Environmental Protection*, 102: 558-566. https://doi.org/10.1016/j.psep.2016.05.010

20. Malik, A. 2004. Metal bioremediation through growing cells. *Environment International*, 30(2): 261-78. https://doi.org/10.1016/j.envint.2003.08.001

21. Modak, J.M. & Natarajan, K.A. 1995. Biosorption of metals using nonliving biomass-A review. *Mining, Metallurgy & Exploration*, 12: 189-196. https://doi.org/10.1007/BF03403102

22. Monod, J. 1949. The growth of bacterial cultures. *Annual Reviews in Microbiology*, 3(1): 371-394. https://mcb.berkeley.edu/labs/garcia/sites/mcb.berkeley.edu.labs.garcia/files/Teaching/2017-MCB137/Monod1949.pdf (Date accessed: 22.11.2020)

23. Pawan, K.R. & Devi, R. 2018. Heavy metal tolerance and adaptability assessment of indigenous filamentous fungi isolated from industrial wastewater and sludge samples. *Beni-Suef University Journal of Basic and Applied Sciences*, 7(4): 688-694. https://doi.org/10.1016/j.bjbas.2018.08.001

24. Podder, M.S. & Majumder, C.B. 2019. Bacteria immobilization on neem leaves/MnFe2O4 composite surface for removal of As(III) and As(V) from wastewater. *Arabian Journal of Chemistry*, 12: 3263-3288. https://doi.org/10.1016/j.arabjc.2015.08.025

25. Raspor P. & Zupan J. 2006. Yeasts in Extreme Environments. pp. 371-372. In: Péter G.& Rosa C.A. (eds). *Biodiversity and Ecophysiology of Yeasts*. Springer-Verlang, Berlin, 580 pp. https://doi.org/10.1007/3-540-30985-3_15

*26.* Razack, S.A., Velayutham, V. & Thangavelu, V. 2013. Medium optimization for the production of exopolysaccharide by *Bacillus subtilis* using synthetic sources and agro wastes. *Turkish Journal of Biology*, 37: 280-288. https://doi.org/10.3906/biy-1206-50

27. Redha, A.A. 2020. Removal of heavy metals from aqueous media by biosorption. *Arab Journal of Basic and Applied Sciences*, 27(1): 183-193. https://doi.org/10.1080/25765299.2020.1756177

28. Rehman, A. & Anjum, M.S. 2011. Multiple metal tolerance and biosorption of cadmium by *Candida tropicalis* isolated from industrial effluents: glutathione as detoxifying agent. *Environmental Monitoring and Assessment*, 174: 585-595. https://doi.org/10.1007/s10661-010-1480-x

29. Rehman, A. & Anjum, M.S. 2010. Cadmium Uptake by Yeast, *Candida tropicalis*, Isolated from Industrial Effluents and Its Potential Use in Wastewater Clean-Up Operations. *Water, Air and Soil Pollution*, 205: 149-159. https://doi.org/10.1007/s11270-009-0062-4

30. Şengör, S.S., Barua, S., Gikas, P., Ginn, T.R., Peyton, B., Sani, R.K., & Spycher, N.F. 2009. Influence Of Heavy Metals On Microbial Growth Kinetics Including Lag Time: Mathematical Modeling And Experimental Verification. *Environmental Toxicology and Chemistry*, 28: 2020-2029. https://doi.org/10.1897/08-273.1

31. Sandell, E.B. 1950. Colorimetric Determination of Traces of Metals Volume III. pp. 304-475. In: Clarke, B.L. & Kolthoff, I.M. (eds). *Chemical Analysis A Series of Monographs on Analytical Chemistry And Its Applications*. Interscience Publishers INC, London, 688 pp.

32. Tchounwou, P.B., Yedjou, C.G., Patlolla, A.K. & Sutton, D. J. 2012. Heavy metal toxicity and the environment. *Experientia Supplementum*, 101: 133-164. https://doi.org/10.1007/978-3-7643-8340-4_6

33. Tripathi, A, & Ranjan, M.R. 2015. Heavy Metal Removal from Wastewater Using Low Cost Adsorbents. *Journal of Bioremediation & Biodegration*, 6: 315-320. http://dx.doi.org/10.4172/2155-6199.1000315

34. Volland, S., Bayer, E., Baumgartner, V., Andosch, A., Lütz, C., Sima, E. & Lütz-Meindl, U. 2014. Rescue of

heavy metal effects on cell physiology of the algal model system Micrasterias by divalent ions. *Journal of Plant Physiology*, 171(2): 154-163. https://doi.org/10.1016/j.jplph.2013.10.002

35. Waldron, K.J. & Robinson, N.J. 2009. How do bacterial cells ensure that metalloproteins get the correct metal? *Nature Reviews Microbiology*, 7: 25-35. https://doi.org/10.1038/nrmicro2057

36. Wołowiec, M., Komorowska-Kaufman, M., Pruss, A., Rzepa, G. & Bajda, T. 2019. Removal of Heavy Metals and Metalloids from Water Using Drinking Water Treatment Residuals as Adsorbents: A Review. *Minerals*, 9(8): 487-504. https://doi.org/10.3390/min9080487

37. Zha, F., Wang, H., Xu, L., Yang, C., Kang, B., Chu, C., Deng, Y. & Tan, X. 2020. Initial feasibility study in adsorption capacity and mechanism of soda residue on lead (II)-contaminated soil in solidification/stabilization technology. *Environmental Earth Sciences*, 79: 1-12. https://doi.org/10.1007/s12665-020-08990-9

*http://dergipark.org.tr/trkjnat*
*Trakya University Journal of Natural Sciences, 22(1): 77-92, 2021*
*ISSN 2147-0294, e-ISSN 2528-9691*
*DOI: 10.23902/trkjnat.805761*

**Research Article**

# THE INTRODUCED NORTH AMERICAN SPECIES OF THE GENUS *Juglans* L. IN THE RIGHT-BANK FOREST-STEPPE OF UKRAINE AND THEIR USE

Halyna ISHCHUK[1], Volodymyr SHLAPAK[1], Liubov ISHCHUK[2*], Olexander BAYURA[1], Svitlana KURKA[1]

[1] Uman National University of Horticulture, Faculty of Forestry and Landscape Gardening, Uman, UKRAIN
[2] Bila Tserkva National Agrarian University, Faculty of Agro-Biotechnology, Bila Tserkva, UKRAIN

**Cite this article as:**

Ishchuk H., Shlapak V., Ishchuk L., Bayura O. & Kurka S. 2021. The introduced North American species of the genus *Juglans* L. in the Right-bank forest-steppe of Ukraine and their use. *Trakya Univ J Nat Sci*, 22(1): 77-92, DOI: 10.23902/trkjnat.805761

Received: 09 October 2020, Accepted: 31 March 2021, Online First: 12 April 2021, Published: 15 April 2021

***Edited by:***
*Vedat Beşkardeş*

****Corresponding Author:***
*Liubov Ishchuk*
*ishchuk29@gmail.comr*

***ORCID iDs of the authors:***
*HI. orcid.org/0000-0002-4969-0933*
*VS. orcid.org/0000-0001-8710-5662*
*LI. orcid.org/0000-0003-2150-0672*
*OB. orcid.org/0000-0003-1679-5840*
*SK. orcid.org/0000-0002-7722-2483*

***Key words:***
*North American Juglans spp.*
*Growth*
*Seasonal rhythm of development*
*Flowering*
*Fruit bearing*
*Winter and frost resistance*
*Introduction*
*Forest crops*

**Abstract:** The article presents generalized scientific researches and experimental data on the bioecological peculiarities of the North American species of the *Juglans* L. genus. The peculiarities of the seasonal rhythm of development are revealed. *Juglans cinerea* L., *J. rupestris* Engelm. and *J. major* (Torr.) A. Heller were the first to wake up and *J. nigra* L., *J. californica* S. Wats., and *J. hindsii* (Jeps.) Jeps. ex R.E. Sm. wake up a little later. The biorhythm of woody plants is closely related to the increase in the sum of active (+10°C) and effective (+5°C) temperatures. *Juglans cinerea* and *J. rupestris* require the smallest sum of effective temperatures for buds swelling, that is 28.9 and 34.1°C, respectively; *J. hindsii* require the largest sum of effective temperatures -57.1°C and *J. nigra* require 50.6°C. Investigation of growth dynamics shows that intensive growth of all species of the *Juglans* genus was observed in May-June. The vegetation period in all *Juglans* species lasts 183-206 days. The development cycle of North American walnuts under research conditions is shifted towards the summer-autumn period. When determining frost resistance, it was found that the species are characterized by an average degree of subfreezing. All species genus are promising for use in ornamental horticulture of the Right-Bank Forest-Steppe of Ukraine, as evidenced by the full acclimatization of *J. nigra* and *J. cinerea*, good acclimatization of *J. rupestris* and *J. major* and satisfactory acclimatization of *J. californica* and *J. hindsii*. It is established that *J. nigra* are promising for the development of highly productive forest plantations.

**Özet:** Bu çalışmada *Juglans* L. cinsinin Kuzey Amerika türlerinin biyolojik özellikleri ile ilgili genel bilimsel araştırmalar ile deneysel bulgular sunulmuştur. Bu türlere ilişkin mevsimsel gelişim özelliklerinin detayları ortaya konmuştur. *Juglans cinerea* L., *J. rupestris* Engelm. ve *J. major* (Torr.) A. Heller ilk uyanan türler iken *J. nigra* L., *J. californica* S. Wats. ve *J. hindsii* (Jeps.) Jeps. ex R.E. Sm. biraz daha geç uyanmışlardır. Odunsu bitkilerin biyolojik ritimleri aktif (+10°C) ve efektif (+5°C) sıcaklık değerlerinin toplamındaki artış ile yakında ilişkilidir. *Juglans cinerea* ve *J. rupestris* tomurcuklanma için en düşük toplam efektif sıcaklık değerlerine (sırasıyla 28.9 °C ve 34.1°C), *J. hindsii* ve J. nigra ise en yüksek değerlere (sırasıyla -57.1°C ve 50.6°C). Büyüme dinamiklerinin incelenmesi tüm *Juglans* türlerindeki yoğun büyümenin Mayıs-Haziranda yaşandığını göstermiştir. Tüm türlerdeki vejetasyon süresi 183-206 gün sürmektedir. Kuzey Amerika kökenli cevizlerin araştırma sahası koşullarındaki gelişim döngüsü yaz-sonbahar dönemine doğru kaymıştır. Dona dayanıklılık tespiti için yapılan çalışmalar tüm türlerin ortalama bir donma derecesi ile karakterize olduklarını göstermiştir. Tüm türler Sağ Yaka Ukrayna orman-step bölgesinde süs bitkiciliği kullanımı için gelecek vaat etmektedirler ki bu durum *J. nigra* ve *J. cinerea*'nın tam, *J. rupestris* ve *J. major*'ın iyi derecede ve *J. californica* ve *J. hindsii*'nin yeterli derecede uyum sağlamış olmalarıyla desteklenmektedir. *Juglans nigra*'nın yüksek üretkenlikte orman alanları oluşturulmasında ümit veren bir tür olduğu düşünülmektedir.

## Introduction

The genus *Juglans* L. is classified in the Juglandaceae family, Juglandales order, Hamamelididae subclass, Magnoliopsida class, Magnoliophyta division according to the system of Takhtadjian (1980). De Candolle (1857), Dode (1909), Engler & Prantl (1894), Linnaei (1759), Martin, Zim & Nelson (1951), Manning (1978), APG IV

(The Angiosperm Phylogeny Group, 2016) studied the systematics of the genus, the history of its origin, the spreading pattern over the world and phylogenetic relations of the North American species of the genus. *Juglans nigra* L. was first described by Carl Linnaeus in 1737, *J. cinerea* L. in 1759, and the other North American species were described in the nineteenth century. Researchers so far identified 10 species in the genus spreading in moderately warm, subtropical and even tropical regions of Eurasia (*J. regia* L., *J. mandshurica* Maxim., *J. cordiformis* Maxim., *J. sieboldiana* Maxim.) and North America (*J. nigra*, *J. cinerea*, *J. rupestris* Engelm., *J. major* (Torr.) A. Heller, *J. californica* S. Wats., *J. hindsii* (Jeps.) Jeps. ex R.E. Sm.) (Fig. 1) (Sokolov 1957).

According to Zhukovsky (1971), *Juglans* genus has four genetic centers of origin as Central Asian, Western Asian, Chinese-Japanese and North American. *Juglans nigra*, *J. cinerea*, *J rupestris*, *J. major*, *J. californica* and *J. hindsii* are the species with North American origin center. The current occurrence areas of species of the genus are the part of one large area that existed in the past geological epochs and disintegrated because of the climate changes.

Numerous fossils indicated that the genus is known from the Upper Cretaceous, and the number of species and their distribution areas changed in past geological epochs. Representatives of the genus in terms of species diversity reached their highest peak in the Eocene, Oligocene and Miocene ages (Ishchuk 2013).

*Juglans nigra* and *J. cinerea* were introduced to Ukraine in the early nineteenth century. *Juglans nigra* was introduced in 1809 by the Osnoviansky Acclimatization Garden. *Juglans cinerea* has been known since 1816 and was first introduced in the Kremenets Botanical Garden in Ternopil region (Barbarich & Horhota 1952, Ishchuk 2007a). Both species underwent a long period of acclimatization and are widely represented in the dendrological collections, forest crops and street plantations of all natural-and-climatic zones of Ukraine. *Juglans rupestris*, *J. major*, *J. californica* and *J. hindsii* were introduced to Ukraine in the 1930s at Nikitsky Botanical Garden and are now rarely found in the dendrological collections of Eastern, Central and Southern Ukraine (Ishchuk 2007b). The period of acclimatization of these species continued to present day. The oldest trees of *J. nigra* are in the O.V. Fomin Botanical Garden in Kyiv (1854) and in the arboretum of Ukrainian National Forestry University in Lviv.

The North American species of the genus are rare in the Right-Bank Forest-Steppe of Ukraine because of insufficient studies on the bioecological peculiarities of their introduction. Only two species, *J. nigra* and *J. cinerea*, are found in the forest crops of this region. Other species, *J. rupestris*, *J. californica*, *J. major* and *J. hindsii*, are only present in the collections of botanical gardens and dendrological parks where they are cultivated as single trees in the territory of Ukraine.

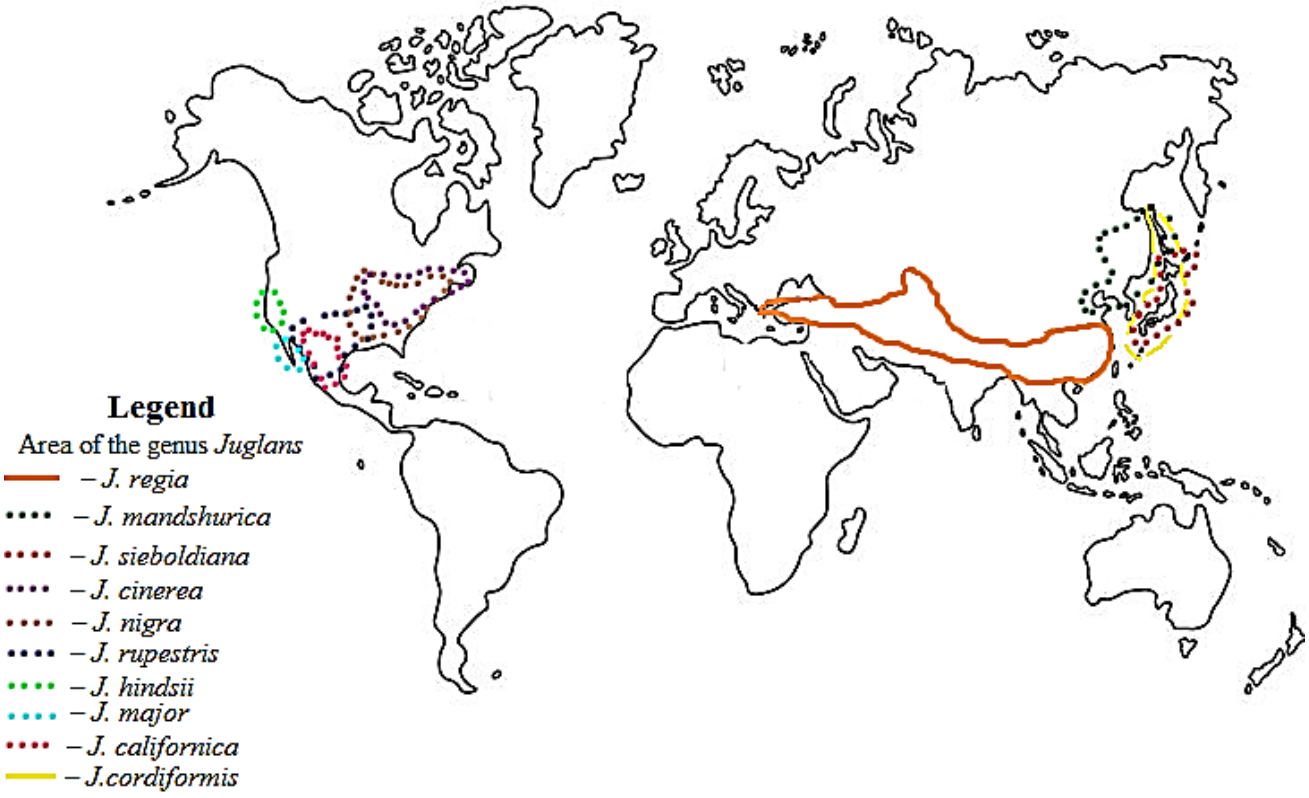


**Fig. 1.** The distributional area of the genus *Juglans* (according to Sokolov, 1957) 1- *J. regia*, 2- *J. mandshurica*, 3- *J. sieboldiana*, 4- *J. cinerea*, 5- *J. nigra*, 6- *J. rupestris* 7- *J. hindsii*, 8- *J. major*, 9- *J. californica*, 10- *J. cordiformis.*

During the last century, Badalov (1971) (selection of nuts and research on bioecological features of hybrids), Shchepotiev (1985) (bioecological features of *J. regia* and partly of *J. nigra* and *J. cinerea*), Bondar (1997), Shvydenko & Tsygankov (1978) (study on *J. nigra* in the forest crops), Kenig (1966), Antoniuk (1968), Hryshko-Bogmenko (1969) (studies on the introduction of some *Juglans* species in Ukraine), Zhyhalova (2007) (review of the systematic features in determining the representatives of the *Juglans* genus), Takhtadjian (1980) (systematics of the genus) were engaged in the study of the representatives of the genus. Analysis of the economic use of *J. nigra* was performed by Dubrovsky & Shved (2019).

However, most of these works were dedicated to *J. regia*, the most common in the Forest-Steppe, which originated from the Balkans, Iran and Asia Minor. In general, these sources contributed only to certain partial information about the North American species *J. nigra* and *J. cinerea* and their hybrids with *J. regia* and with themselves, which were more related to the western and northern parts of the Right-Bank Forest-Steppe and the Left-Bank Forest-Steppe of Ukraine. We found only short reports in the catalogs of botanical gardens and dendrological parks of Ukraine and in the reference books on dendrology about the rest of the North American species *J. rupestris, J. californica, J. major* and *J. hindsii* (Ishchuk 2007b).

Based on the fact that the territory of the Right-Bank Forest-Steppe of Ukraine is located at 45°-50° north latitude, that *J. nigra* and *J. cinerea* will be the most promising species among the North American species of the *Juglans* genus for green building and forest plantations. In North America, they grow at about the same latitude as our research region - the Right-Bank Forest-Steppe of Ukraine.

In this study, we aimed to choose the most promising species of the North American species of the *Juglans* genus for forest plantations and green building of the Right-Bank Forest-Steppe of Ukraine. In this regard, we analyzed the dynamics of growth and development, the degree of frost resistance, peculiarities of flowering, fruiting and seed propagation of North American *Juglans* spp.

**Materials and Methods**

Studies of the North American species of the genus *Juglans* were conducted during 2006-2019 at the research areas of Uman National University of Horticulture, in Moivske, Monastyryshche, Synytsia and Yurkivka forestries of the state enterprises of "Mohyliv-Podilskyi and Uman forestry" (37 sampling areas with the forest crops were laid out), in the street plantations in Uman city (Fig. 2), and by expeditions in the botanical gardens, dendrological parks, ornamental urban and rural plantations of the Forest-Steppe and Steppe of Ukraine (163 trees of the North American species of the *Juglans* genus were investigated).

In studying the species of the genus *Juglans*, we used the following research methods: bioecological, biomorphological, biometric, forest, expeditionary, visual, statistical.

The climate indicators of the region of introduction (Right-Bank Forest-Steppe of Ukraine) of the North American species of the *Juglans* genus according to Moroz & Kosenko (2006) and Buchinskij (1960) are the following: average July temperature 19.2-20.8°C, average January temperature (-5.5) - (-6.1)°C, maximum temperature +37.1°C, minimum temperature -35°C, annual precipitation 500-610 mm, snow cover height 0.3-0.5 m., the duration of the non-frosty period 159-171 days. The climate of the Right-Bank Forest-Steppe of Ukraine is continental, moderately warm with sufficient humidity.

Phenological observations of the species were conducted during 14 growing seasons of 2006-2019 on 5 sample trees of each species. The phases of swelling and budding were observed in April, the phase of flowering in late April and early May, fruit set in May, growth and woodiness of shoots in May-August, the phase of discoloration and leaf fall in September-October, and the phase of fruit ripening and falling was observed in October (Lapin 1975). The sum of effective temperatures (above +5°C) during the recording of the phases of swelling and budding, flowering, fruit set was calculated. The sum of active temperatures (above +10°C) during the recording of the phases of growth and woodiness of shoots, discoloration and leaf fall, and ripening and falling of fruits was calculated for each species.

The sum of effective temperatures is the sum of average daily temperatures deducted from the biological minimum at which plants of a given crop develop (+ 5°C). The sum of active temperatures is an indicator of supply of active plants vegetation by the warm period and consists of average daily temperatures of above +10°C. The sums of temperatures are determined by data on the average daily, average decadal and average monthly temperatures (Chirkov 1986).

Measurements of shoot growth were performed every 5 days on 10 sample trees in the lower, middle and upper part of the crown using a measuring device (ruler) (Molchanov & Smirnov 1967). We measured diameter of the root collar, length of the main root, total length of the root system for every year.

Flowering and fruiting were evaluated by the following scale: 5 points - flowers and fruits are placed on the tree very abundantly and evenly covered the whole tree, 4 points - flowers and fruits are placed on the tree moderately, 3 points - flowers and fruits on the tree are twice less compared to very abundant flowering and fruiting, 2 points - flowers and fruits are widely-spaced on the tree, 1 point - only single flowers and fruits are recorded, 0 point- flowers and fruits are absent (Ivanenko 1962). The score of flowering and fruiting was determined visually on five sample trees of each species.

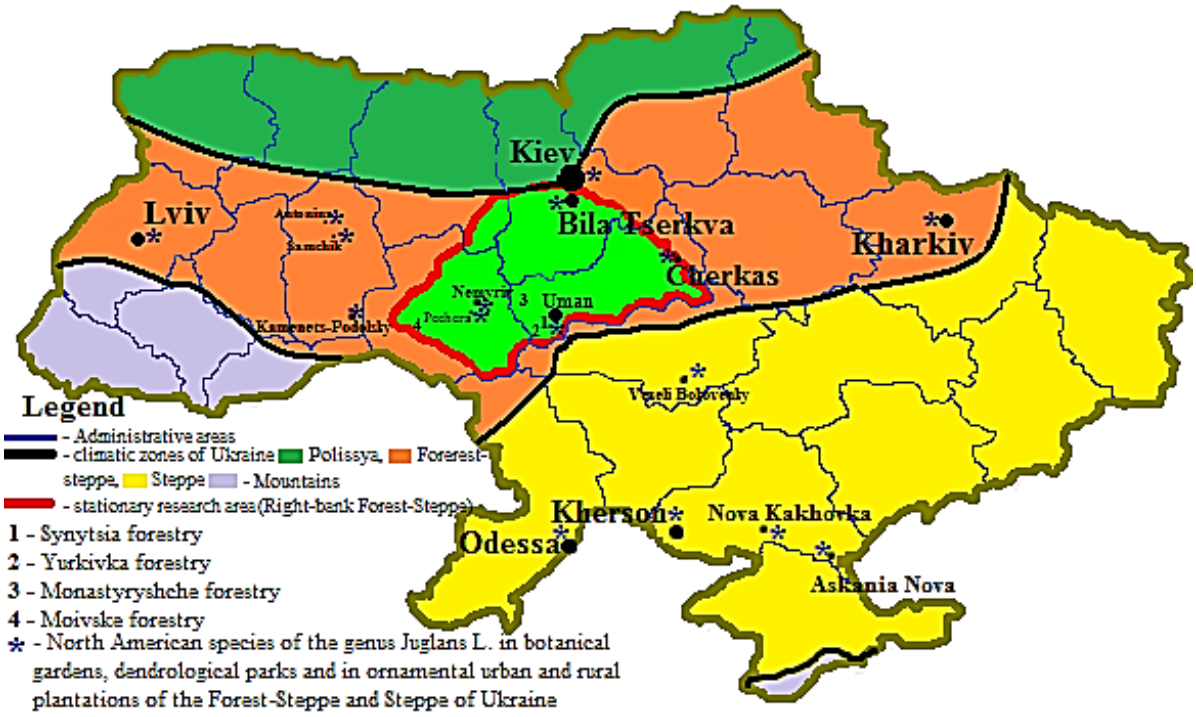


**Fig. 2.** The map showing the research area of the North American species of the *Juglans* genus in Ukraine.

Freezing was carried out in two stages - during the period of deep dormancy (January) at a temperature of -25ºC and -35ºC and during the period of forced dormancy (March) at a temperature of -20ºC and -25ºC (Soloviova 1982). Cuttings without freezing were taken for control. Anatomical and microscopic method to determine the nature and degree of damage of various tissues by the intensity of browning on the transversal section of shoots was used. Conditional coefficients on different physiological significance of tissues were introduced for each of them: 6 - for bark, 8 - for cambium, 4 - for wood, 2 - for core under the general estimation of frost resistance of shoots. The coefficient of 20 was introduced for a bud and the index of frost damage (IFD), i.e. sensitivity to low temperatures was determined (Potanin *et al*. 2005).

100 walnuts of each species for autumn sowing with endocarp to a depth from 2-3 cm. to 8-9 cm. were used to investigate the soil germination of North American walnuts and to determine the optimal depth of their seeds covering (Tsitsin 1980).

Sampling areas were formed in a rectangular shape, they were limited by sight lines at the sight. In each sampling area, 200 trees were selected in pure plantations, 100 trees of each species in mixed plantations, 400 trees of the investigated species in young plantations. The size of the sampling area was not less than 0.02 ha. (Hordiienko 1979). A continuous count of trees by a two-centimetre scale of the thickness degrees was performed on the sampling area. The heights of the trees were measured during the observation (Anuchin 1982). Forestry description of them was performed after limiting the sampling areas at the sight. During the description of the plantation, the type of forest vegetation conditions, soil type, method of crop production (sowing, planting), category of forest areas were determined, as well as the composition of grass vegetation and the nature of its spreading, capacity and composition of forest litter was described. Office processing of the obtained data with determining of all forestry and taxation indicators (planting composition, age of planting, type of planting habitat conditions, average diameter and height of planting, planting bonitet, planting completeness, stock of wood in the planting per 1 ha.) was carried out after the end of the field work on the sampling area.

The degree of acclimatization was determined by the acclimatization value, which is the sum of indicators of growth, generative development, winter hardiness and drought resistance of plants, expressed in points: full acclimatization 100 points, good acclimatization 80 points, satisfactory acclimatization 60 points, poor acclimatization 40 points and no acclimatization 20 points (Kokhno & Kordiuk 1994). The degree of acclimatization of the species was studied on 5 sample trees of each species.

Mathematical processing of the dynamics of shoots growth was performed by the method of descriptive statistics by determination of the arithmetic mean value ($M$), the error of the average value ($m$), the mean-square deviation ($\sigma$), the coefficient of variation ($V$), the accuracy of the study ($P$) (Moseichenko 1992). We also used the analysis of variance program (one-way ANOVA).

## Results

In studies performed to determine the dormancy period of North American species of the *Juglans* genus, we found that the shortest dormancy period was observed in *J. cinerea*, i.e., it was not deep and could be disturbed by frequent winter thaws; then *J. nigra* woke up (Table 1).

However, *J. rupestris*, *J. major J. californica* and *J. hindsii* had an even longer dormancy period, which lasted until the end of January - beginning of February and only then the species entered the forced dormancy (Figs 3-4).

Under environmental conditions of Uman city, a complete small cycle of the development was observed only in *J. nigra*, *J. cinerea* and *J. rupestris* (Table 2). The small cycle was not complete in other species, because they had not yet reached reproductive age (Fig. 5).

**Table 1.** The sum of effective temperatures (above 5°C) at which there is a mass buds swelling and budding in species of the *Juglans* genus under environmental conditions of Uman city (average indicators for 2006-2019).

| Species | Phase of development | | Sum of effective temperatures (°C) necessary for | |
|---|---|---|---|---|
| | date of buds swelling | date of budding | buds swelling | budding |
| ***J. nigra*** | 7-21.04 | 27.04-2.05 | 51.7±7.6 | 103.0±7.2 |
| ***J. cinera*** | 3-12.04 | 21.04-25.04 | 28.9±4.8 | 70.9±8.0 |
| ***J. rupestris*** | 8-14.04 | 26.04-2.05 | 35.5±5.8 | 68.3±4.9 |
| ***J. major*** | 9-13.04 | 26.04-3.05 | 45.6±1.4 | 83.3±7.1 |
| ***J. californica*** | 13-17.04 | 28.04-2.05 | 49.1±4.7 | 86.0±9.9 |
| ***J. hindsii*** | 13-18.04 | 29.04-3.05 | 52.2±3.0 | 91.5±3.9 |

**Table 2.** The sum of active temperatures (°C) necessary for flowering, fruit setting and ripening of the species of the *Juglans* genus under environmental conditions of Uman city (average indicators for 2006-2019).

| Species | Duration of flowering (days) | Sum of active temperatures (above +10°C) necessary for | | | |
|---|---|---|---|---|---|
| | | beginning of flowering | ending of flowering | fruit setting | fruit ripening |
| ***J. nigra*** | 13-17 | 135.2±8.7 | 192.8±3.2 | 720.7±19.1 | 2555.7±15.4 |
| ***J. cenerea*** | 15-17 | 141.4±12.3 | 199.8±7.9 | 855.4±14.9 | 2367.8±12.1 |
| ***J. rupestris*** | 9-16 | 113.0±9.2 | 148.5±10.8 | 810.5±12.8 | 3045.0±14.0 |

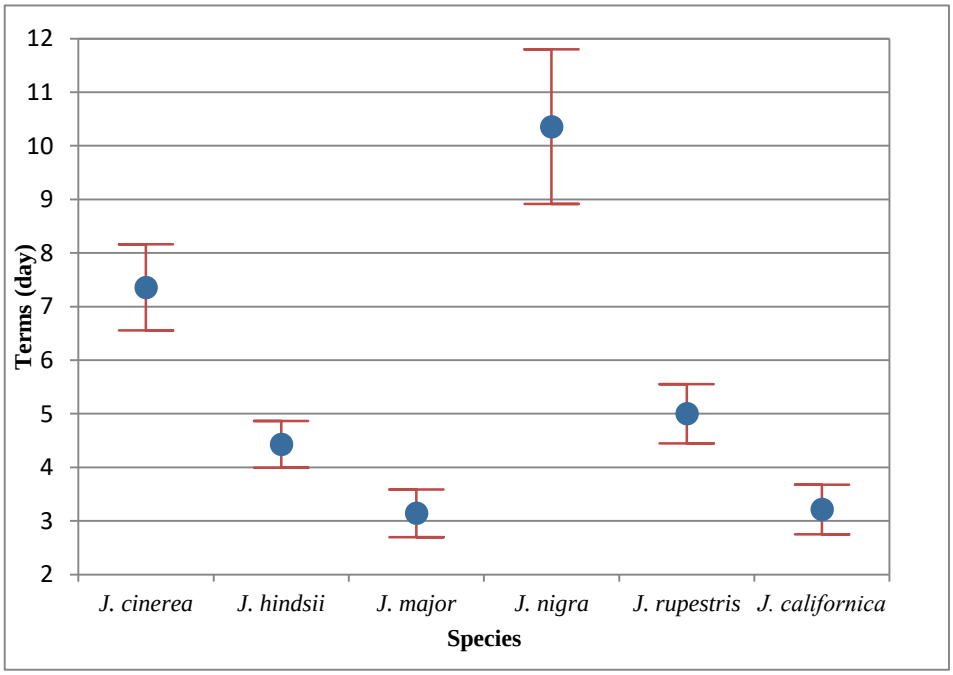


**Fig. 3.** Means plot (95% CI) of the swelling phase of tree buds.

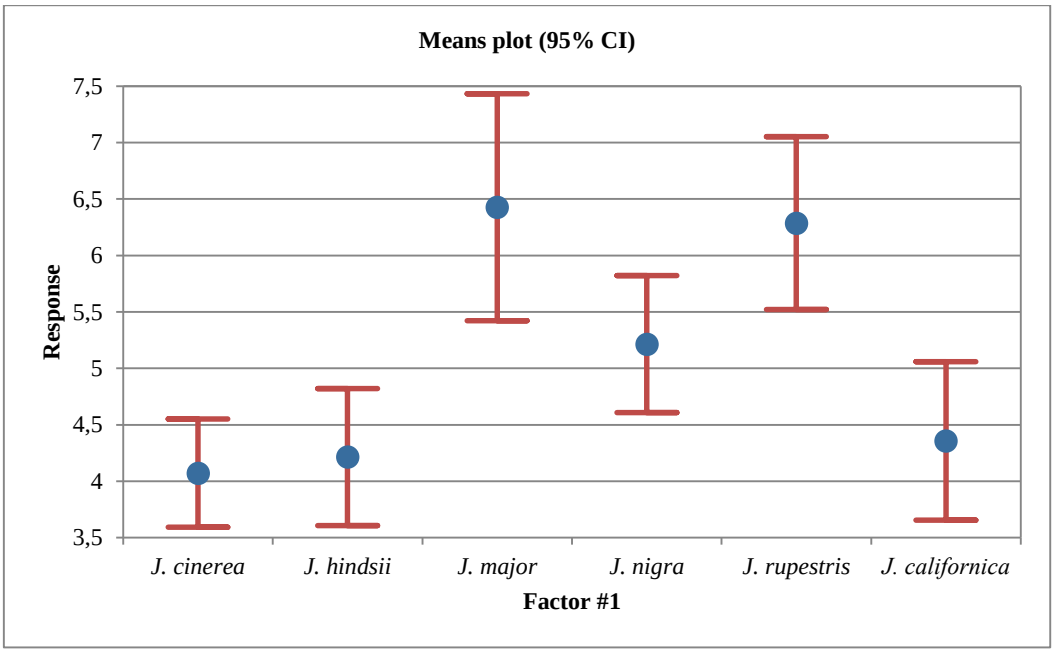


**Fig. 4.** Means plot (95% CI) of duration of bud burst.

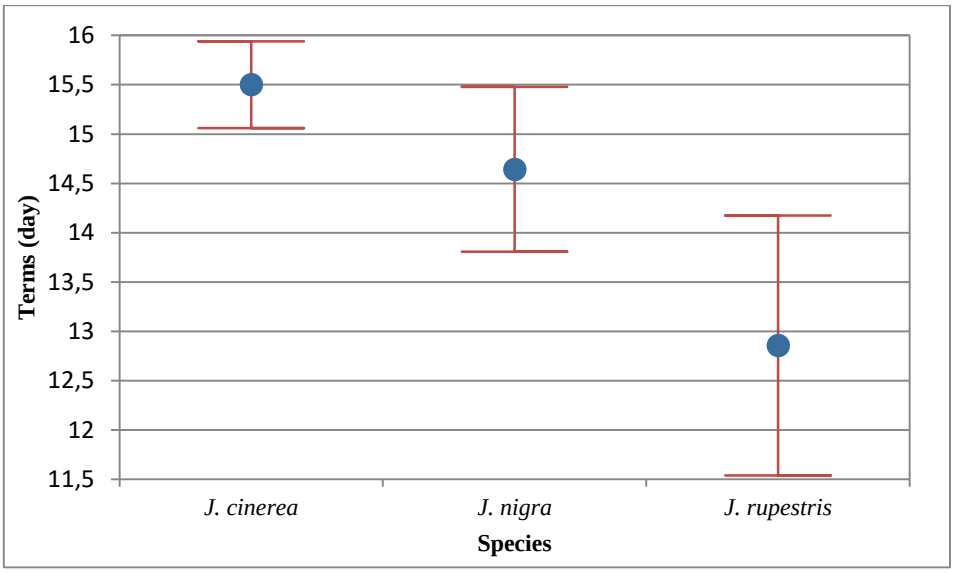


**Fig. 5.** Means plot (95% CI) of flowering duration.

*Juglans cinerea*, *J. rupestris*, and *J. major* were the first to wake up in the conditions of Uman city and *J. nigra*, *J. californica*, *J. hindsii* woke up later. The shoots became completely woody much later in *J. nigra*, *J. rupestris*, *J. major*, *J. californica*, *J. hindsii*, so they freeze more often.

We found that the intensive growth of shoots of all species was observed in May-June; the energy of shoot growth decreased in July and stopped in August. One-year seedlings of *J. nigra* and *J. cinerea* grew to 31.5 cm, *J. rupestris* and *J. major* to 16.2-16.7 cm, and *J. californica* and *J. hindsii* to 14.1-14.3 cm in height. The study was performed on 30 one-year seedlings of each species (Table 3). The growth of annual seedlings was determined on 30 samples of each species. Statistical data processing of the dynamics of growth is presented in Table 4.

The vegetation period in *J. nigra* began on April 8-20 and ended on October 7-12 and lasted for 183 days on average. It began on April 1-11, ended on October 1-5 in *J. cinerea*, and lasted for 184 days on average. The vegetation period in *J. major* and *J. rupestris* began on April 8-10 and ended on November 1-3, lasting for 206-208 days on average. It began on April 12-18 in *J. californica* and *J. hindsii*, and ended the latest on November 2-5, lasting for 201-203 days. The vegetation period in all North American species of the *Juglans* genus was shifted towards the summer-autumn season (Table 5, Fig. 6).

**Table 3.** Characteristics of one-year seedlings of species of the *Juglans* genus under environmental conditions of Uman city.

| Species | Height (cm) | Diameter of the root collar (cm) | Length of the main root (cm) | Total length of the root system (cm) | First branching from the root collar (cm) |
|---|---|---|---|---|---|
| ***J. nigra*** | 31.5±2.3 | 1.0±0.5 | 125.7±2.85 | 453.5±3.9 | 25.1±0.5 |
| ***J. cinerea*** | 31.2±2.6 | 1.0±0.5 | 118.4±3.2 | 420.7±3.7 | 10.3±0.5 |
| ***J. rupestris*** | 16.7±1.7 | 0.8±0.3 | 100.8±1.9 | 285.2±3.2 | 8.8±0.3 |
| ***J. major*** | 16.2±1.4 | 0.5±0.2 | 80.1±1.6 | 215.0±2.9 | 5.2±0.3 |
| ***J. californica*** | 14.3±1.2 | 0.5±0.1 | 74.3±1.5 | 198.6±3.0 | 6.9±0.2 |
| ***J. hindsii*** | 14.1±1.3 | 0.5±0.1 | 92.5±1.1 | 255.9±3.1 | 7.0±0.2 |

**Table 4.** Statistical *data* processing of the dynamics of growth of the North American species of the *Juglans* genus.

| Name of the species | Year of observation | | | | | | | | | | | | | | Height* (cm) | | | | |
|---|---|---|---|---|---|---|---|---|---|---|---|---|---|---|---|---|---|---|---|
| | 2006 | 2007 | 2008 | 2009 | 2010 | 2011 | 2012 | 2013 | 2014 | 2015 | 2016 | 2017 | 2018 | 2019 | *M* | *m* | *σ* | *V* | *P* |
| ***J. nigra*** | 30.5 | 35.2 | 30.5 | 26.9 | 32.5 | 30.4 | 33.5 | 37.5 | 26 | 36.4 | 29.1 | 35 | 27 | 31.1 | 31.54 | 2.33 | 3.50 | 0.11 | 66.49 |
| ***J. cinerea*** | 36.8 | 30 | 36.7 | 30.6 | 36.5 | 25 | 30.1 | 30.2 | 26.6 | 28 | 30.8 | 30.4 | 30.2 | 35.1 | 31.21 | 2.63 | 3.59 | 0.12 | 73.25 |
| ***J. rupestris*** | 17.7 | 16.9 | 13.3 | 16.8 | 16.1 | 15.9 | 14.5 | 17.2 | 16 | 18.3 | 12.5 | 21.2 | 15.5 | 21.9 | 16.70 | 1.70 | 2.51 | 0.15 | 67.76 |
| ***J. major*** | 16 | 14.3 | 16.5 | 16.6 | 21 | 13.7 | 16.9 | 16.8 | 15 | 15.9 | 12.6 | 15.9 | 19.7 | 16.1 | 16.21 | 1.41 | 2.09 | 0.13 | 67.82 |
| ***J. californica*** | 10.2 | 14.9 | 13 | 15.9 | 14 | 15.2 | 16 | 13.5 | 14.8 | 13.6 | 13 | 15.3 | 14.2 | 16.8 | 14.31 | 1.23 | 1.59 | 0.11 | 76.98 |
| ***J. hindsii*** | 15 | 14.4 | 18 | 15 | 12.9 | 11.9 | 14.9 | 14.2 | 8.9 | 14.2 | 13.6 | 15 | 14.8 | 15 | 14.13 | 1.32 | 1.95 | 0.14 | 67.50 |

* *M* is the arithmetic mean value, *m* is the error of the average value, *σ* is the mean-square deviation, *V* is the coefficient of variation, *P* is the accuracy of the study.

**Table 5.** The vegetation period of species of the *Juglans* genus under environmental conditions of Uman city (average indicators for 2006-2019).

| Species | Beginning of the vegetation | Autumn coloring of leaves | Leaf fall | Duration of the vegetation period (days) |
|---|---|---|---|---|
| ***J. nigra*** | 8.04-20.04 | 25.09 -10.10 | 7-12.10 | 183±7 |
| ***J. cinerea*** | 1.04-11.04 | 20.09-1.10 | 1-5.10 | 184±5 |
| ***J. rupestris*** | 8.04-12.04 | 15.10-1.11 | 1.11-3.11 | 208±2 |
| ***J. major*** | 10.04-14.04 | 15.10-23.10 | 1.11-3.11 | 206±2 |
| ***J. californica*** | 12.04-14.04 | 15.10-20.10 | 29.10-2.11 | 201±2 |
| ***J. hindsii*** | 12.04-18.04 | 28.10-4.11 | 2.11-5.11 | 203±1 |

Abundant harvests of nuts were observed in 2007, 2011 and 2018 in the conditions of the Right-Bank Forest-Steppe of Ukraine during 2006-2019. The average score of flowering and fruit bearing of the species in the plantations of Uman city and Synytsia arboretum was 3.5 points for *J. nigra*, 3 points for *J. cinerea* and 1.5 points for *J. rupestris* (Fig. 7).

In our studies on the freezing of shoots, we found that the highest rate of frost damage (from 33.1 in *J. cinerea* to 52.4 in *J. rupestris*) was obtained in the experimental variant for cambium and bark of all species in sections through the apex shoots at t = -35°C during the period of deep dormancy (Table 6). The wood and core of shoots in all species when cutting through the node of the shoot middle was the least damaged. The highest index of frost damage was recorded in *J. rupestris* (57.5) for the bark and cambium of the upper part of the shoots when freezing at t = -25°C during the period of forced dormancy (Table 6). This indicator was much lower (from 30.0 to 48.5) in all species in all tissues of the middle of the shoot at t = -25°C. Determined the degree of frost resistance of 5 shoots of each species in 3 repetitions. Bud had a very high level of damage in all cases of freezing. A medium degree of freezing was characterized for the species.

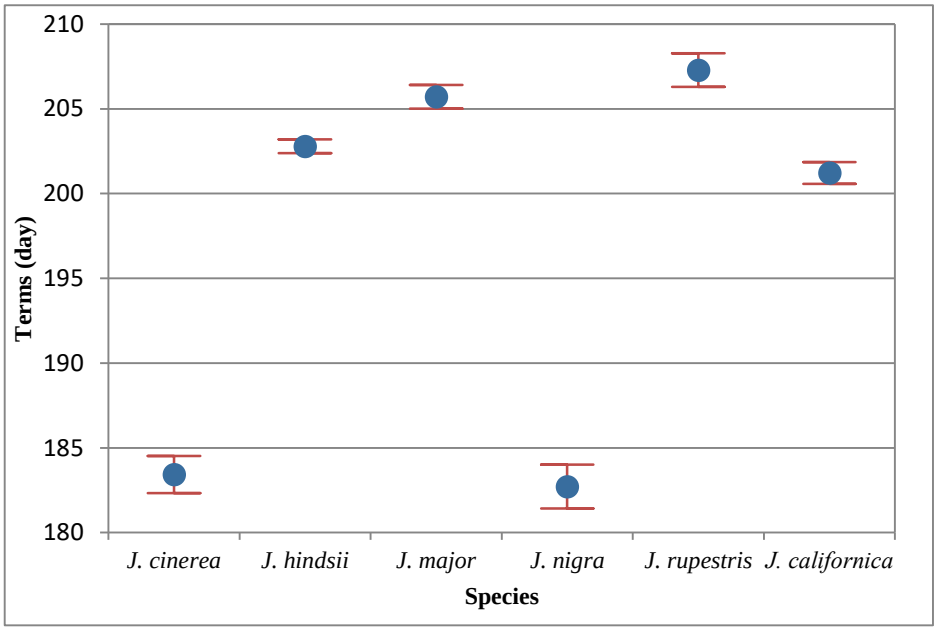


**Fig.6.** Means plot (95% CI) during the growing season.

**Table 6.** Situational and potential frost resistance of *Juglans* species under artificial freezing during deep and forced dormancy.

| Species | Freezing temperature (°C) | Index of frozen damage of different shoot parts | | | |
|---|---|---|---|---|---|
| | | bud | upper internode | middle internode | middle node |
| **I decade of January (period of deep dormancy)** | | | | | |
| | Control | 20.0 | 37.2 | 30.4 | 17.4 |
| ***J. nigra*** | -25 | 32.0 | 39.6 | 27.4 | 37.4 |
| | -35 | 90.0 | 36.2 | 32.5 | 28.4 |
| | Control | 10.0 | 25.0 | 21.5 | 12.5 |
| ***J. cinerea*** | -25 | 28.3 | 37.3 | 34.4 | 26.5 |
| | -35 | 75.0 | 33.1 | 30.2 | 26.5 |
| | Control | 30.0 | 40.2 | 35.0 | 24.6 |
| ***J. rupestris*** | -25 | 41.5 | 52.0 | 46.5 | 38.2 |
| | -35 | 100.0 | 52.4 | 48.6 | 45.5 |
| **I decade of March (period of forced dormancy)** | | | | | |
| | Control | 10.8 | 40.0 | 23.7 | 15.3 |
| ***J. nigra*** | -20 | 28.2 | 20.0 | 14.6 | 10.3 |
| | -25 | 78.5 | 30.9 | 30.0 | 24.0 |
| | Control | 8.5 | 35.6 | 20.6 | 12.5 |
| ***J. cinerea*** | -20 | 25.6 | 20.3 | 12.8 | 10.0 |
| | -25 | 65.8 | 30.0 | 28.5 | 22.4 |
| | Control | 15.6 | 52.0 | 28.4 | 22.5 |
| ***J. rupestris*** | -20 | 38.2 | 30.5 | 22.4 | 18.5 |
| | -25 | 90.0 | 57.5 | 48.5 | 36.4 |

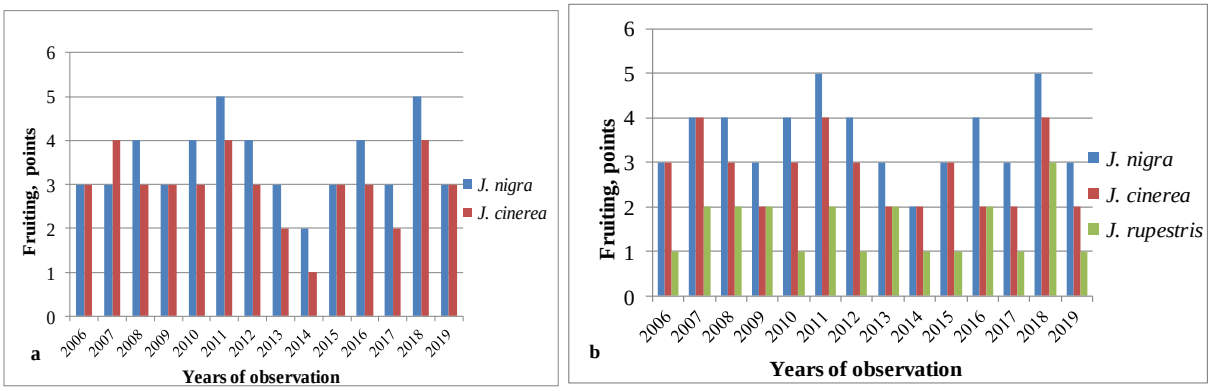


**Fig. 7.** Estimation of fruit bearing of the species of in Uman city (a) and Synytsia arboretum (b).

**Table 7.** Influence of the depth of the seed sowing of the species on their field germination and gum of planting materia (initial number of walnuts was 100 pcs.).

| Species | Depth of seed covering Shved cm) | Field germination (%) | Date of mass nut field germination | Gum of planting materia (%) |
|---|---|---|---|---|
| ***J. nigra*** | 2-3 | 25 | 10.05 | 25.5 |
| | 3-4 | 28 | 12.05 | 28.5 |
| | 4-5 | 54 | 15.05 | 54.5 |
| | 5-6 | 62 | 15.05 | 62.5 |
| | 6-7 | 68 | 20.05 | 70.0 |
| | 7-8 | 70 | 22.05 | 49.5 |
| | 8-9 | 50 | 26.05 | 38.7 |
| ***J. cinerea*** | 2-3 | 20 | 10.05 | 19.5 |
| | 3-4 | 32 | 14.05 | 31.5 |
| | 4-5 | 55 | 17.05 | 54.5 |
| | 5-6 | 62 | 18.05 | 52.5 |
| | 6-7 | 67 | 20.05 | 60.0 |
| | 7-8 | 53 | 23.05 | 66.5 |
| | 8-9 | 20 | 27.05 | 31.5 |
| ***J. rupestris*** | 2-3 | 10 | 18.05 | 9.5 |
| | 3-4 | 15 | 23.05 | 14.5 |
| | 4-5 | 25 | 27.05 | 24.5 |
| | 5-6 | 45 | 28.05 | 44.5 |
| | 6-7 | 41 | 28.05 | 39.5 |
| | 7-8 | 38 | 30.05 | 37.5 |
| | 8-9 | 30 | 3.06 | 29.5 |

Seeds were best sown with endocarp in autumn to a permanent place, or in spring under the condition of the nut's stratification of *J. rupestris, J. major* for 160 days, *J. nigra, J. cinerea* for 120 days and *J. californica, J. hindsii* for 100 days in the wet sand at t = 1-3°C. Seed hardness of fruits could be broken by scarification, hydrothermal and chemical methods. The action of sulfuric acid was the most effective way to break the hardness. The optimal depth of seed covering during spring and autumn sowing was 5-6 cm for *J. rupestris*, 7-8 cm for *J. nigra* and *J. cinerea* and was determined experimentally which allowed to increase germination by 25-30% (Table 7).

*Juglans nigra* and *J. cinerea* under favourable soil and climatic conditions were restored by self-seeding. Self-seeding of *J. cinerea* and *J. nigra* were observed mainly in the botanical gardens and dendrological parks but they were not found in the forest plantations. The best self-seeding of *J. cinerea* was observed in the botanical garden of N.V. Karazin Kharkiv National University, and *J. nigra* - in the Synytsia arboretum of the "Uman Forestry" state enterprise.

Our research established the optimal timing and methods of sowing nuts in forest nurseries. In autumn, in October, nuts together with the endocarp were sown in the seed-plots by band sowing with a width between the rows in the bands of 10-12 cm, and between the bands - 50-55 cm. The distance between the nuts in a row was 3-5 cm. The depth of seed covering was 6-7 cm (Fig. 8).

Pure and mixed forest crops of *J. nigra* in Moivske forestry in Vinnytsia region, Yurkivka, Synytsia and Monastyryshche forestries in Cherkasy region were studied (Table 8).

It is found that forest crops had a good growth and were characterized by high wood and seed productivity. The oldest 87-year-old cultures of *J. nigra* (Fig. 9) in Moivske forestry were presented in the "Filitsianivskyi forest" natural landmark.

**Fig. 8.** *Juglans nigra* in the seed-plot of Moivske forestry of Vinnytsia region.

**Fig. 9.** Forest crops of *J. nigra* in Moivske forestry.

**Table 8.** Characteristics of mixed *J. nigra* plantations of different ages in the forestries of the state enterprises "Mohyliv-Podilskyi forestry" and "Uman forestry".

| Forest planning quarter | Plantation composition (by rows) | Age of planning (year) | Average height (m) | Average diameter (cm) | Forest appraisal index | Forest site type | Stand density | Stand volume ($m^3/ha^{-1}$) |
|---|---|---|---|---|---|---|---|---|
| **Yurkivka forestry** | | | | | | | | |
| 107 | 8 *J. regia*, 2 *J. nigra* | 63 | 17.4±0.6 | 21.0±1.6 | II | new hornbeam-oak wood | 0.6 | 123.6 |
| 108 | 6 *J. regia*, 3 *J. mandschurica* Maxim., 1 *J. nigra* | 65 | 15.2±0.4 | 19.5±1.7 | III | new hornbeam-oak wood | 0.6 | 113.4 |
| 124 | 8 *J. nigra*, 2 *Fraxinus excelsior* L. | 30 | 10.6±0.2 | 17.4±1.0 | Ia | new hornbeam-oak wood | 0.6 | 57.8 |
| **Synytsia forestry** | | | | | | | | |
| 106 | 8 *J. nigra*, 2 *J. regia* | 65 | 21.5±0.7 | 28.3±1.8 | I | new hornbeam-oak wood | 0.7 | 2448 |
| 106 | 6 *J. nigra*, 3 *F. excelsior*, 1 *J. regia* | 59 | 23.1±0.8 | 26.7±1.2 | Ib | new hornbeam-oak wood | 0.8 | 318.2 |
| 108 | 4 *J. nigra*, 4 *J. mandschurica*, 1 *J. regia*, 1 *Betula pendula* Roth. | 34 | 11.6±0.3 | 18.6±1.4 | III | new hornbeam-oak wood | 0.7 | 96.8 |
| **Potash forestry** | | | | | | | | |
| 135 | 5 *Quercus robur* L., 1 *Carpinus betulus* L., 1 *J. nigra*, 1 *Robinia pseudoacacia* L., 2 *Tilia cordata* Mill. | 62 | 22.7±0.7 | 24.2±1.3 | Ia | new hornbeam-oak wood | 0.7 | 220.7 |
| **Moivske forestry** | | | | | | | | |
| 75 | 5 *Q. robur* 2 *F. excelsior*, 1 *T. cordata*, 1 *J. nigra*, 1 *Acer campestre* L. + *C. betulus* + *F. excelsior* | 87 | 22.5±0.5 | 48.5±0.6 | I | new hornbeam-oak wood | 0.7 | 324.5 |

**Table 9.** The degree of acclimatization of *Juglans* species under environmental conditions of the Right-Bank Forest-Steppe of Ukraine (by Kokhno & Kurdiuk 1994).

| Species | Indicators of | | | | Acclimatization value (point) | Acclimatization degree |
|---|---|---|---|---|---|---|
| | growth | generative development | frost-resistance | drought-resistance | | |
| ***J. nigra*** | 10 | 25 | 50 | 15 | 100 | complete |
| ***J. cinerea*** | 10 | 25 | 50 | 15 | 100 | complete |
| ***J. rupestris*** | 8 | 25 | 40 | 15 | 88 | good |
| ***J. major*** | 8 | 25 | 40 | 15 | 88 | good |
| ***J. californica*** | 8 | 25 | 30 | 15 | 78 | satisfactory |
| ***J. hindsii*** | 8 | 25 | 30 | 15 | 78 | satisfactory |

In the forests of the "Uman Forestry" state enterprise forest crops of *J. nigra* were presented in the new oak-hornbeam forests on grey and dark-grey forest soils and loamy chernozem. The oldest plantations of *J. nigra* were investigated in Yurkivka forestry. The age of these plantations was 65 years. The height of *J. nigra* varied from 10.6 to 17.4 m, the diameter of the trunk was in the range of 17.4 to 21.0 cm. The closure of the planting crowns was in the range of 0.6-0.8.

The oldest forest crops in Synytsia forestry in the Pankivske natural landmark were of 59-65 years of age (Fig. 10). These plantations belonged to the forests of I group performing protective functions. Usually, *J. nigra* was planted in a mixture with *J. regia*. The height of *J. nigra* here varied from 21.5 to 23.1 m, and the diameter from 26.7 to 28.3 cm. From the point of view of the recreational evaluation, they were forest crops. The age of the oldest crops in Potash forestry was 62 years. The height of *J. nigra* was 22.7 m and its diameter was 24.2 cm. *Juglans nigra* regularly bore fruit in these plantations, although freezing of branches was observed in some frosty years. In the last 5-8 years, a number of new mixed forest crops were created with the participation of *J. nigra* in Monastyryshche and Mankivka forestries. These plantations appeared to be open forest crops of 1-8 years ages (Fig. 11).

Studies on the complete acclimatization of North American *Juglans* species in the the Right-Bank Forest-Steppe of Ukraine are shown in Table 9.

In view of this, the degree of acclimatization of the North American *Juglans* species confirmed our hypothesis on the prospect of *J. nigra* and *J. cinerea* in green building and forest plantations. The remaining North American species *J. rupestris*, *J. major*, *J. californica* and *J. hindsii* require further experimental research in Ukraine.

**Fig. 10.** Forest crops of *J. nigra* in Synytsia forestry.

**Fig. 11.** Forest crops of *J. nigra* in Monastyryshche and Mankivka forestries.

## Discussion

*Juglans nigra* and *J. cinerea* were introduced to Ukraine in the early 19th century, underwent a long period of acclimatization and were widely presented in the dendrological collections, forest crops and street plantations of all natural-and-climatic zones of the country. *Juglans rupestris*, *J. major*, *J. californica*, and *J. hindsii* were introduced to Ukraine in the 1930s of the previous century, but they were rarely found in the dendrological collections in Eastern, Central and Southern Ukraine. Due to their low distribution and spatial isolation, these species do not interbreed and do not need protection, as *J. hindsii* in natural habitats in North America (Potter *et al.* 2018).

The introduction area (Right-Bank Forest-Steppe of Ukraine) has a certain similarity to the climate of the eastern regions of North America in terms of precipitation (Ishchuk 2009, Buzovkyn 1960, Vitvicki 1953), although there is a significant difference in absolute values. In these areas, most of the precipitation falls during the warm season. Temperatures also have some similarities, although they differ significantly by the indicator of average annual temperature, average minimum and maximum temperatures of the introduction area. All areas are characterized by the presence of some period with an average daily minimum of temperatures below 0°C.

The climatic conditions of the introduction area were favorable for the introduction of all North American species of the *Juglans* genus, although the Right-Bank Forest-Steppe differed from the natural conditions of North America in terms of temperature, light and moisture. The conditions of heat and moisture supply, which affected plants not only directly but also by physical and chemical and microbiological processes occurring in the soil were the most important among the set of climatic factors that determined the success of plant introduction (Ishchuk & Ishchuk 2019).

The small development cycle of *Juglans* species was directly dependent on the sum of active and effective temperatures. The cycle of development of North

American species is shifted towards the summer-autumn period under environmental conditions of the Right-Bank Forest-Steppe of Ukraine. Vegetation of the species began in the period from April 1-20 with swelling of the generative buds. They were characterized by annual, abundant flowering, which began in the I-II decades of May for *J. cinerea*, and in the II-III decades of May for *J. nigra, J. rupestris, J. californica, J. major*, and *J. hindsii* and lasted for 9-17 days depending on the amount of active temperatures. Based on a meta-analysis by Gill *et al.* (2015), we concluded that the phase of autumn leaf coloration was significantly stayed at 25-49° of north latitude. Moreover, Uman city, where we conducted stationary research, is located at 48°45′44″ of north latitude where plants are more sensitive to temperature. In more northern latitudes, the photoperiod affects leaf senescence. The lack of constant connections between air temperature and time of leaf senescence suggests that various factors may influence autumn leaf senescence. The date of the first autumn frosts is variable in temperate and boreal ecosystems and does not always correspond to the linear cooling tendency. Our observations also confirm this fact.

Shoot growth began after buds breaking in late April-early May, and ended in July-August and trees were characterized by good growth of 0.5-0.6 m per year under sufficient moisture. The maximum increase was observed in May-June. The increase in one-year-old plants in height and diameter of the root collar under autumn sowing is twice as large as under spring sowing, which is also proved by experimental data obtained by Zaharova (2016) under environmental conditions of Nizhny Novgorod region of Russia. Growth increased almost twice in two-year seedlings. However, growth in all types of seedlings decreased when the roots were pruned. Our results showed that two-year seedlings of *J. nigra* and *J. cinerea* had the most powerful root system. *Juglans rupestris, J. californica* and *J. hindsii* had a much shorter length of the root system; these species were characterized by weaker growth, the root system was less branched and located in the surface layers of the soil. The biological needs of *J. nigra, J. cinerea, J. rupestris, J. major, J. californica, J. hindsii* were fully met by the natural conditions of the Right-Bank Forest-Steppe of Ukraine during the vegetation period and thermal regime.

Enduring by the North American walnut species, especially *J. rupestris, J. californica, J. major* and *J. hindsii* of some period with an average daily minimum of temperatures below zero without damage under environmental conditions indicates their rather wide biological potential for frost resistance, which was formed during the evolution of species, and the possibility of successful introduction in the context of climate change in Ukraine. A decrease in frost-resistance of tissues in a row: bark-cambium-wood-core in the model experiments with artificial freezing of shoots at temperatures of -25, -30 and -35°C (Ishchuk 2010) and the quantitative microscopic analysis of the level of low-temperature damages was found. This meant that the survival of shoots after overwintering would depend on the ability of cells of the bark and cambium parenchyma to restore physiological processes and form new tissues with the beginning of the favorable temperature conditions of the vegetation period. According to Moroz & Kosenko (2006) and Uman Meteorological Station (https://meteopost.com/weather/climate/), the maximum negative air temperature for the last 50 years in Uman city in January was -32.2°C. Therefore, the North American species of the *Juglans* genus are characterized by a medium degree of freezing.

Studied species needed special care, which should include measures for pruning, enhanced nutrition and watering. They also needed light fertile chernozem or gray forest soils, but they grew satisfactorily on other soil differences under conditions of watering and fertilizing. All the species are light demanding, but they could withstand shading at a young age. In addition, they were resistant to air pollution by carbon, nitrogen, lead compounds, had phytoncidal and antimicrobial properties and deserved widespread introduction into recreational plantations (Ishchuk 2015).

All North American *Juglans* species of the in the crop under environmental conditions of the region included in our study are well propagated by seed. Seed is best sown with endocarp in autumn or spring providing stratification. The optimal stratification time for *J. rupestris, J. major* is 160 days, *J. nigra, J. cinerea* - 120 days and J *californica, J. hindsii* - 100 days in moist sand at a temperature of 1-3°C. In contrast, researchers in the USA consider vermiculite to be better substrate for stratification of *J. nigra* and *J. cinerea* (Cobb *et al.* 2020). The optimal depth of seeding-down of *J. rupestris* seeds is 5-6 cm., and *J. nigra* and *J. cinerea* - 7-8 cm, which allows to increase germination by 25-30%. Our multi-year researches coincide with the data of American researchers (Brauer *et al.* 2010), who consider the best practice of growing high-quality planting material of the North American walnuts by sowing seeds in containers. Our studies showed that the highest germination of seedlings under autumn sowing at a depth of seeding-down was 6-8 cm in *J. nigra* and 6-7 cm in *J. cinerea* which almost coincides with similar investigations made by Zaharova (2016) under environmental conditions of Nizhny Novgorod region of Russia. At the same time, the germination of stratified seed under environmental conditions of dry oak-forest in the south-east of Ukraine was 61-64% (Aboimova & Polyakov 2012), which can be explained by drier soil-and-climatic conditions compared to the Right-Bank Forest-Steppe of Ukraine. In our opinion, the low abundance of seedlings and poor growth of *J. nigra* and *J. cinerea* on site condition of Uman city could be explained by the lack of moisture in the recent drought years in the surface layers of very dense soil and litter for young nut roots, which led to their massive fall from planting. Only a few seedlings survived until the following year.

In recent decades, *J. nigra* was increasingly introduced into both pure and mixed forest crops in the conditions of the Right-Bank Forest-Steppe of Ukraine, in particular, in Vinnytsia and Cherkasy regions. This, in turn, required the expansion of the seed base and the creation of its nurseries in the seed-plots. However, the technology of growing of *J. nigra* planting material in various forestries had its differences. Their sowing in Monastyryshche forestry in Cherkasy region was practiced immediately to a permanent place in the forest due to the fact that walnuts had a tap-root system and bore replanting badly under environmental conditions of the Right-Bank Forest-Steppe. Therefore, nut seedlings were not grown in the seed-plots. There was somewhat different technology of material growing planting in Moivske forestry in Vinnytsia region.

Introduced *J. nigra* in pure and mixed forest crops of Vinnytsia (Ishchuk & Shlapak 2007) and Cherkasy regions grows in different age plantations. Pure *J. nigra* plantations of 159.4 ha (21%) are dominated by the share in the plantation composition on the territory of the Right-Bank Forest-Steppe of Ukraine. Among *J. nigra* plantations, the largest area is occupied by young plants (536.2 ha, 70.7%) and middle-age plantations (196.1 ha, 25.9%). The largest total stock of wood in forest stands of this species (21 thousand $m^3$) is concentrated in middle-age plantations. *Juglans nigra* plantations grown by the first and highest classes of bonitet cover the area of 433.1 ha which is more than half of the area (57%) of their distribution. The division by the type of forest vegetation conditions and by area showed that 72% of black walnut plantations grow under environment conditions of young oak-forest by the I class of bonitet (Filonenko 2017).

Our investigations showed that *J. nigra* is highly competitive with aboriginal forest species (*Quercus robur*, *Fraxinus excelsior*, *Acer campestre*, *Tilia cordata*, *Carpinus betulus*) in terms of forestry-and-taxonomic indicators and has good growth, high quality wood and high seed productivity. The growth of *J. nigra* under conditions of plantation cultivation at the age of 10 in mixed forest crops is higher than in pure single-breed plantations of this species under environmental conditions of the south-east of Ukraine (Aboimova & Polyakov 2012).

We also recommend using *J. nigra* and *J. cinerea* for planting tree belt areas on agricultural lands in the Right-Bank Forest-Steppe of Ukraine. This view is also supported by Gauthier & Jacobs (2010), who studied the effects of lighting and thinning of plantations, and American researchers and Wolz & DeLucia (2019), who propose to plant alley cropping of *J. nigra* on soybean and corn plantations in Midwest of the USA in order to increase productivity of the farm lands.

Complete (A = 100) acclimatization of *J. nigra* and *J. cinerea* was confirmed, good (A = 80) acclimatization of *J. rupestris* and *J. major* and satisfactory (A = 60) acclimatization of *J. californica* and *J. hindsii* in the conditions of the Right-Bank Forest-Steppe of Ukraine was defined by the studies. *Juglans nigra* and *J. cinerea* successfully adapted to the natural conditions of the Right-Bank Forest-Steppe of Ukraine and reached the highest degree of acclimatization - naturalization. Evidence of this fact was their ability to successfully regenerate by natural seed way. The natural regeneration of *J. nigra* and *J. cinerea* was confined to well-lit and moist areas with the presence of the scalping of the upper mineral horizon of the soil.

Obtained results of the success of the introduction concerning *J. nigra* completely coincide with the results of the research of Nicolescu *et al.* (2020), who studied the process of introduction and adaptation of this species into forest plantations in Europe.

**Conclusion**

Biological needs of *J. nigra, J. cinerea, J. rupestris, J. major, J. californica,* and *J. hindsii* were completely satisfied with the natural conditions of the Right-Bank Forest-Steppe of Ukraine during the vegetation period and thermal regime.

Bioecological evaluation of the species of the *Juglans* genus suggested that the studied species, except *J. cinerea*, had a shift of vegetation towards the summer-autumn period. *Juglans cinerea* needed the smallest sum of effective temperatures for growth and development - 28.9 and 72.3°C, respectively, and *J. rupestris* - 34.1 and 66.8°C, the largest sum was required by *J. hindsii* - 51.7 and 90.5 and by *J. nigra* - 50.6 and 105.0°C. Vegetation duration was 183-208 days under the sum of active temperatures of above + 10°C of 2367.8-3050.0°C.

North American nuts in the region of introduction are able to withstand temperatures down to -25°C. Thus, the highest index of frost damage was recorded in *J. rupestris* (57.5) for the bark and cambium of the upper part of the shoots when freezing at t = -25°C during the period of forced dormancy. This indicator was much lower (from 30.0 to 48.5) in all species of *Juglans* in all tissues of the shoot middle at t = -25°C. Buds had a very high level of damage in all cases of freezing.

Forest crops of *J. nigra* could be established both by pure plantings, and in combination with deciduous local forest species. Higher growth rate than the main forest-forming species in terms of the main taxonomic indicators in the young growth phase, and much lower - in the following age groups was characteristics for the introducer.

All North American species of the *Juglans* genus are promising for use in the plantations of the Right Bank Forest-Steppe of Ukraine, as evidenced by the complete acclimatization of *J. nigra* and *J. cinerea*, good acclimatization of *J. rupestris* and *J. major* and satisfactory acclimatization of *J. californica* and *J. hindsii*. These species were suitable for introduction not only into forest plantations, but also into

phytomelioration, garden and park construction of the Right-Bank Forest-Steppe of Ukraine due to high ecological resistance to unfavorable climatic conditions and high decorativeness of both plantations and individual trees.

**Ethics Committee Approval:** Since the article does not contain any studies with human or animal subject, its approval to the ethics committee was not required.

**Author Contributions:** Concept: H.I., Desing: O.B., Execution: H.I., Material Supplying: L.I., Data acquisition: H.I., L.I., O.B. S.K., Data analysis/interpretation: H.I., L.I., Writing: H.I., L.I., Critical Review: V.S.

**Conflict of Interest:** The authors have no conflicts of interest to declare.

**Funding:** The authors declared that this study has received no financial support.

## References


1. Aboimova, A.N. & Polyakov, A.K. 2012. Growth and development of *Juglans nigra* L. in the south-east of Ukraine. *Industrial botany*, 12: 283-286.
2. Antoniuk, N.E. 1968. *Introduction of black nut (Juglans nigra L.) in the Right-Bank Forest-Steppe of the Ukrainian SSR.* Kiev, 27 pp.
3. Anuchin, N.P. 1982. *Forest taxation*. Timber industry. Moscow, 552 pp.
4. Badalov, P.P. 1971. Introduction of nuts of the genus *Juglans* at the Veselobokovenskaya selection and dendrological station Lesovodstvo i agrolesomelioratsiya. *Introduktsiya novykh porod i lesnyye kultury*, 5: 47-52.
5. Barbarich, A.I. & Horhota, A.Y. 1952. *Landscaping of populated areas* – Kiev: Publishing house of the Academy of Architecture of the Ukrainian SSR. 742 pp.
6. Brauer D.K., Brauer D.E., Ares A., Thomas A.L., Burner D. & Idassi, J. 2010. Effects of Seedling Type on the Establishment, Growth and Precocity of Eastern Black nuts (*Juglans nigra* L.) for Nut Production. *The Open Forest Science Journal*, 3: 1-8.
7. Bondar, A.O. 1997. *Forest crops of black nut*. Vinobldrukarnya, Vinnitsya, 48 pp.
8. Buchinskij, I.E. 1960. *Climate of Ukrainy*. Leningrad: Gosmeteoizdat. 256 pp.
9. Buzovkyn, B.A., 1960. *Climate of the United States*. Leningrad: Gidrometeoizdat. 103 pp.
10. Chirkov, Y.I. 1986. *Agrometeorology*. Gidrometeoizdat, Leningrad, 296 p.
11. Cobb, M., Woods, M.J. and McEwan, R.W. 2020. Assessing Seed Handling Processes to Facilitate a Community-Engaged Approach to Regional Forest Restoration. *Forests*, 11(4), 474. DOI:10.3390/f11040474
12. De Candolle, A. 1857. *Introduction. A. l`etude Dela Botanique. Traiteelementaire*. Cans&Compadnie, Bruselles Meline, 334 pp.
13. Dode, L.A. 1909. Contribution a l`etude du genre *Juglans*. *Bulletin de la Société dendrologique de France Bull. Soc. Dendrol. France*. 2: 22-50.
14. Dubrovsky, V.I. & Shved M.V. 2019. Introduction of black nut *(Juglans nigra* L.) in Ukraine and its economic and biological significance. *Gardening*, 74: 100-105.
15. Engler, A. & Prantl, K. 1894. Die naturlichen Pflanzenfamilitn, 1, Teil 3, Halfte 1. *Juglandaceae.* Ver. W. Engelmann, Leipzig. P.19-25.
16. Filonenko, V.V. 2017. General characteristics of black nut (*Juglans nigra* L.), which grows in the Right-Bank Forest-Steppe of Ukraine. Scientific Bulletin of the National University of Life and Environmental Sciences of Ukraine. *Series "Forestry and ornamental horticulture"*, 278: 152-157.
17. Gauthier M.M. & Douglass F.J. 2010. Ecophysiological responses of black nut (*Juglans nigra*) to plantation thinning along a vertical canopy gradient. *Forest Ecology and Management*, 259: 867-874.
18. Gill, A.L., Gallinat, A.S., Sanders-DeMott, R., Rigden, A.J., Short Gianotti, D.J., Mantooth, J.A. & Templer, P.H. 2015. Changes in autumn senescence in northern hemisphere deciduous trees: a meta-analysis of autumn phenology studies. *Annals of Botany*, 116(6): 875-888. DOI: 10.1093/aob/mcv055
19. Hordiienko, M.I. 1979. *Methodological guidelines for the study of forest cultures*. Ukrainian Agricultural Academy. Kiev, 89 pp.
20. Hryshko-Bogmenko, B.K. 1969. *Biological characteristics of species of the genus Juglans L. in the forest-steppe conditions of Ukraine.* Kiev, 255 pp.
21. Ishchuk, H.P. 2007a. History of the introduction of American species of the genus *Juglans* L. *Scientific notes of the Ternopil National Pedagogical University of the name of Volodymyr Hnatyuk. Series: Biology*, 3(33): 145-147.
22. Ishchuk, H.P. 2007b. The current state of North American species of the genus *Juglans* L. in the collections of gardens and parks of Ukraine, Vol. 1, 30-32. Report presented at the International Scientific Conference, June 12-15, Minsk, Belarus.
23. Ishchuk, H.P. 2009. comparative characteristics of climatic conditions of North America and the Right-Bank Forest-Steppe of Ukraine in connection with the introduction of North American species of the genus *Juglans* L. in Ukraine. 41-146. Materials of the international. scientific conference dedicated to the 100th anniversary of the birth of Corresponding Member. USSR Academy of Sciences P.I. Lapin, June 30-July 2, Moscow, Russia.
24. Ishchuk, H.P. 2010. Winter and frost resistance of North American species of the genus *Juglans* L. in the conditions of the Right-Bank Forest-Steppe of Ukraine. *Scientific Bulletin of the National Forestry University of Ukraine*. 20(8): 24-29.
25. Ishchuk, H.P. 2013. History of origin, distribution and phylogenetic relationships of North American species of the genus *Juglans* L. *Scientific Bulletin of the National Forestry University of Ukraine* 23(5): 62-68.

26. Ishchuk, H.P. 2015. Resistance to pollution of North American species of the genus *Juglans* L. 105-108. Proceedings of the international scientific-practical conference, 5-6 November, Zhytomyr, Ukraine ZhNAEU.

27. Ishchuk, L.P. & Ishchuk, H.P. 2019. Comparative characteristics of the climatic conditions of North America and Forest Steppe and Steppe of Ukraine in connection with the introduction of the North American species of *Juglans* L. and *Populus* L. genus. *Journal of Native and Alien Plant Studies*, 15: 34-43.

28. Ishchuk, H.P. & Shlapak, V.P. 2007. Condition of black nut (*Juglans nigra* L.) plantations in Moivsky forestry in Vinnytsia region. *Scientific Bulletin of* Ukrainian National Forestry University, 17(7): 20-26.

29. Ivanenko, B.I. 1962. *Phenology of tree and shrub species*. Publishing house of agricultural literature, Moscow, 184 pp.

30. Kenig, A.E. 1966. *Introduction of species of the genus Juglans L. in the forests of the forest-steppe of the Ukrainian SSR*. Kiev, 20 pp.

31. Kokhno, N.A. & Kurdiuk, A.M. 1994. *Theoretical foundations and experience of the introduction of woody plants in Ukraine*. Naukova dumka, Kiev, 188 pp.

32. Lapin, P.I. (Ed.) 1975. *The methodology of phenological observations in the botanical gardens of the USSR*. 1975. Moscow, 27 pp.

33. Linnaei, C. 1759. *Systema Naturae*. HALAE, Volume II, 1272 pp.

34. Manning, W.E. 1978. The Classification Within the *Juglandaceae*. *Annals of the Missouri botanical garden*, 65(4): 1058-1087.

35. Martin, A.C., Zim, H.S. & Nelson, A.L. 1951. *American wildlife and plants: A guide to wildlife food habits*. Dover Publications. New York, 512 pp.

36. Molchanov, A.A. & Smirnov, V.V. 1967. *Technique of studying the growth of woody plants*. Nauka, Moskov, 95 pp.

37. Moroz, P.I. & Kosenko, I.S. 2006. *Nature of the Shevchenko region: Monograph*. Uman: Uman National University of Horticulture, 413 pp.

38. Moseichenko, V.F. 1992. Fundamentals of scientific research in fruit growing, vegetable growing, viticulture and storage technology for fruit and vegetable products. Kiev, 364 pp.

39. Nicolescu, V.-N., Redei, K., Vor T., Bastien, J.-Ch., Brus, R., Bencat, T., Dodan, M., Cvjetkovic,·B., Andrasev, S., La Porta, N., Lavnyy, V., Petkova, K., Peric, S., Bartlett, D., Hernea, C., Pastor, M., Mataruga, M., Podrazsky, V., Sfecla, V., Stefancik, I. 2020. A review of black nut (*Juglans nigra* L.) ecology and management in Europe. Trees, 34: 1087-1112. https://doi.org/10.1007/s00468-020-01988-7

40. Potanin, D.V., Grokholsky, V.V. & Kitaev, O.I. 2005. Determination of frost resistance of fruit species by the laboratory method of direct freezing. *Garden*, 56: 170-180.

41. Potter, D., Bartosh, D., Dangl, G., Yang, J., Bittman, R. & Preece, J. 2018. "Clarifying the Conservation Status of Northern California Black nut (*Juglans hindsii*) Using Microsatellite Markers," *Madrono* 65 (3), 131-140, (1 July 2018). https://doi.org/10.3120/0024-9637- 65.3.131

42. Shchepotiev, F.L. 1985 *Walnut forest and horticultural crops*. Agropromizdat, Moscow 224 pp.

43. Shvydenko, A.I. & Tsygankov, P.A. 1978. *Black nut culture*. Vyscha school, Lviv, 92 pp.

44. Sokolov, S.Y. 1957. *The current state of the theory of plant acclimatization and introduction*. Plant introduction and green building. Moscow-Leningrad. 5 pp.

45. Soloviova, M.A. 1982. *Methods for determining the winter hardiness of fruit crops*. Gidrometeoizdat, Leningrad, 36 pp.

46. Takhtadjian, A.L. 1980. *Juglandaceae* P. 329–342. In A.L. Takhtadzhyan Plant life. Vol. 5.1. Flowering plants. Moscow, 430 pp.

47. The Angiosperm Phylogeny Group. 2016. An update of the Angiosperm Phylogeny Group classification for the orders and families of flowering plants: APG IV. *Botanical Journal of the Linnean Society*, 181(1): 1-20. DOI:10.1111/boj.12385

48. Tsitsin, N.V. (Ed.) 1980. *Methodical instructions for seed science of introduced species*. Science, Moscow, 64 pp.

49. Vitvicki, G.N. 1953. *Climates of North America*: Geografgiz, 287 pp.

50. Wolz, K.J. & DeLucia, E.H. 2019. Black walnut alley cropping is economically competitive with row crops in the Midwest USA. *Ecological Applications*, 29(1): e01829. https://doi.org/10.1002/eap.1829

51. Zaharova, E.I. 2016. Comparative analysis of immature plants of the genus *Juglans* L., grown in the Nizhny Novgorod region. *International Research Journal*, 3(45): 17-19.

52. Zhukovsky, P.M. 1971. *Cultivated plants and their relatives*. Kolos, Lviv, 751 pp.

53. Zhyhalova, S.L. 2007. Genus *Juglans* L. (*Juglandaceae*) in Ukraine (Morphological-biological and geographical features, systematic position and economic significance): dissertation author's abstract for the degree of candidate of biological sciences: specialty: 03.05.00 Botany. Kiev, 21 pp.

*http://dergipark.org.tr/trkjnat*
*Trakya University Journal of Natural Sciences, 22(1): 93-100, 2021*
*ISSN 2147-0294, e-ISSN 2528-9691*
*DOI: 10.23902/trkjnat.863506*

**Research Article**

# MOLECULAR IDENTIFICATION OF *Diplodia seriata* De Not. CAUSING DIEBACK EFFECT ON GRAPEVINES AND EVALUATION OF *in vitro* EFFICACY OF FIVE DIFFERENT SYNTHETIC FUNGICIDES AGAINST THIS DISEASE

Nurdan GÜNGÖR SAVAŞ*, Murat YILDIZ

Manisa Viticulture Research Institute, Plant Protection Department, 45125 Yunusemre, Manisa, TURKEY

**Cite this article as:**

Güngör Savaş N. & Yıldız M. 2021. Molecular identification of *Diplodia seriata* De Not. causing dieback effect on grapevines and evaluation of *in vitro* efficacy of five different synthetic fungicides against this disease. *Trakya Univ J Nat Sci*, 22(1): 93-100, DOI: 10.23902/trkjnat.863506

Received: 18 January 2021, Accepted: 13 April 2021, Published: 15 April 2021

**Abstract:** The aim of this study was to realize the molecular identification of *Diplodia seriata* De Not., a member of the Botryosphaericea family, isolated from 2-10 years old vines in vineyards showing symptoms of dieback disease. The susceptibility of the pathogen against the fungicides with the fosetyl-Al+triadimenol, azoxystorbin+difecanozole, fludioxanil+cyprodinil, metrafenone, fluopyram+tebuconazole combinations were evaluated. The isolates obtained from the root and crown parts of the vine samples were identified as *D. seriata* according to the morphological and molecular methods. In molecular identification, the ITS (Internal Transcribed Spacer) and TUB2 (β-tubulin) gene regions of the isolates were amplified by Real-Time PCR and the nucleotide sequences were obtained in these gene regions. After using the MEGA 7 software, ITS and TUB2 sequences were aligned and a combined phylogenetic tree was made. It has been molecularly confirmed that the *D. seriata* isolate has a 100% similarity index with *Diplodia* species according to the phylogenetic analyses. The mean effective concentration ($EC_{50}$) values of fungicides used with different concentrations (0, 1, 3, 10, 30, 50, 100 µL mL-1) were determined by Probit analysis. Cyprodinil + fludioxonil showed the highest efficacy (100%) at a concentration of 1 µL $mL^{-1}$. According to $EC_{50}$ values, cyprodinil + fludioxonil (0.001 µL $mL^{-1}$) was recorded as the most effective fungicide followed by fluopyram + tebuconazole (0.520 µL $mL^{-1}$) and, azoxystrobin + difenoconazole (2.958 µL $mL^{-1}$), respectively.

**Özet:** Bu çalışmanın amacı, geriye doğru ölüm hastalığı belirtileri gösteren bağlardaki 2-10 yaşındaki asmalardan izole edilen Botryosphaericea ailesinin bir üyesi olan *Diplodia seriata* De Not.'nın, moleküler tanılamasını gerçekleştirmektir. Patojenin duyarlılığı, fosetil-Al+triadimenol, azoxystorbin+difecanozole, fludioxanil+cyprodinil, metrafenon, fluopyram+tebuconazole dâhil olmak üzere çeşitli fungisitlere karşı değerlendirilmiştir. Üreticiler tarafından getirilen asma örneklerinin kök ve kök boğazı kısımlarından elde edilen izolatlar, morfolojik ve moleküler yöntemlere göre *D. seriata* olarak tanımlanmıştır. Moleküler tanımlamada izolatların ITS (Internal Transcribed Spacer) ve TUB2 (β-tubulin) gen bölgeleri Real-Time PCR ile çoğaltılmış ve bu gen bölgelerinden nükleotid dizileri elde edilmiştir. Daha sonra MEGA 7 yazılımı kullanılarak ITS ve TUB2 dizileri hizalanmış ve kombine bir filogenetik ağaç çizilmiştir. *Diplodia seriata* izolatının filogenetik analizlere göre *Diplodia* türleri ile % 100 benzerlik indeksine sahip olduğu moleküler olarak doğrulanmıştır. Farklı konsantrasyonlarda (0, 1, 3, 10, 30, 50, 100 µL $mL^{-1}$) kullanılan fungisitlerin ortalama etkili konsantrasyon ($EC_{50}$) değerleri Probit analiziyle belirlenmiştir. Cyprodinil+fludioxonil 1 µL $mL^{-1}$ konsantrasyonunda en yüksek etkinliği (%100) göstermiştir. $EC_{50}$ değerlerine göre cyprodinil+fludioxonil (0.001 µL $mL^{-1}$) en etkili fungisit olarak kaydedilmiş, ardından fluopyram+tebuconazole (0.520 µL $mL^{-1}$) ve azoxystrobin+difenokonazol (2.958 µL $mL^{-1}$) izlemiştir.

***Edited by:***
*Mehmet Bora Kaydan*

***Corresponding Author:***
*Nurdan Güngör Savaş*
*nurdangngrsvs10@gmail.com*

***ORCID iDs of the authors:***
*NGS. orcid.org/0000-0002-3450-4747*
*MY. orcid.org/0000-0002-0758-0429*

***Key words:***
*Botryosphaeriaceae*
*Dieback*
*Diplodia seriata*
*Vitis vinifera L.*

## Introduction

Turkey is one of the countries including the most geographically favorable areas for viticulture. According to FAO 2019 statistics, Turkey has the 6th largest land area devoted to vineyards with 470,000 hectares and is the 5th largest grape producer in the world with 4.1 million tons per year (FAO 2019). In the country, the Aegean region ranks first in terms of both area (1,392,082 da) and production (1,952,356 tons per year) and the Manisa

province ranks first in Aegean region with 809,123 da and 1,372,571 tons per year (Anonymous 2019). More than 30% of the country's production is provided by this region. Manisa province supplies 90% of Turkey's dried grape production and is the leader in Sultani seedless grape production used for export (Anonymous 2019).

Botryosphaeria dieback, caused by members of the fungi family Botryosphaeriaceae, is an important disease in vines seen all over the world and in Turkey. Members of Botryosphaeriaceae in the Dothideomycetes class are found largely as endophytes, parasites, and saprophytes in both annual and perennial plants under different ecological conditions in many regions of the world (Slippers & Wingfield 2007). The importance of these disease agents in vines was understood after it was first reported as a pathogen in the 2000s (Phillips 2002). The Eutypa dieback disease caused by *Eutypa lata* (Pers.) Tul. & C. Tul. has been thought to be responsible for cancers and deaths seen on vines in Australia for many years (Highet & Wicks 1998, Pascoe & Cottral 2000, Castillo-Pando *et al*. 2001, Siebert 2001). In Turkey, dieback, symptoms on vine leaves, and the development of brown color in wood tissue, which the shape of a “V”, have been associated with Esca or Eutypa dieback disease as in Australia.

Identification of *Botryosphaeria* Ces. & De. Not. diseases is problematic because symptoms occurring on vines in the field are very similar to other diseases such as Phomopsis dead arm disease caused by *Phomopsis viticola* (Sacc.) and Eutypa dieback caused by *Eutypa lata* (Castillo-Pando *et al*. 2001). Species of *Botryosphaeria* Ces. & De. Not., *Diplodia* Fr., *Lasiodiplodia* Ellis & Everh., *Neofusicoccum* Slippers & A.J.L. Phillips in the family Botryosphaeriaceae have been isolated and described for the first time from vines showing dieback symptoms (Akgül *et al*. 2014). *Diplodia seriata* De Not. and *Neofusicoccum luteum* (Pennycook & Samuels 1985) Crous, Slippers & A.J.L. Phillips 2006 were often isolated from stems, branches and shoots that show symptoms during surveys conducted in vineyards in the sub-tropical region of eastern Australia (Savocchia *et al*. 2007).

Members of the genera *Diplodia* and *Botryosphaeria* have often been isolated from the root and crown parts of vine samples delivered to Manisa viticulture research institute plant health laboratory by producers in Aegean region. It has been reported that varieties of *Vitis vinifera* L. are generally more susceptible to disease (Larignon *et al*. 2001). *Diplodia* and *Botryosphaeria* species shorten the life of the vineyards, allow late awakening of the vines, lead to the formation of yellow dots on the leaves followed by necrotic spots with zebra pattern, killing of the shoots and the stem and eventually drying the vine backward, which are defined as important signs of the disease (Gramaje *et al*. 2018, Kühn *et al*. 2017). In addition to the *Botryosphaeria* species, fungi from the fungal families *Botryosphaeria* species, as well as fungi from *Phaeoacremonium* W. Gams, Crous, M. J. Wingf. & Mugnai, *Phaeomoniella* Crous & W. Gams, and *Phomopsis* Sacc. & Roum were generally isolated the necrotic wood tissues showing symptoms of the disease. *Botryosphaeria* colonies are similar to *Alternaria* Nees colonies and are not noticed during the diagnostic phase based on colony development (Pitt *et al*. 2010, Úrbez-Torres 2011). The asexual spores of *Diplodia* spp. with spores of anamorphic of *Botryosphaeria* species are very similar, and a classification based only on the sexual situation is not suitable, especially since it is known that some species have only the asexual structures, and in some species, sexual development is extremely rare. Given these conditions, it has been determined that there are too many features in Botryosphaeriaceae that make it difficult to classify species (Slippers *et al*. 2013). For this reason, molecular diagnostics and even phylogenetic analysis are recommended. Ozben (2011) pointed to the presence of *Botryosphaeria obtusa* (Schwein.) Shoemaker and *B. rhodina* (Pat.) Griffon & Maubl. in the vineyard areas of Ankara, but the presence of these species has not been approved molecularly and phylogenetically. In a study conducted in the Aegean region, Akgül *et al*. (2015) morphologically and molecularly identified the presence of *B. dothidea* and *D. seriata* in Sultani seedless vineyards, but phylogenetic analyses were not performed. Between 2015 and 2018, 22 Botryosphaeriaceae cultures were isolated from the vineyard areas in the Mediterranean and Southern Anatolia regions and they were phylogenetically separated (Akgül *et al*. 2020). It is very difficult to combat wood trunk diseases contained in wood tissue, and the applications for accurate diagnostics and combating are extremely important. Therefore, the present study was performed in order to evaluate the molecular characterization of *Diplodia seriata* isolated from the vineyards in Aegean Region and its sensitivity against five different fungicides.

## Materials and Methods

### *Isolation of the Disease Pathogen*

Sultani seedless vines (N=23 samples) showing dieback disease symptoms were obtained from growers in 2019 and 2020 from the vineyard areas in Manisa and Denizli province in Aegean Region. In addition to the symptoms the samples (including root regions) were those which dried in the vineyards. The information about the rootstock of the vines and the area where the vineyards were located were noted for those where *D. seriate* could have been isolated (Table 1). Preliminary examinations of the root, crown, and trunks revealed thick-fine lines in the wood tissue or brown necrosis spread over a wider area in the form of "V". 23 symptomatic samples from roots and cordons were cut, surface disinfection was performed by dipping into 1% (v/v) sodium hypochlorite for 2 min, and small pieces from the edge of necrotic and healthy tissues were removed and plated on potato dextrose agar (PDA) (Darmstadt, Germany). Petri dishes containing PDA were incubated for 4-5 days in the dark at 25°C, and micelle structures taken from fungal colonies that developed around tissues were purified by transferring them to new Petri dishes containing PDA according to colony properties and morphological structures (Phillips *et al*. 2007).

**Table 1.** Provincial, county-village, and rootstock information of Sultani seedless vine samples showing signs of dieback.

| Sample No | Isolate code | Province | County-village | Vine rootstock | Age of the vines in years |
|---|---|---|---|---|---|
| **1** | *MBAE234N | Manisa | Yunusemre-Horozköy | 5BB | 9 |
| **2** | MBAE244N | Manisa | Yunusemre-Muradiye | 1103Paulsen | 6 |
| **3** | MBAE275N | Manisa | Yunusemre-Evrenos | 110R | 3 |
| **4** | MBAE288N | Manisa | Yunusemre-Horozköy | 1103Paulsen | 5 |
| **5** | MBAE312N | Manisa | Yunusemre-Horozköy | 1103Paulsen | 4 |
| **6** | MBAE313N | Manisa | Akhisar-Sazoba | SO4 | 10 |
| **7** | MBAE336N | Manisa | Şehzadeler-Hacıhaliller | 1103Paulsen | 4 |
| **8** | MBAE344N | Manisa | Gölmarmara-Kayaaltı | 1103Paulsen | 2 |
| **9** | MBAE358N | Manisa | Saruhanlı-Nuriye | 5BB | 7 |
| **10** | MBAE359MN | Denizli | Çal | 5BB | 3 |
| **11** | MBAE368MN | Denizli | Buldan-Yenicekent | 110R | 6 |

* Naming MBAE is an abbreviation for the research institute where isolates were isolated. Number is the sequence number in the cultural collection. N/NM next to the number is the name abbreviation of the person/persons isolating it.

The mycelial discs from pure cultures were then transferred to Eppendorf tubes containing sterile 30% glycerol and stored at -80°C.

*Molecular diagnosis of Diplodia seriata and phylogenetic analysis*

Molecular diagnosis and phylogenetic analyses were carried out by selecting two isolates (MBAE359NM, MBAE368NM) from 11 *D. seriata* isolates obtained purely and very similar to each other from morphological-microscopic aspects. A total of 50 mg fresh mycelial mass was taken from the colonies of these two isolates, and DNA extraction was carried out. The micelle were put into sterile 1.5 mL Eppendorf tubes and crushed with Evolution Homogenizer (Precellys® Evolution, Paris, France), and 550 µL DNA extraction buffer (200 mM Tris-HCl) was added. DNA was obtained according to the proposed method of Cenis (1992) using 250 mM NaCl, 25 mM EDTA and 2% Sodium Dodecyl Sulphate. The concentration and purity of the isolated DNA were determined with a Multiscan GO µ-drop plate (Thermo Scientific, Vantaa, Finland). In PCR studies, the internal transcribed spacers (ITS) rDNA region was amplified with the ITS4 (5′-TCCTCCGCTTATTGATATGC-3′) and ITS5 (5′-GGAAGTAAAAGTCGTAACAAGG-3′) primer pair (White *et al.* 1990), and the β-tubulin (TUB2) gene region was amplified with βt-2a (5′-GGTAACCAAATCGGTGCTGCTTTC-3′) and βt-2b (5′-ACCCTCAGTGTAGTGACCCTTGGC-3′) primer pair (Glass & Donaldson 1995). In real-time PCR reactions, 0.3 µL 20 µM forward primer, 0.3 µL 20 µM reverse primer, 2 µL DNA, and 10 µL 2x FastStart Essential DNA Green Master Mix were added into sterile PCR tubes, and the final volume was completed with DNase/RNase pure water to 20 µL. Real-time PCR (Roche Light Cycler® Nano) amplification conditions included the initial denaturation for 10 min at 95°C, denaturation for 30 s at 95°C, 54°C for annealing temperature of ITS, 58°C for TUB2, and 35 cycles for 1 min. at 72°C. After PCR amplification, melting analysis eliminated non-specific amplifications such as primer dimers and determined whether the replicated area was the target region. Sequence data of the PCR products were obtained by a two-way genome sequencing service from a laboratory that provides Sanger sequence service (by TrioGene firm). Chromatogram files of sequence data were analyzed with ChromasPro 1.7.6 chromatogram analysis software, and consensus sequences were obtained by combining sequence data with forward and reverse sequences. BLASTn analyzes fungal species were performed using the consensus sequences obtained for each gene region in the National Center for Biotechnology Information (NCBI) GenBank database. According to these results, access numbers were obtained from the NCBI GenBank library of diagnosed isolates. For phylogenetic analyses, sequences belonging to an isolate were primarily aligned with Bioedit 7.2.5 sequence alignment software, then similarity ratios of nucleotide sequences were determined by the Clustal W software. The dendrogram of data of nucleotide sequences was created using the Mega 7 software and the Maximum likelihood model (Tamura *et al.* 2011) and confirmation of the obtained phylogenetic tree was made with 1000 repetitions (Bootstrap, p-distance, pairwise deletion). The access numbers of the isolates obtained in this study and the references from the GenBank database in the phylogenetic tree are listed in Table 2.

*Evaluation of susceptibility of Diplodia seriata to fungicides in in-vitro conditions*

To test the effect of fungicides on the development of mycelia in *in vitro* conditions, the fungicides given in Table 3 were used. The MBAE368MN isolate was used for this experimental step. The fungicidal activity of the fungicides was evaluated in the growth culture containing the same concentrations (0, 1.0, 3.0, 10.0, 30.0, 50.0, 100.0 PDA containing µg/mL). Stock solutions of each fungicide were prepared and concentrations from stock solutions were mixed into a sterile PDA medium cooled to 50°C and poured into Petri dishes (Isolab, 90x100 mm). As a control, Petri dishes with a PDA medium free from fungicides were used. Six mm diameter mycelial discs cut from the edges of the fungal colony of the 5-day-old *D. seriata* isolate (MBAE368NM) were placed to the center

**Table 2.** Isolates obtained from the GenBank database and references in the phylogenetic tree.

| Species | Isolate | Host | Origin | GenBank Accession Nos. | |
|---|---|---|---|---|---|
| | | | | ITS | TUB2 |
| *Diplodia seriata* | MBAE359MN* | *V. vinifera* | Turkey | MT880771 | MT914171 |
| *Diplodia seriata* | MBAE368MN* | *V. vinifera* | Turkey | MT880774 | MT914174 |
| *Diplodia seriata* | CBS:114791 | *V. vinifera* | South Africa | KX464107 | KX464833 |
| *Botryosphaeria obtusa* | CBS 112555 | *V. vinifera* | Portugal | AY259094 | DQ458856 |
| *Diplodia seriata* | CBS 113527 | *V. vinifera* | South Africa | KX464106 | KX464832 |
| *Diplodia mutila* | CBS 136014 | *Populus alba* L. | Portugal | KJ361837 | MG015815 |
| *Diplodia mutila* | CBS 431.82 | *V. vinifera* | France | KU198424 | KU198426 |
| *Lasiodiplodia theobromae* (Pat.) Griffon & Maubl. | CBS 111530 | Proteaceae | Netherlands | FJ150695 | KU887531 |
| *Lasiodiplodia theobromae* | CBS 164.96 | Fruit along coral reef coast | Papua New Guinea | NR_111174.1 | EU673110.1 |
| *Neofusicoccum parvum* (Pennycook & Samuels) Crous, Slippers & A.J.L. Phillips | CBS 123652 | *Syzygium cordatum* (Hochst.) | South Africa | KX464184 | KX464996 |
| *Neofusicoccum parvum* | CBS 257.77 | *Cocos nucifera* L. | India | KX464197 | KX465012 |
| *Neofusicoccum luteum* | CBS 562.92 | *Actinidia deliciosa* (A.Chev.) C.F.Liang & A.R.Ferguson | New Zeland | KX464170 | KX464968 |
| *Neofusicoccum luteum* | CBS 612.83 | *Persea Americana* Mill | USA | KX464171 | KX464969 |
| *Tiarosporella tritici* B. Sutton & Marasas | CBS 118719 | *Triticum* sp. | South Africa | KF531830 | KF531810 |

* Isolates registered in GenBank and their accession numbers.

**Table 3.** The active ingredient, formulation, and company information of the fungicides used in determining fungicidal activity in *in vitro* conditions.

| Active ingredient % | Commercial Name | Firm | Formulation Type* |
|---|---|---|---|
| Cyprodinil+Fludioxonil, %37.5+%25 | Switch 62.5 | Syngenta | WG |
| Fluopyram+Tebuconazole, 200 g/L +200 g/L | Luna Experience | Bayer | SC |
| Azoxystrobin+Difenoconazole, 200 g+125 g | Quadris Maxx | Syngenta | SC |
| Folpet+Triadimenol, 700 g/kg+20 g/kg | Shavit F 72 | Adama | WDG |
| Metrafenone, 500 gr/L | Vivando | Basf | SC |

*WG, WDG: Water dispersible granule of formulation type, SC: Water soluble concentrate of formulation type.

of the growth culture containing fungicide concentrations. All inoculated application and control Petri dishes were incubated in darkness at 20°C for 7 days. During this period, the rates of blocking micelle by fungicides (%) were examined by measuring the radial development of fungal micelles (Uysal & Kurt 2019).

In the trials, randomized controlled trials were established so that each Petri dish represented one replication and each concentration has 3 replications. The experiment was repeated at 2 different times.

*Calculations and Statistical Evaluation*

*In vitro* trials were set up to have 3 replications for each application, according to the randomized controlled trial. For establishing antifungal efficacy in petri dishes containing fungicide concentrations, variation analysis was carried out with one-way ANOVA using SPSS Statistics (Version 17.0, SPSS Inc., Chicago, IL, USA) without converting the blocking rates of micelle development in petri dishes ($p \leq 0.05$). Effective concentrations of fungicides that inhibit the development of micelles at 50% level ($EC_{50}$) were determined by Probit analysis with the help of the SPSS statistics using the values obtained in different concentrations for each chemical.

## Results

*Isolation and morphological characteristics of the disease agent*

Eleven *Diplodia seriata* isolates were obtained during the isolation from the root and crown regions of the samples taken from Sultani seedless vine varieties showing signs of dieback in the vineyards in Manisa and Denizli provinces. Wedge-shaped brown lines and necrotic tissues ranging from brown to black color were observed in the root areas of the isolated samples. On the upper part of the vine, yellow spots in the form of dots on the leaves, necrotic spots with zebra pattern, and backward drying on the shoots were found to be remarkable.

Colonies that develop in a PDA medium were initially colorless or light olive green-gray in color but darkened and blacken in time (Fig. 1A and B). The conidia were dark brown in colour and oval, broad at the apex and truncated or rounded at the base, and its wall was rough. Immature spores were without compartment and formed darker brown single-compartment spores as they matured. Forty conidia per isolate were measured by light microscopy (Olympus BX-51 connected with Olympus Camedia-4501X, Hamburg, Germany). The

size of the conidia was measured as 27.4 ± 0.31 x 10.8 ± 0.15 µm, with no significant differences between the isolates, and it was determined to be the same as the characteristics of *D. seriata* (teleomorph: *Botryosphaeria obtusa*) specified in morphological diagnostics made by Phillips *et al*. (2007).

*Molecular diagnosis and phylogenetic analyses*

By using primers specific to ITS (ITS-1 and ITS-4), TUB2 (βt-2a and βt-2b) gene regions, PCR, and DNA sequencing of MBAE359MN and MBAE368MN isolates selected among the fungal isolates resulted in the 580 bp and 434 bp bands, respectively. By comparing the nucleotide sequences with sequences in the NCBI GenBank (BLASTn), the isolates were found to be *D. seriata*. As a result of Blast comparison with species registered in GenBank, they were found to have a 97-100% resemblance to MBAE359MN and MBAE368MN *D. seriata* isolates (for ITS and TUB gene regions, the access numbers are KX464107, KX464833, and KX464106, KX464832, respectively). The nucleotide sequences of *D. seriata* MBAE359MN and MBAE368MN isolates, which were morphologically and molecularly determined, were uploaded to the GenBank database and obtained the access number MT880771 and MT880773 were obtained for the ITS gene and MT914171 and MT914174 for the TUB2 gene. A combined dendrogram was obtained for the ITS and TUB 2 genes with MEGA 7 software using the maximum likelihood method (Fig. 2). According to the dendrogram, MBAE359MN and MBAE368MN isolates were in the same group as *D. seriata* CBS: 114791, CBS 112555, and CBS:113527 isolates. *Tiarosporella tiritici* CBS 118719 was determined as an external group (Fig. 2).

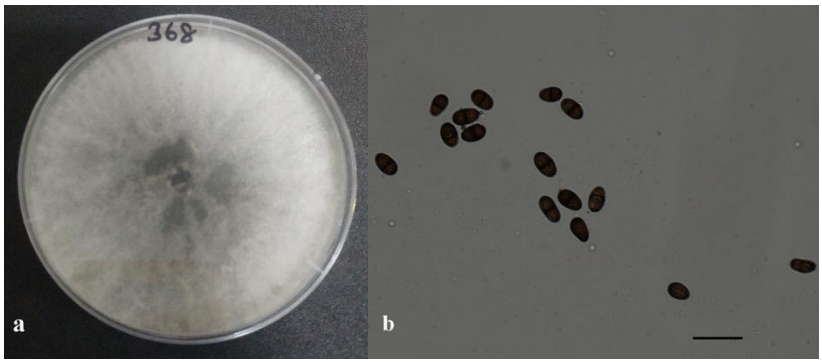


**Fig. 1.** *Diplodia seriata;* **a.** 7-day views of young colonies on PDA, **b.** Conidia, scale 10 µm.

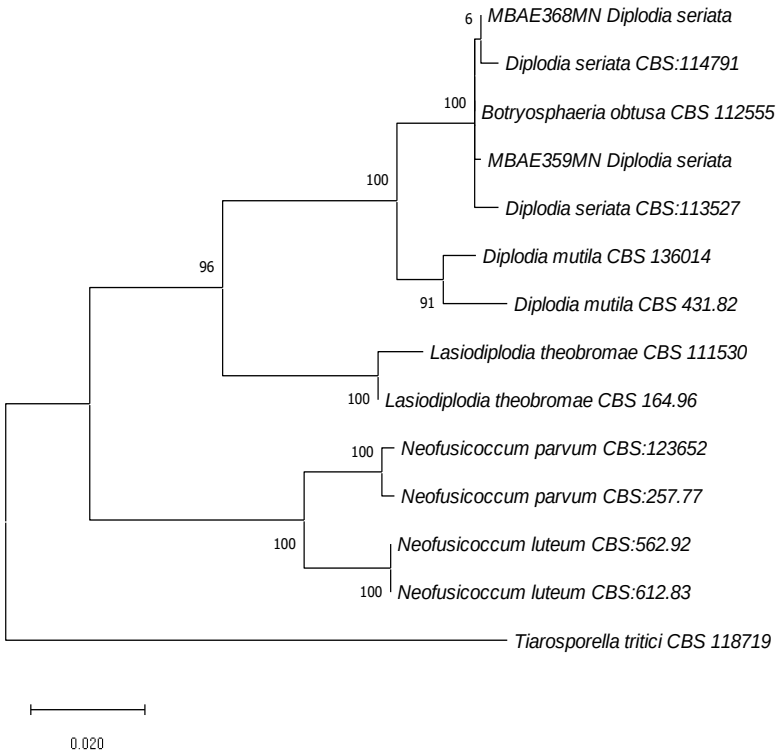


**Fig. 2.** Phylogenetic relationships of some Botryosphaeriaceae species according to the maximum similarity model obtained by the combination of ITS and TUB2 gene regions (Maximum Likelihood). The reliability of the phylogenetic tree was calculated with 1000 replications by the Bootstrap method. Bootstrap values below 50% were not shown. *Tiarosporella tritici* (CBS 118719) is the outside group. The scale bar shows the number of nucleotide changes.

**Table 4.** Antifungal effects of the tested fungicides on *Diplodia seriata* MBAEM368MN isolate as revealed by *in vitro*-micelle growth prevention.

| Active substance | Replication 1 $EC_{50}$ value ** (µg $mL^{-1}$) | Replication 2 $EC_{50}$ value (µg $mL^{-1}$) | Replication 3 $EC_{50}$ value (µg $mL^{-1}$) | Average $EC_{50}$ value (µg $mL^{-1}$)* |
|---|---|---|---|---|
| **Cyprodinil+Fludioxonil,** | 0.001 | 0.001 | 0.001 | 0.001±0.00 a |
| **Fluopyram+Tebuconazole** | 0.453 | 0.434 | 0.673 | 0.520±0.08 a |
| **Azoxystrobin+Difenoconazole** | 2.847 | 2.006 | 4.021 | 2.958±0.58 a |
| **Folpet+Triadimenol** | 4.962 | 5.721 | 7.546 | 6.076±0.76 ab |
| **Metrafenone** | 4.996 | 21.090 | 7.585 | 11.223±4.99 b |

***** Different letters next to the mean $EC_{50}$ (µg/$mL^{-1}$ ± S.E) in the row indicate that the difference between the applications is statistically significant according to the Duncan Multiple Comparison Test ($p<0.05$).
******Effective concentrations ($EC_{50}$) of fungicides that inhibit micelle growth by 50% were estimated by using the values obtained at different concentrations for each fungicide by Probit analysis with the help of SPSS statistical software (Version 17.0, SPSS Inc., Chicago, IL, USA).

*Determination of susceptibility of the disease agent to fungicides in in-vitro conditions*

The effective concentration ($EC_{50}$) values required for fungicides used in the study to prevent micelle development of disease factor *D. seriata* by 50% were determined by the SPSS statistical software Probit analysis. When the antifungal effects of fungicides with different active substances preventing micelle growth of *D. seriata* MBAEM368MN isolate in *in vitro* conditions were examined, it was observed that the disease agent was quite sensitive to other fungicides except for metrafenone. Among the fungicides, cyprodinil+fludioxonil showed the highest efficacy (100%) at a concentration of 1µg $mL^{-1}$. The highest activity was recorded as cyprodinil+fludioxonil with the lowest $EC_{50}$ value as 0.001 µg $mL^{-1}$, followed by fluopyram+tebuconazole with 0.520 µg $mL^{-1}$, azoxystrobin+difenoconazole with 2.958 µg $mL^{-1}$, and folpet+triadimenol with 6.076 µg $mL^{-1}$ respectively. The lowest efficacy was obtained from metrafenone active substance with the highest $EC_{50}$ value of 11.223 µg $mL^{-1}$ (Table 4). Cyprodinil+fludioxonil, fluopyram+tebuconazole, azoxystrobin+difenoconazole fungicides were in the same statistical group with low $EC_{50}$ values and were determined as the most effective fungicides against *D. seriata* MBAEM368MN isolate.

## Discussion

*Diplodia seriata* was isolated from the root and crown parts of the Sultani seedless vine varieties between of 2-10 years old, grafted on different rootstocks in Denizli and Manisa in Aegean Region. In a study examining cross infections of *Ilyonectria* spp. and Botryosphaeriaceae family that cause dieback in young vines in Australia; *D. seriata*, *D. mutila* (Fries) Montagne, and *Lasiodiplodia theobromae* were isolated from 79.8% and 8% of Chardonny and Ramsey rootstocks, respectively. *Diplodia seriata* and *D. mutila* were detected from the roots of 10% and 5% of the plants showing the symptoms, respectively (Pitt *et al.* 2010). In a study conducted in 2015 in the Sultani seedless vineyard areas in Aegean Region, it was reported that at least one grapevine stem disease was seen in more than 80% of the vineyards who were at least 10 years old, and *Botryosphaeriaceae* species were the most isolated pathogens with 1.3% (Akgul *et al*. 2015). However, Billones-Baaijens *et al.* (2013) found that *D. seriata* and *D. mutila* were less virulent in green shoots compared to the three *Neofusicoccum* species. These *Diplodia* species were equally virulent when grafted into rooted strawberries, and these species may be tissue-specific pathogens also may be explain the reason for the endophytic behavior of these pathogens as their high availability from asymptomatic breeding materials and nurseries.

It is difficult to differentiate *Diplodia* species based on their conidial morphology because they are very similar to each other. The time of onset of conidia pigmentation in *Diplodia* species, and very small differences in color and compartments aid in distinction (Phillips *et al*. 2008, 2012). It is noted that the conidia in most *Diplodia* species remains hyaline for a long time and may never actually be brown. However, species within the group are characterized by brown, aseptate conidia (such as *D. seriata* and *D. sapinea* (Fries) Fuckel), pigmented conidia (Phillips *et al*. 2013). In our study, the isolates obtained based on morphological characters of fungal structures of diseased plants were described as *D. seriata* De Not (teleomorph "*Botryosphaeria*" obtusa) (Phillips *et al*. 2007, Chebil *et al*. 2017). By phylogenetic analysis, the two *Diplodia* species were clustered on two different branches in the same group. It has been molecularly confirmed that the *Diplodia seriata* isolate has a 100% similarity index with *Diplodia* species. In a study on species in the Botryosphaeriaceae family associated with dieback in Vine in China, *Lasiodiplodia theobromae*, *Neofusicoccum parvum, Botryosphaeria dothidea* and, *D. seriata* were determined as pathogens by their molecular characterization of the ITS, TUB, and EF1-α gene regions (Yan *et al*. 2013).

A number of studies have been carried out on members of the Botryosphaeriaceae family, which leads to dieback in vines (Luque *et al.* 2009, Urbez-Torres & Gubler 2009). In a study that evaluated fungicides for the control of Botryosphaeria dieback disease in vines in New Zealand, 8 of the 16 tested fungicides were been found to be effective in preventing conidial germination and mycelial growth in against *Neofusicoccum australe* (Slippers, Crous & Wingfield) Crous, Slippers & Phillips,

*N. luteum*, and *D. mutila*. Flusilazole, carbendazim, tebuconazole, prochlorase, procymidone, iprodione, fenarimol, thiophanate methyl, chlorothalonil, and mancozeb 1 µg $mL^{-1}$ were found to be the most effective against these three *Botryosphaeria* species in *in vitro* with lower average $EC_{50}$ values (Amponsha *et al*. 2012). The effectiveness of 20 different fungicides used against *Botryosphaeria* cancer in the vineyards in Australia was revealed by *in vitro* trials using *B. dothidea*, *N. parvum*, *L. theobromae*, and *D. seriata*. Fludioxonil, carbendazim, fluazinam, tebuconazole, flusilazole, penconazole, procymidone, iprodione, myclobutanil, and pyraclostrobin, with a value of <1.0 mg $L^{-1}$, were identified as the most effective fungicides (Pitt *et al*. 2012).

*Diplodia seriata*, isolated in the present study was determined as the dieback disease in vines in Manisa and Denizli provinces in Aegean region. It is thought that this agent can be found in the root and crown region and accelerates dieback according to the region in which it is located.

The effects of fungicides with different chemical structures against the disease agent isolated from the vineyard were tested for the first time in *in vitro* conditions. Cyprodinil + fludioxonil and fluopyram + tebuconazole were found to be the most effective fungicides against *D. seriata* MBAEM368MN isolate with low $EC_{50}$ values. For complete control of dieback disease, an integrated control system that encompasses the entire life cycle of grapevines is necessary. In future studies, integration of well-planned cultural methods and chemical control practices that will provide optimum protection in field conditions can be realized. It may also be recommended to add the Switch 62.5 and Luna Experience fungicides with good results according to $EC_{50}$ values in chemical control applications.

**Acknowledgement**

This study was carried out in the laboratory of The Plant Health Clinic of the Directorate of Manisa Viticulture Research Institute. A part of this study was presented as a short summary at II. International Agricultural, Biological & Life Science Conference (E-Agbiol), held in Edirne, Turkey, from September 1 to 3, 2020.

**Ethics Committee Approval:** Since the article does not contain any studies with human or animal subject, its approval to the ethics committee was not required.

**Author Contributions:** Concept: N.G.S., M.Y., Desing: N.G.S., M.Y., Execution: N.G.S., M.Y., Material supplying: N.G.S., M.Y., Data acquisition: N.G.S., M.Y., Data analysis/interpretation: N.G.S., M.Y., Writing: N.G.S., M.Y.

**Conflict of Interest:** The authors have no conflicts of interest to declare.

**Funding:** The authors declared that this study has received no financial support.

**References**

1. Akgül, D.S., Savas, N.G. & Eskalen, A. 2014. First report of wood canker caused by *Botryosphaeria dothidea*, *Diplodia seriata*, *Neofusicoccum parvum*, and *Lasiodiplodia theobromae* on grapevine in Turkey. *Plant Diseases*, 98: 568.
2. Akgül, D.S., Savas, N.G., Teker, T., Keykubat, B., Mayorquin, J.S. & Eskalen, A. 2015. Fungal trunk pathogens of Sultana seedless vineyards in Aegean region of Turkey. *Phytopathologia Mediterranea*, 54(2): 380-393.
3. Akgül, D.S., Ozarslandan, M. & Erkılıç, A. 2020. Phylogenetic discrimination and pathogenicity of fungi causing Botryosphaeria dieback disease on grapevine in Southern Turkey. *Plant Protection Bulletin*, 60(2): 63-72.
4. Amponsah N.T., Jones E., Ridgway H.J. & Jaspers M.J. 2012.Evaluation of fungicides for the management of Botryosphaeria dieback diseases of grapevines. *Pest Management Science*, 68: 676-683.
5. Anonymous, 2019. Agricultural Products Markets GRAPE. https://arastirma.tarimorman.gov.tr/tepge/Belgeler/PDF%20Tar%C4%B1m%20%C3%9Cr%C3%BCnleri%20Piyasalar%C4%B1/2019Ocak%20Tar%C4%B1m%20%C3%9Cr%C3%BCnleri%20Raporu/2019-Ocak%20%C3%9Cz%C3%BCm.pdf. (Data Accessed: May 2020).
6. Billones-Baaijens, R., Ridgway, H.J., Jones, E.E. & Jaspers, M.V. 2013. Prevalence and distribution of Botryosphaeriaceae species in New Zealand grapevine nurseries. *European Journal of Plant Pathology*, 135: 175-85.
7. Castillo-Pando, M., Somers, A., Green, C.D., Priest, M. & Sriskanthades, M. 2001. Fungi associated with dieback of Semillon grapevines in the Hunter Valley of New South Wales. *Australasian Plant Pathology*, 30: 59-63.
8. Chebil, S., Fersi, R., Bouzid, M., Quaglino, F., Chenenaoui, S., Melki, I., Durante, G., Zacchi, E., Bahri, B.A., Bianco, P.A. & Rhouma, A. 2017. Fungi from the Diaporthaceae and Botryosphaeriaceae families associated with grapevine decline in Tunisia. *Ciencia e Investigación Agraria*, 44(2): 127-138.
9. FAO. 2019. Food and Agricultural Organization, Statistics Division. http://www.fao.org. (Date Accessed: April 2020).
10. Glass, N. & Donalds, G.C. 1995. Development of primer sets designed for use with the PCR to amplify conserved genes from filamentous ascomycetes. *Applied and Environmental Microbiology*, 61(4): 1323-30.
11. Gramaje D., Úrbez-Torres, J.R. & Sosnowski, M.R. 2018. Managing Grapevine Trunk Diseases with respect to etiology and epidemiology: Current Strategies and Future Prospects. *Plant Diseases*, 102(1): 12-39.
12. Highet, A. & Wicks, T. 1998. The incidence of Eutypa dieback in South Australia vineyards. Annual Technical Issue. The Australian Grape Grower and Wine-maker, 414: 135-136.

13. Kühn A., Zappata, A., Gold, R.E., Zito, R. & Kortekamp, A. 2017. Susceptibility of grape pruning wounds to grapevine trunk diseases and effectiveness of a new BASF wound protectant. *Phytopathologia Mediterranea*, 56(3): 536 (abstract).

**14.** Larignon, P., Fulchıc, R., Cere, L. & Dubos, B. 2001. Observation on black dead arm in French vineyards. *Phytopathologia Mediterranea*, 40: 336-342**.**

**15.** Luque J., Martos, S., Aroca, A., Raposoand, R. & Garcia-Fihueres, F. 2009. Symptoms and fungi associated with declining mature grapevine plants in northeast Spain. *Journal of Plant Pathology*, 91: 381-390**.**

16. Ozben, S. 2011. Determination of Fungal Diseases and Their Prevalence in Vineyard in Ankara Provinces. Ankara University Graduate School of Natural and Applied Sciences Department of Plant Protection, *Master Thesis*, Ankara, 134pp.

17. Pascoe, I. & Cottral, E. 2000. Developments in grapevine trunk diseases research. *Phytopathologia Mediterranea*, 39: 68-75.

18. Phillips, A.J.L. 2002. Botryosphaeria species associated with diseases of grapevines in Portugal. *Phytopathologia Mediterranea*, 41: 3-18.

19. Phillips, A.J.L., Crous, P.W & Alves, A. 2007. *Diplodia seriata*, the anamorph of "*Botryosphaeria*" *obtusa*. *Fungal Diversity*, 25: 141-155.

20. Phillips, A.J.L., Alves, A., Pennycook, S.R., Johnston, P.R. & Ramaley, A. 2008. Resolving the phylogenetic and taxonomic status of dark-spored teleomorph genera in the Botryosphaeriaceae. *Molecular Phylogeny and Evolution of Fungi*, 21: 2955.

21. Phillips, A.J.L., Lopes, J., Abdollahzadeh, J., Bobev, S. & Alves, A. 2012. Resolving the *Diplodia* complex on apple and other Rosaceae hosts. *Molecular Phylogeny and Evolution of Fungi*, 29: 29-38.

22. Phillips, A.J.L., Alves, A., Abdollahzadeh, J., Slippers, B., Wingfield, M.J., Groenewald, J.Z. & Crous, P.W. 2013. The Botryosphaeriaceae: genera and species known from culture. *Studies in Mycology*, 76: 51-167.

23. Pitt, W.M., Sosnowski, M.R., Huang, R., Qiu, Y., Steel, C.C. & Savocchia, S. 2012. Evaluation of fungicides for the management of Botryosphaeria canker of grapevines. *Plant Diseases*, 96: 1303-1308.

24. Pitt, W.M., Huang, R. & Steel, C.C. 2010. Identification, distribution and current taxonomy of Botryosphaeriaceae species associated with grapevine decline in New South Wales and South Australia. *Australian Journal of Grape and Wine Research*, 16: 258-271.

25. Savocchia S., Steel C.C., Stodart, B.J. & Somers, A., 2007. Pathogenicity of Botryosphaeria species from declining grapevines in subtropical regions of Eastern Australia. *Vitis*, 46(1): 27-32.

26. Siebert, J.B. 2001. *Eutypa*: the economic toll on vineyards. *Wines and Vines*, 4: 50-56.

27. Slippers, B. & Wingfield, M.J. 2007. Botryosphaeriaceae as endophytes and latent pathogens of woody plants-diversity, ecology and impact. *Fungal Biology Reviews*, 21: 90-106.

28. Slippers, B., Boissin, E., Phillips, A.J.L., Groenewald, J.Z. & Wingfield, M.J. 2013. Phylogenetic lineages in the *Botryosphaeriales*: A systematic and evolutionary framework. *Studies in Mycology*, 76: 31-49.

29. Tamura, K., Peterson, D., Peterson, N., Stecher, G., Nei, M. & Kumar, S. 2011. MEGA5: molecular evolutionary genetics analysis using maximum likelihood, evolutionary distance, and maximum parsimony methods. *Molecular Biology and Evolution*, 28: 2731-2739.

30. Úrbez-Torres, J.R. & Gubler, W.D. 2009. Pathogenicity of Botryosphaeriaceae species isolated from grapevine cankers in California. *Plant Disease*, 93: 584-592.

31. Úrbez-Torres, J.R. 2011. The status of Botryosphaeriaceae species infecting grapevines. *Phytopathologia Mediterranea*, 50: 5-45.

32. Uysal, A. & Kurt, S. 2019. In vitro sensitivity of anthracnose disease agent, Colletotrichum gloeosporioides (Penz.) Penz. & Sacc., to some fungicides on lemon. *Plant Protection Bulletin*, 59(1): 53-62.

33. Yan, JY., Xie, Y., Zhang, W., Wang, Y., Liu, JK., Hyde, KD., Seem, RC., Zhang, GZ.,Wang, ZY, Yao, SW., Bai, XJ., Dissanayake, AJ., Peng, YL. & Li, XH. 2013. Species of Botryosphaeriaceae involved in grapevine dieback in China. *Fungal Diversity*, 61: 221-236.

# Trakya University Journal of Natural Sciences (TUJNS)

# Copyright Release Form

Trakya University
Institute of Natural Sciences
Balkan Campus, Institutions Building
22030 EDİRNE, TURKEY

Telephone : 0 284 2358230
Fax : 0 284 2358237
e-mail : tujns@trakya.edu.tr

I, the undersigned, declare that I transfer the copyright and all related financial rights of the article with the title given below to Trakya University, granting Trakya University for rights of publishing and accepting University Publishing Regulations and Trakya University Publication Application Instructions for printing process.

**Article Name:**

**Author(s):**

Name, Surname :
Title :
Signature :
Date :

Name, Surname :
Title :
Signature :
Date :

Name, Surname :
Title :
Signature :
Date :

Name, Surname :
Title :
Signature :
Date :

Name, Surname :
Title :
Signature :
Date :

*Additional page(s) can be used if the author number exceeds 5. All co-authors of the study are required to sign this form.*

# Yazım Kuralları

# Trakya University Journal of Natural Sciences

# (Trakya Univ J Nat Sci)

**Trakya University Journal of Natural Sciences,** her yıl Nisan ve Ekim aylarında olmak üzere yılda iki sayı olarak çıkar ve **Biyoloji, Biyoteknoloji, Çevre Bilimleri, Biyokimya, Biyofizik, Su Ürünleri, Ziraat, Veterinerlik, Ormancılık, Hayvancılık, Genetik, Gıda, Temel Tıp Bilimleri** alanlarındaki teorik ve deneysel yazıları yayınlar. Dergide yazılar İngilizce olarak yayınlanır. Ancak, yazıda Türkçe özet olmalıdır. Yabancı yazarlar için Türkçe özet desteği verilecektir. Özet kısmında kısaca giriş, materyal ve metot, sonuçlar ve tartışma başlıkları yer almalıdır. Dergide orijinal çalışma, araştırma notu, derleme, teknik not, editöre mektup, kitap tanıtımı yayınlanabilir. Değerlendirilmek üzere dergiye gönderilen yazıların yazımında ulusal ve uluslararası geçerli etik kurallara Committee on Publication Ethics (COPE) uyularak araştırma ve yayın etiğine dikkat edilmesi gerekmektedir. Yazılara konu olarak seçilen deney hayvanları için etik kurul onayı alınmış olmalı ve yazının sunumu esnasında dergi sistemine ek dosya olarak eklenerek belgelendirilmelidir. Basılacak yazıların daha önce hiçbir yerde yayınlanmamış ve yayın haklarının verilmemiş olması gerekir. Dergide yayınlanacak yazıların her türlü sorumluluğu yazar(lar)ına aittir.

## Yazıların sunulması

Yazılar http://dergipark.gov.tr/trkjnat web adresi üzerinden gönderilmelidir. Dergiye yazı gönderimi mutlaka online olarak yapılmalıdır.

Yazı gönderiminde daha önce Dergi Park sistemine giriş yapmış olan kullanıcılar, üye girişinden kullanıcı adı ve şifreleri ile giriş yapabilirler.

Yazı gönderiminde sisteme ilk kez giriş yapacak ve yazı gönderecek yazarlar **"GİRİŞ"** bölümünden "**KAYDOL**" butonunu kullanacaklardır.

Yazarlar dergipark sistemine kaydolduktan sonra **"YAZAR"** bölümünden girecek ve yazıyı sisteme, yönergelere uygun olarak yükleyeceklerdir.

## Yazı hazırlama ilkeleri

Yazılar, Yayın Komisyonu'na **MS Word** kelime işlemcisiyle **12 punto** büyüklüğündeki **Times New Roman** tipi yazı karakteriyle ve 1,5 aralıklı yazılmış olarak gönderilmelidir. İletişim bilgileri yazının ilk sayfasında tek başına yazılmalı, daha sonraki sayfada yazar isimleri ve iletişim bilgileri bulunmamalıdır. Tüm yazı her sayfası kendi arasında **satır numaraları** içerecek şekilde numaralandırılmalıdır. Yazar adları yazılırken herhangi bir akademik unvan belirtilmemelidir. Çalışma herhangi bir kurumun desteği ile yapılmış ise, teşekkür kısmında kurumun; kişilerin desteğini almış ise kişilerin bu çalışmayı desteklediği yazılmalıdır.

Yazı aşağıdaki sıraya göre düzenlenmelidir:

**Yazarlar:** Yazının ilk sayfasında sadece yazar isimleri ve adresleri bulunmalıdır. Adlar kısaltmasız, soyadlar büyük harfle ve ortalanarak yazılmalıdır. Adres(ler) tam yazılmalı, kısaltma kullanılmamalıdır. Birden fazla yazarlı çalışmalarda, yazışmaların hangi yazarla yapılacağı yazar ismi altı çizilerek belirtilmeli (sorumlu yazar) ve **yazışma yapılacak yazarın adres ve e-posta adresi yazar isimlerinin hemen altına yazılmalıdır. Bu sayfaya yazı ile ilgili başka bir bilgi yazılmamalıdır. Yazı, takip eden sayfada bulunmalı ve yazar-iletişim bilgisi içermemelidir.**

**Başlık:** İngilizce olarak Kısa ve açıklayıcı olmalı, büyük harfle ve ortalanarak yazılmalıdır.

**Özet ve Anahtar kelimeler:** Türkçe ve İngilizce özet 250 kelimeyi geçmemelidir. Özetin altına küçük harflerle anahtar kelimeler ibaresi yazılmalı ve yanına anahtar kelimeler virgül konularak sıralanmalıdır. Anahtar kelimeler, zorunlu olmadıkça başlıktakilerin tekrarı olmamalıdır. İngilizce özet koyu harflerle "Abstract" sözcüğü ile başlamalı ve başlık, İngilizce özetin üstüne büyük harflerle ortalanarak yazılmalıdır. Yazıdaki ana başlıklar ve varsa alt başlıklara **numara verilmemelidir.**

**Giriş:** Çalışmanın amacı ve geçmişte yapılan çalışmalar bu kısımda belirtilmelidir. Yazıda SI (Systeme International) birimleri ve kısaltmaları kullanılmalıdır. Diğer kısaltmalar kullanıldığında, metinde ilk geçtiği yerde 1 kez açıklanmalıdır. Kısaltma yapılmış birimlerin sonuna nokta konmamalıdır (45 m mesafe tespit edilmiştir). Kısaltma cümle sonunda ise nokta konmalıdır (… tespit edilen mesafe 45 m. Dolayısıyla…).

**Materyal ve Metod:** Eğer çalışma deneysel ise kullanılan deneysel yöntemler detaylı ve açıklayıcı bir biçimde verilmelidir. Yazıda kullanılan metod/metodlar, başkaları tarafından tekrarlanabilecek şekilde açıklayıcı olmalıdır. Fakat kullanılan deneysel yöntem herkes tarafından bilinen bir yöntem ise ayrıntılı açıklamaya gerek olmayıp sadece yöntemin adı verilmeli veya yöntemin ilk kullanıldığı çalışmaya atıf yapılmalıdır.

**Sonuçlar**: Bu bölümde elde edilen sonuçlar verilmeli, yorum yapılmamalıdır**.** Sonuçlar gerekirse tablo, şekil ve grafiklerle de desteklenerek açıklanabilir.

**Tartışma:** Sonuçlar mutlaka tartışılmalı fakat gereksiz tekrarlardan kaçınılmalıdır. Bu kısımda, literatür bilgileri vermekten çok, çalışmanın sonuçlarına yoğunlaşmalı, sonuçların daha önce yapılmış araştırmalarla benzerlik ve farklılıkları verilmeli, bunların muhtemel nedenleri tartışılmalıdır. Bu bölümde, elde edilen sonuçların bilime katkısı ve önemine de mümkün olduğu kadar yer verilmelidir.

**Teşekkür:** Mümkün olduğunca kısa olmalıdır. Teşekkür, genellikle çalışmaya maddi destek sağlayan kurumlara, kişilere veya yazı yayına gönderilmeden önce inceleyip önerilerde bulunan uzmanlara yapılır. Teşekkür bölümü kaynaklardan önce ve ayrı bir başlık altında yapılır.

**Kaynaklar**: Yayınlanmamış bilgiler kaynak olarak verilmemelidir (*Yayınlanmamış kaynaklara örnekler: Hazırlanmakta olan veya yayına gönderilen yazılar, yayınlanmamış bilgiler veya gözlemler, kişilerle görüşülerek elde edilen bilgiler, raporlar, ders notları, seminerler gibi*). Ancak, tamamlanmış ve jüriden geçmiş tezler ve DOI numarası olan yazılar kaynak olarak verilebilir. Kaynaklar, yazı sonunda alfabetik sırada (yazarların soyadlarına göre) sıra numarası ile belirtilerek verilmelidir.

**Kaynak yazım şekli:**

Kaynak yazım şekli için Endnote stilini indirebilirsiniz.

Veya aşağıdaki yönergeyi kullanabilirsiniz.

Yazıların ve kitapların referans olarak veriliş şekilleri aşağıdaki gibidir:

**Makale:** Yazarın soyadı, adının baş harfi, basıldığı yıl. Makalenin başlığı, *derginin adı*, cilt numarası, sayı, sayfa numarası. Dergi adı italik yazılır.

*Örnek:*

*Tek yazarlı Makale için*

Soyadı, A. Yıl. Makalenin adı. (Sözcüklerin ilk harfi küçük). *Yayınlandığı derginin açık ve tam adı*, Cilt(Sayı)**:** Sayfa aralığı.

Kıvan, M. 1998. *Eurygaster integriceps* Put. (Heteroptera: Scuteleridae)'nin yumurta parazitoiti *Trissolcus semistriatus* Nees (Hymenoptera: Scelionidae)'un biyolojisi üzerinde araştırmalar*. Türkiye Entomoloji Dergisi*, 22(4): 243-257.

*İki ya da daha çok yazarlı makale için*

Soyadı1, A1. & Soyadı2**,** A2. Yıl. Makalenin adı**.** (Sözcüklerin ilk harfi küçük). *Yayınlandığı derginin tam adı*, Cilt(Sayı): Sayfa aralığı.

Lodos, N. & Önder, F. 1979. Controbution to the study on the Turkish Pentatomoidea (Heteroptera) IV. Family: Acanthasomatidae Stal 1864. *Türkiye Bitki Koruma Dergisi*, 3(3): 139-160.

Soyadı1, A1., Soyadı2, A2. & Soyadı3, A3**.** Yıl. Makalenin adı**.** (Sözcüklerin ilk harfi küçük). *Yayınlandığı derginin tam adı*, Cilt (Sayı): Sayfa aralığı.

Önder, F., Ünal, A. & Ünal, E. 1981. Heteroptera fauna collected by light traps in some districts of Northwestern part of Anatolia. *Türkiye Bitki Koruma Dergisi***,** 5(3): 151-169.

**Kitap:** Yazarın soyadı, adının baş harfi, basıldığı yıl. Kitabın adı (varsa derleyen veya çeviren ya da editör), cilt numarası, baskı numarası, basımevi, basıldığı şehir,toplam sayfa sayısı.

*Örnek*:

Soyadı, A., Yıl. *Kitabın adı*. (Sözcüklerin ilk harfi büyük, italik). Basımevi, basıldığı şehir, toplam sayfa sayısı s./pp.

Önder F., Karsavuran, Y., Tezcan, S. & Fent, M. 2006. *Türkiye Heteroptera (Insecta) Kataloğu*. Meta Basım Matbaacılık, İzmir, 164 s.

Lodos, N., Önder, F., Pehlivan, E., Atalay, R., Erkin, E., Karsavuran, Y., Tezcan, S. & Aksoy, S. 1999. Faunistic *Studies on Lygaeidae (Heteroptera) of Western Black Sea, Central Anatolia and Mediterranean Regions of Turkey.* Ege University, İzmir, ix + 58 pp.

**Kitapta Bölüm:** Yazarın soyadı, adının baş harfi basıldığı yıl. Bölüm adı, sayfa numaraları. Parantez içinde: Kitabın editörü/editörleri, *kitabın adı*, yayınlayan şirket veya kurum, yayınlandığı yer, toplam sayfa sayısı.

*Örnek*:

Soyadı, A., Yıl. Bölüm adı, sayfa aralığı. In: (editör/editörler). *Kitabın adı*. (Sözcüklerin ilk harfi büyük, italik). Basımevi, basıldığı şehir, toplam sayfa sayısı s./pp.

Jansson, A. 1995. Family Corixidae Leach, 1815—The water boatmen. Pp. 26–56. In: Aukema, B. & Rieger, C.H. (eds). *Catalogue of the Heteroptera of the Palaearctic Region.* Vol. 1. Enicocephalomorpha, Dipsocoromorpha, Nepomorpha, Gerromorpha and Leptopodomorpha. The Netherlands Entomological Society, Amsterdam, xxvi + 222 pp.

**Kongre, Sempozyum:** Yazarlar, Yıl. "Bildirinin adı (Sözcüklerin ilk harfi küçük), sayfa aralığı". Kongre/Sempozyum Adı, Tarihi (gün aralığı ve ay), Yayınlayan Kurum, Yayınlanma Yeri.

*Örnek:*

Bracko, G., Kiran, K., & Karaman, C. 2015. The ant fauna of Greek Thrace, 33-34. Paper presented at the 6th Central European Workshop of Myrmecology, 24-27 July, Debrecen-Hungary.

**Internet:** Eğer bir bilgi herhangi bir internet sayfasından alınmış ise (*internetten alınan ve dergilerde yayınlanan yazılar hariç*), kaynaklar bölümüne internet sitesinin ismi tam olarak yazılmalı, siteye erişim tarihi verilmelidir.

Soyadı**,** A. Yıl. Çalışmanın adı. (Sözcüklerin ilk harfi küçük) http://www..... (Date accessed: 12.08.2009).

Hatch, S., 2001. Studentsperception of online education. Multimedia CBT Systems. http://www.scu.edu.au/schools/sawd/moconf/papers2001/hatch.pdf (Date accessed: 12.08.2009).

Kaynaklara metin içinde numara verilmemeli ve aşağıdaki örneklerde olduğu gibi belirtilmelidir.

Örnekler:
... x maddesi atmosferde kirliliğe neden olmaktadır (Landen 2002). Landen (2002) x maddesinin atmosferde kirliliğe neden olduğunu belirtmiştir. İki yazarlı bir çalışma kaynak olarak verilecekse, (Landen & Bruce 2002) veya Landen & Bruce (2002)'ye göre. ... şeklinde olmuştur; diye verilmelidir. Üç veya daha fazla yazar söz konusu ise, (Landen *et al.* 2002) veya Landen *et al.* (2002)'ye göre .... olduğu gösterilmiştir; diye yazılmalıdır.

**Şekil ve Tablolar:** Tablo dışında kalan fotoğraf, resim, çizim ve grafik gibi göstermeler "Fig." olarak verilmelidir. Resim, şekil ve grafikler, net ve ofset baskı tekniğine uygun olmalıdır. Her tablo ve şeklin metin içindeki yerlerine konmalıdır. Tüm tablo ve şekiller yazı boyunca sırayla numaralandırılmalı (Table 1, Fig. 1, Figs 3, 4), başlık ve açıklamalar içermelidir. Şekillerin sıra numaraları ve başlıkları, alta, tabloların ki ise üstlerine yazılır.

Şekiller (tablo dışında kalan fotoğraf, resim, çizim ve grafik gibi) tek tek dosyalar halinde en az **300 dpi** çözünürlükte ve **tif** dosyası olarak şekil numaraları dosya isminde belirtilmiş şekilde ayrıca sisteme ek dosya olarak yüklenmelidir.

Sunulan yazılar, öncelikle Dergi Yayın Kurulu tarafından ön incelemeye tabii tutulur. **Dergi Yayın Kurulu, yayınlanabilecek nitelikte bulmadığı veya yazım kurallarına uygun hazırlanmayan yazıları hakemlere göndermeden red kararı verme hakkına sahiptir.** Değerlendirmeye alınabilecek olan yazılar, incelenmek üzere iki ayrı hakeme gönderilir. Dergi Yayın Kurulu, hakem raporlarını dikkate alarak yazıların yayınlanmak üzere kabul edilip edilmemesine karar verir.

## SUİSTİMAL İNCELEMELERİ VE ŞİKAYETLER

Dergide yayınlanmış veya yayınlanma sürecine girmiş her türlü yazı hakkındaki suistimal şüphesi ve suistimal şüphesiyle yapılan şikayetler dergi Yayın Kurulu tarafından değerlendirilir. Yayın kurulu suistimal şüphesini veya şikayeti değerlendirirken COPE (Committee on Publication Ethics)'un yönergelerine bağlı kalır. Şüphe veya şikayet sürecinde şikayet taraflarıyla hiçbir bağlantısı olmayan bir ombudsman belirlenerek karar verilir. Şikayetler baş editöre tujns@trakya.edu.tr adresi kullanılarak yapılabilir.

## TELIF HAKKI

Telif hakkı, makalenin yayınlandığı andan itibaren (Erken Görünüm dahil) herhangi bir kısıtlama olmaksızın makalenin yazarına / yazarlarına devredilir.

## YAYIN SONRASI DEĞİŞİKLİK VE GERİÇEKME İSTEĞİ

Dergide yazının yayınlanması sonrası yazar sırasında değişiklik, yazar ismi çıkarma, ekleme ya da yazının geriçekilmesi tujns@trakya.edu.tr adresine yapılacak bir başvuru ile gerçekleştirilebilir. Gönderilecek e-postada mutlaka gerekçe ve kanıtlar sunulmalıdır. Sunulan gerekçe ve kanıtlar Yayın Kurulu tarafından görüşülüp karara bağlanır. Yukarıda belirtilen değişiklik ve geri çekme istekleri oluştuğunda tüm yazarların dergiye gönderecekleri yazılar işlem süresi içerisinde otomatik olarak reddedilir.

## ÜYELİK/AYRI BASKI/ERİŞİM

Dergi üyelik gerektirmeyip Açık Erişime sahiptir. Dergide yazısı basılan tüm sorumlu yazarlara 15 ayrı baskı ve yazının çıktığı 1 dergi ücretsiz gönderilmektedir. Dergide yayınlanan tüm yazılara erişim ücretsiz olup full-text pdf dosyaları CC-BY 4.0 uluslararası lisansı kapsamında kullanılabilir.

## REKLAM VERME

Dergiye reklam vermek üzere tujns@trakya.edu.tr adresine yapılacak başvurular dergi sahibi tarafından değerlendirilecektir.

**Baş Editör** **:** Prof. Dr. Kadri KIRAN

Trakya Üniversitesi
Fen Bilimleri Enstitüsü
Balkan Yerleşkesi
22030 - EDİRNE

Tel : 0284 235 82 30
Fax : 0284 235 82 37
e-mail : tujns@trakya.edu.tr

# Trakya University Journal of Natural Sciences
# (Trakya Univ J Nat Sci)

**Trakya University Journal of Natural Sciences,** is published twice a year in April and in October and includes theoretical and experimental articles in the fields of **Biology, Biotechnology, Environmental Sciences, Biochemistry, Biophysics, Fisheries Sciences, Agriculture, Veterinary and Animal Sciences, Forestry, Genetics, Food Sciences** and **Basic Medicine Sciences**. Original studies, research notes, reviews, technical notes, letters to the Editor and book reviews can be published in the journal. The publishing language for all articles in the journal is **English**. On the other hand, authors are required to provide a Turkish abstract also. The Turkish version of the abstract will be supply by the journal for foreign authors. Abstracts should include introduction, material and methods, results and discussion sections in summary. The authors should pay attention to research and publication ethics Committee on Publication Ethics (COPE) in preparation of their manuscripts before submission by considering national and international valid ethics. An approval of Ethics and Animal Welfare Committee is mandatory for submissions based on experimental animals and this approval should be provided during submission of the manuscripts. Articles which have not been published elsewhere previously and whose copyright has not been given to anywhere else should be submitted. All responsibilities related to published articles in Trakya University Journal of Natural Sciences belong to the authors.

**Submitting articles**

Articles should be submitted on the web through http://dergipark.gov.tr/trkjnat and all submissions should be performed online.

Authors, who are already a member of the DergiPark system, can enter in the login section using their "user name" and "password" to submit their articles.

Authors entering the DergiPark system for the first time to submit an article will enter in the "**REGISTER**" section to submit their articles.

**Article preparation rules**

Articles should be submitted to the Journal using **MS Word** preparing **12 points Times New Roman** font and 1.5 raw spacing. Author names and contact info must be in first page, article must continue in second page without author names and contact info. Whole article should have numbered with **line number** restarting each page. The author's name must not be specified any academic titles. If studies supported by a foundation, this support should have been written in the acknowledgement section.

Articles should be arranged as below:

**Authors:** The name(s) of the author(s) should not be abbreviated and must be written under the title one by one, with surnames in capital letters. Address(es) should be written in full. Corresponding authors in multiple authored submissions should be indicated, and the address and e-mail of the corresponding author should be written just under the author(s) list. **No other information about the manuscript should be included in this page. The main manuscript text should start with the following new page and should not include any author-contact information.**

**Title:** Should be short and explanatory and written in capital letters and centered.

**Abstract and keywords:** Turkish and English abstracts should not exceed 250 words. "Keywords" should be written under the abstract in small letters and all keywords should be written using a comma after all. Keywords should not be replica of the title words, if it is not obligatory. Abstract should begin "Abstract" word from the left side of the page. The main and sub headers (if present) should not be numbered.

**Introduction:** The aim of the submitted and history of the previous studies should be indicated in this section. SI (Systeme International) system and abbreviation should be used in the article. Other abbreviations- should be explained once in their first appearance in the text. No "." sign should be used after abbreviations except those used at the end of a sentence (…the determined distance is 45 m. Therefore, …).

**Material and Method:** If the submitted study is experimental, methods of the experiments should be given in detail. The method(s) used in the article should be descriptive for others to repeat. If a widely known experimental method is used, the method does not need to be explained in detail. In this situation, indicating only the name of the experimental method or citing the study who used the method for the first time will be enough.

**Results**: Obtained results should be given in this section without any comment. Results can be explained with tables, figures or graphics, if necessary.

**Discussion:** Results must be discussed, but unnecessary duplications should be avoided. In this section, rather than giving literature data, authors should focus on their results considering similarities and differences with and between previously conducted researches, and should discuss possible reasons of similarities and differences. The contribution to science and importance of the obtained results should also be mentioned as much as possible in this section.

**Acknowledgements:** Should be as short as possible. Thanks are usually made to institutions or individuals who support the study or to experts who reviewed the article before submitting to the journal. Acknowledgement section should be given before the references section in a separate header.

**References**: Unpublished information should not be given as a reference (examples of unpublished references: articles in preparation or submitted somewhere, unpublished data or observations, data obtained based on interviews with individuals, reports, lecture notes, seminars, etc.). However, thesis completed and signed by a jury and articles with DOI numbers given can be used as reference. References should be given at the end of the text, sorted alphabetically by author's surname and should be given with numbering.

**Reference style:**

You can download the Endnote style of TUJNS from http://www.researchsoftware.com.

Or you can follow the instruction below.

**Articles:** Surname of author, first letter of author's first name, publication year, article title, the *name of the journal,* volume, issue, page numbers. Journal name is written in italics.

*Example:*

*Articles with single author*

Surname, N. Year. Article title (First letter of all words small). *Whole name of journal*, Volume (Issue)**:** page range.

Aybeke, M. 2016. The detection of appropriate organic fertilizer and mycorrhizal method enhancing salt stress tolerance in rice (*Oryza sativa* L.) under field conditions. *Trakya University Journal of Natural Sciences,* 17(1): 17-27.

*Articles with two or more authors*

Surname1, N1. & Surname2**,** N2. Year. Article title (First letter of all words small). *Whole name of journal*, Volume (Issue)**:** page range.

Dursun, A. & Fent, M. 2016. Contributions to The Cicadomorpha and Fulgoromorpha (Hemiptera) fauna of Turkish Thrace region. *Trakya University Journal of Natural Sciences,* 17(2): 123-128.

Surname1, N1., Surname2**,** N2. & Surname3, N. Year. Article title (First letter of words small). *Whole name of journal*, Volume (Issue)**:** page range.

Becenen, N., Uluçam, G. & Altun, Ö. 2017. Synthesis and antimicrobial activity of iron cyclohexanedicarboxylic acid and examination of pH effect on extraction in water and organic phases.*Trakya University Journal of Natural Sciences,* 18(1): 1-7.

**Book:** Surname of author, first letter of author's first name, Year. *Book title* (name of translator or book editor if present), volume, edition number, press, city, page number.

*Example*:

Surname, N. Year. *Book Title* (First letter of words small and italic), volume, edition number, press, city, page number.

Czechowski, W., Radchenko, A., Czechowska, W. & Vepsäläinen, K. 2012. *The ants of Poland with reference to the myrmecofauna of Europe*. Museum and Institute of Zoology PAS, Warsaw, 496 pp.

**Book Section:** Surname of author, first letter of the author's first name, Year. Section name, page range. In: (Editor(s) of Book, *Book title,* press, city, page number).

*Example*:

Surname, N. Year. Section name, page range. In: (Editor of Book, *Book title* (First letter of words small and italic), press, city, page number)

Jansson, A. 1995. Family Corixidae Leach, 1815—The water boatmen. pp. 26-56. In: Aukema, B. & Rieger, C.H. (eds). *Catalogue of the Heteroptera of the Palaearctic Region.* Vol. 1. Enicocephalomorpha, Dipsocoromorpha, Nepomorpha, Gerromorphaand Leptopodomorpha. The Netherlands Entomological Society, Amsterdam, xxvi + 222 pp.

**Congress, Symposium:** Surname, N. Year. Presentation title (first letters of all words small), page range. Name of Congress/Symposium, Date (day range and month), place.

*Example:*

Bracko, G., Kiran, K., & Karaman, C. 2015. The ant fauna of Greek Thrace, 33-34. Paper presented at the 6th Central European Workshop of Myrmecology, 24-27 July, Debrecen-Hungary.

**Internet:** If any information is taken from an internet source (articles published in journals and taken from internet excluded), internet address should be written in full in references section and access date should be indicated.

Surname**,** N. Year. Name of study (First letter of words small). http://www..... (Date accessed: 12.08.2009).

Hatch, S. 2001. Student sperception of online education. Multimedia CBT Systems. http://www.scu.edu.au/schools/sawd/moconf/papers2001/hatch.pdf (Date accessed: 12.08.2009).

References within the text should not be numbered and indicated as in the following examples.

Examples:

... atmospheric pollution is causing by x matter (Landen 2002). If an article has two authors, it should be indicated in the text as (Landen & Bruce 2002) or ... according to Landen & Bruce (2002) .... If there are three or more authors, references should be indicated as (Landen *et al.* 2002) or according to Landen *et al.* 2002 ...

**Graphics and tables:** All photos, pictures, drawings and graphics except tables should be indicated as Figures. Pictures, figures and graphics should be clear and ready to print with offset technique. The places of all tables and figures should be indicated in the text. All tables and figures should be numbered within the text respectively (Table 1, Fig. 1, Figs 3, 4). Figure numbers and legends are written below the figures, table numbers and legends are written above the tables.

All figures (all pictures, drawings and graphics except table) should also be uploaded to the system separately with 300dpi resolution at least as .tif file using the figure numbers in the files name.

Submitted articles are subjected to prior review by the Editorial Board. Editorial Board has the right to reject the articles which are considered of low quality for publish or those which are insufficiently prepared according to the author guidelines. The articles accepted for consideration for evaluation will be sent to two different referees. Editorial Board decides to accept or reject the submissions for publication by taking into account the reports of referees.

**EXPLOITATION ENQUIRY AND COMPLAINTS**

All kinds of exploitation doubts and complaints about manuscripts, either published or in publication process, are evaluated by the Editorial Board. The Editorial Board strictly follows the directives of COPE (Committee on Publication Ethics) during the evaluations. An ombudsman who has no connection with the parts in any stage of the complaint is appointed and a decision is made. Complaints can be sent to the editor in chief by sending an e-mail to tujns@trakya.edu.tr.

**POST-PUBLICATION CHANGE AND WITHDRAWAL OF A MANUSCRIPT**

Changes in author ordering, removal or addition of a new author in and withdrawal of a published manuscript can be realized by sending an application to tujns@trakya.edu.tr. The application e-mail should include the reason of the requested change with the evidences. The reasons and the evidences are discussed and finalized by the Editorial Board. Further submissions of authors of a formerly accepted manuscript undergoing a change process are automatically sent back to the authors until the final decision of the manuscript in process.

**ADVERTISING**

Advertising applications send to tujns@trakya.edu.tr will be evaluated by the journal owner.

**Editor-in-Chief** **:** Prof. Dr. Kadri KIRAN

Trakya Üniversitesi
Fen Bilimleri Enstitüsü
Balkan Yerleşkesi
22030 - EDİRNE-TURKEY

Phone : +90 284 235 82 30
Fax : +90 284 235 82 37
e-mail : tujns@trakya.edu.tr